

**THE UNIVERSITY OF TULSA
THE GRADUATE SCHOOL**

**A NEW EFFICIENT FULLY INTEGRATED APPROACH TO
COMPOSITIONAL RESERVOIR SIMULATION**

by
Fawzi M. Guehria

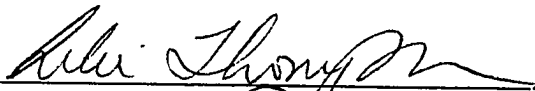


**A dissertation submitted in partial fulfillment of
the requirements for the degree of Doctor of Philosophy
in the Discipline of Petroleum Engineering
The Graduate School
The University of Tulsa
1991**

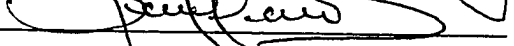
THE UNIVERSITY OF TULSA
THE GRADUATE SCHOOL

A NEW EFFICIENT FULLY INTEGRATED APPROACH TO
COMPOSITIONAL RESERVOIR SIMULATION

A DISSERTATION
APPROVED FOR THE DISCIPLINE OF
PETROLEUM ENGINEERING

By Dissertation Committee


_____, Co-Chairperson

_____, Co-Chairperson




ABSTRACT

Guehria, Fawzi M. (Doctor of Philosophy in Petroleum Engineering)

A New Efficient Fully Integrated Approach to Compositional Reservoir Simulation
(297 pp. - Chapter VI)

Co-Directed by Professors Albert C. Reynolds and Leslie G. Thompson

(350 WORDS)

Reservoir processes generally requiring compositional modeling are depletion and/or cycling of volatile oil and retrograde gas condensate reservoirs and miscible flooding with multiple-contact-miscibility generated in-situ. Most compositional models described in the literature use explicit transmissibilities. Because of the complexity of the equations and the use of a large number of components, the explicit formulation has been the only feasible approach to field-scale simulation. The drawback of the explicit formulation is the severe time step size limitation which excludes its application in single well models that are used to study productivity impairment as a result of condensate dropout around the well. Some attempts have been made to develop a fully-implicit equation of state model. However, the application of such a model has been restricted to very small problems because of the prohibitive cost associated with it.

We present a novel highly efficient approach to the discretization and solution of the flow and thermodynamic equations describing multicomponent fluid flow in a porous medium. Comparisons with a standard fully-implicit compositional simulator, which utilizes Newton's method, indicates that typical execution times for our simulator are five to seven times faster than the fully-implicit model, and that these speeds are achieved with no degradation in accuracy, stability or robustness. In fact, our simulator does not experience

convergence difficulties (oscillations) during phase transitions (crossing phase envelopes) that have been routinely observed in other simulators. The remarkable speed achieved by our simulator (with time step sizes controlled by accuracy requirements rather than stability requirements) arises from our radically novel approach to the linearization and solution of the discretized flow equations and thermodynamic equilibrium equations. An incremental gain in efficiency is also achieved by solving the minimum number of equations necessary for accurate flow description at each time step. For an N_c - component system, our model solves a maximum of N_c equations at each gridblock containing two phases (e.g., oil and gas). This reduction in equations is achieved by rigorously and explicitly incorporating the thermodynamic equilibrium equations in the component mass balance equations at the beginning of each time step.

ACKNOWLEDGEMENTS

This dissertation is dedicated to the memory of my late father Ali and my two brothers, Mohamed Cherif and Abdelhamid.

I would like to extend my most heartfelt thanks to Professor Albert C. Reynolds and Professor Leslie G. Thompson for their encouragement, guidance, support, and patience shown over the course of this research and for reading the countless revisions required in the development of this dissertation to its present form. Essentially, this work exists because of the belief they placed in my ability. Much gratitude is extended to both of Dr. Ramon Cerro and Dr. William Coberly for their constructive comments. I also wish to express my sincere appreciation to Dr. Richard Redner for his assistance in the use of the \TeX macros to produce this manuscript.

I wish to thank Phillips Petroleum Foundation, Inc. for providing a Doctoral Fellowship which financed the major part of my Ph.D studies. The financial support of the Tulsa University Petroleum Reservoir Exploitation Projects is also gratefully acknowledged. Funds for computer time were provided by the University of Tulsa.

Finally, I wish to thank my wife for enduring the many late night jaunts to the Computer Laboratory.

I wish to dedicate this work to my mother, all my brothers and sisters, my loving and caring wife Farida and my newborn son Adel for their endless patience and understanding.

TABLE OF CONTENTS

TITLE PAGE	i
APPROVAL PAGE	ii
ABSTRACT	iii
ACKNOWLEDGEMENTS	v
TABLE OF CONTENTS	vi
LIST OF TABLES	xii
LIST OF FIGURES	xv
CHAPTER I INTRODUCTION	1
1.1 Review of Compositional Simulators	1
1.1.1 Fussell and Fussell Formulation	2
1.1.2 Coats Formulation	3
1.1.3 Nghiem et al. Formulation	4
1.1.4 Young and Stephenson Formulation	5
1.1.5 Acs et al. Formulation	5
1.1.6 Watts Formulation	6
1.1.7 Chien et al. Formulation	6
1.1.8 Collins et al. Formulation	7
1.2 Discussion	8
1.3 TUCOMP	10
CHAPTER II PHASE BEHAVIOR CALCULATIONS	12
2.1 Introduction	12
2.2 Equations of State (EOS)	14
2.2.1 Pure Compounds	14
2.2.1.a Ideal Gas	14
2.2.1.b Van der Waals	14

2.2.1.c	Redlich-Kwong (RK)	17
2.2.1.d	Soave-Redlich-Kwong (SRK)	19
2.2.1.e	Peng-Robinson (PR)	20
2.2.1.f	Schmidt-Wenzel (SW)	21
2.2.2	Mixtures	23
2.2.2.a	Redlich-Kwong; Mixtures	26
2.2.2.b	Zudkevitch-Joffe-Redlich-Kwong; Mixtures	27
2.2.2.c	Soave-Redlich-Kwong; Mixtures	27
2.2.2.d	Peng-Robinson; Mixtures	27
2.2.2.e	Schmidt-Wenzel; Mixtures	28
2.2.2.f	Generalized EOS; Mixtures	29
2.3	Equilibrium and Fugacity Functions	30
2.4	Single-Stage Separation Equations	33
2.5	Successive Substitution Method	35
2.6	Minimum Variable Newton-Raphson Method (MVNR)	39
2.6.1	Overall Scheme	39
2.6.2	Dew Point Computation ($p - x$ iteration)	40
2.6.3	Bubble Point Computation ($p - y$ iteration)	42
2.6.4	Flash Calculations ($p < p_{sat}$)	43
2.6.5	Initial Estimates	46
2.6.5.a	K -Values Approach	46

2.6.5.b Baker and Luks Approach	47
2.7 Phase Viscosities	50
2.8 Results and Accuracy of Computations	52
2.8.1 Z - factor	52
2.8.2 Saturation Points	52
2.8.3 Flash Calculations	59
2.9 Use and Capabilities	62
 CHAPTER III FLOW EQUATIONS	 63
3.1 Continuity Equation and Flow with Change of Phase	 63
3.1.1 General Continuity Equation	63
3.1.2 Fluid Flow in Porous Media with Change of Phase	 65
3.1.3 Source/Sink Term	67
3.2 Radial flow Problem Formulation	70
3.2.1 Partial Differential Equations and Auxiliary Conditions	 70
3.2.2 Initial Conditions	71
3.2.3 Inner Boundary Conditions	72
3.2.4 Outer Boundary Conditions	72
 CHAPTER IV NEW NUMERICAL SOLUTION PROCEDURE	 75
4.1 Discretization	75
4.1.1 Radial Grid System	75
4.1.2 Finite Difference Equations	76
4.1.3 Simulation of the Skin Zone	80
4.2 Overall Numerical Scheme	82
4.3 Single-Phase Fluid with Known Initial Composition, $j \in N_{r1}$	 84
4.4 Two-Phase Flow Formulation, $j \in N_{r2}$	89

4.4.1	Multicomponent Systems ($N_c > 2$)	90
4.4.1.a	Treatment of the Equilibrium	
	Equations	90
4.4.1.b	Overall Mass Balance Equation	94
4.4.1.c	Component Flow Equations	99
4.4.1.d	Flow Equation of	
	Component i , $2 \leq i \leq N_c - 1$	103
4.4.1.e	Flow Equation of Component N_c	105
4.4.2	Binary Systems ($N_c = 2$)	106
4.5	Single-Phase Fluid with	
	Varying Composition, $j \in N_{r3}$	109
4.5.1	Block $j \equiv 2$ and Block $j + 1 \equiv 1$	111
4.5.1.a	Overall Mass Balance Equation	111
4.5.1.b	Component Flow Equations	112
4.5.2	Block $j \equiv 2$ and Block $j + 1 \equiv 5$	113
4.5.2.a	Overall Mass Balance Equation	113
4.5.2.b	Component Flow Equations	114
4.5.3	Block $j \equiv 2$ and Block $j + 1 \equiv 2$	116
4.5.3.a	Overall Mass Balance Equation	116
4.5.3.b	Component Flow Equations	117
4.5.4	Block $j \equiv 2$ and Block $j + 1 \equiv 4$	118
4.5.4.a	Overall Mass Balance Equation	118
4.5.4.b	Component Flow Equations	118
4.6	Structure of the Matrix	120
4.7	Automatic Time Step Selector	123
4.8	Appearance and Disappearance of a Phase	126
4.8.1	Block $j \equiv 1, 3$	126
4.8.2	Block $j \equiv 2, 4$	126
4.8.3	Disappearance of a Phase	127
4.9	Material Balance	128

4.10	Summary of the Overall Computational Procedure of the Simulator	129
CHAPTER V	MODEL VALIDATION AND DISCUSSION	131
5.1	Analytical Results	131
5.1.1	Single-Phase Gas Flow	131
5.1.1.a	Transient	
	Single-Phase Gas Flow	132
5.1.1.b	Boundary-Dominated	
	Single-Phase Gas Flow	133
5.1.2	The Steady-State Model Problem	134
5.2	Fluid and Rock Properties	140
5.2.1	Description of Fluids Used	140
5.2.2	Rock Properties Description	148
5.3	Single-Phase Flow Results	152
5.3.1	Single-Phase Gas	152
5.3.2	Single-Phase Oil	152
5.4	Two-Phase Flow Results	161
5.4.1	Boltzmann Variable as a	
	Correlating Parameter	161
5.4.1.a	Binary Systems	161
5.4.1.b	Ternary Systems	168
5.4.1.c	14-Component	
	Volatile System	178
5.4.1.d	17-Component	
	Gas Condensate System	186
5.4.2	Steady-State	186
5.4.3	Comparison with the Fully-Implicit	
	Model (Coats Approach)	191
5.4.3.a	Constant Rate Production	191

5.4.3.b Constant Pressure Production . . .	198
5.4.4 Other Results	198
5.4.5 Isochronal Tests	203
5.4.5.a Test 1	203
5.4.5.b Test 2	208
5.4.6 Gas Cycling	211
 CHAPTER VI CONCLUSIONS	 214
6.1 PVT Package	215
6.2 Reservoir Model	216
NOMENCLATURE	218
REFERENCES	228
APPENDIX A REIDEL'S VAPOR PRESSURE EQUATION	234
APPENDIX B COATS' METHOD FOR Ω_a and Ω_b (ZJRK EOS)	235
APPENDIX C EVALUATION OF PARTIAL DERIVATIVES	237
APPENDIX D PHASE DENSITY AND DENSITY DERIVATIVES	244
APPENDIX E EXAMPLE RUN	245

LIST OF TABLES

<u>Table</u>	<u>Page</u>
2.1	Comparison of Calculated and Experimental <i>Z</i> - factors for the GPA condensed fluid Peng-Robinson and Schmidt-Wenzel EOS 53
2.2	Comparison of Calculated and Experimental Results $C_1/nC_4/nC_{10}$ Zudkevitch-Joffe-Redlich-Kwong EOS 54
2.3	Comparison of Calculated and Experimental Results $C_1/nC_4/nC_{10}$ Peng-Robinson EOS 55
2.4	Comparison of Calculated and Experimental Results $C_1/nC_4/nC_{10}$ Schmidt-Wenzel EOS 56
2.5	Computation of Saturation Points $CO_2/C_1 - C_{13+}$ Peng-Robinson EOS 57
2.6	Computation of Saturation Points $N_2 - CO_2/C_1 - C_{15+}$ Peng-Robinson EOS 58
2.7	Flash Calculations near the Critical Region $C_1 - nC_{10}$ Soave-Redlich-Kwong EOS 60

LIST OF TABLES (Continued)

<u>Table</u>	<u>Page</u>
2.8	Flash Calculations for Reservoir Oil Results $N_2 - CO_2/C_1 - C_{7+}$ Soave-Redlich-Kwong EOS 61
5.1	Summary of the Binary Volatile Oil Data 141
5.2	Summary of the Binary Gas Condensate Data 142
5.3	Saturation Point Properties for the Ternary System $C_1/nC_4/nC_{10}$ Zudkevitch-Joffe-Redlich-Kwong EOS 143
5.4	Composition and Characterization of 14-Component Reservoir Oil MIX 6: $N_2 - CO_2/C_1 - nC_{10+}$ Peng-Robinson EOS 144
5.5	Composition and Characterization of 17-Component Retrograde Gas Condensate MIX 7: $N_2 - CO_2/C_1 - nC_{15+}$ Schmidt-Wenzel EOS 145
5.6	Summary of Input Reservoir Data Single-Phase and Binary Systems 153
5.7	Summary of Input Reservoir Data Retrograde Gas Condensate 162
5.8	Summary of Input Reservoir Data Volatile Oil 163
5.9	Summary of Input Reservoir Data Black-Oil 164
5.10	Summary of Input Reservoir Data Steady-State and Gas Cycling Runs 187

LIST OF TABLES (Continued)

<u>Table</u>		<u>Page</u>
5.11	L_2 Norm Square Error on Fugacities for 17-Component Mixture	204
5.12	Comparison of Simulator and Phase Package Results MIX 2: Retrograde Gas Condensate	205
5.13	Isochronal Test 1	206
5.14	Isochronal Test 2	207

LIST OF FIGURES

<u>Figure</u>	<u>Page</u>
2.1	Diagram of a cubic EOS in the two-phase region 15
2.2	Conditions for the existence of a solution of $\Gamma(V)$ in $[0, 1]$ (Ref. 23) 37
5.1	Constant composition expansion data; retrograde gas condensate, ternary systems 146
5.2	Constant composition expansion data; volatile and black-oil, ternary systems 147
5.3	Relative permeability data; Set 1, imbibition 149
5.4	Relative permeability data; Sets 2 and 3, drainage 151
5.5	Single-phase gas; constant rate production: transient flow 154
5.6	Single-phase gas; constant pressure production: transient flow 155
5.7	Single-phase gas; constant rate production: boundary-dominated flow 156
5.8	Single-phase oil; constant rate production: transient flow 158
5.9	Single-phase oil; constant pressure production: transient flow 159
5.10	Single-phase oil; constant rate production: boundary-dominated flow 160

LIST OF FIGURES (Continued)

<u>Figure</u>	<u>Page</u>
5.11	Correlation of pressure in terms of inverse Boltzmann variable 165
5.12	Correlation of gas saturation in terms of inverse Boltzmann variable 166
5.13	Correlation of composition in terms of inverse Boltzmann variable 167
5.14	Plot of gas saturation as function of pressure 169
5.15	Correlation of gas saturation in terms of inverse Boltzmann variable; retrograde gas condensate, ternary system, $s = 0$ 170
5.16	Correlation of pressure in terms of inverse Boltzmann variable; retrograde gas condensate, ternary system, $s = 0$ 171
5.17	Correlation of gas saturation in terms of inverse Boltzmann variable; retrograde gas condensate, ternary system, $s = 0$ 172
5.18	Correlation of pressure in terms of inverse Boltzmann variable; retrograde gas condensate, ternary system, $s = 0$ 173
5.19	Plot of gas saturation as function of pressure; retrograde gas condensate, ternary system, $s = 0$ 174
5.20	Correlation of composition in terms of inverse Boltzmann variable; retrograde gas condensate, ternary system, $s = 0$ 175
5.21	Correlation of liquid composition in terms of inverse Boltzmann variable; retrograde gas condensate, ternary system, $s = 0$ 176

LIST OF FIGURES (Continued)

<u>Figure</u>	<u>Page</u>
5.22	Correlation of gas composition in terms of inverse Boltzmann variable; retrograde gas condensate, ternary system, $s = 0$ 177
5.23	Correlation of gas saturation in terms of inverse Boltzmann variable; volatile oil, ternary system, $s = 0$ 179
5.24	Correlation of pressure in terms of inverse Boltzmann variable; volatile oil, ternary system, $s = 0$ 180
5.25	Plot of gas saturation as function of pressure; volatile oil, ternary system, $s = 0$ 181
5.26	Correlation of composition in terms of inverse Boltzmann variable; volatile oil, ternary system, $s = 0$ 182
5.27	Correlation of liquid composition in terms of inverse Boltzmann variable; volatile oil, ternary system, $s = 0$ 183
5.28	Correlation of gas composition in terms of inverse Boltzmann variable; volatile oil, ternary system, $s = 0$ 184
5.29	Correlation of pressure and gas saturation in terms of inverse Boltzmann variable; volatile oil, $s = 0$ 185
5.30	Correlation of pressure and gas saturation in terms of inverse Boltzmann variable; retrograde gas condensate, $s = 0$ 188

LIST OF FIGURES (Continued)

<u>Figure</u>	<u>Page</u>
5.31	Comparison of simulator results with steady-state theory predictions; overall flowing mole fractions 189
5.32	Comparison of simulator results with steady-state theory predictions; liquid phase mole fractions 190
5.33	Comparison of simulator results with steady-state theory predictions; gas saturation 192
5.34	Comparison of simulator results with steady-state theory predictions; pseudopressure drop distribution 193
5.35	Comparison of implicit model and new formulation pressure results; retrograde gas condensate, $s = 0$ 194
5.36	Comparison of implicit model and new formulation saturation results; retrograde gas condensate, $s = 0$ 195
5.37	Comparison of implicit model and new formulation gas composition results; retrograde gas condensate, $s = 0$ 196
5.38	Comparison of implicit model and new formulation liquid composition results; retrograde gas condensate, $s = 0$ 197
5.39	Comparison of CPU time used by implicit and new formulation models; constant time step, $\Delta t = 10^{-3}$ days 199

LIST OF FIGURES (Continued)

<u>Figure</u>		<u>Page</u>
5.40	Comparison of CPU time used by implicit and new formulation models; automatic time step selection	200
5.41	Comparison of implicit and new formulation models results; black oil constant rate, $s = 0$	201
5.42	Comparison of implicit and new formulation models results; black oil constant flowing bottomhole pressure, $s = 0$	202
5.43	Variation in sandface saturation during an isochronal test; retrograde gas condensate, $s = 7$, $r_{sD} = 6.03$	209
5.44	Variation in sandface saturation during an isochronal test; retrograde gas condensate, $s = 0$	210
5.45	Sandface pressure and saturation profiles during gas cycling; retrograde gas condensate, ternary system	212
5.46	Sandface gas composition profiles during gas cycling; retrograde gas condensate, ternary system	213

CHAPTER I

INTRODUCTION

1.1 Review of Compositional Simulators

Techniques to predict oil and gas reservoir performance have progressed from volumetric and trend analysis calculations to the development of “mathematical models”, or reservoir simulators. These models, in general, utilize finite difference approximations to the rather complex partial differential equations that mathematically describe the physics and the thermodynamics of fluid flow in porous media. The standard method of developing a model for two-phase fluid flow in a porous medium is to solve simultaneously the continuity equation (after applying Darcy’s Law), and the equation of state for each phase under the prescribed initial and boundary equations. Black oil reservoir simulators are used to model and predict the results of conventional recovery techniques by considering two hydrocarbon components, and assuming that the fluid properties can be expressed as functions of pressure and saturation pressure. However, in reality, interphase mass transfer may take place with mutual changes in both the intensive and extensive thermodynamic properties of each phase. This phenomenon, which is not accounted for by black oil models, led researchers to include an additional relation which more closely models mass transfer between phases. Compositional models are used whenever the variations in the fluid properties and composition are thought to be large enough to affect simulation predictions. Reservoir processes that require compositional modeling can be divided into two major types. The first type is depletion and/or cycling of volatile oil and gas condensate reservoirs. The second type is miscible flooding

with multiple-contact-miscibility generated in-situ. Compositional models are also needed for a variety of chemical flooding processes, but these are beyond the scope of this study.

In a compositional model, the principles of mass conservation and phase equilibria are employed to compute pressure, saturations and phase compositions at each gridblock in the reservoir. Fussell and Fussell¹ (1979) developed a compositional simulator for gas flooding using an equation of state for both equilibria and density calculations. This approach overcame nonconvergence problems of previous models²⁻⁶ which did not utilize an equation of state. The major nonconvergence problem was due to the use of inconsistent fluid property correlations based on equilibrium K -values.

Coats⁷ (1980) developed a fully-implicit formulation and Nghiem et al.⁸ (1981) developed an IMPES-type (implicit pressure, explicit saturation) formulation for miscible gas flooding. Young and Stephenson⁹ (1983) developed a formulation similar to, but more general and efficient than Fussell and Fussell's¹. Thele et al.¹⁰ (1983) compared the Coats⁷, Nghiem et al.⁸ and Young and Stephenson⁹ formulations in terms of computer storage, accuracy, number of iterations and computer time. Acs et al.¹¹ developed an IMPES-type formulation which shared the sequential approach used by Nghiem et al.⁸ while solving a pressure equation that was more closely related to that of the Young and Stephenson⁹ formulation. Watts¹² (1986) later combined and extended the ideas of Acs et al.¹¹ and Spillette et al.¹³ to form a sequential implicit compositional formulation. Chien et al.¹⁴ proposed a new fully-implicit formulation which differs from the Coats⁷ formulation mainly in the selection of unknown variables. Collins et al.¹⁵ (1986) presented an adaptive-implicit formulation.

1.1.1 Fussell and Fussell Formulation

As mentioned before, Fussell and Fussell¹ (1979) presented the first compositional simulator for miscible gas flooding using an equation of state for both the phase equilibrium and density calculations. A modified Redlich-Kwong equation

of state (Zudkevitch and Joffe¹⁶, 1970) was used to model hydrocarbon fluid behavior. Their model used a Newton-Raphson method to simultaneously solve an equation equivalent to the saturation constraint (phase saturations sum to one) and the phase equilibrium constraints for pressure and phase compositions. The algorithm was called a "Minimum Variable Newton-Raphson" iterative method since the authors attempted to minimize the number of variables for which simultaneous solution was required. Different sets of independent variables were selected for a gridblock depending on whether the fluid in the gridblock is single-phase, two-phase predominantly vapor, or two-phase predominantly liquid. Comparison of the hydrocarbon saturation pressure with the gridblock pressure determined whether the hydrocarbon fluid in the gridblock was undersaturated vapor, undersaturated oil, or two-phase at the reservoir conditions. The formulation accounts for a water phase, but does not allow for mass transfer between the aqueous and the non-aqueous phases. For a single hydrocarbon phase gridblock, only the saturation constraint equation entered into the Jacobian, and pressure was the corresponding unknown. For each gridblock containing two phases, $N_c + 1$ equations were entered into the Jacobian, where N_c denotes the number of components in the fluid mixture. These equations would be the N_c phase equilibrium equations and the saturation constraint. Explicit flow coefficients (phase mobility, density and mole fraction composition) were used in constructing the Jacobian.

1.1.2 Coats Formulation

Coats⁷ formulation (1980) also used the Zudkevitch and Joffe¹⁶ version of the Redlich-Kwong equation of state for computing hydrocarbon phase densities and fugacities. The formulation assumptions included mutual insolubility of the aqueous phase and the hydrocarbon components. The Newton-Raphson method was used to compute pressures, saturations and phase compositions simultaneously. The implicit formulation required a Jacobian of order $N_c + 1$ for each gridblock. The $N_c + 1$ equations were the mass conservation equations and the unknowns were pressure, oil and gas saturations, and $N_c - 2$ oil phase compositions. This implicit formulation

treated the flow coefficients implicitly and thus required more computing time per gridblock per time step than an IMPES (implicit pressure, explicit saturation) type model. Like Fussell and Fussell, Coats compared the hydrocarbon saturation pressure with the gridblock pressure to determine whether a gridblock changed from one to two hydrocarbon phases. In addition, if either oil or gas saturation was negative during an iteration, it was set to zero before initiating the next iteration.

1.1.3 Nghiem et al. Formulation

Unlike Fussell and Fussell¹ (1979) and Coats⁷ (1980), Nghiem et al.⁸ (1981) developed an IMPES-type compositional simulator which solved for pressure and phase compositions separately. The Peng-Robinson¹⁷ (1976) equation of state was used for hydrocarbon phase equilibrium and density calculations. The solution procedure was iterative and sequential in nature. First, the mass conservations equations were combined to form a pressure equation, which was linearized with respect to pressure (but not to compositions) using an “approximated” Newton-Raphson method and solved for pressure implicitly. In solving for pressure, the flow coefficients in the pressure equation were computed explicitly. Secondly, the component flow equations were solved for the overall compositions explicitly. Then flash calculations were used to compute phase compositions and densities. The number of moles of vapor at the termination of the flash calculation was used to determine the number of phases present at equilibrium and if it was single-phase, whether the phase was oil or gas. For each time step, the procedure was repeated until convergence was achieved. Using an “approximated” Newton-Raphson method, the Nghiem et al.⁸ formulation yielded a symmetric and diagonally dominant Jacobian matrix of order equal to the number of blocks in the reservoir. Nghiem et al.⁸ computed the derivatives in the Jacobian analytically rather than numerically. Later, Mansoori¹⁸ (1982) observed that the pressure iterates sometimes oscillated when using these approximations. He suggested using numerical approximations but this would require an additional flash calculation per gridblock per iteration. Nghiem¹⁹

(1982) then recommended using a damping factor on the pressure iterates to avoid oscillation.

1.1.4 Young and Stephenson Formulation

Young and Stephenson⁹ (1983) modified Fussell and Fussell's¹ formulation to form a more efficient simulator. They assumed no mass transfer between the aqueous and hydrocarbon phases, and the Redlich-Kwong²⁰ (1949) equation of state was used to model hydrocarbon phase behavior. Like Fussell and Fussell¹, Young and Stephenson's⁹ formulation employed the Newton-Raphson method to compute pressure, the compositions of one phase and the number of moles of vapor simultaneously, and used explicit flow coefficients to compute elements of the Jacobian. The principal difference between these two formulations were the ordering of equations and the selection of variables explicitly appearing in the Jacobian. With the Young and Stephenson⁹ changes, a single set of variables was used under all circumstances; different fluid correlations could be easily implemented; the sparsity of the Jacobian was better utilized and a more efficient formulation resulted. For each gridblock containing two hydrocarbon phases, the Young and Stephenson⁹ formulation results in a Jacobian of order $2N_c + 2$ which was twice the order of the Jacobian in the Fussell and Fussell's¹ formulation. However, the Jacobian was sparse and nearly upper triangular. This set of equations could be solved efficiently, for example, by Gaussian elimination to remove the few elements below the main diagonal and then using backward substitution. Flash calculations were used to test single-phase gridblocks to determine whether they became two-phase. Testing was done only once per time step.

1.1.5 Acs et al. Formulation

Acs et al.¹¹ developed an IMPES-type formulation which shared the sequential nature of the Nghiem et al.⁸ formulation. However Acs et al. considered the composition-dependent terms in the development of the pressure equation, and the

solution of the pressure equation was done once per time step with the flow coefficients computed explicitly. The maximum number of phases that could flow simultaneously was not mentioned and the simulation was not tied to a specific equation of state. In their application example, the fluid properties were calculated by empirical correlations.

The pressure equation of the Acs et al. formulation was derived on the premise of “volume balance”; i.e., the pore volume should be filled completely by the total fluid volume. The coefficients of the pressure equation were computed explicitly, and the “partial mass volume” which was needed for determining the coefficients was computed numerically rather than analytically. Once the pressure was obtained, the mass balance equation was solved explicitly for component mass. With the newly computed pressure and composition, all the fluid properties were updated prior to proceeding to the next time step.

1.1.6 Watts Formulation

The Watts (1986) formulation¹² was a combination and extension of the ideas of Acs et al.¹¹ and Spillette et al.¹³ (1973). Watts constructed a pressure equation which was similar to that of the Acs et al. formulation and solved the equation for pressure implicitly at the new time level. Unlike the Acs et al. formulation, Watts developed a compositional saturation equation, and employed the sequential semi-implicit approach of Spillette et al. to solve the equation for saturation at the new time level. The relative permeability was treated implicitly in this step. The pressure and saturations were then used to compute phase velocities and to solve the mass balance equations for component mass. The paper gave no details concerning phase behavior modeling.

1.1.7 Chien et al. Formulation

Chien et al.¹⁴ (1985) proposed a fully-implicit formulation. The model uses the Peng-Robinson¹⁷ equation of state to describe hydrocarbon phase behavior.

Rather than solving for pressure, saturations and phase compositions as in the Coats⁷ formulation, they solved for pressure, overall composition and equilibrium K -values simultaneously using the Newton-Raphson method. They claimed that this change of variables improved numerical stability and computational efficiency.

1.1.8 Collins et al. Formulation

Collins et al.¹⁵ (1986) developed an adaptive-implicit simulator. The idea behind using an adaptive-implicit method was that at a given time step only a small number of gridblocks needed to be solved implicitly, while the remaining gridblocks were solved in an explicit manner. The criteria for switching explicit gridblocks to implicit gridblocks were based on saturation and overall composition changes over a time step.

The Newton-Raphson method was used to compute pressure and overall composition simultaneously and then flash calculations were used to determine saturations and phase compositions explicitly.

1.2 Discussion

The compositional formulations that have been discussed include two fully-implicit formulations (Coats⁷, 1980; Chien et al.¹⁴ 1985), a sequential semi-implicit formulation (Watts¹², 1986), an adaptive-implicit scheme (Collins et al.¹⁵, 1986), two IMPES-type formulations (Nghiem et al.⁸, 1981; Acs et al.¹¹, 1985), and two formulations which solve for pressure and composition simultaneously, but use explicit flow coefficients (Fussell and Fussell¹, 1979; Young and Stephenson⁹, 1983).

The fully-implicit formulations allow larger time step sizes during simulation than the formulations with explicit flow coefficients. However, the computer memory and CPU time required for the fully-implicit models are its major disadvantages. Furthermore, the program coding is more complicated and the implementation of physical properties models is more difficult than those of the IMPES-type formulations.

The adaptive-implicit approach can partially solve the memory and CPU time problems exhibited by the fully-implicit models while allowing the time step sizes that approach those of the fully-implicit formulation. In addition, the other major drawback of this formulation is the complexity of the program since both fully-implicit and IMPES-type formulations are included. Finally, flash calculations are required to compute phase compositions.

The Nghiem et al.⁸ formulation requires less computer memory. Unfortunately, it does not converge under certain circumstances as reported by Thele et al.¹⁰. The Young and Stephenson⁹ formulation does not have convergence problems and requires minimum flash calculations, but is more complicated. The memory requirements for the Young and Stephenson⁹ formulation are larger than those of the IMPES-type formulation.

The properties and solution procedure of the Acs et al.¹¹ formulation are very similar to those of Nghiem et al.⁸ formulation. The Acs et al.¹¹ method requires flash calculations. However, only one flash calculation is needed for each gridblock at a time step since the method is non-iterative over a time step. The matrix problem in this formulation can be nonsymmetric and nondiagonally dominant.

Both the memory requirements and program complexity of the Watts¹² formulation are greater than those of the Acs et al.¹¹ formulation. However, it allows larger time steps since it is more implicit than the Acs et al.¹¹ formulation.

1.3 TUCOMP

Considering stability, computational efficiency, accuracy, memory requirement, and simplicity of implementing physical properties models, a new solution scheme was developed in this work. The solution procedure has been implemented in a radial flow compositional simulator, TUCOMP. For an N_c - component system, our model solves a maximum of N_c flow equations at each gridblock containing two phases (e.g., oil and gas). The additional N_c thermodynamic equilibrium constraints are rigorously and explicitly incorporated into the component mass balance equations at the beginning of each time step. By equating the phase fugacities of each component and by using a simple Taylor series expansion of this equality, this technique coupled with linearization procedures and semi-implicit treatment of the flow coefficients (phase mobilities, phase densities and phase compositions) yields a robust numerical solution procedure which is on the order of five times faster than a comparable fully-implicit method discussed in Ref. 7. It is hoped that the new solution procedure will form the basis for developing a wide variety of commercial and research reservoir simulators which can achieve the robustness and accuracy necessary for easy and reliable application with a practically reasonable allocation of computer resources.

In chapter two, we present and discuss all the details required in building a reliable PVT package. We also review five equations of state lumped into a generalized expression that degenerates to any of the equations by an appropriate choice of the parameters involved.

In chapter three, we use the general continuity equation to derive the multidimensional equation of flow of fluids in porous media with change of phase. We then restrict our attention to the discretized form of the one-dimensional equation that represents the single well model.

Chapter four contains the new solution procedure developed to efficiently handle this highly nonlinear problem. The details of the techniques to model any type of phase behavior are included.

In chapter five, we validate the new formulation by matching simulation results with a published steady-state analytical solution. Further, during the transient period, we confirm that all dependent variables are unique functions of the Boltzmann variable in a homogeneous reservoir. Comparison with an available fully-implicit simulator based on Coats⁷ procedure, show that, for typical problems, a speedup in execution times of 500% may be obtained without any loss of accuracy. This chapter also contains the successful application of the model to a wide variety of mixtures (ranging from binary systems to 17-component complex mixtures containing non-hydrocarbon components (N_2 and CO_2)). Simulation runs include primary depletion of retrograde gas condensate and volatile oil reservoirs, during which sequences of drawdown are interspersed by buildups to simulate isochronal tests. We also simulate dry gas injection for gas cycling of a retrograde gas condensate reservoir. Simulation of these processes serve as severe tests to the model robustness, since at any particular time it is possible for the reservoir to exhibit fluid behavior varying from black oil to retrograde gas condensate depending on the location in the reservoir.

The final chapter discusses the contribution of this work as well as it presents a short review of the formulation.

CHAPTER II

PHASE BEHAVIOR CALCULATIONS

2.1 Introduction

Calculation of fluid properties and phase equilibrium is important as a general petroleum engineering tool. Knowledge of these properties is required especially when studying multiple - contact miscible displacement processes that involve injection of carbon dioxide and/or rich gas. The ability to perform phase equilibrium calculations numerically using equations of state is extremely important because laboratory analysis is expensive and labor intensive. In this chapter, we discuss a phase package which was designed either to be incorporated into compositional simulators or used independently, e.g., to perform flash calculations, compute phase compressibility factors, or saturation pressures.

This package can be used to perform phase equilibrium calculations based on any of the five commonly used equations of state in the oil industry, namely the Redlich-Kwong²⁰, Zudkevitch-Joffe-Redlich-Kwong¹⁶, Soave-Redlich-Kwong²¹, Peng-Robinson¹⁷ and Schmidt-Wenzel²² equations of state.

The package is designed to enable the user to generate a wide variety of fluid properties, such as densities, compressibility factors, and viscosities. Moreover, the package offers the option of using one, or a combination of two numerical techniques, to solve the single-stage separation equations which describe the thermodynamic equilibrium of fluids, depending on whether the mixtures considered are single-phase, single-phase saturated, or two-phase (Liquid and Vapor). The first

numerical technique is a special version of the commonly known successive substitution method²³. Its two major advantages are its ability to detect the single-phase region without having to compute the saturation pressure, and its simplicity. Unfortunately, this successive substitution method converges very slowly or does not converge at all near the critical region. When the successive substitution method demonstrates slow convergence, our computer program automatically switches to a more robust technique called the Minimum-Variable Newton-Raphson (MVNR) method²⁴.

The MVNR procedure may be used exclusively provided the phase state (single-phase liquid, single-phase gas or two-phase) at a given pressure and overall composition is determined *a priori*, and the set of phase compositions and the number of moles of vapor or liquid must be known at a given pressure before using the MVNR method at chosen pressure increments along the fixed isotherm. If the fluid mixture is single-phase, initial estimates of the saturation pressure and forming mole fraction composition must be provided. Under these conditions, the package is capable of determining the saturation pressure, p_{sat} , and the equilibrium mole fraction composition of the phase which develops at p_{sat} , $\{x_i\}_{i=1}^{N_c}$ or $\{y_i\}_{i=1}^{N_c}$. (See Nomenclature for a definition of the symbols used). Here N_c is the number of components which characterize the fluid. Given pressure and temperature, the package can also perform a constant composition flash calculation to determine the liquid and vapor compositions, the moles of liquid and moles of vapor per mole of fluid mixture at any pressure.

Finally, the package uses correlations to determine the phase viscosities²⁵⁻²⁸ as functions of pressure, temperature and phase compositions.

2.2 Equations of State (EOS)

2.2.1 Pure Compounds

An equation of state is an algebraic relation between pressure, temperature and volume. Throughout, we work in terms of the molar volume. Several equations of state have been proposed for a real gas, from which the molar volume or density can be estimated at a given pressure and temperature. Each equation of state (EOS) has distinct advantages, but no single EOS perfectly describes all fluid properties.

2.2.1.a Ideal Gas

The earliest equation of state is the ideal gas-law which results from Boyle's and Charles' laws and is given by

$$pV = RT, \quad (2.2.1)$$

where throughout, V is the molar volume in units of $ft^3/lbmole$. Eq. 2.2.1 does not adequately describe the behavior of gases except at very low pressures. Consequently, many attempts have been made to develop an equation of state to describe the behavior of real fluids.

2.2.1.b Van der Waals

The most famous EOS is that of van der Waals (1873) given by

$$p = \frac{RT}{V - b} - \frac{a}{V^2}. \quad (2.2.2)$$

Equation 2.2.2 strictly applies to a pure compound; here a and b are parameters which account for the finite size of molecules and are called the attraction and repulsion parameters, respectively, and are determined as follows.

On a $p - V$ diagram, the critical point (see Fig. 2.1)) (critical volume) is an inflection point on the critical isotherm which is mathematically described via the following relationships:

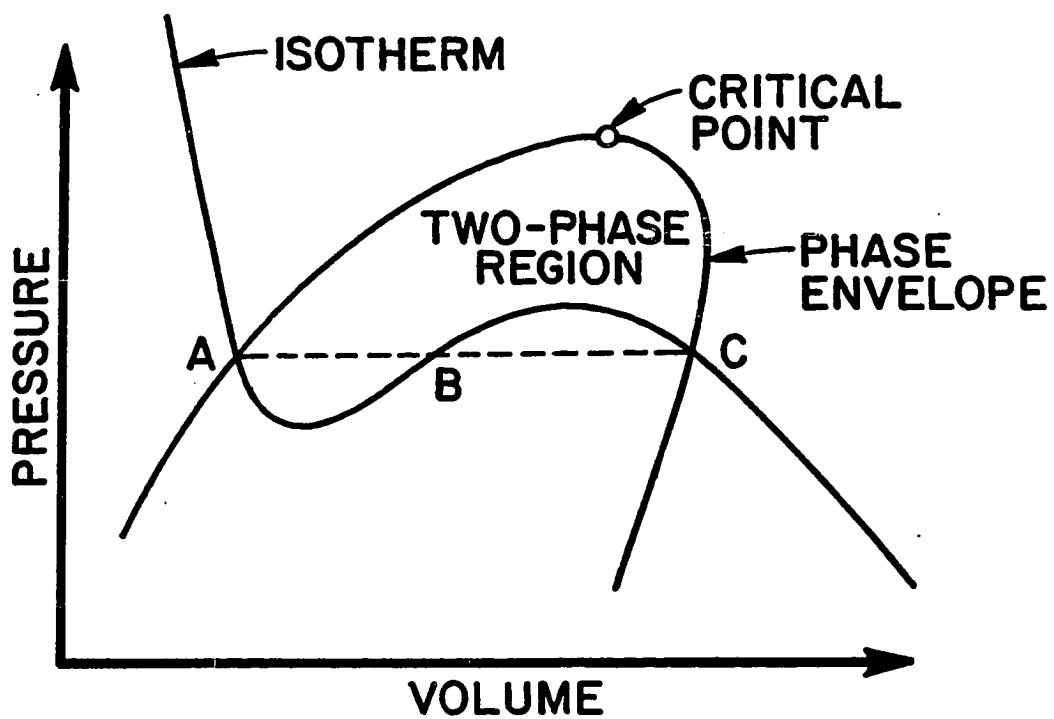


Fig. 2.1 - Diagram of a cubic EOS in the two-phase region.

$$\left(\frac{\partial p}{\partial V}\right)_T = \left(\frac{\partial^2 p}{\partial V^2}\right)_T = 0. \quad (2.2.3)$$

As is well known, applying Eqs. 2.2.2 and 2.2.3 at the critical point gives

$$a = \Omega_a \frac{R^2 T_c^2}{p_c} \quad (2.2.4)$$

and

$$b = \Omega_b \frac{RT_c}{p_c}, \quad (2.2.5)$$

where Ω_a and Ω_b are called the van der Waals coefficients and are equal to 27/64 and 1/8, respectively.

The van der Waals equation, Eq. 2.2.2 may also be expressed as equivalent polynomials in V and in Z . Rearranging Eq. 2.2.2, we obtain

$$V^3 - \left(b + \frac{RT}{p}\right)V^2 + \frac{a}{p}V - \frac{ab}{p} = 0. \quad (2.2.6)$$

Using the gas-law deviation factor equation, $Z = pV/RT$, in Eq. 2.2.6 and rearranging the resulting equation gives

$$Z^3 - \left(1 + \frac{bp}{RT}\right)Z^2 + \frac{ap}{(RT)^2}Z - \frac{abp^2}{(RT)^3} = 0. \quad (2.2.7)$$

Solving the cubic equations, 2.2.6 and 2.2.7 for V and Z , respectively, will yield one real root for a supercritical isotherm and three real positive roots for a subcritical isotherm. In the latter case, the smallest root is interpreted as the specific molar volume (Eq. 2.2.6) or the Z factor (Eq. 2.2.7), respectively, of a liquid phase, while the largest root is interpreted as the specific molar volume (Eq. 2.2.6) or the Z factor (Eq. 2.2.7) for the gas phase. The intermediary real roots of Eqs. 2.2.6 and 2.2.7 are physically insignificant.

It is easy to see through the derivation of Eqs. 2.2.4 and 2.2.5 that the critical compressibility, Z_c , predicted by the van der Waals equation of state is 0.375. This value is considerably higher than those of real fluids. For instance, the critical

compressibility factors of hydrocarbons are all less than 0.29. Only a small number of gases (mostly quantum gases), have critical compressibilities slightly greater than 0.3.

A number of investigators have modified the van der Waals equation of state to improve the accuracy and the most significant improvement of the equation was made by Redlich and Kwong²⁰. Later, Zudkevitch and Joffe¹⁶ and Soave²¹ modified the parameters of the Redlich-Kwong equation of state to improve its capability. Peng and Robinson¹⁷, and Schmidt and Wenzel²² proposed new equations of state in order to improve the poor estimates of liquid density predicted by the Redlich-Kwong types of equations of state.

In this work, we consider five equations of state and we will write a generalized form of the equation of state that degenerates to any of the five widely used equations of state considered here. In the following, we focus on each of these equations of state.

2.2.1.c Redlich-Kwong (RK)

The Redlich-Kwong equation of state gives reasonably accurate predictions of gas phase volumetric properties of hydrocarbons. For a pure compound, it is given by

$$p = \frac{RT}{V-b} - \frac{a}{V(V+b)}, \quad (2.2.8)$$

where a is expressed as a product of a temperature-independent parameter, \tilde{a} , and a temperature dependent term, $\psi(T)$, and is defined as follows:

$$a = \tilde{a}\psi(T). \quad (2.2.9)$$

In the original Redlich-Kwong equation, $\psi(T) = 1/\sqrt{T}$.

The parameters \tilde{a} and b are found by applying the criticality conditions, (Eq. 2.2.3), in a manner similar to that discussed for the van der Waals equation. The resulting expressions are given by the two following equations:

$$a_c = \Omega_a \frac{R^2 T_c^2}{p_c}, \quad (2.2.10)$$

$$b = \Omega_b \frac{RT_c}{p_c}. \quad (2.2.11)$$

Here Ω_a and Ω_b are called the van der Waals coefficients relative to the Redlich-Kwong equation and are equal to 0.42748 and 0.08664, respectively. The critical compressibility, Z_c , predicted by the Redlich-Kwong equation of state becomes a universal constant which is equal to 1/3 for all fluids. Because of this shortcoming, the Redlich-Kwong equation is inaccurate around the critical region. Note that, following Eq. 2.2.9, $a_c = \tilde{a}\psi(T_c)$, and thus, if we define $\alpha = \psi(T)/\psi(T_c)$, it follows that

$$a = a_c \alpha. \quad (2.2.12)$$

If we define

$$A = \frac{ap}{R^2 T^2}, \quad (2.2.13)$$

$$B = \frac{bp}{RT} \quad (2.2.14)$$

and

$$Z = \frac{pV}{RT}, \quad (2.2.15)$$

(note that Z is the gas-law deviation factor) the Redlich - Kwong equation becomes

$$Z^3 - Z^2 - (B^2 + B - A)Z - AB = 0, \quad (2.2.16)$$

which is the Redlich-Kwong analog of the cubic equation given by 2.2.7. Eq. 2.2.16 can be solved either iteratively or analytically. In the two-phase region, the cubic equation yields three roots for Z . As discussed previously, the largest root is that

of the vapor, the smallest is that of the liquid, and the intermediate root is without physical significance, (refer to Fig. 2.1).

Combining Eq. 2.2.13 with 2.2.10 and Eqs. 2.2.12 and 2.2.14 with 2.2.11 gives

$$A = \Omega_a \frac{p_r}{T_r^2} \alpha \quad (2.2.17)$$

and

$$B = \Omega_b \frac{p_r}{T_r}, \quad (2.2.18)$$

where p_r is the reduced pressure, p/p_c , and T_r is the reduced temperature, T/T_c . The only difference in the original Redlich-Kwong and the Soave (defined below) equations is the expression for α . At $T = T_c$, where $\alpha = 1$, the two equations become identical.

In the original Redlich-Kwong equation, the α expression is

$$\alpha = \frac{1}{\sqrt{T_r}}. \quad (2.2.19)$$

Redlich and Kwong²⁰ determined the α expression as an integral part of their equation of state development, without considering the variation of individual fluids, but Soave included the variation by expressing α as a function of reduced temperature and an additional parameter which will be discussed next.

2.2.1.d Soave-Redlich-Kwong (SRK)

The Redlich-Kwong EOS was modified by Soave to improve property predictions in the liquid region. The Soave modification forces the equation to reproduce experimentally determined vapor pressures of pure substances at $T = 0.7T_c$ by introducing a third parameter, the acentric factor denoted by ω . The term α is defined as a function of T_r as follows:

$$\alpha = \left[1 + (0.48508 + 1.55171\omega - 0.15613\omega^2) (1 - \sqrt{T_r}) \right]^2. \quad (2.2.20)$$

With this definition of α , Eqs. 2.2.10 through 2.2.18 still apply.

According to Pitzer (1977) (see Ref. 29), the acentric factor ω is said to “measure the deviation of intermolecular potential functions from that of simple spherical molecules such as argon (where ω is essentially zero).” This new parameter actually describes the deviation of the reduced vapor pressure (p/p_c) of a particular substance from the expected behavior for simple spherical molecules; it is defined as

$$\omega = -1 - \log p_{vp,r}. \quad (2.2.21)$$

Here, $p_{vp,r}$ is the reduced pressure, p_{vp}/p_c , of saturated vapor, evaluated at the reduced temperature $T/T_c = 0.7$. The saturated vapor pressure is computed via the Reidel’s vapor equation³² which, in the interest of completeness, is included in Appendix A.

2.2.1.e Peng-Robinson (PR)

The original Redlich-Kwong equation and the modifications by Soave have a common shortcoming; i.e., they predict poor liquid densities. Peng and Robinson proposed an equation of state similar to the Redlich-Kwong equation, which gives better predictions of vapor pressures, liquid densities and phase equilibrium, particularly near the critical region. The equation is of the form

$$p = \frac{RT}{V-b} - \frac{a}{V(V+b) + b(V-b)}, \quad (2.2.22)$$

where a and b are defined by Eq. 2.2.12 and 2.2.11, respectively. The function α was modified to

$$\alpha = \left[1 + (0.37464 + 1.54226\omega - 0.26992\omega^2) (1 - \sqrt{T_r}) \right]^2. \quad (2.2.23)$$

Also A is given by Eq. Eq. 2.2.13, or equivalently, Eq. 2.2.17 and B is given by Eq. 2.2.14, or equivalently, Eq. 2.2.18, but the van der Waals coefficients have different values; i.e., $\Omega_a = 0.45724$ and $\Omega_b = 0.00778$.

The compressibility factor satisfies the following cubic polynomial:

$$Z^3 - (1 - B)Z^2 + (A - 3B^2 - 2B)Z - (AB - B^2 - B^3) = 0. \quad (2.2.24)$$

For both the Soave-Redlich-Kwong method and the Peng-Robinson method, solving the cubic for the compressibility factor would yield three values of Z in the two-phase region. The largest value of Z represents the Z - factor for the vapor phase, the smallest value is the Z - factor the liquid phase the intermediate root is ignored.

2.2.1.f Schmidt-Wenzel (SW)

The final equation considered is due to Schmidt and Wenzel. Schmidt and Wenzel²² noted the shortcomings of the Soave-Redlich-Kwong and Peng-Robinson equations to predict more accurate densities of the saturated liquids and the critical volumes. They suggested the following equation, where the denominator V^2 in the attraction term of the original van der Waals equation (Eq. 2.2.2) is replaced by a quadratic expression in volume; i.e.,

$$p = \frac{RT}{(V - b)} - \frac{a}{(V^2 + UV + Wb^2)}. \quad (2.2.25)$$

Here, the parameters U and W are independent of temperature, and are related to the acentric factor, ω , as follows,

$$U = 1 + 3\omega \quad (2.2.26)$$

and

$$W = -3\omega. \quad (2.2.27)$$

In Eq. 2.2.25, the terms a and b are defined by Eqs. 2.2.12 and 2.2.11, respectively. For subcritical temperatures, the function α is given by

$$\alpha = \left[1 + k \left(1 - \sqrt{T_r}\right)\right]^2, \quad T < T_c \quad (2.2.28a)$$

where

$$k = \begin{cases} k_1, & \text{if } \omega \leq 0.4, \\ k_2, & \text{if } \omega \geq 0.55, \\ \left(\frac{\omega-0.4}{0.15}\right) k_1 + \left(\frac{0.55-\omega}{0.15}\right) k_2, & \text{if } 0.4 < \omega < 0.55, \end{cases}$$

with

$$k_1 = k_0 + \left(\frac{1}{70}\right) (5T_r - 3k_0 - 1)^2,$$

$$k_2 = k_0 + 0.71 (T_r - 0.779)^2,$$

$$k_0 = \begin{cases} 0.465 + 1.347\omega - 0.528\omega^2, & \text{if } \omega \leq 0.3671, \\ 0.5361 + 0.9593\omega, & \text{if } \omega > 0.3671. \end{cases}$$

For supercritical temperatures, α is given by

$$\alpha = 1.0 - (0.4774 + 1.328\omega) \ln T_r, \quad T > T_c. \quad (2.2.28b)$$

Here T_r is the reduced temperature and ω is the acentric factor of the component considered.

The compressibility factor is represented by the following cubic polynomial

$$Z^3 - (B + 1 - UB)Z^2 + (A - UB - UB^2 + WB^2)Z - (AB + WB^2 + WB^3) = 0, \quad (2.2.29)$$

Schmidt and Wenzel²² use the parameters A and B given by Eqs. 2.2.17 and 2.2.18, respectively, but treat the coefficients Ω_a and Ω_b as functions of the component acentric factor; i.e., for each given value of ω , the cubic

$$(6\omega + 1)\beta_c^3 + 3\beta_c^2 + 3\beta_c - 1 = 0 \quad (2.2.30a)$$

is solved for β_c . If an iterative method (such as Newton-Raphson) is used to solve this cubic, then an initial guess is provided by

$$\beta_c = 0.25989 - 0.0217\omega + 0.00375\omega^2. \quad (2.2.30b)$$

The smallest root of Eq. 2.2.30a is used to compute an intermediary parameter ξ_c via

$$\xi_c = \frac{1}{3(1 + \beta_c\omega)}. \quad (2.2.31)$$

Finally, Ω_a and Ω_b are given by the following expressions:

$$\Omega_a = [1 - \xi_c(1 - \beta_c)]^3 \quad (2.2.32)$$

and

$$\Omega_b = \beta_c\xi_c. \quad (2.2.33)$$

With Ω_a and Ω_b obtained from Eqs. 2.2.32 and 2.2.33, respectively, Eqs. 2.2.10 through 2.2.15 and Eqs. 2.2.17 and 2.2.18 still apply.

2.2.2 Mixtures

The utility of an equation of state is greatly increased when it can be applied to mixtures of pure compounds. Essentially all pure-component equations of state can be applied to mixtures; the difficulty in their application lies in defining rules to obtain mixture parameters which account for the mixture composition. This is achieved by writing the parameters a and b in each equation of state in terms of other parameters involving the composition of the pure compounds which make up the mixture. These parameters are determined via some "mixing rules" which account for interaction between compounds in the mixture.

To begin, we note that Eqs. 2.2.10 - 2.2.12 apply for any pure component i . To emphasize this, we record these equations as

$$a_{c,i} = \Omega_{a,i} \frac{R^2 T_{c,i}^2}{p_{c,i}}, \quad 1 \leq i \leq N_c, \quad (2.2.34)$$

$$b_i = \Omega_{b,i} \frac{RT_{c,i}}{p_{c,i}}, \quad 1 \leq i \leq N_c \quad (2.2.35)$$

and

$$a_i = a_{c,i} \alpha_i, \quad 1 \leq i \leq N_c, \quad (2.2.36)$$

where the subscript i refers to component i and N_c is the number of components in the mixture under consideration. We have also allowed the van der Waals coefficients $\Omega_{a,i}$ and $\Omega_{b,i}$ to vary with i , although in most cases $\Omega_{a,i}$ and $\Omega_{b,i}$ are independent of i ; i.e., independent of temperature, pressure and composition. The parameter, α_i , and acentric factor, ω_i , may also vary from component to component. We summarize the proper equations for each of these parameters for each equation of state later.

For the van der Waals equation of state, Lohrenz (1881) and Berthelot (1898) (see Refs. 29 and 30) assumed that Eq. 2.2.2 is valid for mixtures provided the parameters a and b are replaced by the expressions:

$$a_m = \sum_{i=1}^{N_c} \sum_{j=1}^{N_c} x_{i,m} x_{j,m} \sqrt{a_i a_j}, \quad (2.2.37)$$

$$b_m = \sum_{i=1}^{N_c} x_{i,m} b_i. \quad (2.2.38)$$

Here a_i and b_i are defined by Eqs. 2.2.36 and 2.2.35, respectively, and $\{x_{i,m}\}_{i=1}^{N_c}$ is the mole fraction composition of the component i in phase m in the mixture.

Similar to the van der Waals equation, the equations of state considered in this work, (i.e., Redlich-Kwong, Zudkevitch-Joffe-Redlich-Kwong, Soave-Redlich-Kwong, Peng - Robinson and Schmidt-Wenzel) contain only two basic parameters a and b ; however, other equations of state contain more than two parameters in order to be more representative of the data considered.

For mixtures, Redlich and Kwong suggested the same mixing rules as for the van der Waals equation, i.e. Eqs. 2.2.37 and 2.2.38, where a_i and b_i are given by Eqs. 2.2.36 and 2.2.35, respectively.

Later, Zudkevitch and Joffe¹⁶ modified these mixing rules by introducing a new parameter $k_{i,j}$, which represents the deviation of $\sqrt{a_i a_j}$ from the classical geometric mean assumption; thus Eq. 2.2.37 becomes

$$a_m = \sum_{i=1}^{N_c} \sum_{j=1}^{N_c} (1 - k_{i,j}) x_{i,m} x_{j,m} \sqrt{a_i a_j}. \quad (2.2.39)$$

With this modification, the Redlich-Kwong EOS is called the Zudkevitch-Joffe-Redlich-Kwong (ZJRK) EOS. Note that if we set $k_{i,j} = 0, 1 \leq i, j \leq N_c$, Eq. 2.2.39 reduces to Eq. 2.2.37.

The term $k_{i,j}$ is called the binary interaction parameter that is specific to the i - j binary and is assumed to be independent of the composition, system pressure or system temperature. It is obtained from experimental data on each i - j binary. It is used in most multicomponent mixtures under the assumption that higher order interactions (e.g. between j , k , and l for ternary systems) are negligible. Most equations developed in recent years, and all those considered in this work, take the binary interaction parameter into account. While $k_{i,j}$ is a small number, the results obtained from an EOS are extremely sensitive to the value used for $k_{i,j}$ (see Ref. 30). In all cases, $k_{i,i}$ is taken to be zero. Note that Eq. 2.2.39 applies to the Soave-Redlich-Kwong, Peng-Robinson and Schmidt-Wenzel equations of state.

Recall that for the Redlich-Kwong and Soave-Redlich-Kwong equations of state, $\Omega_a = 0.4274802327$ and $\Omega_b = 0.08664035$ and are independent of temperature, pressure, composition, and individual component. Zudkevitch and Joffe¹⁶ showed that experimental data could be matched better by using different values of $\Omega_{a,i}$ and $\Omega_{b,i}$ for each component. These values depend only on the temperature. They developed a method of computing $\Omega_{a,i}$ and $\Omega_{b,i}$ for each component i at a given temperature using the component's vapor pressure, saturated liquid density and Lyckman's fugacity coefficient. An extensive application of the RK EOS to reservoir fluids was made by Yarborough³¹. He considered $\Omega_{a,i}$ and $\Omega_{b,i}$ to be functions of reduced temperature and the acentric factor and used binary interaction parameters developed from laboratory data for the cases he considered.

For the ZJRK EOS, our package offers the flexibility to input the $\Omega_{a,i}$'s and $\Omega_{b,i}$'s as data or to evaluate them using a method reported by Coats⁷ that we present in Appendix B.

2.2.2.a Redlich-Kwong: Mixtures.

The RK EOS is

$$p = \frac{RT}{V_m - b_m} - \frac{a_m}{V_m(V_m + b_m)}, \quad (2.2.40)$$

where a_m and b_m are given by Eqs. 2.2.37 and 2.2.38, respectively, and Eqs. 2.2.34 through 2.2.36 still apply. Also

$$\Omega_{a,i} = 0.42748, \quad 1 \leq i \leq N_c, \quad (2.2.41a)$$

$$\Omega_{b,i} = 0.08664, \quad 1 \leq i \leq N_c \quad (2.2.41b)$$

and

$$\alpha_i = \frac{1}{\sqrt{T_{r,i}}}, \quad 1 \leq i \leq N_c, \quad (2.2.42)$$

where $T_{r,i}$ is the reduced temperature for component i , i.e., $T_{r,i} = T/T_{c,i}$.

The Z factor satisfies the cubic polynomial

$$Z_m^3 - Z_m^2 - (B_m^2 + B_m - A_m) Z_m - A_m B_m = 0, \quad (2.2.43)$$

where

$$A_m = \frac{a_m p}{R^2 T^2} \quad (2.2.44)$$

and

$$B_m = \frac{b_m p}{RT}. \quad (2.2.45)$$

2.2.2.b Zudkevitch-Joffe-Redlich-Kwong; Mixtures.

For the ZJRK EOS, Eqs. 2.2.40 - 2.2.45 apply provided we define a_m by Eq. 2.2.39 instead of Eq. 2.2.37. In addition the van der Waals coefficients defined in Eqs. 2.2.41a and 2.2.41b are allowed to vary with component i .

2.2.2.c Soave-Redlich-Kwong; Mixtures.

All equations for the SRK EOS are identical to those for the RK EOS discussed in the preceding subsection provided we define

$$\alpha_i = \left[1 + (0.48508 + 1.55171\omega_i - 0.15613\omega_i^2) (1 - \sqrt{T_{r,i}}) \right]^2, \quad (2.2.46)$$

and use the ZJRK EOS mixing rules, i.e., Eqs. 2.2.38 and 2.2.39.

2.2.2.d Peng-Robinson; Mixtures.

The PR EOS is given by

$$p = \frac{RT}{V_m - b_m} - \frac{a_m}{V_m(V_m + b_m) + b_m(V_m - b_m)}, \quad (2.2.47)$$

where a_m and b_m are given by Eqs. 2.2.39 and 2.2.38, respectively, and Eqs. 2.2.34 - 2.2.36 apply. Also

$$\Omega_{a,i} = 0.45724, \quad 1 \leq i \leq N_c, \quad (2.2.48a)$$

$$\Omega_{b,i} = 0.00778, \quad 1 \leq i \leq N_c \quad (2.2.48b)$$

and

$$\alpha_i = \left[1 + (0.37464 + 1.54226\omega_i - 0.26992\omega_i^2) (1 - \sqrt{T_{r,i}}) \right]^2. \quad (2.2.49)$$

The Z factor satisfies the cubic polynomial

$$Z_m^3 - (1 - B_m) Z_m^2 + (A_m - 3B_m^2 - 2B_m) Z_m - (A_m B_m - B_m^2 - B_m^3) = 0, \quad (2.2.50)$$

where A_m and B_m are given by Eqs. 2.2.44 and 2.2.45, respectively.

2.2.2.e Schmidt-Wenzel: Mixtures.

The SW EOS is given by

$$p = \frac{RT}{(V_m - b_m)} - \frac{a_m}{(V_m^2 + UV_m + Wb_m^2)}, \quad (2.2.51)$$

where a_m and b_m are given by Eqs. 2.2.39 and 2.2.38, respectively, and Eqs. 2.2.34 - 2.2.36 apply provided we use α_i defined by Eqs. 2.2.28a and 2.2.28b. Also U and W are defined as

$$U = 1 + 3\omega_{mix} \quad (2.2.52)$$

and

$$W = -3\omega_{mix}. \quad (2.2.53)$$

Here, the mixing acentric factor, ω_{mix} , is defined as

$$\omega_{mix} = \frac{\sum_{i=1}^{N_c} \omega_i x_{i,m} b_i^{0.7}}{\sum_{i=1}^{N_c} x_{i,m} b_i^{0.7}}. \quad (2.2.54)$$

The Z factor satisfies the cubic polynomial

$$Z_m^3 - (B_m + 1 - UB_m) Z_m^2 + (A_m - UB_m - UB_m^2 + WB_m^2) Z_m - (A_m B_m + WB_m^2 + WB_m^3) = 0, \quad (2.2.55)$$

where A_m and B_m are given by Eqs. 2.2.44 and 2.2.45, respectively, with the coefficients $\Omega_{a,i}$ and $\Omega_{b,i}$ evaluated as functions of the component acentric factor via Eqs. 2.2.32 and 2.2.33, respectively.

2.2.2.f Generalized EOS; Mixtures.

A generalized equation of state which includes the SW (Schmidt-Wenzel), PR (Peng-Robinson), SRK (Soave-Redlich-Kwong), ZJRK (Zudkevitch-Joffe-Redlich-Kwong) and RK (Redlich-Kwong) equations of state for phase m is written as

$$p = \frac{RT}{(V_m - b_m)} - \frac{a_m}{(V_m^2 + Ub_mV_m + Wb_m^2)}, \quad (2.2.56)$$

where b_m is given by Eq. 2.2.38. For the RK EOS, a_m is defined by Eq. 2.2.37 and for the other remaining four equations, it is given by Eq. 2.2.39. Eqs. 2.2.34 - 2.2.36 apply for all EOS with α_i defined by Eqs. 2.2.42, 2.2.46, 2.2.49 and 2.2.28a - 2.2.28b, for the RK and ZJRK, SRK, PR and SW EOS, respectively.

Note that the RK, ZJRK, SRK and PR equations are special forms of the SW EOS. For the PR EOS, $U = 2$ and $W = -1$, and for the RK, ZJRK and SRK EOS, $U = 1$ and $W = 0$. This implies that $\omega_{mix} = \frac{1}{3}$ for the PR EOS and $\omega_{mix} = 0$ for the RK, ZJRK and SRK EOS.

Written as a cubic equation in Z_m , the generalized form of the cubic equation follows Eq. 2.2.55 where A_m and B_m are given by Eqs. 2.2.44 and 2.2.45, respectively, with the coefficients $\Omega_{a,i}$ and $\Omega_{b,i}$ depending on the EOS used; i.e., we use Eqs. 2.2.41a - 2.2.41b for the RK and SRK EOS; we evaluate both coefficients as unique functions of temperature for each component i for the ZJRK EOS; we apply Eqs. 2.2.48a - 2.2.48b for the PR EOS and for the SW EOS, $\Omega_{a,i}$ and $\Omega_{b,i}$ are evaluated as functions of the component acentric factor via Eqs. 2.2.32 and 2.2.33, respectively.

2.3 Equilibrium and Fugacity Functions

We now focus our attention on the case where multiple phases coexist at a given pressure and temperature. Our objective in this section will be to define useful mathematical relationships which describe the condition of thermodynamic equilibrium between the phases. Note that throughout this work, multiple phases are assumed to coexist only under the constraint of thermodynamic equilibrium.

Chemical potentials play an important role in defining equilibrium states. Just as the temperature can be looked upon as “potential” for heat flux and the pressure as “potential” for volume changes, the chemical potential can be looked upon as “potential” for the flux of chemical species. The chemical potential provides the force not only for the flow of matter from point to point, but also for its changes of phase and for chemical reactions. At equilibrium, chemical potentials are equal in all phases for multiphase systems so it is desirable to calculate such chemical potentials. However, there are some drawbacks to this function. First, the numerical value of any chemical potential can only be determined within an arbitrary constant. Second, chemical potentials monotonically decrease to negative infinity when the system pressure decreases. Third, for a low concentration of a particular component in a mixture, the chemical potential becomes negatively infinite. For these reasons, a new function, the fugacity, was introduced. This new function may be employed instead of the chemical potential to define phase equilibrium and other properties that are not relevant to this discussion. The major advantages are that it can be determined numerically and is a well-behaved function at both low pressures and/or small concentrations.

An explicit expression for the fugacity which can be evaluated numerically can be derived from any equation of state. Since an equation of state is of the form $p = f(V, T, N)$, where N is the number of moles, the most appropriate energy function to be used would be the Helmholtz energy function since the basis for this function is the set of independent variables (V, T, N) . By using the energy departure concept (which measures the difference between the property in the real state and

in an ideal gas state at the same temperature), we would finally obtain the following relationship for the fugacity of component i in phase m of a mixture, $f_{i,m}$ as

$$RT \ln \left(\frac{f_{i,m}}{px_{i,m}} \right) = - \int_{\infty}^{V_m} \left(\frac{\partial p}{\partial N_{i,m}} - \frac{RT}{V_m} \right) dV_m - RT \ln \frac{V^*}{V_m}, \quad (2.3.1)$$

where V^* is the ideal gas volume which is determined by

$$V^* = \frac{NRT}{p}, \quad (2.3.2)$$

and V_m is the total volume in ft^3 , of phase m given by

$$V_m = Z_m \frac{NRT}{p}. \quad (2.3.3)$$

In the above equations, $N_{i,m}$ is the number of moles of component i in phase m , N is the total number of moles in phase m and Z_m is the compressibility factor of phase m .

Using Eqs. 2.3.2 and 2.3.3 in Eq. 2.3.1 we obtain

$$RT \ln \left(\frac{f_{i,m}}{px_{i,m}} \right) = - \int_{\infty}^{V_m} \left(\frac{\partial p}{\partial N_{i,m}} - \frac{RT}{V_m} \right) dV_m - RT \ln Z_m. \quad (2.3.4)$$

Note that the lower limit of the integral in Eq. 2.3.1 is infinity which represents the ideal state (i.e., low p , infinite V).

Values for the compressibility factors are given by solving the appropriate cubic polynomial. We recall the generalized form of the cubic equation is given by

$$Z_m^3 - (B_m + 1 - UB_m) Z_m^2 + (A_m - UB_m - UB_m^2 + WB_m^2) Z_m - (A_mB_m + WB_m^2 + WB_m^3) = 0, \quad (2.3.5)$$

where U , W depend on the EOS used, and A_m , B_m are given by

$$A_m = \frac{a_m p}{R^2 T^2} \quad (2.3.6)$$

and

$$B_m = \frac{b_m p}{RT}. \quad (2.3.7)$$

The integration in Eq. 2.3.4 can be carried out in the following manner: First, evaluate the partial derivative of pressure with respect to the number of moles of component i from the EOS (Eq. 2.2.56), second, integrate, and finally use the polynomial form (Eq. 2.3.5) and the appropriate mixing rules to obtain a generalized expression of the partial fugacity of component i in the mixture. The resulting expression assumes the following generalized form:

$$\begin{aligned} \ln \left(\frac{f_{i,m}}{p x_{i,m}} \right) = & -\ln(Z_m - B_m) + \frac{b_i}{b_m} (Z_m - 1) \\ & + \frac{A_m}{B_m \sqrt{U^2 - 4W}} \ln \left(\frac{2Z_m + UB_m + B_m \sqrt{U^2 - 4W}}{2Z_m + UB_m - B_m \sqrt{U^2 - 4W}} \right) \\ & \times \left(\frac{b_i}{b_m} - \frac{2}{a_m} \sum_{k=1}^{N_c} x_{k,m} a_{i,k} + 3 \frac{U+2}{U^2 - 4W} \frac{b_i^{0.7}}{\sum_{k=1}^{N_c} x_{k,m} b_k^{0.7}} (\omega_i - \omega) \right) \\ & + \left[\left(1 - \frac{1}{Z_m - B_m} \right) \frac{3}{U^2 - 4W} \frac{b_i^{0.7}}{\sum_{k=1}^{N_c} x_{k,m} b_k^{0.7}} (\omega_i - \omega) \right] \\ & \times (2Z_m + UZ_m + 2WB_m + UB_m). \end{aligned} \quad (2.3.8)$$

Equation (2.3.8) represents the partial fugacity of component i for the SW EOS. It reduces to the PR, SRK and RK cases by setting $\omega_i - \omega = 0$ and by using the appropriate coefficients A_m , B_m , U and W (as discussed in the previous section). This equation will be used throughout the remaining of this work.

2.4 Single-Stage Separation Equations

The condition of thermodynamic equilibrium between coexisting phases is described by the mathematical equations given below.

(i) The overall material balance is given by

$$L + V = 1, \quad (2.4.1)$$

where L is the moles of liquid per mole of fluid mixture and V is the moles of vapor per mole of fluid mixture.

(ii) The component material balance is given by

$$z_i = Lx_i + Vy_i, \quad 1 \leq i \leq N_c, \quad (2.4.2)$$

where $\{z_i\}_{i=1}^{N_c}$ is the mole fraction composition of the initial fluid and $\{x_i\}_{i=1}^{N_c}$ and $\{y_i\}_{i=1}^{N_c}$ are the mole fraction compositions of the liquid and gas phases, respectively, at pressure p and temperature T .

Note that Eq. 2.4.2 shows that z_i moles of component i , when equilibrated, will be distributed as Lx_i moles of component i in the liquid phase and Vy_i moles of component i in the vapor phase.

(iii) The mole fraction constraints are given by the following three equations:

$$\sum_{i=1}^{N_c} z_i = 1, \quad (2.4.3)$$

$$\sum_{i=1}^{N_c} x_i = 1, \quad (2.4.4a)$$

$$\sum_{i=1}^{N_c} y_i = 1. \quad (2.4.4b)$$

Note that both of equations 2.4.4a and 2.4.4b cannot be used simultaneously because, given one, the second may be derived by combining the given equation with Eqs. 2.4.1 and 2.4.2 and 2.4.3.

(iv) Finally, the criterion for thermodynamic equilibrium is

$$f_{i,L} = f_{i,V}, \quad 1 \leq i \leq N_c, \quad (2.4.5)$$

where $f_{i,L}$ is the fugacity of component i in the liquid phase at pressure p and temperature T and $f_{i,V}$ is the fugacity of component i in the vapor phase at pressure p and temperature T .

We have chosen to use Eq. 2.4.5 to develop a criterion for thermodynamic equilibrium since fugacities are easily obtainable as functions of pressure, temperature and composition from an equation of state. This criterion of thermodynamic equilibrium can be replaced by the use of the equilibrium ratios, K -values given by

$$K_i = \frac{y_i}{x_i}, \quad 1 \leq i \leq N_c, \quad (2.4.6)$$

where the K -values are tabulated. We will use Eq. 2.4.6 only to obtain initial estimates needed for the solution method. The equation of state approach (and hence Eq. 2.4.5) is more desirable than the K -values method because the latter becomes unstable near the critical region.

Equations 2.4.1, 2.4.2, one of Eqs. 2.4.4a and 2.4.4b, and Eq. 2.4.5 represent a system of $(2N_c + 2)$ equations in the $(2N_c + 2)$ unknowns L , V , $\{x_i\}_{i=1}^{N_c}$, and $\{y_i\}_{i=1}^{N_c}$. Note that these equations apply at a given pressure p , and temperature T . As discussed later, we will need an additional modification in order to solve for saturation pressure.

Our phase package has the option of using the special version of the commonly known successive substitution method or the more robust iterative method known as the Minimum-Variable Newton-Raphson scheme (MVNR) (presented by Fussell and Yanosik²⁴). In the following, we present both methods in detail.

2.5 Successive Substitution Method

Eqs. 2.4.1, 2.4.2, 2.4.3 and 2.4.6 can be combined to yield the following equations:

$$x_i = \frac{z_i}{1 + V(K_i - 1)}, \quad 1 \leq i \leq N_c, \quad (2.5.1)$$

$$y_i = \frac{K_i z_i}{1 + V(K_i - 1)}, \quad 1 \leq i \leq N_c \quad (2.5.2)$$

and

$$\Gamma(V) = \sum_{i=1}^{N_c} \frac{z_i(K_i - 1)}{1 + V(K_i - 1)} = 0. \quad (2.5.3)$$

The criterion for the thermodynamic equilibrium (Eq. 2.4.5) can be rewritten as

$$F_i = \frac{f_{i,L}}{f_{i,V}} = 1, \quad 1 \leq i \leq N_c. \quad (2.5.4)$$

It is easy to see that the equilibrium K - values are related to the fugacities via the following equation:

$$K_i = \frac{(f_{i,L}/x_i p)}{(f_{i,V}/y_i p)} = F_i \frac{y_i}{x_i}, \quad 1 \leq i \leq N_c. \quad (2.5.5)$$

We present a discussion on the behavior of the function given by Eq. 2.5.3. The derivative of Γ is given by

$$\frac{d\Gamma}{dV} = - \sum_{i=1}^{N_c} \frac{z_i(K_i - 1)^2}{(1 + V(K_i - 1))^2}. \quad (2.5.6)$$

The preceding equation indicates that the derivative is always negative, and hence, the function Γ is monotonically decreasing with asymptotes given by

$$V = \frac{1}{(1 - K_i)}, \quad 1 \leq i \leq N_c. \quad (2.5.7)$$

The set of K - values has a maximum and a minimum denoted as K_l and K_s , respectively. For the function $\Gamma(V)$ to have a root in $[0,1]$, it is necessary that $[0,1]$ be a subinterval of $[\frac{1}{(1-K_l)}, \frac{1}{(1-K_s)}]$ (See Fig. 2.2). Following Nghiem et al.²³, three cases are possible:

Case (1) $\Gamma(0) \geq 0$ and $\Gamma(1) \leq 0$. We use Newton-Raphson method or the bisection method to determine the root of Eq. 2.5.3 in $(0,1)$. This case occurs when the system is two-phase.

Case (2) $\Gamma(0) < 0$. The root is negative; Nghiem et al. suggest that we set V equal to 0.5 at the first iteration then to 0.0 at subsequent iterations.

Case (3) $\Gamma(1) > 0$. The root is greater than unity. Again, we set V equal to 0.5 at the first iteration but to 1.0 at subsequent iterations.

The last two cases represent a single-phase system, in which the F_i ratios could converge to a number different than one.

We now describe the method of successive substitution assuming that values of p , T and $\{z_i\}_{i=1}^{N_c}$ are given.

Step (1) Use a set of K - values obtained from Eq. 2.5.5 to solve Eq. 2.5.4 for V , then use Eqs. 2.5.1 and 2.5.2 to obtain the sets $\{x_i\}_{i=1}^{N_c}$ and $\{y_i\}_{i=1}^{N_c}$. At the first iteration, the K - values are given by the following relationship

$$K_i = \frac{p_{c,i} \exp \left[5.37 (1 + \omega_i) \left(1 - \frac{T_{c,i}}{T} \right) \right]}{p}. \quad (2.5.8)$$

Step (2) Update the fugacities using Eq. 2.3.8 and check the convergence criterion

$$\sum_{i=1}^{N_c} (F_i - 1)^2 \leq \epsilon, \quad (2.5.9)$$

where ϵ is a small tolerance. If Eq. 2.5.9 is satisfied, convergence has been obtained, if not repeat Step (1). Typically, we use $\epsilon = 10^{-4}$ in Eq. 2.5.9.

Contrary to the classical successive substitution method, this special version can detect the single-phase region without having to compute the saturation pressure. This method is appealing because of its simplicity, but unfortunately, like the

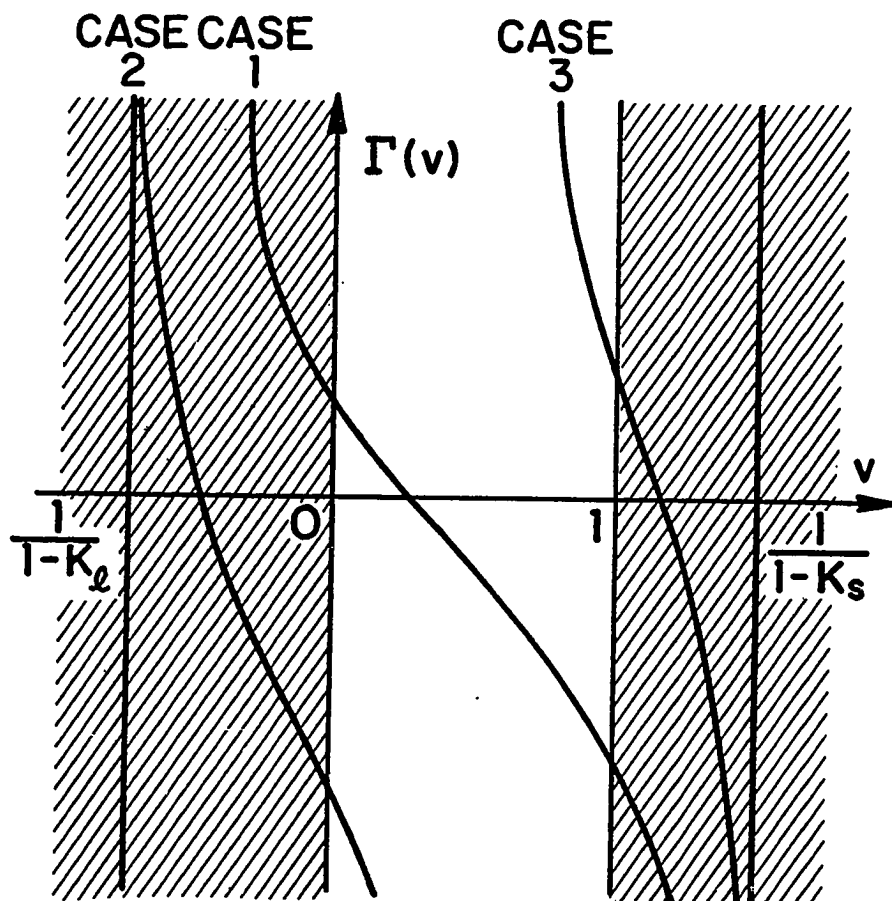


Fig. 2.2 - Conditions for the existence of a solution of $\Gamma(V)$ in $[0, 1]$ (Ref. 23).

classical version, it demonstrates poor convergence or no convergence at all near the critical region.

Our package takes advantage of this successive substitution method to detect the single-phase region and to provide an initial guess to a more robust algorithm that we will describe in the next section.

2.6 Minimum Variable Newton-Raphson Method(MVNR)

2.6.1 Overall Scheme

With the partial fugacities computed from the equations of state, the single-stage separation equations (Eqs. 2.4.1, 2.4.2, 2.4.4a or 2.4.4b and 2.4.5) form a non-linear system of $(2N_c + 2)$ equations in the $(2N_c + 2)$ unknowns L , V , $\{x_i\}_{i=1}^{N_c}$, and $\{y_i\}_{i=1}^{N_c}$.

The idea behind the MVNR is to use some of the equations to eliminate the maximum number of variables in the remaining equations. Then the remaining equations are used to update the uneliminated variables via the multidimensional Newton - Raphson method.

We form two sets of variables, a set of dependent variables and a set of iteration variables. We solve for each of the dependent variables using one of the equations in the total system, one equation for each dependent variable. Following Fussell and Yanosik²⁴, we call such equations the defining equations. Then we use the remaining equations as error equations for the Newton-Raphson iteration. The overall scheme of the MVNR is as follows:

Step (1): - Pick the iteration variables and assign initial values to them as discussed later.

Step (2): - Evaluate the dependent variables from the defining equations.

Step (3): - Use the values from step (1) and (2) to compute the error from the error equations. If the error is within a small tolerance, then the scheme has converged. Otherwise, use the multidimensional Newton-Raphson method to update the iteration variables, then repeat step (2).

We will apply this procedure both to the detection of the boundary region (i.e., saturation pressure computation) and to the performance of a flash calculation. We begin by describing how the above scheme is applied to the computation of saturation pressure and forming phase composition.

Following Fussell and Yanosik²⁴, we will refer to the scheme as the $p-x$ iteration if the saturation point is a dew point or as the $p-y$ iteration if the saturation point is a bubble point. Both iteration procedures are analogous.

2.6.2 Dew Point Computation ($p - x$ iteration)

At a dew point, Eq. 2.4.1 reduces to $V = 1$, since the number of moles of liquid is infinitesimal. This infinitesimal quantity of liquid mole fraction composition $\{x_i\}_{i=1}^{N_c}$, is in equilibrium with the vapor phase composition $\{y_i\}_{i=1}^{N_c}$. Since the amount of forming liquid is negligible, the variation of the vapor mole fraction composition as the pressure changes from just above the dew point to the dew point must also be negligible. Therefore, when $p \geq p_{dew}$, Eq. 2.4.2 becomes

$$y_i = z_i, \quad 1 \leq i \leq N_c. \quad (2.6.1)$$

Note that z_i is the mole fraction composition of the initial fluid in place which is known. Thus the only unknowns left to solve for are p_{dew} and $\{x_i\}_{i=1}^{N_c}$, that is $(N_c + 1)$ unknowns. These unknowns are the prime candidates for the iteration variables required by the MVNR method (Step (1)). The remaining equations not used so far are the N_c equilibrium equations (Eq. 2.4.5) and the constraint equation (Eq. 2.4.4a) which should constitute the error equations needed for the update. However, Fussell and Yanosik²⁴ introduced the following equation to replace Eq. 2.4.4a:

$$p_{dew} = \sum_{i=1}^{N_c} \frac{f_{i,V}}{\psi_{i,L}}, \quad (2.6.2)$$

where

$$\psi_{i,L} = \frac{f_{i,L}}{px_i}. \quad (2.6.3)$$

We can see that at equilibrium (i.e., at convergence) $p = p_{dew}$. (Later, contrary to Fussell and Yanosik²⁴, Coats⁷ used Eq. 2.4.4a and claimed he obtained faster convergence. In this work, we chose to use the original idea, that is, Eqs. 2.6.2 and 2.6.3. Note that step (2) is not needed here since the dependent variables L , V , and $\{y_i\}_{i=1}^{N_c}$ are already known.

The error equations are defined as follows:

(i) The residual of the thermodynamic phase equilibrium equation:

$$E_i = f_{i,L} - f_{i,V}, \quad 1 \leq i \leq N_c, \quad (2.6.4)$$

(ii) The additional error equation as defined by Fussell and Yanosik²⁴:

$$E_{N_c+1} = p - \sum_{i=1}^{N_c} \frac{f_{i,V}}{f_{i,L}} p x_i. \quad (2.6.5)$$

The $(N_c + 1)$ equations given by Eqs. 2.6.4 and 2.6.5 can be solved by Newton's method which takes the form:

$$J^k (\mathbf{R}^{k+1} - \mathbf{R}^k) = -\mathbf{E}^k. \quad (2.6.6)$$

Here, the superscript k represents the old iteration level, J is the Jacobian matrix, \mathbf{E} is the residual vector as defined in Eqs. 2.6.4 and 2.6.5. This set of simultaneous linear equations is solved for the elements of the vector $\Delta \mathbf{R}^{k+1} = \mathbf{R}^{k+1} - \mathbf{R}^k$ and then $\mathbf{R}^{k+1} = \mathbf{R}^k + \Delta \mathbf{R}^{k+1}$ where

$$\mathbf{R}^{k+1} = (x_1^{k+1}, x_2^{k+1}, \dots, x_{N_c}^{k+1}, p^{k+1})^t. \quad (2.6.7)$$

The Jacobian matrix is ordered as

$$J = \begin{pmatrix} \frac{\partial E_1}{\partial x_1} & \frac{\partial E_1}{\partial x_2} & \cdots & \frac{\partial E_1}{\partial x_{N_c}} & \frac{\partial E_1}{\partial p} \\ \frac{\partial E_2}{\partial x_1} & \frac{\partial E_2}{\partial x_2} & \cdots & \frac{\partial E_2}{\partial x_{N_c}} & \frac{\partial E_2}{\partial p} \\ \vdots & \vdots & \ddots & \ddots & \vdots \\ \frac{\partial E_{N_c}}{\partial x_1} & \frac{\partial E_{N_c}}{\partial x_2} & \cdots & \frac{\partial E_{N_c}}{\partial x_{N_c}} & \frac{\partial E_{N_c}}{\partial p} \\ \frac{\partial E_{N_c+1}}{\partial x_1} & \frac{\partial E_{N_c+1}}{\partial x_2} & \cdots & \frac{\partial E_{N_c+1}}{\partial x_{N_c}} & \frac{\partial E_{N_c+1}}{\partial p} \end{pmatrix} \quad (2.6.8)$$

The elements of the Jacobian are evaluated as

$$\frac{\partial E_i}{\partial x_j} = \frac{\partial f_{i,L}}{\partial x_j}, \quad 1 \leq i, j \leq N_c, \quad (2.6.9)$$

$$\frac{\partial E_i}{\partial p} = \frac{\partial f_{i,L}}{\partial p} - \frac{\partial f_{i,V}}{\partial p}, \quad 1 \leq i \leq N_c, \quad (2.6.10)$$

$$\frac{\partial E_{N_c+1}}{\partial x_j} = -\frac{f_{j,V}}{f_{j,L}} p + \sum_{i=1}^{N_c} p x_i \frac{f_{i,V}}{f_{i,L}^2} \frac{\partial f_{i,L}}{\partial x_j}, \quad 1 \leq j \leq N_c, \quad (2.6.11)$$

$$\frac{\partial E_{N_c+1}}{\partial p} = 1 - \sum_{i=1}^{N_c} \frac{p x_i}{f_{i,L}} \left(\frac{\partial f_{i,V}}{\partial p} + \frac{f_{i,V}}{p} - \frac{f_{i,V}}{f_{i,L}} \frac{\partial f_{i,L}}{\partial p} \right). \quad (2.6.12a)$$

The convergence is determined from the Euclidean norm of the E'_i 's, i.e.,

$$\sqrt{\sum_{i=1}^{N_c+1} E_i'^2} \leq \epsilon,$$

where ϵ is some small tolerance. Typically, we use $\epsilon = 10^{-4}$

If the norm is less than the error tolerance, the sequence is converged and the iteration ends. Methods for obtaining initial estimates for the $p-x$ iteration and the $p-y$ iteration presented immediately below are discussed later in Section 2.6.5.

2.6.3 Bubble Point Computation ($p-y$ iteration)

The logic behind the $p-x$ iteration is valid for the $p-y$ iteration. At the bubble point pressure, $L = 1$, $V = 0$ and $x_i = z_i$, $1 \leq i \leq N_c$, so that the set $\{L, V, \{x_i\}_{i=1}^{N_c}\}$ is known and therefore selected to be the set of dependent variables, whereas the set $\{p, \{y_i\}_{i=1}^{N_c}\}$ becomes the set of iteration variables. The equations derived for the dew point calculation will be used provided we interchange L and V , x_i and y_i , $f_{i,L}$ and $f_{i,V}$ in Eqs. 2.6.2, 2.6.3, 2.6.7 and 2.6.9 - 2.6.12a. For example, Eq. 2.6.12a is replaced by

$$\frac{\partial E_{N_c+1}}{\partial p} = 1 - \sum_{i=1}^{N_c} \frac{p y_i}{f_{i,V}} \left(\frac{\partial f_{i,L}}{\partial p} + \frac{f_{i,L}}{p} - \frac{f_{i,L}}{f_{i,V}} \frac{\partial f_{i,V}}{\partial p} \right). \quad (2.6.12b)$$

Initial estimates of p and $\{x_i\}_{i=1}^{N_c}$ for the $p-x$ iteration and of p and $\{y_i\}_{i=1}^{N_c}$ for the $p-y$ iteration are required. We will present the different methods of obtaining these values after we discuss the MVNR for pressures below the saturation pressure.

2.6.4 Flash Calculations ($p < p_{sat}$)

Once the saturation pressure is known, we proceed by chosen pressure increments along the fixed isotherm through the two-phase region. At each step, the pressure p and temperature T are both fixed and the overall composition is assumed to be known and fixed. The set of unknowns is $\{ L, V, \{x_i\}_{i=1}^{N_c}, \{y_i\}_{i=1}^{N_c} \}$. Again, we need to divide this set into two sets, a set of iteration variables and a set of dependent variables. Two sets of iteration variables that satisfy the MVNR criteria would be $\{ L, \{x_i\}_{i=1}^{N_c} \}$ and $\{ V, \{y_i\}_{i=1}^{N_c} \}$. The MVNR that uses the first set will be referred to as the $L - x$ iteration, and the MVNR that uses the second set will be referred to as the $V - y$ iteration. The $V - y$ iteration is used for a fluid system that is predominantly liquid (i.e., when $L > V$) and the $L - x$ iteration is used for a fluid that is predominantly vapor (i.e., when $V > L$). The initial estimates for either the $L - x$ or the $V - y$ iteration are the values of the variables calculated at the previous pressure. The initial estimates for the first two-phase calculations are the values obtained from the saturation pressure computation. Due to the symmetry of the two cases, we describe only the procedure for the $V - y$ iteration.

Recall that the basic objective of the MVNR is to minimize the set of iteration variables. Following Fussell and Yanosik²⁴, we use the constraint equation (Eq. 2.4.4b) on the vapor mole fraction composition so that

$$y_1 = 1 - \sum_{i=2}^{N_c} y_i. \quad (2.6.13)$$

Then the set of iteration variables is reduced by one and the set of iteration variables becomes $\{ V, \{y_i\}_{i=2}^{N_c} \}$; in this case, Eq. 2.6.13 becomes a defining equation. The overall material balance (Eq. 2.4.1) can be used as a second defining equation, by solving for L ,

$$L = 1 - V. \quad (2.6.14)$$

Finally, the component material balances (Eq. 2.4.2) is equivalent to

$$x_i = \frac{(z_i - Vy_i)}{L}, \quad 1 \leq i \leq N_c. \quad (2.6.15)$$

Eqs. 2.6.13 - 2.6.15 represent the defining equations and the set of dependent variables is $\{ L, y_1, \{x_i\}_{i=1}^{N_c} \}$. The remaining N_c equilibrium equations (Eq. 2.4.5) will be used to define the error equations for the N_c iteration variables as follows

$$E_i = f_{i,L} - f_{i,V}, \quad 1 \leq i \leq N_c. \quad (2.6.16)$$

The N_c equations given by (2.6.16) are solved by Newton's method which takes the form

$$J^k (\mathbf{R}^{k+1} - \mathbf{R}^k) = -\mathbf{E}^k, \quad (2.6.17)$$

where k denotes the iteration level, and J^k is the Jacobian matrix evaluated at the old iterate.

This set of simultaneous linear equations is solved for the elements of the vector $\Delta \mathbf{R}^{k+1} = \mathbf{R}^{k+1} - \mathbf{R}^k$ and then $\mathbf{R}^{k+1} = \mathbf{R}^k + \Delta \mathbf{R}^{k+1}$ where

$$\mathbf{R}^{k+1} = (V, y_2^{k+1}, y_3^{k+1}, \dots, y_{N_c}^{k+1})^t. \quad (2.6.18)$$

The Jacobian matrix is ordered as

$$J = \begin{pmatrix} \frac{\partial E_1}{\partial V} & \frac{\partial E_1}{\partial y_2} & \cdots & \frac{\partial E_1}{\partial y_{N_c}} \\ \frac{\partial E_2}{\partial V} & \frac{\partial E_2}{\partial y_2} & \cdots & \frac{\partial E_2}{\partial y_{N_c}} \\ \vdots & \vdots & \ddots & \vdots \\ \frac{\partial E_{N_c}}{\partial V} & \frac{\partial E_{N_c}}{\partial y_2} & \cdots & \frac{\partial E_{N_c}}{\partial y_{N_c}} \end{pmatrix}, \quad (2.6.19)$$

where the elements of the Jacobian are evaluated as

$$\frac{\partial E_i}{\partial V} = -\frac{1}{L} \sum_{j=2}^{N_c} \frac{\partial f_{i,L}}{\partial x_j} (y_j - x_j), \quad 1 \leq i \leq N_c \quad (2.6.20)$$

and

$$\frac{\partial E_i}{\partial y_j} = -\frac{V}{L} \frac{\partial f_{i,L}}{\partial x_j} - \frac{\partial f_{i,V}}{\partial y_j}, \quad 1 \leq i \leq N_c, \quad 2 \leq j \leq N_c. \quad (2.6.21)$$

Note that Eqs. 2.6.20 and 2.6.21 are obtained by using the following facts:

(i) From the overall material balance,

$$\frac{\partial L}{\partial V} = -1. \quad (2.6.22)$$

(ii) From Eq. 2.6.13,

$$\frac{\partial y_1}{\partial y_j} = -1, \quad 2 \leq j \leq N_c \quad (2.6.23)$$

and

$$\frac{\partial y_i}{\partial y_j} = \delta_{i,j}, \quad 2 \leq i, j \leq N_c, \quad (2.6.24)$$

where $\delta_{i,j}$ is the Kroenecker delta, i.e.,

$$\delta_{i,j} = \begin{cases} 1, & \text{if } i = j, \\ 0, & \text{if } i \neq j. \end{cases}$$

Since z_i is fixed and known (constant overall composition), then

$$\frac{\partial x_i}{\partial V} = \frac{x_i - y_i}{L}, \quad 1 \leq i \leq N_c \quad (2.6.25)$$

and

$$\frac{\partial x_i}{\partial y_j} = -\frac{V}{L} \delta_{i,j}. \quad (2.6.26)$$

For the $L - x$ iteration, the set of iteration variables is $\{ L, \{x_i\}_{i=2}^{N_c} \}$. The elements of the Jacobian will be given by

$$\frac{\partial E_i}{\partial L} = -\frac{1}{V} \sum_{j=2}^{N_c} \frac{\partial f_{i,V}}{\partial y_j} (y_j - x_j), \quad 1 \leq i \leq N_c \quad (2.6.27)$$

and

$$\frac{\partial E_i}{\partial x_j} = \frac{\partial f_{i,L}}{\partial x_j} + \frac{L}{V} \frac{\partial f_{i,V}}{\partial y_j}, \quad 1 \leq i \leq N_c, \quad 2 \leq j \leq N_c \quad (2.6.28)$$

In Appendix C, we provide detailed expressions for the partial derivatives of fugacity with respect to the various independent variables.

2.6.5 Initial estimates

We now describe methods of obtaining initial estimates of saturation pressure and of liquid or vapor compositions, required by the $p - x$ and/or $p - y$ iterations.

For $p - x$ and $p - y$ iterations, we require initial estimates of the saturation pressure, p_{sat} , and the mole fraction composition of the developing vapor phase, i.e., $\{y_i\}_{i=1}^{N_c}$, for $p - y$ iterations, or, the mole fraction composition of the developing phase, $\{y_i\}_{i=1}^{N_c}$, for $p - y$ iterations.

2.6.5.a K - Values Approach

Fussell and Yanosik²⁴ recommend that the single-phase fluid initially in place be flashed at an estimate of the saturation pressure using individual component K - values obtained from the relation known as Wilson's equation, which is derived by integrating the Clausius - Clayperon equation and then using Raoult's law. Wilson's equation is given by

$$K_i = \frac{p_{c,i} \exp \left[5.37 (1 + \omega_i) \left(1 - \frac{T_{c,i}}{T} \right) \right]}{p_{sat}} \quad (2.5.8)$$

The saturation pressure is found by a trial and error iterative method. We flash the overall fluid mixture at the system temperature and an estimated saturation pressure. The flash calculations result in liquid and vapor compositions and hence a value of $K_i = y_i/x_i$. If our estimate of p_{sat} is correct, this value of K_i should be equal to the K_i -value predicted by Eq. 2.5.8. Depending on the iteration used ($p - x$ or $p - y$), the appropriate phase compositions are used as initial estimates of the iteration variables, x_i or y_i . The other phase composition is equal to the composition of the overall fluid mixture (Eq. 2.6.1). However, if the system temperature is at or near the critical temperature, or the initial overall composition is within a few percent of the critical composition, this method becomes quite unstable. Moreover,

it has been observed that this correlation (Eq. 2.5.8) gave unsatisfactory results for fluid systems containing only light components²² such as CH_4 , CO_2 and N_2 .

For this reason, a second method was proposed by Baker and Luks³³. They applied it only to the ZJRK EOS; however, we have successfully applied it to the other equations of state discussed in this work.

2.6.5.b Baker and Luks³³ Approach

Baker and Luks³³ noted the limitations of the K - values approach and presented an alternative method to obtain the needed initial estimates. Their method uses an equation of state, and thus, has the advantage of being consistent with all other calculations.

We define the partial fugacity coefficient in phase m as

$$\psi_{i,m} = \frac{f_{i,m}}{px_{i,m}}, \quad 1 \leq i \leq N_c. \quad (2.6.29)$$

We first consider a bubble point calculation. For a bubble point calculation, the x_i 's are known (equal to z_i 's for the overall fluid mixture in-place) and the vapor phase composition is given by

$$y_i = \frac{(p\psi_{i,L}x_i)}{(p\psi_{i,V})} = \left(\frac{\psi_{i,L}}{\psi_{i,V}} \right) x_i, \quad 1 \leq i \leq N_c \quad (2.6.30a)$$

and

$$x_i = z_i, \quad 1 \leq i \leq N_c. \quad (2.6.30b)$$

The Baker and Luks³³ method involves the following steps:

Step (1): Choose a pressure increment Δp . Baker and Luks³³ suggest using a pressure increment, $100 \leq \Delta p \leq 300$. Also choose an error tolerance, ϵ .

Step (2): First iteration ($k = 1$), pick a very low pressure, e.g., $p^1 = 10$ psia, set $\psi_{i,V} = 1, 1 \leq i \leq N_c$, and evaluate $\psi_{i,L}, 1 \leq i \leq N_c$ from Eq. 2.6.29 with $x_{i,m} = x_i = z_i, 1 \leq i \leq N_c$, then go to step 4.

Step (3): Compute $\psi_{i,V}, 1 \leq i \leq N_c$ and $\psi_{i,L}, 1 \leq i \leq N_c$ from Eq. 2.6.9, i.e.,

$$\psi_{i,V} = \frac{f_{i,V}^k}{p^k y_i^k}, \quad 1 \leq i \leq N_c$$

and

$$\psi_{i,L} = \frac{f_{i,L}^k}{p^k x_i^k}, \quad 1 \leq i \leq N_c.$$

Step (4): Compute y_i^k , $1 \leq i \leq N_c$ from Eq. 2.6.30a.

Step (5): (a) If $\sum_{i=1}^{N_c} y_i^k > 1$ then p^k is less than the saturation pressure and we proceed to step (6). (b) If $\sum_{i=1}^{N_c} y_i^k < 1$ then p^k is greater than the saturation pressure; thus, we replace Δp by $\Delta p/2$ and proceed to step (6).

Step (6): Set $p^{k+1} = p^k + \Delta p$ and $y_i^{k+1} = y_i^k$, $1 \leq i \leq N_c$, then set $k = k + 1$ so that the latest iterates for pressure and vapor mole fractions are denoted by p^k and y_i^k , $1 \leq i \leq N_c$, respectively.

Step (7): Check for convergence. If $\Delta p > \epsilon$, we have not achieved convergence and we go to step (3).

Once the preceding iterative procedure converges, the resulting vapor composition and pressure is then used to start the $p - y$ iteration of the MVNR method.

The preceding algorithm can be easily modified to compute the upper dew point pressure. In this case $y_i = z_i$, $1 \leq i \leq N_c$ at all iterations and at each iteration we must compute an estimate of the liquid mole fraction x_i^k , $1 \leq i \leq N_c$. Also in Step (2), we compute $\psi_{i,V}$, $1 \leq i \leq N_c$ from Eq. 2.6.29, i.e.,

$$\psi_{i,V} = \frac{f_{i,V}}{py_i} = \frac{f_{i,V}}{pz_i}, \quad 1 \leq i \leq N_c,$$

but compute $\psi_{i,L}$ as follows:

$$\psi_{i,L} = \psi_{i,L}^0 \exp \left[Z_L^0 \left(\frac{p}{p_{vp,i}} - 1 \right) \right], \quad (2.6.31)$$

where Z_L^0 is the compressibility factor at the pure component i vapor pressure $p_{vp,i}$ obtained by solving the appropriate equation of state. $\psi_{i,L}^0$ is the pure component partial fugacity coefficient evaluated at the pure component i vapor pressure $p_{vp,i}$, i.e., $\psi_{i,L}^0 = f_{i,L}/p_{vp,i}$.

Once the bubble point or the upper dew point has been found, then we can modify the preceding algorithm to determine the lower dew point as follows:

Case (a): If the upper dew point is known, then in Step (2), set the first pressure iterate, p^1 , equal to the upper dew point pressure and compute $\psi_{i,L}, 1 \leq i \leq N_c$ from Eq. 2.6.29, using the mole fraction composition relative to the upper dew point. Finally, in Step (5), if $\sum_{i=1}^{N_c} x_i^k < 1$ then p^k is less than the saturation pressure and we proceed to step (6). Otherwise, p^k is greater than the saturation pressure; thus we replace Δp by $\Delta p/2$ and proceed to step (6).

Case (b): If the bubble point is known, then in Step (2), set the first pressure iterate, p^1 , equal to the bubble point pressure and compute $\psi_{i,L}, 1 \leq i \leq N_c$ from Eq. 2.6.29, using the mole fraction composition relative to the upper dew point. Finally, in Step (5), if $\sum_{i=1}^{N_c} x_i^k < 1$ then p^k is less than the saturation pressure and we proceed to step (6). Otherwise, p^k is greater than the saturation pressure; thus we replace Δp by $\Delta p/2$ and proceed to step (6).

2.7 Phase Viscosities

We determine phase viscosities following the procedure presented by Lohrenz and Bray²⁵. This procedure applies to both the gas and liquid phases, and a description of the method follows.

The phase viscosities are first calculated at low pressure and subsequently corrected to the system pressure. The correlation reported by Stiel and Thodos²⁸ is employed to calculate the low pressure viscosity, μ_i^* of component i , from the following equations:

$$\mu_i^* \tau_i = \begin{cases} 1.778 \times 10^{-4} \left(94.58 \frac{T}{T_{c,i}} - 1.67 \right)^{\frac{5}{8}}, & \text{if } T > 1.5T_{c,i}; \\ 3.4 \times 10^{-4} \left(\frac{T}{T_{c,i}} \right)^{0.94}, & \text{if } T \leq 1.5T_{c,i}, \end{cases}$$

where $T_{c,i}$ is the critical temperature of component i expressed in $^{\circ}K$, T is the system temperature in $^{\circ}K$ and τ_i is given by

$$\tau_i = \frac{T_{c,i}^{\frac{1}{8}}}{\sqrt{M_i} p_{c,i}^{\frac{2}{3}}}. \quad (2.7.1)$$

Here, the critical pressure $p_{c,i}$ is expressed in atmospheres and M_i denotes the molecular weight of component i .

The Hering and Zipperer²⁷ equation is used to calculate the low pressure mixture viscosity in cp at the system temperature, T ; i.e.,

$$\mu_m^* = \frac{\sum_{i=1}^{N_c} (x_{i,m} \mu_i^* \sqrt{M_i})}{\sum_{i=1}^{N_c} (x_{i,m} \sqrt{M_i})}, \quad (2.7.2)$$

where $x_{i,m}$ is the mole fraction of component i in phase m (liquid or gas).

Jossi, Stiel and Thodos²⁶ developed a relationship between the low pressure viscosity and the viscosity at system pressure, μ_m , in terms of the reduced phase molar density, $\rho_{r,m}$ (lbmoles/ft³) as follows

$$\begin{aligned} [(\mu_m - \mu_m^*) \xi + 10^{-4}]^{\frac{1}{4}} = & 0.1023 + 0.023364 \rho_{r,m} + 0.058533 \rho_{r,m}^2 \\ & - 0.040758 \rho_{r,m}^3 + 0.0093324 \rho_{r,m}^4. \end{aligned} \quad (2.7.3)$$

Here ξ is called the mixture viscosity parameter and is given by

$$\xi = \frac{\left[\sum_{i=1}^{N_c} (x_{i,m} T_{c,i}) \right]^{\frac{1}{6}}}{\sqrt{\sum_{i=1}^{N_c} (x_{i,m} M_i)} \left[\sum_{i=1}^{N_c} x_{i,m} p_{c,i} \right]^{\frac{2}{3}}} \quad (2.7.4)$$

The reduced density of phase m is defined as

$$\rho_{r,m} = \frac{\rho_m}{\rho_{c,m}}, \quad (2.7.5)$$

where ρ_m is obtained from

$$\rho_m = \frac{p}{Z_m RT}, \quad (2.7.6)$$

and Z_m is the appropriate root of the cubic equation considered.

Lohrenz et. al.²⁵ calculate the pseudocritical density of phase m , $\rho_{c,m}$ as

$$\rho_{c,m} = \frac{1}{\sum_{i=1}^{N_c} x_{i,m} V_{c,i}} \quad (2.7.7)$$

where $V_{c,i}$ is the critical volume of component i , computed using the tabulated critical values³², in ft³/lbmole.

2.8 Results and Accuracy of Computations

The package has been extensively tested for each equation of state and here, we compare our results with published results.

2.8.1 Z - factor

First, we compare the solution of the cubic equation (Eq. 2.3.5) from two equations of state, (Peng -Robinson and Schmidt-Wenzel EOS, (Eq. 2.2.25). Table 2.1 compares Z - factors for a condensate fluid with analogous results from Ref. 34 for a variety of pressures and temperatures. Our package solves the cubic equation using an explicit formula (Ref. 35, Eq. 3.8.2). Note the close agreement between our results and the published data³⁴.

2.8.2 Saturation Points

Tables 2.2 - 2.6 compare saturation point computations from three equations of state, (Zudkevitch - Joffe - Redlich-Kwong, Peng-Robinson and Schmidt-Wenzel EOS).

As mentioned earlier, one of the modifications made by Zudkevitch and Joffe to the original Redlich - Kwong equation is the variation of the van der Waals coefficients Ω_a and Ω_b as functions of temperature and acentric factor. Table 2.2 shows the computation of the bubble point pressure and the composition of the forming gas in the methane/butane/decane system, by use of the ZJRK EOS. We used the same set of binary interaction parameters as Ref. 7, i.e., $k_{i,j} = 0$, except for $k_{1,2} = k_{2,1} = 0.024$ and $k_{2,3} = k_{3,2} = 0.025$ (Here, methane, butane and decane are referred to as components 1, 2, 3, respectively).

For $T = 160$ °F, we used the same values for $\Omega_{a,i}$ and $\Omega_{b,i}$ as Ref. 7, but for $T = 280$ °F, we used the the set of coefficients originally determined experimentally by Zudkevitch and Joffe¹⁶. The experimental and package results agreed within 4% for pressure and within 3% for K - values for all cases. $T = 160$ °F, the results of our package are in excellent agreement with those of Ref. 7.

TABLE 2.1

**Comparison of Calculated and Experimental
Z - factors for the GPA condensed fluid**

Peng-Robinson and Schmidt-Wenzel EOS

T (°F)	Pressure (psia)	Ref. 34			Package	
		Lab.	PR	SW	PR	SW
100	6,000	1.133	1.044	1.104	1.043	1.104
	5,500	1.050	0.978	1.033	0.977	1.034
	5,000	0.978	0.911	0.962	0.911	0.962
	4,500	0.906	0.843	0.890	0.844	0.890
	4,000	0.828	0.775	0.817	0.774	0.817
150	6,000	1.101	1.034	1.089	1.034	1.089
	5,500	1.037	0.974	1.025	0.973	1.024
	5,000	0.970	0.914	0.961	0.914	0.961
	4,500	0.903	0.854	0.897	0.855	0.898
	4,000	0.834	0.794	0.833	0.793	0.833
200	6,000	1.107	1.034	1.085	1.034	1.086
	5,500	1.042	0.980	1.027	0.980	1.027
	5,000	0.979	0.927	0.970	0.928	0.972
	4,500	0.913	0.874	0.914	0.873	0.913
	4,000	0.833	0.859	0.823	0.858	0.822
250	6,000	1.082	1.040	1.087	1.040	1.087
	5,500	1.035	0.992	1.036	0.992	1.036
	5,000	0.972	0.945	0.985	0.945	0.985
	4,500	0.918	0.900	0.936	0.901	0.936
	4,000	0.868	0.856	0.889	0.855	0.887

TABLE 2.2

Comparison of Calculated and Experimental Results

 $C_1/nC_4/nC_{10}$

Zudkevitch-Joffe-Redlich-Kwong EOS

T (°F)	x_i	Pressure (psia)			K-Value		
		Lab.	Ref. 7	Package	Lab.	Ref. 7	Package
280	0.203	1000	1019.7	995	3.813	3.773	3.736
	0.346				0.613	0.637	0.656
	0.451				0.032	0.031	0.032
280	0.402	2000	1970.5	1912	1.861	1.867	1.850
	0.370				0.605	0.613	0.629
	0.228				0.122	0.099	0.103
280	0.575	3000	2997.6	2915	1.459	1.475	1.470
	0.179				0.631	0.635	0.645
	0.246				0.193	0.156	0.157
160	0.253	1000	972.7	976	3.174	3.173	3.173
	0.661				0.297	0.297	0.297
	0.086				0.013	0.008	0.008
160	0.459	2000	1950.9	1960	1.854	1.862	1.861
	0.390				0.367	0.361	0.362
	0.151				0.039	0.028	0.028
160	0.663	3000	3128.2	3143	1.213	1.254	1.252
	0.229				0.703	0.633	0.636
	0.108				0.330	0.218	0.221

TABLE 2.3

Comparison of Calculated and Experimental Results

 $C_1/nC_4/nC_{10}$

Peng-Robinson EOS

T (°F)	x_i	Pressure (psia)			K-Value		
		Lab.	Ref. 34	Package	Lab.	Ref. 34	Package
280	0.203	1000	1009	1009	3.813	3.800	3.800
	0.346				0.613	0.615	0.615
	0.451				0.032	0.035	0.035
280	0.402	2000	1940	1941	1.861	1.844	1.844
	0.370				0.605	0.625	0.625
	0.228				0.122	0.119	0.119
280	0.575	3000	2999	3000	1.459	1.460	1.462
	0.179				0.631	0.639	0.639
	0.246				0.193	0.180	0.181
160	0.253	1000	952	954	3.174	3.130	3.126
	0.661				0.297	0.313	0.315
	0.086				0.013	0.009	0.009
160	0.459	2000	1937	1940	1.854	1.850	1.848
	0.390				0.367	0.374	0.376
	0.151				0.039	0.034	0.034
160	0.663	3000	3113	3117	1.213	1.247	1.245
	0.229				0.703	0.643	0.646
	0.108				0.330	0.241	0.244

TABLE 2.4

Comparison of Calculated and Experimental Results
 $C_1/nC_4/nC_{10}$

Schmidt-Wenzel EOS

T (°F)	x_i	Pressure (psia)			K-Value		
		Lab.	Ref. 8	Package	Lab.	Ref. 8	Package
280	0.203	1000	1012	1012	3.813	3.850	3.851
	0.346				0.613	0.587	0.587
	0.451				0.032	0.033	0.033
280	0.402	2000	1927	1928	1.861	1.873	1.873
	0.370				0.605	0.600	0.600
	0.228				0.122	0.109	0.109
280	0.575	3000	2955	2957	1.459	1.479	1.479
	0.179				0.631	0.608	0.609
	0.246				0.193	0.165	0.166
160	0.253	1000	951	952	3.174	3.155	3.152
	0.661				0.297	0.304	0.305
	0.086				0.013	0.006	0.007
160	0.459	2000	1940	1943	1.854	1.867	1.866
	0.390				0.367	0.355	0.357
	0.151				0.039	0.028	0.029
160	0.663	3000	3105	3109	1.213	1.263	1.261
	0.229				0.703	0.611	0.614
	0.108				0.330	0.211	0.214

TABLE 2.5
Computation of Saturation Points
 $CO_2/C_1 - C_{13+}$
Peng-Robinson EOS

Property	Ref. 36	Package
Bubble Point (<i>psia</i>)		
with 0% CO_2	1651	1653
20%	1860	1857
40%	2088	2085
60%	2228	2234
65%	2637	2630
Dew Point (<i>psia</i>)		
with 60% CO_2	2113	2110
65%	2487	2485
70%	3868	3865
75%	3182	3179
80%	3769	3773

TABLE 2.6

Computation of Saturation Points

 $N_2 - CO_2/C_1 - C_{15+}$

Peng-Robinson EOS

Property	Ref. 36	Package
Bubble Point (<i>psia</i>)		
with 0% N_2	3990	3993
5%	4742	4745
10%	5603	5606
15%	6604	6608
20%	7787	7790
25%	9217	9221
Dew Point (<i>psia</i>)		
with 0% N_2	3565	3567
10%	4080	4081
20%	4644	4646
30%	5259	5260
40%	5921	5924
50%	6609	6612

Tables 2.3 and 2.4 show the saturation point computations using the Peng-Robinson and Schmidt-Wenzel equations of state, respectively. The results of the package agree very closely with the results of Ref. 34.

The results of Table 2.5 were obtained by using the Peng-Robinson equation to simulate the variation of the bubble point and dew point pressures of a mixture containing thirteen hydrocarbon components plus a concentration of CO_2 ranging from 0 to 80%. Table 2.6 shows the results for a seventeen component mixture that includes a fixed concentration of CO_2 plus a concentration of N_2 ranging from 0 to 50%. In both cases, our phase package yields results that agree well with published data³⁶.

Note that in all cases, we used the Baker and Luks³³ method to evaluate the initial estimates of the saturation pressures.

2.8.3 Flash Calculations

Here, we present the results of flash calculations using both the SS and MVNR methods.

For a ten component system, Table 2.7 shows the results obtained for a range of pressure including the critical point at 2810 psia and 162.2 °F. The SRK EOS was used and as expected, the SS method did not converge near the critical region whereas the more robust MVNR predicted properties that agree closely with those of Ref. 23. Note that Ref. 23 uses Powell's method^{37,38} instead of the MVNR.

Another flash computation using the SRK EOS was performed for a fifteen component system which included N_2 and CO_2 . Our package predicted the bubble point at 4948 psia. (The analogous pressure from Ref. 23 was 4952 psia). Table 2.8 shows excellent agreement between computed and published values of number of moles of gas per number of moles of mixture.

TABLE 2.7

Flash Calculations near the Critical Region

 $C_1 - nC_{10}$

Soave-Redlich-Kwong EOS

Pressure (<i>psia</i>)	<i>V</i> Ref. 23	<i>V</i> Package
2700	0.575	0.577
2710	0.572	0.573
2720	0.568	0.570
2730	0.565	0.566
2740	0.559	0.561
2750	0.556	0.558
2760	0.552	0.554
2770	0.548	0.549
2780	0.541	0.543
2790	0.536	0.537
2800	0.530	0.532
2810*	0.519	0.522

TABLE 2.8

Flash Calculations for Reservoir Oil

 $N_2 - CO_2/C_1 - C_{7+}$

Soave-Redlich-Kwong EOS

Pressure (<i>psia</i>)	<i>V</i> Ref. 23	<i>V</i> Package
4950	0.0116	0.0000
4925	0.1144	0.1150
4900	0.1770	0.1775
4875	0.2206	0.2218
4825	0.2536	0.2543
4800	0.3016	0.3025
4750	0.3358	0.3364
4700	0.3623	0.3627
4650	0.3838	0.3844
4600	0.4019	0.4025
4550	0.4175	0.4181
4500	0.4313	0.4320

2.9 Use and Capabilities

Our package handles any fluid mixture containing up to 38 pure components and 7 pseudocomponents. All the pure components critical properties and acentric factors are stored and used upon request. In case the mixture contains a pseudocomponent, the user needs to input the boiling point, the molecular weight and the API gravity so that the program generates all critical properties, acentric factors and other parameters needed to compute the heat of vaporization required for the computation of saturation points.

CHAPTER III

FLOW EQUATIONS

3.1 Continuity Equation and Flow with Change of Phase

3.1.1 General Continuity Equation

In flow phenomena of any kind, conservation principles enable us to describe the physics in terms of differential equations. The conservation principle that is relevant to the fluid flow phenomenon considered in this work is the conservation of mass. In general, the conservation of a quantity (energy, mass or momentum) is written as

$$\text{Rate of Change in Quantity} = 0.$$

where “quantity” can represent mass, energy or momentum. We assume that the physical quantity is flowing in some region $E \subseteq R^3$. Let D be a subset of E with volume V , i.e., $D \subset E$. Let the concentration of the quantity be C , expressed in units of amount per unit volume, let the S be the surface bounding D and let \mathbf{F} be the flux through the surface S in units transported per unit time per unit cross-sectional area. Furthermore, let the physical quantity in question be added from the interior of D at the rate Q in units of amount per unit time per unit volume, i.e., Q represents an internal source. C , \mathbf{F} and Q are all variable quantities. Since the physical quantity must be conserved, it follows that, we can write the conservation principle over D (volume V) as

(amount in) – (amount out) + (amount generated) = (increase in content),
or in terms of rates as

$$(\text{rate in}) - (\text{rate out}) + (\text{internal sources}) = (\text{rate of increase}).$$

The amount of the quantity in V at any time t is given by

$$A(t) = \iiint_V C \, dV, \quad (3.1.1)$$

and thus, the rate of increase is

$$\frac{dA}{dt} = \iiint_V \frac{\partial C}{\partial t} \, dV, \quad (3.1.2)$$

where, since the volume element is considered fixed, the time derivative is taken inside the integral as a partial derivative operator on C . Since the physical quantity must be conserved, it follows that for the arbitrary element of volume V , the conservation principle is expressed as

$$-\iint_S \mathbf{F} \cdot \mathbf{n} \, dS + \iiint_V Q \, dV = \iiint_V \frac{\partial C}{\partial t} \, dV, \quad (3.1.3)$$

where \mathbf{n} is an outer normal vector to the surface S . The negative of the surface integral (first term in Eq. 3.1.3) taken over the closed surface of the volume element represents the difference of rates in and out of the cross-sectional area and the first volume integral represents the contribution due to fluid sources or sinks within D .

Applying the divergence theorem to the surface integral and rearranging gives

$$\iiint_V \left(-\nabla \cdot \mathbf{F} + Q - \frac{\partial C}{\partial t} \right) \, dV = 0. \quad (3.1.4)$$

Because this must hold for any arbitrary volume element, if the integrand is continuous on D , then it must be identically zero on D , i.e.,

$$-\nabla \cdot \mathbf{F} = \frac{\partial C}{\partial t} - Q. \quad (3.1.5)$$

Eq. 3.1.5 is a mathematical expression of the conservation of a physical quantity flowing through a region D in R^3 where C is the concentration of the given quantity per unit volume.

3.1.2 Fluid Flow in Porous Media with Change of Phase

In the flow of a compressible fluid through a porous medium, mass transfer of hydrocarbon components between phases occurs. Therefore, the mass of a phase is not conserved but the mass of each component is conserved. In our model, we consider the two-phase flow of oil (liquid) and gas (vapor) and component i may flow in both phases. The mass flux of phase m in $lbm/(ft^2 - day)$ is given by

$$\mathbf{F}_m = \rho_m \mathbf{v}_m, \quad (3.1.6)$$

where ρ_m is the fluid density of phase m in lbm/ft^3 and \mathbf{v}_m denotes the velocity in ft/day . As we use oil field units, the velocity of phase m will be given by Darcy's law (see Eq. 3.1.8 below) in units of $RB/(ft^2 - day)$. Thus from here on, we assume \mathbf{v}_m is given in $RB/(ft^2 - day)$, so $5.615\mathbf{v}_m$ gives the velocity in ft/day and Eq. 3.1.6 becomes

$$\mathbf{F}_m = 5.615\rho_m \mathbf{v}_m. \quad (3.1.7)$$

The multiphase Darcy's law³⁹ can be used to obtain an expression for the oil and gas phase velocities. For velocity in $RB/(ft^2 - day)$, The relation is

$$\mathbf{v}_m = -1.127 \times 10^{-3} \frac{[k]k_{rm}}{\mu_m} (\nabla p_m - \gamma_m \nabla z'), \quad (3.1.8)$$

where $m = o$ or g , $[k]$ is the absolute permeability tensor, k_{rm} is the phase m relative permeability, μ_m is the phase m viscosity, γ_m is the specific weight of the fluid in phase m and z' is positive in the vertical downward direction, or more precisely, z' is the direction in which gravity acts. In our work, we consider only the two-phase flow of oil and gas and we assume that k_{rm} is a single-valued function of gas saturation, S_g , i.e.,

$$k_{rm} = k_{rm}(S_g). \quad (3.1.9)$$

Throughout this work, we characterize the fluid by its mole fraction composition in each phase where N_c denotes the number of components. Conserving the

mass of hydrocarbon component i is equivalent to conserving the total number of moles of component i . The number of moles of component i per unit bulk volume of porous medium, i.e., the concentration of component i , is

$$C_i = \phi \left(x_i \frac{\rho_o}{M_o} S_o + y_i \frac{\rho_g}{M_g} S_g \right), \quad 1 \leq i \leq N_c, \quad (3.1.10)$$

where S_o and S_g are liquid and gas saturations, and M_o and M_g are mean molecular weights of liquid and gas, respectively. The following equations always apply :

$$\sum_{i=1}^{N_c} x_i = 1 \quad (3.1.11a)$$

and

$$\sum_{i=1}^{N_c} y_i = 1. \quad (3.1.11b)$$

Thus,

$$M_o = \sum_{i=1}^{N_c} x_i M_i \quad (3.1.12a)$$

and

$$M_g = \sum_{i=1}^{N_c} y_i M_i, \quad (3.1.12b)$$

where M_i denotes molecular weight of component i .

Also, the fluid densities, ρ_o and ρ_g , and the fluid viscosities, μ_o and μ_g are known functions of composition, pressure and temperature. Thus,

$$\rho_o = \rho_o \left(\{x_i\}_{i=2}^{N_c}, p, T \right), \quad (3.1.13a)$$

$$\rho_g = \rho_g \left(\{y_i\}_{i=2}^{N_c}, p, T \right) \quad (3.1.13b)$$

and

$$\mu_o = \mu_o \left(\{x_i\}_{i=2}^{N_c}, p, T \right), \quad (3.1.14a)$$

$$\mu_g = \mu_g \left(\{y_i\}_{i=2}^{N_c}, p, T \right). \quad (3.1.14b)$$

The molar flux density of the i^{th} component is obtained by observing that any component may be transported in both liquid and gas phases. Thus,

$$\mathbf{F}_i = 5.615 \left(x_i \frac{\rho_o}{M_o} \mathbf{v}_o + y_i \frac{\rho_g}{M_g} \mathbf{v}_g \right), \quad 1 \leq i \leq N_c \quad (3.1.15)$$

is the flux of component i in *moles/ft²/day*. We assume that the porosity ϕ is constant and there are no internal sources or sinks within the porous medium volume considered. Then, using Eqs. 3.1.10 and 3.1.15 in 3.1.5 gives

$$-5.615 \nabla \cdot \left[x_i \frac{\rho_o}{M_o} \mathbf{v}_o + y_i \frac{\rho_g}{M_g} \mathbf{v}_g \right] = \phi \frac{\partial}{\partial t} \left[x_i \frac{\rho_o}{M_o} S_o + y_i \frac{\rho_g}{M_g} S_g \right], \quad 1 \leq i \leq N_c. \quad (3.1.16)$$

We assume no connate water is included. Thus,

$$S_o + S_g = 1. \quad (3.1.17)$$

A common assumption in compositional simulation is that in petroleum reservoirs the liquid and gas phases at any point of the reservoir are at thermodynamic equilibrium. Thus,

$$f_{i,L} = f_{i,V}, \quad 1 \leq i \leq N_c. \quad (3.1.18)$$

3.1.3 Source/Sink Term

The source or sink term in Eq. 3.1.5 usually represents the boundary condition for production or injection at a well. In our work, we will apply the correct boundary condition and thus, we need no internal source or sink terms in Eq. 3.1.16.

If we consider flow in a three dimensional region defined by

$$\Omega = \{(r, \theta, z) \mid r_w \leq r \leq r_e, 0 \leq z \leq h, 0 \leq \theta \leq 2\pi\},$$

where r_w and r_e are the wellbore and reservoir radius, respectively and h is the total reservoir thickness, then the overall mass flux out of the reservoir into the well is given by

$$5.615 \iint_S (\rho_o \mathbf{v}_o + \rho_g \mathbf{v}_g) \cdot \mathbf{n} \, dS. \quad (3.1.19)$$

In Eq. 3.1.19, S corresponds to the area of the perforated surface of the wellbore which is adjacent to the producing zone, and \mathbf{n} is the unit outward normal vector to the reservoir at the wellbore, i.e., in our case,

$$\mathbf{n} = (n_r, n_\theta, n_z) = (-1, 0, 0). \quad (3.1.20)$$

For the case where Eq. 3.1.20 applies,

$$\mathbf{v}_m \cdot \mathbf{n} = (v_{m,r}, v_{m,\theta}, v_{m,z}) \cdot (-1, 0, 0) = -v_{m,r}, \quad m = o, g. \quad (3.1.21)$$

where $v_{m,r}$ is the component of \mathbf{v}_m in the r - direction. We let ρ_m denotes the molar density of phase m , i.e., $\rho_o = \rho_o/M_o$ and $\rho_g = \rho_g/M_g$. Then using Eqs. 3.1.19 and 3.1.21, it is easy to see that the total rate of production in *lbmoles/day*, is given by

$$\begin{aligned} q_t &= 5.615 \iint_S (\rho_o \mathbf{v}_o + \rho_g \mathbf{v}_g) \cdot \mathbf{n} \, dS \\ &= -5.615 \int_{h_1}^{h_2} [\rho_o v_{o,r} + \rho_g v_{g,r}]_{r_w} r_w \, d\theta dz. \end{aligned} \quad (3.1.22)$$

If we let $C_1 = 0.00633$, and use Darcy's Law (Eq. 3.1.8), then Eq. 3.1.22 becomes

$$q_t = C_1 \int_{h_1}^{h_2} \int_0^{2\pi} k \left[\rho_o \frac{k_{ro}}{\mu_o} \left(\frac{\partial p}{\partial r} - \gamma_o \frac{\partial z'}{\partial r} \right) + \rho_g \frac{k_{rg}}{\mu_g} \left(\frac{\partial p}{\partial r} - \gamma_g \frac{\partial z'}{\partial r} \right) \right]_{r_w} r_w \, d\theta dz. \quad (3.1.23a)$$

Here, $z = h_1$ represents the top of the perforated interval and $z = h_2$ the bottom of the perforated interval. Throughout the remainder of this work, we assume $z = z'$

and that axial symmetry (pressure, saturation or composition), is independent of θ . Under these assumptions, Eq. 3.1.23a becomes

$$q_t = C_1(2\pi r_w) \int_{h_1}^{h_2} k \left[\rho_o \frac{k_{ro}}{\mu_o} \frac{\partial p}{\partial r} + \rho_g \frac{k_{rg}}{\mu_g} \frac{\partial p}{\partial r} \right]_{r_w} dz. \quad (3.1.23b)$$

Eq. 3.1.23 applies to layered reservoirs where k varies with depth, z . To obtain an analog equation for rates of individual components, the phase mobility terms need to be multiplied by the appropriate phase mole fraction composition of each individual component.

3.2 Radial Flow Problem Formulation

Although the basic theoretical concepts involved in our new numerical formulation appear to be general, i.e., independent of the coordinate system used, we present and implement it only for a radial flow.

3.2.1 Partial Differential Equations and Auxiliary Conditions

We consider a bounded cylindrical reservoir which is produced from a single completely-penetrating well located at its center. The reservoir may be initially filled with a single-phase gas, a single-phase liquid or a two-phase fluid with an initial pressure p_i above, below or equal to the saturation pressure. Throughout, we assume that no water exists within the reservoir. Reservoir temperature T may be higher or lower than the critical temperature but remains constant throughout any flow or thermodynamic equilibrium process. We further assume that at any "point" in the reservoir where two phases coexist, thermodynamic equilibrium is instantly achieved. We neglect dispersion, gravity and capillary effects. We assume that flow in the reservoir is purely radial and that the reservoir is homogeneous except for a small concentric region near the wellbore region where the permeability is altered to model a skin effect as suggested by Hawkins⁴⁰, i.e.,

$$s = \left(\frac{k}{k_s} - 1 \right) \ln \left(\frac{r_s}{r_w} \right), \quad (3.2.1)$$

where k_s is the skin zone radial permeability, r_s is the skin zone radius and r_w is the wellbore radius.

The hydrocarbon reservoir fluid consists of N_c components distributed between two phases (Liquid and Vapor). The material balance on each component (Eq. 3.1.16) may be rewritten in the radial coordinates as

$$-5.615 \frac{1}{r} \frac{\partial}{\partial r} [r (\rho_o v_{o,r} x_i + \rho_g v_{g,r} y_i)] = \phi \frac{\partial}{\partial t} (\rho_o S_o x_i + \rho_g S_g y_i), \quad 1 \leq i \leq N_c. \quad (3.2.2)$$

where ρ_o and ρ_g denote the molar densities in $lbmoles/ft^3$. Using the radial flow version of Eq. 3.1.8 with gravity neglected, in Eq. 3.2.2 gives

$$C_1 \frac{1}{r} \frac{\partial}{\partial r} \left[rk \left(\rho_o \frac{k_{ro}}{\mu_o} x_i + \rho_g \frac{k_{rg}}{\mu_g} y_i \right) \frac{\partial p}{\partial r} \right] = \phi \frac{\partial}{\partial t} (\rho_o S_o x_i + \rho_g S_g y_i), \quad 1 \leq i \leq N_c, \quad (3.2.3)$$

for $r_w < r < r_e$ and $t > 0$, under the constraints that

$$\sum_{i=1}^{N_c} x_i = 1, \quad (3.2.4a)$$

$$\sum_{i=1}^{N_c} y_i = 1 \quad (3.2.4b)$$

and

$$S_o + S_g = 1. \quad (3.2.5)$$

The flow equations are subject to the following initial and boundary conditions.

3.2.2 Initial Conditions

$$p(r, 0) = g_1(r), \quad (3.2.6)$$

$$S_g(r, 0) = g_2(r), \quad (3.2.7)$$

$$z_i(r, 0) = g_3(r), \quad 1 \leq i \leq N_c, \quad (3.2.8)$$

for $r_w < r \leq r_e$. Here z_i represents the overall composition of component i throughout the reservoir and g_1 , g_2 and g_3 are functions of r only. While Eqs. 3.2.6 - 3.2.8 allow an arbitrary initial condition, for all numerical results presented, we assume uniform initial conditions, e.g., $p(r, 0) = p_i$ for $r_w \leq r \leq r_e$ where the initial pressure p_i is a constant.

3.2.3 Inner Boundary Conditions

We allow two modes of production at the well, production at a constant sandface total molar rate or production against a fixed sandface pressure, p_{wf} . Thus, we consider two possibilities:

- (1) Specified constant total molar rate

$$q_t = 0.00633(2\pi r_w h) \left[\left(\rho_o \frac{kk_{ro}}{\mu_o} + \rho_g \frac{kk_{rg}}{\mu_g} \right) \left(\frac{\partial p}{\partial r} \right) \right]_{r=r_w}, \quad t > 0 \quad (3.2.9)$$

and

- (2) Specified constant bottomhole pressure

$$p(r_w, t) = p_{wf}, \quad t > 0. \quad (3.2.10)$$

3.2.4 Outer Boundary Conditions

At the outer boundary, r_e , of the reservoir, we also allow two possible boundary conditions. We consider the case of a closed outer boundary given by

$$\left(\frac{\partial p}{\partial r} \right)_{r=r_e} = 0, \quad t > 0. \quad (3.2.11a)$$

We may also hold the pressure at the outer boundary fixed at some pressure, p_e . For this case, we must also specify the mole fraction composition of the fluid at the outer boundary. This fixed composition, denoted by $y_{i,I}$, $1 \leq i \leq N_c$, will in all cases of constant pressure outer boundary be held fixed at the mole fraction composition of the initial in-place gas, or at some other arbitrary mole fraction composition to simulate a gas injection process. Thus, the required equations are

$$p(r_e, t) = p_e, \quad t > 0, \quad (3.2.11b)$$

$$z_i(r_e, t) = y_{i,I}, \quad t > 0, \quad 1 \leq i \leq N_c. \quad (3.2.11c)$$

Eqs. 3.2.3 - 3.2.11 represent the basic system of partial differential equations and boundary conditions which are to be solved. The densities and viscosities are functions of pressure, temperature and composition through an equation of state and the Lohrenz, Bray and Clark²⁵ viscosity correlations. The phase relative permeabilities are considered unique functions of gas saturation.

We wish to solve our system of equations for pressure, phase saturations, and phase mole fraction composition as functions of radial distance and time. The solution set,

$$\{p(r, t), S_o(r, t), S_g(r, t), \{x_i\}_{i=1}^{N_c}, \{y_i\}_{i=1}^{N_c}\}, \quad (3.2.12)$$

contains $(2N_c + 3)$ unknown variables, but thus far, we have specified only $N_c + 3$ equations, (Eqs. 3.2.3 - 3.2.5). (Note that the initial and boundary conditions are not additional equations, but merely constraints necessary to determine the unique solution of the partial differential equations, Eq. 3.2.3.)

To complete the system of equations, we invoke the assumption of thermodynamic equilibrium stated earlier. We present a formulation that includes the compositional treatment of the reservoir via an equation of state. Fugacities are easily obtainable as functions of pressure, temperature and composition from an equation of state.

Assuming that the equilibrium between the phases is achieved instantly, the thermodynamic equilibrium is expressed by minimizing the Gibbs free energy via the fugacities³⁰ of both phases. This yields the remaining N_c equations needed in the form

$$f_{i,L}(\{x_l\}_{l=2}^{N_c}, p, T) = f_{i,V}(\{y_l\}_{l=2}^{N_c}, p, T), \quad 1 \leq i \leq N_c. \quad (3.2.13)$$

In Eq. 3.2.13, $f_{i,L}$ and $f_{i,V}$ are the fugacities of component i in the liquid and vapor phases respectively; the fugacity functions are calculated using an equation of state.

Eqs. 3.2.3 - 3.2.5 and 3.2.13 constitute the system of $(2N_c + 3)$ equations solved to obtain the values of the $(2N_c + 3)$ variables in the set defined by Eq. 3.2.12.

Often, it is convenient to work in terms of an overall mass balance equation. This is obtained by summing the N_c flow equations, Eq. 3.2.3, over all components and applying the constraint equations, Eq. 3.2.4a and 3.2.4b, to yield

$$0.00633 \frac{1}{r} \frac{\partial}{\partial r} \left[r k \left(\rho_o \frac{k_{ro}}{\mu_o} + \rho_g \frac{k_{rg}}{\mu_g} \right) \frac{\partial p}{\partial r} \right] = \phi \frac{\partial}{\partial t} (\rho_o S_o + \rho_g S_g). \quad (3.2.14)$$

Note that Eq. 3.2.14 and any $N_c - 1$ flow equations from Eq. 3.2.3 form a linearly independent set. The single-phase formulation may be regarded as a reduced form of the overall mass balance equation, Eq. 3.2.14, and is expressed as

$$0.00633 \frac{1}{r} \frac{\partial}{\partial r} \left(r k \frac{\rho_m}{\mu_m} \frac{\partial p}{\partial r} \right) = \phi \frac{\partial \rho_m}{\partial t}, \quad m = o, g. \quad (3.2.15)$$

The multiphase flow problem outlined above represents a highly non-linear system and no general analytical methods exist by which a solution can be obtained. A variety of numerical methods for solution of this system have appeared in the literature, ranging from IMPES-type to fully-implicit methods. The high cost of running fully-implicit models based on Newton's method motivated us to seek an alternative method with the same desirable stability usually exhibited by Newton's method. Here, we present a method which preserves implicitness but runs significantly faster than standard implicit models.

CHAPTER IV

NEW NUMERICAL SOLUTION PROCEDURE

The only currently available method of solving the highly nonlinear system of equations developed in the last chapter is to resort to approximate methods of solution. The most common approach is to apply finite difference techniques. This involves defining a grid on the region of interest, expressing the partial differential equations in term of algebraic approximations, and solving the resulting set of algebraic equations coupled through the auxiliary relationships.

4.1 Discretization

4.1.1 Radial Grid System

The finite difference representation of the partial differential equations is independent of the grid system and spacing employed; i.e., they are identical for both block and point-centered grids. Moreover, the precise arrangement of the grid points does not depend on the type of outer boundary conditions (Dirichlet or Neumann) specified.

Following standard practice in developing difference equations, we lay a geometrically spaced radial grid on the region of interest following the procedure suggested by Coats⁴¹. The relation between successive gridpoints is given by

$$r_j = \alpha r_{j-1}, \quad 1 \leq j \leq N_r, \quad (4.1.1)$$

where N_r is the total number of meshpoints interior to the reservoir. The radial distances to block boundaries, (denoted by half integer indices), are defined from

$$r_{j+\frac{1}{2}} = \frac{r_{j+1} - r_j}{\ln \alpha}. \quad (4.1.2)$$

We require that the wellbore radius, r_w , be equal to the block boundary, $r_{\frac{1}{2}}$ and that $r_e = r_{N_r+\frac{1}{2}}$. As shown in Ref. 41, it follows that

$$r_0 = \frac{r_w \ln \alpha}{(\alpha - 1)}. \quad (4.1.3)$$

and

$$\alpha = \left(\frac{r_e}{r_w} \right)^{\frac{1}{N_r}} \quad (4.1.4)$$

4.1.2 Finite Difference Equations

Now, we develop finite difference approximations to the partial derivatives.

We define the following finite difference linear operators:

$$\Delta_r X_j^n = X_{j+\frac{1}{2}}^n - X_{j-\frac{1}{2}}^n \quad (4.1.5)$$

and

$$\Delta_t X_j = X_j^{n+1} - X_j^n. \quad (4.1.6)$$

Eq. 4.1.6 represents the standard backward difference in time⁴². Following standard convention, we write the approximation to Eq. 3.2.2 at grid block j , time level $(n+1)$ for flowing component i as follows

$$-\frac{5.615(2)}{\left(r_{j+\frac{1}{2}}^2 - r_{j-\frac{1}{2}}^2\right)} \Delta_r [r(\rho_o v_o x_i + \rho_g v_g y_i)]_j^{n+1} = \frac{\phi}{\Delta t} \Delta_t (\rho_o S_o x_i + \rho_g S_g y_i)_j, \quad 1 \leq i \leq N_c, \quad (4.1.7)$$

where ρ_o and ρ_g denote the molar densities of the vapor and liquid phases respectively, in $lbmoles/ft^3$. For the remainder of this work, we consider only radial flow.

Thus, we use v_o and v_g (instead of $v_{o,r}$ and $v_{g,r}$) to denote the radial component of the Darcy velocities in $RB/(ft^2 - day)$ given by

$$v_m = -1.127 \times 10^{-3} \frac{k k_{rm}}{\mu_m} \frac{\partial p}{\partial r}, \quad m = o, g. \quad (4.1.8)$$

Throughout, Δt is the time step size (in *days*) defined as

$$\Delta t = t^{n+1} - t^n. \quad (4.1.9)$$

Using Eq. 4.1.5, the spatial derivatives in Eq. 4.1.7 may be expanded as

$$\Delta_r(r\rho_m v_m x_{i,m})_j^{n+1} = (r\rho_m v_m x_{i,m})_{j+\frac{1}{2}}^{n+1} - (r\rho_m v_m x_{i,m})_{j-\frac{1}{2}}^{n+1}, \quad (4.1.10a)$$

where, here and throughout, we use (for ease of notation) $x_{i,m}$ to denote the mole fraction of component i in phase m , $m = L$ (or o) for liquid (oil) and $m = V$ (or g) for vapor (gas) but we also use x_i as the mole fraction of component i in the liquid phase and y_i as the mole fraction of component i in the vapor phase, i.e., $x_{i,L} = x_i$ and $x_{i,V} = y_i$. Note that by substituting Eq. 4.1.8 into Eq. 4.1.10a both terms in the right-hand side of Eq. 4.1.10a will involve pressure spatial derivatives that are approximated as follows:

$$\left(\frac{\partial p}{\partial r}\right)_{j+\frac{1}{2}}^{n+1} = \frac{p_{j+1}^{n+1} - p_j^{n+1}}{r_{j+1} - r_j}. \quad (4.1.10b)$$

Using Eqs. 4.1.8, 4.1.10a - 4.1.10b, the standard fully-implicit, finite difference form of the component equations, Eq. 4.1.7, for gridblock j (assuming two phases exist in the gridblock) is given by

$$\begin{aligned} & \left(\frac{2}{r_{j+\frac{1}{2}}^2 + r_{j-\frac{1}{2}}^2}\right) \left[(\lambda_{t,i})_{j+\frac{1}{2}}^{n+1} k_{j+\frac{1}{2}} r_{j+\frac{1}{2}} \frac{p_{j+1}^{n+1} - p_j^{n+1}}{r_{j+1} - r_j} - (\lambda_{t,i})_{j-\frac{1}{2}}^{n+1} k_{j-\frac{1}{2}} r_{j-\frac{1}{2}} \frac{p_j^{n+1} - p_{j-1}^{n+1}}{r_j - r_{j-1}} \right] \\ & = \frac{\phi}{C_1 \Delta t} \Delta_t (\rho_o S_o x_i + \rho_g S_g y_i)_j, \quad 1 \leq i \leq N_c, \quad 1 \leq j \leq N_r, \end{aligned} \quad (4.1.11a)$$

where C_1 is a unit conversion factor ($C_1 = 0.00633$) and where $\lambda_{t,i}$ is defined as

$$\lambda_{t,i} = \rho_o \frac{k_{ro}}{\mu_o} x_i + \rho_g \frac{k_{rg}}{\mu_g} y_i. \quad (4.1.11b)$$

Multiplying both sides of Eq. 4.1.11a by $\pi h (r_{j+\frac{1}{2}}^2 - r_{j-\frac{1}{2}}^2)$, we obtain

$$\begin{aligned} & U_{j+\frac{1}{2}} \left[\left(\rho_o \frac{k_{ro}}{\mu_o} x_i + \rho_g \frac{k_{rg}}{\mu_g} y_i \right)_{j+\frac{1}{2}}^{n+1} (p_{j+1}^{n+1} - p_j^{n+1}) \right] \\ & - U_{j-\frac{1}{2}} \left[\left(\rho_o \frac{k_{ro}}{\mu_o} x_i + \rho_g \frac{k_{rg}}{\mu_g} y_i \right)_{j-\frac{1}{2}}^{n+1} (p_j^{n+1} - p_{j-1}^{n+1}) \right] \\ & = \frac{V_{pj}}{C_1 \Delta t} \Delta t (\rho_o S_o x_i + \rho_g S_g y_i)_j, \quad 1 \leq i \leq N_c, \quad 2 \leq j \leq N_r - 1, \end{aligned} \quad (4.1.12)$$

where

$$U_{j+\frac{1}{2}} = \frac{2\pi h k_{j+\frac{1}{2}} r_{j+\frac{1}{2}}}{r_{j+1} - r_j}, \quad 1 \leq j \leq N_r - 1, \quad (4.1.13a)$$

and where V_{pj} is the pore volume of block j given by

$$V_{pj} = \phi \pi h (r_{j+\frac{1}{2}}^2 - r_{j-\frac{1}{2}}^2), \quad 1 \leq j \leq N_r - 1. \quad (4.1.13b)$$

In Eq. 4.1.13a, $k_{j+\frac{1}{2}}$ denotes the permeability at $r_{j+\frac{1}{2}}$ and is taken to be the harmonic average⁴² of the absolute permeabilities in the upstream and downstream blocks, i.e.,

$$k_{j+\frac{1}{2}} = \frac{k_{j+1} k_j \ln \alpha}{k_j \ln \left(\frac{\alpha-1}{\ln \alpha} \right) + k_{j+1} \ln \left(\frac{\alpha \ln \alpha}{\alpha-1} \right)}. \quad (4.1.14)$$

Similarly, the overall mass balance equation, Eq. 3.2.14, assumes the following finite difference form:

$$\begin{aligned} & U_{j+\frac{1}{2}} \left[\left(\rho_o \frac{k_{ro}}{\mu_o} + \rho_g \frac{k_{rg}}{\mu_g} \right)_{j+\frac{1}{2}}^{n+1} (p_{j+1}^{n+1} - p_j^{n+1}) \right] \\ & - U_{j-\frac{1}{2}} \left[\left(\rho_o \frac{k_{ro}}{\mu_o} + \rho_g \frac{k_{rg}}{\mu_g} \right)_{j-\frac{1}{2}}^{n+1} (p_j^{n+1} - p_{j-1}^{n+1}) \right] \\ & = \frac{V_{pj}}{C_1 \Delta t} \Delta t (\rho_o S_o + \rho_g S_g)_j, \quad 2 \leq j \leq N_r - 1. \end{aligned} \quad (4.1.15)$$

In Eqs. 4.1.12 and 4.1.15, the densities, viscosities, relative permeabilities and mole fractions for both phases are to be evaluated at block boundaries. In our model, we upstream weight all of these quantities⁴¹.

The constraints, Eqs. 3.2.4 - 3.2.5 and 3.2.13 are approximated at time level $(n + 1)$ and meshpoint j by

$$\sum_{i=1}^{N_c} x_{i,j}^{n+1} = 1 \quad (4.1.16a)$$

$$\sum_{i=1}^{N_c} y_{i,j}^{n+1} = 1 \quad (4.1.16b)$$

and

$$S_{o,j}^{n+1} + S_{g,j}^{n+1} = 1 \quad (4.1.17)$$

$$f_{i,L,j}^{n+1}(\{x_{l,j}\}_{l=2}^{N_c}, p_j, T) = f_{i,V,j}^{n+1}(\{y_{l,j}\}_{l=2}^{N_c}, p_j, T), \quad 1 \leq i \leq N_c. \quad (4.1.18)$$

The finite difference form of the inner boundary condition (Eq. 3.2.9), is similarly written as follows

$$(0.00633)U_{\frac{1}{2}} \left[\left(\rho_o \frac{k_{ro}}{\mu_o} + \rho_g \frac{k_{rg}}{\mu_g} \right)_1^{n+1} (p_1^{n+1} - p_{\frac{1}{2}}^{n+1}) \right] = q_t, \quad (4.1.19)$$

where $U_{\frac{1}{2}}$ is defined as

$$U_{\frac{1}{2}} = \frac{2\pi k_{\frac{1}{2}} h r_w}{r_1 - r_w}, \quad (4.1.20)$$

where $k_{\frac{1}{2}} = k_1$, the absolute permeability in the first gridblock. Here, again, upstream weighting is used for all phase properties and relative permeabilities. Eq. 4.1.19 introduces the unknown sandface pressure $p(r_w, t) = p_{\frac{1}{2}}$, for which we must solve if production is at a constant rate. For the second possible inner boundary condition, constant pressure production, we set

$$p_{\frac{1}{2}}^{n+1} = p_{wf}, \quad (4.1.21)$$

where p_{wf} is the specified constant value of flowing bottomhole pressure. The initial pressure condition, i.e., Eq. 3.2.6 becomes $p_j^0 = (g_1)_j$.

The no flow outer boundary condition, Eq. 3.2.11a, is automatically satisfied if we set $k_{N_r+\frac{1}{2}} = 0$ or $U_{N_r+\frac{1}{2}} = 0$. In general, $U_{N_r+\frac{1}{2}}$ is defined by

$$U_{N_r+\frac{1}{2}} = \frac{2\pi h k_{N_r+\frac{1}{2}} r_{N_r+\frac{1}{2}}}{r_{N_r+\frac{1}{2}} - r_{N_r}} = \frac{2\pi h k_{N_r} r_e}{r_e - r_{N_r}} \quad (4.1.22)$$

With the definition of $U_{N_r+\frac{1}{2}}$ given by Eq. 4.1.22, Eqs. 4.1.12 and 4.1.15 apply at $j = N_r$ provided we replace $p_{j+1}^{n+1} - p_j^{n+1}$ by $p_{N_r+\frac{1}{2}}^{n+1} - p_{N_r}^{n+1}$.

The constant pressure outer boundary conditions, Eqs. 3.2.11b and 3.2.11c, become

$$p_{N_r+\frac{1}{2}}^{n+1} = p_e \quad (4.1.23)$$

and

$$z_{i,N_r+\frac{1}{2}} = z_{i,e} = y_{i,I}, \quad 1 \leq i \leq N_{cI}, \quad (4.1.24)$$

where p_e is the specified pressure at the outer boundary and N_{cI} is the number of components in the injected fluid. Normally, for gas condensate reservoirs, $p_e = p_i$ where $p_i \geq p_{dew}$, the dew point of the initial in-place gas. The overall composition of the fluid at $r = r_e$, $z_{i,e}$, $1 \leq i \leq N_c$, may be the same or different from the original in-place composition. In using p_e greater than p_{dew} , we are basically assuming that any cycling operations would be performed such that a minimum of the reservoir is subject to two-phase flow.

4.1.3 Simulation of the Skin Zone

We simulate the presence of mechanical damage in the near wellbore region by assuming a zone of altered permeability k_s and radius r_s . The Hawkins⁴⁰ formula, Eq. 3.2.1, is used to relate the magnitude of the skin factor, s , the skin zone

permeability, k_s , the formation permeability, k , and dimensionless radius $r_{sD} = r_s/r_w$.

To incorporate the discontinuity that this formulation requires in permeability at the block boundary between the skin zone and the formation, we use a harmonic average of the skin zone permeability and the formation permeability to determine the half-integer numbered permeability at the block boundary at the edge of the skin zone, i.e.,

$$k_{ns+\frac{1}{2}} = \frac{k_{ns+1}k_{ns} \ln\left(\frac{r_{ns+1}}{r_{ns}}\right)}{k_{ns} \ln\left(\frac{r_{ns+1}}{r_{ns+\frac{1}{2}}}\right) + k_{ns+1} \ln\left(\frac{r_{ns+\frac{1}{2}}}{r_{ns}}\right)}, \quad (4.1.25)$$

where ns is the number of the blocks assigned to the skin zone. This choice is consistent with Eq. 4.1.14. In particular, $k_{\frac{1}{2}} = k_1 = k_s$, the permeability of the skin zone.

4.2 Overall Numerical Solution Procedure

Equations 4.1.12, 4.1.16 - 4.1.18, 4.1.19 and 4.1.21 represent the finite difference equations which approximate Eqs. 3.2.3 - 3.2.5, 3.2.9 - 3.2.10 and 3.2.13. For a reservoir where two-phase flow exists at all points, the N_c flow equations of Eq. 4.1.12, the $(N_c + 3)$ constraint equations given by Eqs. 4.1.16 - 4.1.18, and the inner boundary condition, Eq. 4.1.19, form a system of $N_r(2N_c + 3) + 1$ equations which must be solved for the $N_r(2N_c + 3) + 1$ variables in the set

$$Q = \bigcup_{j=1}^{N_r} \{p, S_o, S_g, \{x_i\}_{i=1}^{N_c}, \{y_i\}_{i=1}^{N_c}\}_j^{n+1} \cup \{p_{wf}\}. \quad (4.2.1)$$

We refer to the set Q as the full set of variables. The boundary conditions either specify completely the values of the variables on the boundary or allow us to solve for these boundary values.

In this work, the solution method we present is based on solving the minimum number of equations necessary for accurate flow description at each time step; i.e., the set Q may be reduced depending on whether the whole reservoir or part of it is subject to two-phase flow. In applying the discrete flow equations, Eq. 4.1.12 or 4.1.15 at any reservoir gridblock j during the course of a simulation run, there are three possible conditions which could be encountered; i.e., the gridblock contains (i) a single-phase fluid (Liquid or Vapor) with fixed known composition; (ii) two hydrocarbon phases at thermodynamic equilibrium or (iii) a single-phase fluid with varying composition. The latter case occurs when fluid flowing into the gridblock has a composition different from that locally present; e.g., for gas cycling or miscible flooding operations, or, possibly during production following a pressure buildup when one of the two phases in the gridblock has disappeared during buildup.

One of the features incorporated into our solution procedure is to solve the minimum number of equations required to completely describe the flow in each gridblock. For example, if part of the reservoir is subject to a single-phase flow with initial composition, then, only one equation per single-phase block is solved for pressure. If, on the other hand, some blocks are subject to single-phase flow with

varying composition, then we solve a maximum of N_c equations at these blocks, for pressure and $N_c - 1$ varying mole fraction compositions. We rewrite Eq. 4.2.1 as

$$Q = \bigcup_{j \in N_{r1}} Q_j \bigcup_{j \in N_{r2}} Q_j \bigcup_{j \in N_{r3}} Q_j \cup \{p_{wf}\},$$

where N_{r1} represents the set of gridblocks containing a single-phase fluid with initial (fixed) composition, N_{r2} is the set of gridblocks containing two hydrocarbon phases, and N_{r3} is the set of gridblocks containing only one phase where the composition of this phase may vary with time. N_{r3} is important in simulating cycling processes. Q_j is defined as the minimum subset of changing variables in block j ; thus three types of subsets are considered:

1. Single-Phase with Fixed (Initial) Composition System, $j \in N_{r1}$:

$$Q_j = \{p\}_j^{n+1}. \quad (4.2.2)$$

2. Two-Phase System, $j \in N_{r2}$:

$$Q_j = \{p, S_o, S_g, \{x_i\}_{i=1}^{N_c}, \{y_i\}_{i=1}^{N_c}\}_j^{n+1}. \quad (4.2.3)$$

3. Single-Phase with Varying Composition System, $j \in N_{r3}$:

$$Q_j = \{p, \{x_{i,m}\}_{i=1}^{N_c}\}_j^{n+1}, \quad (4.2.4)$$

where $x_{i,m}$ represents the mole fractions for the phase present. (Recall that in Eq. 4.2.4 and throughout, $x_{i,m}$ denotes the mole fraction of component i in phase m , $m = o$ for liquid (oil) and $m = g$ for vapor (gas), but we also use x_i as the mole fraction of component i in the liquid phase and y_i as the mole fraction of component i in the vapor phase, i.e., $x_{i,o} = x_i$ and $x_{i,g} = y_i$).

4.3 Single-Phase Fluid with Known Initial Composition, $j \in N_{r1}$

For reservoirs filled with a single-phase fluid with fixed (initial) composition, the solution set Q in Eq. 4.2.1 is reduced to $\bigcup_{j=1}^{N_r} \{p\}_j^{n+1} \cup \{p_{wf}\}$, i.e., during depletion and shut-in periods, the initial phase composition is fixed and is not subject to changes due to pressure changes above the saturation point; thus, for each block, only one equation, (e.g., the finite difference equation for Eq. 3.2.15), is needed to solve for pressure i.e.,

$$\begin{aligned} & U_{j+\frac{1}{2}} \left[\left(\frac{\rho_m}{\mu_m} \right)_{j+\frac{1}{2}}^{n+1} (p_{j+1}^{n+1} - p_j^{n+1}) \right] \\ & - U_{j-\frac{1}{2}} \left[\left(\frac{\rho_m}{\mu_m} \right)_{j-\frac{1}{2}}^{n+1} (p_j^{n+1} - p_{j-1}^{n+1}) \right] \\ & = \frac{V_{pj}}{C_1} \left(\frac{\partial \rho_m}{\partial t} \right)_j, \quad 2 \leq j \leq N_r - 1. \end{aligned} \quad (4.3.1)$$

We recall that the density of phase m is function of pressure, composition and temperature, thus, its derivative with respect to time at a specified radius is given by

$$\begin{aligned} \left(\frac{\partial \rho_m}{\partial t} \right)_r &= \left(\frac{\partial \rho_m}{\partial p} \right)_{\{x_{i,m}\}_{i=2}^{N_c}, T} \left(\frac{\partial p}{\partial t} \right)_r + \sum_{i=2}^{N_c} \left(\frac{\partial \rho_m}{\partial x_{i,m}} \right)_{x_{k,m}, p, T, k \neq 1, i} \left(\frac{\partial x_{i,m}}{\partial t} \right)_r \\ &+ \left(\frac{\partial \rho_m}{\partial T} \right)_{\{x_{i,m}\}_{i=2}^{N_c}, p} \left(\frac{\partial T}{\partial t} \right)_r. \end{aligned} \quad (4.3.2)$$

Since the reservoir is single-phase with initial composition, no variations of composition due to pressure changes will occur, so $\left(\frac{\partial x_{i,m}}{\partial t} \right)_r = 0$. Moreover, since the flow process is isothermal, $\left(\frac{\partial T}{\partial t} \right)_r = 0$. Thus, substituting Eq. 4.3.2 into Eq. 4.3.1 yields

$$U_{j+\frac{1}{2}} \left[\left(\frac{\rho_m}{\mu_m} \right)_{j+\frac{1}{2}}^{n+1} (p_{j+1}^{n+1} - p_j^{n+1}) \right]$$

$$\begin{aligned}
& -U_{j-\frac{1}{2}} \left[\left(\frac{\rho_m}{\mu_m} \right)_{j-\frac{1}{2}}^{n+1} (p_j^{n+1} - p_{j-1}^{n+1}) \right] \\
& = \frac{V_{pj}}{C_1 \Delta t} \left(\frac{\partial \rho_m}{\partial p} \right)_j^{n+1} \Delta_t p_j, \quad 2 \leq j \leq N_r - 1.
\end{aligned} \tag{4.3.3}$$

For production at a specified rate, the discretized constant rate boundary condition, Eq. 4.1.19 is used as an additional equation to enable one to solve for the solution set

$$\bigcup_{j=1}^{N_r} \{p\}_j^{n+1} \cup \{p_{wf}\}, \tag{4.3.4}$$

The outer boundary condition, the discretized form of Eq. 3.2.11a, or Eq. 4.1.23 remains unchanged. The saturation and fugacity constraints, Eq. 4.1.17 and Eq. 4.1.18, respectively, are not applicable since the system is single-phase.

Eq. 4.3.3 may be rewritten as

$$\begin{aligned}
& \left[T_{m,j-\frac{1}{2}}^{n+1} \right] p_{j-1}^{n+1} \\
& - \left[T_{m,j-\frac{1}{2}}^{n+1} + T_{m,j+\frac{1}{2}}^{n+1} + \frac{V_{pj}}{C_1 \Delta t} \left(\frac{\partial \rho_m}{\partial p} \right)_j^{n+1} \right] p_j^{n+1} \\
& + \left[T_{m,j+\frac{1}{2}}^{n+1} \right] p_{j+1}^{n+1} \\
& = -\frac{V_{pj}}{C_1 \Delta t} \left(\frac{\partial \rho_m}{\partial p} \right)_j^{n+1} p_j^n, \quad 2 \leq j \leq N_r - 1,
\end{aligned} \tag{4.3.5}$$

where we define the transmissibility terms as follows

$$T_{m,j+\frac{1}{2}}^{n+1} = U_{j+\frac{1}{2}} \left(\frac{\rho_m}{\mu_m} \right)_{j+\frac{1}{2}}^{n+1}, \quad 0 \leq j \leq N_r. \tag{4.3.6a}$$

For simplicity, we will assume that block $j + 1$ is upstream of block j , then Eq. 4.3.6a becomes

$$T_{m,j+\frac{1}{2}}^{n+1} = U_{j+\frac{1}{2}} \left(\frac{\rho_m}{\mu_m} \right)_{j+1}^{n+1}, \quad 0 \leq j \leq N_r - 1 \tag{4.3.6b}$$

and

$$T_{m, N_r + \frac{1}{2}}^{n+1} = U_{N_r + \frac{1}{2}} \left(\frac{\rho_m}{\mu_m} \right)_{r_e}^{n+1} \quad (4.3.6c)$$

For $j = 1$, Eq. 4.3.5 is modified as

$$\begin{aligned} & \left[T_{m, \frac{1}{2}}^{n+1} \right] p_{wf}^{n+1} \\ & - \left[T_{m, \frac{1}{2}}^{n+1} + T_{m, \frac{3}{2}}^{n+1} + \frac{V_{p1}}{C_1 \Delta t} \left(\frac{\partial \rho_m}{\partial p} \right)_1^{n+1} \right] p_1^{n+1} \\ & + \left[T_{m, \frac{3}{2}}^{n+1} \right] p_2^{n+1} \\ & = - \frac{V_{p1}}{C_1 \Delta t} \left(\frac{\partial \rho_m}{\partial p} \right)_1^{n+1} p_1^n, \end{aligned} \quad (4.3.7)$$

The inner boundary condition, Eq. 4.1.19, may be rewritten as follows

$$C_1 U_{\frac{1}{2}} \left(\rho_m \frac{k_{rm}}{\mu_m} \right)_1^{n+1} (p_1^{n+1} - p_{\frac{1}{2}}^{n+1}) = q_t, \quad (4.3.8)$$

Eq. 4.3.8 is the additional equation needed to solve for the flowing wellbore pressure, i.e., p_{wf} .

The outer boundary equations are also incorporated directly in Eq. 4.3.5 for $j = N_r$. For a sealed outer boundary, we set $U_{N_r + \frac{1}{2}} = 0$, or, equivalently $T_{m, N_r + \frac{1}{2}} = 0$, thus, the $j = N_r$ analogous of Eq. 4.3.5 is

$$\begin{aligned} & \left[T_{m, N_r - \frac{1}{2}}^{n+1} \right] p_{N_r - 1}^{n+1} \\ & - \left[T_{m, N_r - \frac{1}{2}}^{n+1} + \frac{V_{pN_r}}{C_1 \Delta t} \left(\frac{\partial \rho_m}{\partial p} \right)_{N_r}^{n+1} \right] p_{N_r}^{n+1} \\ & = - \frac{V_{pN_r}}{C_1 \Delta t} \left(\frac{\partial \rho_m}{\partial p} \right)_{N_r}^{n+1} p_{N_r}^n, \end{aligned} \quad (4.3.9)$$

whereas, for a constant outer boundary pressure, using Eq. 4.1.23 in Eq. 4.3.5 (with $j = 1$) yields

$$\begin{aligned}
& \left[T_{m,N_r-\frac{1}{2}}^{n+1} \right] p_{N_r-1}^{n+1} \\
& - \left[T_{m,N_r-\frac{1}{2}}^{n+1} + T_{m,N_r+\frac{1}{2}}^{n+1} + \frac{V_{pN_r}}{C_1 \Delta t} \left(\frac{\partial \rho_m}{\partial p} \right)_{N_r}^{n+1} \right] p_{N_r}^{n+1} \\
& = - \frac{V_{pN_r}}{C_1 \Delta t} \left(\frac{\partial \rho_m}{\partial p} \right)_{N_r}^{n+1} p_{N_r}^n - T_{m,N_r+\frac{1}{2}}^{n+1} p_e,
\end{aligned} \tag{4.3.10}$$

The nonlinearities that appear in the pressure-dependent terms, i.e., $T_{j+\frac{1}{2}}^{n+1}$ and $\left(\frac{\partial \rho_m}{\partial p} \right)_j^{n+1}$, in Eq. 4.3.5 may be treated by using an iterative scheme where these terms are evaluated at the old iteration level, i.e., through the following matrix problem,

$$J^{n+1,k} \mathbf{P}^{n+1,k+1} = \mathbf{R}, \tag{4.3.11}$$

where k denotes the iteration level, J is a tridiagonal matrix containing the coefficients of pressure in Eqs. 4.3.5, 4.3.9 and 4.3.10, \mathbf{R} is the right-hand side vector and \mathbf{P} is the pressure solution vector

$$\mathbf{P} = [p_{wf}, p_1, p_2, \dots, p_{N_r}]^t. \tag{4.3.12}$$

The transmissibility terms are updated at each iteration by evaluating the densities $\rho_{m,j}^{n+1,k}$ and viscosities $\mu_{m,j}^{n+1,k}$ at the latest value of pressure with the known (fixed) fluid composition via an equation of state. At the first iteration, $\left(\frac{\partial \rho_m}{\partial p} \right)_j^{n+1,k}$ is evaluated analytically using an equation of state (see Appendix D). Thereafter, the following chord slope expression is employed, provided $p_j^{n+1,k} \neq p_j^n$.

$$\left(\frac{\partial \rho_m}{\partial p} \right)_j^{n+1,k} \approx \left(\frac{\rho_m(p_j^{n+1,k}) - \rho_m(p_j^n)}{p_j^{n+1,k} - p_j^n} \right). \tag{4.3.13}$$

Note that the finite difference approximation

$$\left(\frac{\partial \rho_m}{\partial t} \right)_j^{n+1,k} \approx \frac{\rho_m(p_j^{n+1,k}) - \rho_m(p_j^n)}{\Delta t}. \tag{4.3.14}$$

is rigorously honored at convergence, when Eq. 4.3.13 is used for the derivative of density with respect to pressure, i.e.,

$$\begin{aligned}
 \left(\frac{\partial \rho_m}{\partial t}\right)_j &= \left(\frac{\partial \rho_m}{\partial p}\right)_j \left(\frac{\partial p}{\partial t}\right)_j \\
 &\approx \left(\frac{\rho_m(p_j^{n+1,k}) - \rho_m(p_j^n)}{p_j^{n+1,k} - p_j^n}\right) \left(\frac{p_j^{n+1,k+1} - p_j^n}{\Delta t}\right) \\
 &= \frac{\rho_m(p_j^{n+1}) - \rho_m(p_j^n)}{\Delta t}.
 \end{aligned} \tag{4.3.15}$$

This iteration process is performed until the differences in absolute value between successive pressure values are less than some specified tolerance. We always use the values of the variables at time level n as the starting guess to begin the iterations for any time step. This completes the outline of the solution method for a single-phase fluid with fixed composition equal to the initial composition.

4.4 Two-Phase Flow Formulation, $j \in N_{r2}$

Throughout, we assume that the adjacent blocks also contain a two-phase fluid. This case clearly represents the most complex situation which can occur at a grid-block. We recall the set of changing variables, Q_j , in a block j containing a two-phase mixture is defined as

$$Q_j = \{p, S_o, S_g, \{x_i\}_{i=1}^{N_c}, \{y_i\}_{i=1}^{N_c}\}_j^{n+1}.$$

We define the following subsets of Q_j :

$$\left\{ \begin{array}{l} Q'_j = \{p, S_g, \{x_i\}_{i=2}^{N_c-1}\}_j^{n+1} ; \\ Q''_j = \{\{y_i\}_{i=2}^{N_c}, x_{N_c}\}_j^{n+1} \end{array} \right\} \text{ or } \left\{ \begin{array}{l} Q'_j = \{p, S_g, \{y_i\}_{i=2}^{N_c-1}\}_j^{n+1} ; \\ Q''_j = \{\{x_i\}_{i=2}^{N_c}, y_{N_c}\}_j^{n+1} \end{array} \right\},$$

for $N_c > 2$ and

$$\left\{ \begin{array}{l} Q'_j = \{p, S_g\}_j^{n+1} ; \\ Q''_j = \{x_2, y_2\}_j^{n+1} \end{array} \right\}$$

for a binary system.

We refer to Q'_j as the set of primary variables which are obtained by solving the flow equations. The set Q''_j is referred to as the set of secondary variables. For $N_c > 2$, this set includes the block pressure, gas saturation and $N_c - 2$ mole fraction compositions which may be arbitrarily chosen. Without loss of generality, we assume that this set contains the variable $\{p, S_g, \{y_i\}_{i=2}^{N_c-1}\}_j^{n+1}$. The remaining mole fraction compositions contained in Q''_j form a set of "equilibrium" variables to be determined using the thermodynamic equilibrium equations. In the remainder of this work, this set will be assumed to contain $\{\{x_i\}_{i=2}^{N_c}, y_{N_c}\}_j^{n+1}$. In the first step of our solution procedure, we explicitly incorporate the thermodynamic equilibrium equations into the flow equations. Our procedure ensures that upon convergence to the solution for the set of primary variables, Q'_j , the "equilibrium" variables solution is automatically satisfied, i.e., Q''_j is "implicit" to the solution of the flow

equations; that is, the solution of the flow equations automatically ensures that we also solve for the variables in the set Q''_j .

4.4.1 Multicomponent Systems ($N_c > 2$)

For binary mixtures, the solution procedure is slightly different than for multicomponent mixtures. Since the latter case may easily degenerate to the binary mixture case, we first choose to present the multicomponent case.

4.4.1.a Treatment of the Phase Equilibrium Equations

One of the keys to our method lies in the way we treat the nonlinear thermodynamic equilibrium constraints.

Since we will assume that for any block j where two phases coexist, the flow equations are solved for the set of primary variables $\{p, S_g, \{y_i\}_{i=2}^{N_c-1}\}_j^{n+1}$, we will use a new discretized version of the equations of thermodynamic equilibrium, (Eq. 4.1.18), to generate the N_c remaining variables, $\{x_{i,j}\}_{i=2}^{N_c}$ and $y_{N_c,j}$.

Since the phase fugacity function $f_{i,m,j}$ of component i in phase m at any two-phase block j is continuously differentiable, we can expand it as a first order Taylor's series about any equilibrium point, $(p_j^n, \{x_{i,m,j}^*\}_{i=2}^{N_c})$. We choose this point to be at the old time level n where phase equilibrium has been achieved. Thus, it follows that

$$f_{i,L,j}^{n+1} = f_{i,L,j}^n + \left(\frac{\partial f_{i,L,j}}{\partial p_j} \right)_{\{x_k^n\}_{k=2}^{N_c}} (p_j^{n+1} - p_j^n) + \sum_{l=2}^{N_c} \left(\frac{\partial f_{i,L,j}}{\partial x_{l,j}} \right)_{x_{k,j}^n, p_j^n, k \neq 1, l} (x_{l,j}^{n+1} - x_{l,j}^n) + O(\Delta t^2), \quad (4.4.1a)$$

and

$$f_{i,V,j}^{n+1} = f_{i,V,j}^n + \left(\frac{\partial f_{i,V,j}}{\partial p_j} \right)_{\{y_k^n\}_{k=2}^{N_c}} (p_j^{n+1} - p_j^n) + \sum_{l=2}^{N_c} \left(\frac{\partial f_{i,V,j}}{\partial y_{l,j}} \right)_{y_{k,j}^n, p_j^n, k \neq 1, l} (y_{l,j}^{n+1} - y_{l,j}^n) + O(\Delta t^2), \quad (4.4.1b)$$

where $\left(\frac{\partial f_{i,m,i}}{\partial p_j}\right)_{\{x_{k,m}^n\}_{k=2}^{N_c}}$ is the partial derivative of the fugacity of component i in phase m with respect to pressure and $\left(\frac{\partial f_{i,m,i}}{\partial x_{l,m,j}}\right)_{x_{k,m,j}^n, p_j^n}_{k \neq 1, l}$ is the partial derivative of the fugacity of component i in phase m with respect to the mole fraction composition of component l in phase m . Analytical expressions for both derivatives are evaluated using the generalized equation of state. The truncation error associated with these expansions is $O(\Delta t^2)$, whereas, the time truncation error associated with the flow difference equations (Eqs. 4.1.12 and 4.1.15) is $O(\Delta t)$. This indicates that as the time step size is reduced, the time truncation error associated with Eqs. 4.4.1a and 4.4.1b diminishes more rapidly than the time truncation error associated with the discrete flow equations. The thermodynamic equilibrium criterion, Eq. 4.1.18, may be expressed by subtracting Eq. 4.4.1b from Eq. 4.4.1a,

$$\left[\left(\frac{\partial f_{i,L,j}}{\partial p_j}\right)^n - \left(\frac{\partial f_{i,V,j}}{\partial p_j}\right)^n\right] \Delta_t p_j + \sum_{l=2}^{N_c} \left(\frac{\partial f_{i,L,j}}{\partial x_{l,j}}\right)^n \Delta_t x_{l,j} - \left(\frac{\partial f_{i,V,j}}{\partial y_{l,j}}\right)^n \Delta_t y_{l,j} = 0, \quad (4.4.2)$$

where we have employed the fact that $f_{i,L,j}^n = f_{i,V,j}^n$, $1 \leq i \leq N_c$, since thermodynamic equilibrium was achieved at the old time level n at block j . Note that for simplicity of notation, the parameters that remain constant during a partial differentiation process are omitted in Eq. 4.4.2 and throughout the remainder of this work. Eq. 4.4.2 is a key equation in our new solution procedure. It allows us to express the changes in the N_c variables, $\{\Delta_t x_{i,j}\}_{i=2}^{N_c}$ and $\Delta_t y_{N_c}$ over a time step explicitly in terms of changes in the set of $N_c - 1$ primary variables, $\{\Delta_t y_{i,j}\}_{i=2}^{N_c-1}$ and $\Delta_t p_j$. As is shown below, by incorporating these relations into the finite difference approximations of the flow equations, we effectively obtain a “fully-implicit” finite difference scheme.

Eq. 4.4.2 represents an $N_c \times N_c$ matrix problem of the form

$$M_j \Delta_t \mathbf{X}_j = \mathbf{B}_j,$$

or equivalently,

$$\Delta_t \mathbf{X}_j = M_j^{-1} \mathbf{B}_j, \quad (4.4.3)$$

where M_j^{-1} denotes the inverse matrix of M_j . According to Eq. 4.4.3, the vector

$$\Delta_t \mathbf{X}_j = (\Delta_t x_{2,j}, \Delta_t x_{3,j}, \dots, \Delta_t x_{N_c,j}, \Delta_t y_{N_c,j})^t \quad (4.4.4)$$

can be evaluated by direct matrix multiplication. The matrix M_j and the right-hand side column vector B_j are defined, respectively, as follows

$$M_j = \begin{pmatrix} \left(\frac{\partial f_{1,L,j}}{\partial x_{2,j}} \right)^n & \left(\frac{\partial f_{1,L,j}}{\partial x_{3,j}} \right)^n & \dots & \left(\frac{\partial f_{1,L,j}}{\partial x_{N_c,j}} \right)^n & - \left(\frac{\partial f_{1,V,j}}{\partial y_{N_c,j}} \right)^n \\ \left(\frac{\partial f_{2,L,j}}{\partial x_{2,j}} \right)^n & \left(\frac{\partial f_{2,L,j}}{\partial x_{3,j}} \right)^n & \dots & \left(\frac{\partial f_{2,L,j}}{\partial x_{N_c,j}} \right)^n & - \left(\frac{\partial f_{2,V,j}}{\partial y_{N_c,j}} \right)^n \\ \vdots & \vdots & \ddots & \vdots & \vdots \\ \left(\frac{\partial f_{N_c,L,j}}{\partial x_{2,j}} \right)^n & \left(\frac{\partial f_{N_c,L,j}}{\partial x_{3,j}} \right)^n & \dots & \left(\frac{\partial f_{N_c,L,j}}{\partial x_{N_c,j}} \right)^n & - \left(\frac{\partial f_{N_c,V,j}}{\partial y_{N_c,j}} \right)^n \end{pmatrix} \quad (4.4.5a)$$

and

$$\mathbf{B}_j = \begin{pmatrix} - \left[\left(\frac{\partial f_{1,L,j}}{\partial p_j} \right)^n - \left(\frac{\partial f_{1,V,j}}{\partial p_j} \right)^n \right] \Delta_t p_j + \sum_{l=2}^{N_c-1} \left(\frac{\partial f_{1,V,j}}{\partial y_{l,j}} \right)^n \Delta_t y_{l,j} \\ - \left[\left(\frac{\partial f_{2,L,j}}{\partial p_j} \right)^n - \left(\frac{\partial f_{2,V,j}}{\partial p_j} \right)^n \right] \Delta_t p_j + \sum_{l=2}^{N_c-1} \left(\frac{\partial f_{2,V,j}}{\partial y_{l,j}} \right)^n \Delta_t y_{l,j} \\ \vdots \\ - \left[\left(\frac{\partial f_{N_c,L,j}}{\partial p_j} \right)^n - \left(\frac{\partial f_{N_c,V,j}}{\partial p_j} \right)^n \right] \Delta_t p_j + \sum_{l=2}^{N_c-1} \left(\frac{\partial f_{N_c,V,j}}{\partial y_{l,j}} \right)^n \Delta_t y_{l,j} \end{pmatrix} \quad (4.4.5b)$$

Note that Eq. 4.4.3 explicitly relates the N_c variables in Q_j'' to $N_c - 1$ primary variables in Q_j' , since the coefficients of the matrix M_j are evaluated at the old time level. Note that the matrix M_j is inverted only once per time step.

For ease of notation, we define the following

$$\hat{b}_{i,j} = - \left[\left(\frac{\partial f_{i,L,j}}{\partial p_j} \right)^n - \left(\frac{\partial f_{i,V,j}}{\partial p_j} \right)^n \right], \quad (4.4.6a)$$

and

$$\hat{c}_{i,l,j} = \left(\frac{\partial f_{i,V,j}}{\partial y_{l,j}} \right)^n. \quad (4.4.6b)$$

We also let $M_j^{-1} = [\hat{a}_{i,k,j}]$ denote the inverse of M_j ; so $\hat{a}_{i,k,j}$ denotes the element in the i^{th} row and k^{th} column of M_j^{-1} . Thus, the solution of Eq. 4.4.3 is computed as follows

$$\Delta_t x_{i+1,j} = \left(\sum_{k=1}^{N_c} \hat{a}_{i,k,j} \hat{b}_{k,j} \right) \Delta_t p_j + \sum_{k=1}^{N_c} \hat{a}_{i,k,j} \sum_{l=2}^{N_c-1} \hat{c}_{k,l,j} \Delta_t y_{l,j}, \quad 1 \leq i \leq N_c - 1, \quad (4.4.6c)$$

and

$$\Delta_t y_{N_c,j} = \left(\sum_{k=1}^{N_c} \hat{a}_{N_c,k,j} \hat{b}_{k,j} \right) \Delta_t p_j + \sum_{k=1}^{N_c} \hat{a}_{N_c,k,j} \sum_{l=2}^{N_c-1} \hat{c}_{k,l,j} \Delta_t y_{l,j}. \quad (4.4.6d)$$

The thermodynamic equilibrium condition, i.e., the $N_c \times N_c$ matrix problem, Eq. 4.4.3, is solved at every iteration at each block where two phases coexist, until convergence has been achieved. We emphasize that the matrix entries for M_j and M_j^{-1} are computed only once every time step and the inverse matrix M_j^{-1} is stored. However, the right-hand side vector \mathbf{B}_j must be recomputed at every iteration because it contains terms involving primary variables, i.e., $\Delta_t p_j$ and $\{\Delta_t y_{l,j}\}_{l=2}^{N_c-1}$.

In our scheme, we choose to solve the overall mass balance equation (Eq. 4.1.15) and $N_c - 1$ component equations (Eq. 4.1.12), $i = 2, \dots, N_c - 1$ for the set of primary variables

$$Q'_j = \{p, \Delta_t S_g, \{\Delta_t y_i\}_{i=2}^{N_c-1}\}_j^{n+1}.$$

The phase density-mobility terms in the overall equation, Eq. 4.1.15 and component equations, Eq. 4.1.12, are, respectively, given by

$$\left(\rho_m \frac{k_{rm}}{\mu_m} \right)_{j+\frac{1}{2}}^{n+1}, \quad m = o, g \quad (4.4.7a)$$

and

$$\left(\rho_m \frac{k_{rm}}{\mu_m} x_{i,m} \right)_{j+\frac{1}{2}}^{n+1}, \quad m = o, g, \quad 2 \leq i \leq N_c. \quad (4.4.7b)$$

Since Eq. 4.4.3 expresses all secondary variables in terms of the primary variable set, the expressions in Eqs. 4.4.7a and 4.4.7b are effectively known as functions of the primary variables, i.e., pressure, saturation and the vapor mole fractions, y_i , $2 \leq i \leq N_c - 1$. In the following, we describe how we treat nonlinearities in the relative permeability term and in mole fraction composition terms.

4.4.1.b Overall Mass Balance Equation

In the overall mass balance equation, (similar to the single-phase flow equation, Eq. 4.3.3), the phase density and viscosity appearing in Eq. 4.4.7a are evaluated at the old iteration level, whereas the relative permeability is linearized as described below.

Since we assume the relative permeability of phase m , i.e., k_{rm} , is a single-valued function of gas saturation, S_g , we may expand it in the manner suggested by Letkman and Ridings⁴³, i.e.,

$$k_{rm,j+\frac{1}{2}}^{n+1} \approx k_{rm,j+\frac{1}{2}}^n + \left(\frac{dk_{rm}}{dS_g} \right)_{j+\frac{1}{2}}^{n,k} (\Delta_t S_g)_{j+\frac{1}{2}}, \quad m = o, g, \quad (4.4.8)$$

where

$$(\Delta_t S_g)_{j+\frac{1}{2}} = S_{g,j+\frac{1}{2}}^{n+1,k+1} - S_{g,j+\frac{1}{2}}^n. \quad (4.4.9a)$$

Similar to our discussion for the single-phase case (section 4.3), we assume for simplicity that gridblock $j+1$ is upstream of gridblock j . In this case, we use upstream

weighting as defined by Eqs. 4.3.6b and 4.3.6c. We also upstream weight the relative permeability term, i.e., $k_{rm,j+\frac{1}{2}}$ will be replaced by $k_{rm,j+1}$ and $(\Delta_t S_g)_{j+\frac{1}{2}}$ by $(\Delta_t S_g)_{j+1}$.

For the first iteration and any other iteration when $S_g^{n+1,k} = S_g^n$, we evaluate $\left(\frac{dk_{rm}}{dS_g}\right)_{j+1}^{n,k}$ as the chord slope of the input relative permeability versus saturation data at the block saturation. Otherwise, we evaluate via

$$\left(\frac{dk_{rm}}{dS_g}\right)_{j+1}^{n,k} = \left(\frac{k_{rm}^{n+1,k} - k_{rm}^n}{S_g^{n+1,k} - S_g^n}\right)_{j+1}, \quad m = o, g. \quad (4.4.9b)$$

Recall that the superscript k ($k = 1, 2, \dots$) denotes the iteration level and at convergence, Eq. 4.4.8 is an equality.

Following Letkman and Ridings⁴³, the nonlinearity that appears in the saturation change-pressure gradients products, i.e., $\Delta_t S_{g,j+1}(p_{j+1}^{n+1,k+1} - p_j^{n+1,k+1})$ and $\Delta_t S_{g,j}(p_j^{n+1,k+1} - p_{j-1}^{n+1,k+1})$, is resolved by evaluating the pressure terms at the old iteration level, k . We introduce the following notation

$$\tilde{T}_{m,j+\frac{1}{2}}^{n+1,k} = T_{m,j+\frac{1}{2}}^{n+1,k} k_{rm}^n, \quad (4.4.10a)$$

$$D_{m,j+\frac{1}{2}}^{n+1,k} = T_{m,j+\frac{1}{2}}^{n+1,k} \left(\frac{dk_{rm}}{dS_g}\right)_{j+1}^{n,k} (p_{j+1}^{n+1,k} - p_j^{n+1,k}), \quad (4.4.10b)$$

for $0 \leq j \leq N_r - 1$ and $m = o, g$, where $T_{m,j+\frac{1}{2}}^{n+1,k}$ is defined by Eqs. 4.3.6a and 4.3.6b. Using Eq. 4.4.8 (with upstream weighting) in Eq. 4.1.15, and using the notation of Eqs. 4.4.10a and 4.4.10b in the overall mass balance equation, Eq. 4.1.15, and rearranging gives

$$\begin{aligned} & \left[\tilde{T}_{o,j-\frac{1}{2}}^{n+1,k} + \tilde{T}_{g,j-\frac{1}{2}}^{n+1,k} \right] p_{j-1}^{n+1,k+1} \\ & - \left[\tilde{T}_{o,j-\frac{1}{2}}^{n+1,k} + \tilde{T}_{g,j-\frac{1}{2}}^{n+1,k} + \tilde{T}_{o,j+\frac{1}{2}}^{n+1,k} + \tilde{T}_{g,j+\frac{1}{2}}^{n+1,k} \right] p_j^{n+1,k+1} \\ & - \left[D_{o,j-\frac{1}{2}}^{n+1,k} + D_{g,j-\frac{1}{2}}^{n+1,k} \right] \Delta_t S_{g,j} \\ & + \left[\tilde{T}_{o,j+\frac{1}{2}}^{n+1,k} + \tilde{T}_{g,j+\frac{1}{2}}^{n+1,k} \right] p_{j+1}^{n+1,k+1} \end{aligned}$$

$$\begin{aligned}
& + \left[D_{o,j+\frac{1}{2}}^{n+1,k} + D_{g,j+\frac{1}{2}}^{n+1,k} \right] \Delta_t S_{g,j+1} \\
& = \frac{V_{pj}}{C_1 \Delta t} \Delta_t (\rho_o S_o + \rho_g S_g)_j.
\end{aligned} \tag{4.4.11}$$

We now consider the finite-difference expansion of the terms which appear on the right-hand side of the overall mass balance equation, Eq. 4.4.11. We use the following expansions :

$$\Delta_t (\rho_m S_m)_j = S_{m,j}^n \Delta_t \rho_{m,j} + \rho_{m,j}^{n+1,k} \Delta_t S_{m,j}. \tag{4.4.12}$$

The term $\Delta_t \rho_{m,j}$ will also appear in the expansion of the right-hand side of the component flow equations, Eq. 4.1.12. In all cases, we will use one of the following options for evaluating $\Delta_t \rho_{m,j}$. The simplest procedure is to use

$$\Delta_t \rho_{m,j} = \rho_{m,j}^{n+1,k} - \rho_{m,j}^n. \tag{4.4.13}$$

On the other hand, we know that the phase density is function of pressure and phase composition; i.e.,

$$\rho_{m,j} = f(p_j, x_{2,m,j}, x_{3,m,j}, \dots, x_{N_c,m,j}) \tag{4.4.14}$$

and thus,

$$\left(\frac{\partial \rho_m}{\partial t} \right)_r = \left(\frac{\partial \rho_m}{\partial p} \right)_{\{x_{i,m}\}_{i=2}^{N_c}} \left(\frac{\partial p}{\partial t} \right)_r + \sum_{i=2}^{N_c} \left(\frac{\partial \rho_m}{\partial x_{i,m}} \right)_{\substack{x_{k,m,p} \\ k \neq 1,i}} \left(\frac{\partial x_{i,m}}{\partial t} \right)_r. \tag{4.4.15}$$

Eq. 4.4.15 may be approximated by

$$\Delta_t \rho_{m,j} = \left(\left(\frac{\partial \rho_m}{\partial p} \right)_{\{x_{i,m}\}_{i=2}^{N_c}} \right)_j^{n+1,k} \Delta_t p_j + \sum_{i=2}^{N_c} \left(\left(\frac{\partial \rho_m}{\partial x_{i,m}} \right)_{\substack{x_{k,m,p} \\ k \neq 1,i}} \right)_j^{n+1,k} \Delta_t x_{i,m,j}, \tag{4.4.16}$$

Note that both partial derivatives of phase density with respect to pressure and phase composition are computed analytically via the equation of state, and are

provided in Appendix D. For problems considered to date, changing from Eq. 4.4.13 to Eq. 4.4.16 did not significantly change the numerical results obtained. Thus, Eq. 4.4.13 seems preferable because its evaluation requires less computational work than is required to evaluate Eq. 4.4.16, however, for the purpose of completeness, we outline the incorporation of Eq. 4.4.16 into the flow equations, Eq. 4.1.12 and Eq. 4.4.11.

Eq. 4.4.16 contains the "equilibrium" variables $\{\Delta_t x_{i,j}\}_{i=2}^{N_c}$ for $m = o$ and $\Delta_t y_{N_c,j}$ for $m = g$. These variables are expressed in terms of the primary variables $\{\Delta_t y_{i,j}\}_{i=2}^{N_c-1}$ and $\Delta_t p_j$ as defined by Eqs. 4.4.6c and 4.4.6d, so that for $m = o$, Eq. 4.4.16 may be rewritten as

$$\Delta_t \rho_{o,j} = O_{p,j} \Delta_t p_j + \sum_{l=2}^{N_c-1} O_{y_l,j} \Delta_t y_{l,j}, \quad (4.4.17)$$

and for $m = g$, the analog equation of Eq. 4.4.17 is

$$\Delta_t \rho_{g,j} = G_{p,j} \Delta_t p_j + \sum_{l=2}^{N_c-1} G_{y_l,j} \Delta_t y_{l,j} \quad (4.4.18)$$

where $O_{p,j}$, $O_{y_l,j}$, $G_{p,j}$ and $G_{y_l,j}$ are defined as follows

$$O_{p,j} = \left(\left(\frac{\partial \rho_o}{\partial p} \right)_{\{x_i\}_{i=2}^{N_c}} \right)_j^{n+1,k} + \sum_{i=2}^{N_c} \left(\left(\frac{\partial \rho_o}{\partial x_i} \right)_{\substack{x_{k,p} \\ k \neq 1,i}} \right)_j^{n+1,k} \sum_{k=1}^{N_c} \hat{a}_{i-1,k,j} \hat{b}_{k,j}, \quad (4.4.19a)$$

$$O_{y_l,j} = \sum_{i=2}^{N_c} \left(\left(\frac{\partial \rho_o}{\partial x_i} \right)_{\substack{x_{k,p} \\ k \neq 1,i}} \right)_j^{n+1,k} \sum_{k=1}^{N_c} \hat{a}_{i-1,k,j} \hat{c}_{k,l,j}, \quad (4.4.19b)$$

$$G_{p,j} = \left(\left(\frac{\partial \rho_g}{\partial p} \right)_{\{y_i\}_{i=2}^{N_c}} \right)_j^{n+1,k} + \sum_{i=2}^{N_c} \left(\left(\frac{\partial \rho_g}{\partial y_i} \right)_{\substack{y_{k,p} \\ k \neq 1,i}} \right)_j^{n+1,k} \sum_{k=1}^{N_c} \hat{a}_{N_c,k,j} \hat{b}_{k,j}, \quad (4.4.20a)$$

and

$$G_{y_l,j} = \left(\left(\frac{\partial \rho_g}{\partial y_l} \right)_{\substack{y_{k,p} \\ k \neq 1,l}} \right)_j^{n+1,k} + \left(\left(\frac{\partial \rho_g}{\partial y_{N_c}} \right)_{\substack{y_{k,p} \\ k \neq 1,N_c}} \right)_j^{n+1,k} \sum_{k=1}^{N_c} \hat{a}_{N_c,k,j} \hat{c}_{k,l,j}. \quad (4.4.20b)$$

Using Eq. 4.4.12 for both phases, Eqs. 4.4.17 and 4.4.18 and the saturation constraint, Eq. 4.1.17, the term on the right-hand side of the overall equation, Eq. 4.4.11, may be written as

$$\begin{aligned} \Delta_t(\rho_o S_o + \rho_g S_g)_j = & \left[[S_{g,j}^n (G_{p,j} - O_{p,j}) + O_{p,j}] \Delta_t p_j \right. \\ & + \sum_{l=2}^{N_c-1} [S_{g,j}^n (G_{y_l,j} - O_{y_l,j}) + O_{y_l,j}] \Delta_t y_{l,j} \\ & \left. + (\rho_g^{n+1,k} - \rho_o^{n+1,k}) \Delta_t S_{g,j} \right]. \quad (4.4.20c) \end{aligned}$$

Using Eq. 4.4.20c into the right-hand side of the overall mass balance equation, Eq. 4.4.11, and rearranging gives

$$\begin{aligned} & \left[\tilde{T}_{o,j-\frac{1}{2}}^{n+1,k} + \tilde{T}_{g,j-\frac{1}{2}}^{n+1,k} \right] p_{j-1}^{n+1,k+1} \\ & - \left[\tilde{T}_{o,j-\frac{1}{2}}^{n+1,k} + \tilde{T}_{g,j-\frac{1}{2}}^{n+1,k} + \tilde{T}_{o,j+\frac{1}{2}}^{n+1,k} + \tilde{T}_{g,j+\frac{1}{2}}^{n+1,k} \right. \\ & \quad \left. + \frac{V_{pj}}{C_1 \Delta t} (S_{g,j}^n (G_{p,j} - O_{p,j}) + O_{p,j}) \right] p_j^{n+1,k+1} \\ & - \left[D_{o,j-\frac{1}{2}}^{n+1,k} + D_{g,j-\frac{1}{2}}^{n+1,k} - \frac{V_{pj}}{C_1 \Delta t} (\rho_{g,j}^{n+1,k} - \rho_{o,j}^{n+1,k}) \right] \Delta_t S_{g,j} \\ & - \frac{V_{pj}}{C_1 \Delta t} \sum_{l=2}^{N_c-1} [S_{g,j}^n (G_{y_l,j} - O_{y_l,j}) + O_{y_l,j}] \Delta_t y_{l,j} \\ & + \left[\tilde{T}_{o,j+\frac{1}{2}}^{n+1,k} + \tilde{T}_{g,j+\frac{1}{2}}^{n+1,k} \right] p_{j+1}^{n+1,k+1} \\ & + \left[D_{o,j+\frac{1}{2}}^{n+1,k} + D_{g,j+\frac{1}{2}}^{n+1,k} \right] \Delta_t S_{g,j+1} \\ & = - \frac{V_{pj}}{C_1 \Delta t} [S_{g,j}^n (G_{p,j} - O_{p,j}) + O_{p,j}] p_j^n, \quad (4.4.21) \end{aligned}$$

4.4.1.c Component Flow Equations

The phase relative permeability terms appearing in the component flow equations, Eq. 4.1.12, are linearized the same way as for the overall mass balance equation, i.e.,

$$\begin{aligned}
& \left[\tilde{T}_{o,j-\frac{1}{2}}^{n+1,k} x_{i,j-\frac{1}{2}}^{n+1,k+1} + \tilde{T}_{g,j-\frac{1}{2}}^{n+1,k} y_{i,j-\frac{1}{2}}^{n+1,k+1} \right] p_{j-1}^{n+1,k+1} \\
& - \left[\tilde{T}_{o,j-\frac{1}{2}}^{n+1,k} x_{i,j-\frac{1}{2}}^{n+1,k+1} + \tilde{T}_{g,j-\frac{1}{2}}^{n+1,k} y_{i,j-\frac{1}{2}}^{n+1,k+1} \right. \\
& \quad \left. + \tilde{T}_{o,j+\frac{1}{2}}^{n+1,k} x_{i,j+\frac{1}{2}}^{n+1,k+1} + \tilde{T}_{g,j+\frac{1}{2}}^{n+1,k} y_{i,j+\frac{1}{2}}^{n+1,k+1} \right] p_j^{n+1,k+1} \\
& - \left[D_{o,j-\frac{1}{2}}^{n+1,k} x_{i,j-\frac{1}{2}}^{n+1,k+1} + D_{g,j-\frac{1}{2}}^{n+1,k} y_{i,j-\frac{1}{2}}^{n+1,k+1} \right] \Delta_t S_{g,j} \\
& + \left[\tilde{T}_{o,j+\frac{1}{2}}^{n+1,k} x_{i,j+\frac{1}{2}}^{n+1,k+1} + \tilde{T}_{g,j+\frac{1}{2}}^{n+1,k} y_{i,j+\frac{1}{2}}^{n+1,k+1} \right] p_{j+1}^{n+1,k+1} \\
& + \left[D_{o,j+\frac{1}{2}}^{n+1,k} x_{i,j+\frac{1}{2}}^{n+1,k+1} + D_{g,j+\frac{1}{2}}^{n+1,k} y_{i,j+\frac{1}{2}}^{n+1,k+1} \right] \Delta_t S_{g,j+1} \\
& = \frac{V_{pj}}{C_1 \Delta t} \Delta_t (x_i \rho_o S_o + y_i \rho_g S_g)_j, \quad 2 \leq i \leq N_c. \tag{4.4.22}
\end{aligned}$$

The variables x_i and y_i are evaluated by upstream weighting, similar to the relative permeability terms.

The component flow equations, Eq. 4.4.22, involve nonlinear terms of the form $x_{i,m}^{n+1,k+1} p^{n+1,k+1}$ and $x_{i,m}^{n+1,k+1} \Delta_t S_g$. As a first step in linearizing such terms, we introduce the following identities:

$$\tilde{T}_{m,j+\frac{1}{2}}^{n+1,k} x_{i,m,j+1}^{n+1,k+1} = \tilde{T}_{m,j+\frac{1}{2}}^{n+1,k} \Delta_t x_{i,m,j+1} + \tilde{T}_{m,j+\frac{1}{2}}^{n+1,k} x_{i,m,j+1}^n, \tag{4.4.23a}$$

and

$$D_{m,j+\frac{1}{2}}^{n+1,k} x_{i,m,j+1}^{n+1,k+1} = D_{m,j+\frac{1}{2}}^{n+1,k} \Delta_t x_{i,m,j+1} + D_{m,j+\frac{1}{2}}^{n+1,k} x_{i,m,j+1}^n \tag{4.4.23b}$$

where \tilde{T}_m and D_m are given by Eqs. 4.4.10a and 4.4.10b. Using these identities (Eqs. 4.4.23a and 4.4.23b) in the component flow equations, Eq. 4.4.22, yields

$$\begin{aligned}
& \left[\tilde{T}_{o,j-\frac{1}{2}}^{n+1,k} x_{i,j}^n + \tilde{T}_{g,j-\frac{1}{2}}^{n+1,k} y_{i,j}^n \right] p_{j-1}^{n+1,k+1} \\
& + \left[\tilde{T}_{o,j-\frac{1}{2}}^{n+1,k} \Delta_t x_{i,j} + \tilde{T}_{g,j-\frac{1}{2}}^{n+1,k} \Delta_t y_{i,j} \right] p_{j-1}^{n+1,k+1} \\
& - \left[\tilde{T}_{o,j-\frac{1}{2}}^{n+1,k} x_{i,j}^n + \tilde{T}_{g,j-\frac{1}{2}}^{n+1,k} y_{i,j}^n + \tilde{T}_{o,j+\frac{1}{2}}^{n+1,k} x_{i,j+1}^n + \tilde{T}_{g,j+\frac{1}{2}}^{n+1,k} y_{i,j+1}^n \right] p_j^{n+1,k+1} \\
& - \left[\tilde{T}_{o,j-\frac{1}{2}}^{n+1,k} \Delta_t x_{i,j} + \tilde{T}_{g,j-\frac{1}{2}}^{n+1,k} \Delta_t y_{i,j} \right. \\
& \quad \left. + \tilde{T}_{o,j+\frac{1}{2}}^{n+1,k} \Delta_t x_{i,j+1} + \tilde{T}_{g,j+\frac{1}{2}}^{n+1,k} \Delta_t y_{i,j+1} \right] p_j^{n+1,k+1} \\
& - \left[D_{o,j-\frac{1}{2}}^{n+1,k} x_{i,j}^n + D_{g,j-\frac{1}{2}}^{n+1,k} y_{i,j}^n \right] \Delta_t S_{g,j} \\
& - \left[D_{o,j-\frac{1}{2}}^{n+1,k} \Delta_t x_{i,j} + D_{g,j-\frac{1}{2}}^{n+1,k} \Delta_t y_{i,j} \right] \Delta_t S_{g,j} \\
& + \left[\tilde{T}_{o,j+\frac{1}{2}}^{n+1,k} x_{i,j+1}^n + \tilde{T}_{g,j+\frac{1}{2}}^{n+1,k} y_{i,j+1}^n \right] p_{j+1}^{n+1,k+1} \\
& + \left[\tilde{T}_{o,j+\frac{1}{2}}^{n+1,k} \Delta_t x_{i,j+1} + \tilde{T}_{g,j+\frac{1}{2}}^{n+1,k} \Delta_t y_{i,j+1} \right] p_{j+1}^{n+1,k+1} \\
& + \left[D_{o,j+\frac{1}{2}}^{n+1,k} x_{i,j+1}^n + D_{g,j+\frac{1}{2}}^{n+1,k} y_{i,j+1}^n \right] \Delta_t S_{g,j+1} \\
& + \left[D_{o,j+\frac{1}{2}}^{n+1,k} \Delta_t x_{i,j+1} + D_{g,j+\frac{1}{2}}^{n+1,k} \Delta_t y_{i,j+1} \right] \Delta_t S_{g,j+1} \\
& = \frac{V_{pj}}{C_1 \Delta t} \Delta_t (x_i \rho_o S_o + y_i \rho_g S_g)_j, \quad 2 \leq i \leq N_c. \tag{4.4.24a}
\end{aligned}$$

The first terms of both equations 4.4.23a and 4.4.23b, $\Delta_t x_{i,m}$, are multiplied by the primary variables, $p^{n+1,k+1}$ and $\Delta_t S_g$, respectively as is shown by Eq. 4.4.24a. To overcome these new nonlinearities, we suggest that pressure terms be evaluated at the old iteration level, k , and that $\Delta_t S_g$ be replaced by $\delta_t S_g = S_g^{n+1,k} - S_g^n$, i.e., we use the approximations $\Delta_t x_{i,m} p^{n+1,k+1} = \Delta_t x_{i,m} p^{n+1,k}$ and $\Delta_t x_{i,m} \Delta_t S_g = \Delta_t x_{i,m} \delta_t S_g$. Thus, Eq. 4.4.24a becomes

$$\begin{aligned}
& \left[\tilde{T}_{o,j-\frac{1}{2}}^{n+1,k} x_{i,j}^n + \tilde{T}_{g,j-\frac{1}{2}}^{n+1,k} y_{i,j}^n \right] p_{j-1}^{n+1,k+1} \\
& + \left[\tilde{T}_{o,j-\frac{1}{2}}^{n+1,k} (p_{j-1}^{n+1,k} - p_j^{n+1,k}) - D_{o,j-\frac{1}{2}}^{n+1,k} \delta_t S_{g,j} \right] \Delta_t x_{i,j} \\
& + \left[\tilde{T}_{g,j-\frac{1}{2}}^{n+1,k} (p_{j-1}^{n+1,k} - p_j^{n+1,k}) - D_{g,j-\frac{1}{2}}^{n+1,k} \delta_t S_{g,j} \right] \Delta_t y_{i,j}
\end{aligned}$$

$$\begin{aligned}
& - \left[\tilde{T}_{o,j-\frac{1}{2}}^{n+1,k} x_{i,j}^n + \tilde{T}_{g,j-\frac{1}{2}}^{n+1,k} y_{i,j}^n + \tilde{T}_{o,j+\frac{1}{2}}^{n+1,k} x_{i,j+1}^n + \tilde{T}_{g,j+\frac{1}{2}}^{n+1,k} y_{i,j+1}^n \right] p_j^{n+1,k+1} \\
& - \left[D_{o,j-\frac{1}{2}}^{n+1,k} x_{i,j}^n + D_{g,j-\frac{1}{2}}^{n+1,k} y_{i,j}^n \right] \Delta_t S_{g,j} \\
& + \left[\tilde{T}_{o,j+\frac{1}{2}}^{n+1,k} x_{i,j+1}^n + \tilde{T}_{g,j+\frac{1}{2}}^{n+1,k} y_{i,j+1}^n \right] p_{j+1}^{n+1,k+1} \\
& + \left[D_{o,j+\frac{1}{2}}^{n+1,k} x_{i,j+1}^n + D_{g,j+\frac{1}{2}}^{n+1,k} y_{i,j+1}^n \right] \Delta_t S_{g,j+1} \\
& + \left[\tilde{T}_{o,j+\frac{1}{2}}^{n+1,k} (p_{j+1}^{n+1,k} - p_j^{n+1,k}) + D_{o,j+\frac{1}{2}}^{n+1,k} \delta_t S_{g,j+1} \right] \Delta_t x_{i,j+1} \\
& + \left[\tilde{T}_{g,j+\frac{1}{2}}^{n+1,k} (p_{j+1}^{n+1,k} - p_j^{n+1,k}) + D_{g,j+\frac{1}{2}}^{n+1,k} \delta_t S_{g,j+1} \right] \Delta_t y_{i,j+1} \\
& = \frac{V_{pj}}{C_1 \Delta t} \Delta_t (x_i \rho_o S_o + y_i \rho_g S_g)_j, \quad 2 \leq i \leq N_c. \tag{4.4.24b}
\end{aligned}$$

Eq. 4.4.24b may be rewritten as

$$\begin{aligned}
& \left[\hat{T}_{i,j-\frac{1}{2}} \right] p_{j-1}^{n+1,k+1} \\
& - \left[\hat{T}_{i,j-\frac{1}{2}} + \hat{T}_{i,j+\frac{1}{2}} \right] p_j^{n+1,k+1} \\
& - \left[\hat{D}_{i,j-\frac{1}{2}} \right] \Delta_t S_{g,j} \\
& + \left[\hat{A}_{o,j-\frac{1}{2}} \right] \Delta_t x_{i,j} \\
& + \left[\hat{A}_{g,j-\frac{1}{2}} \right] \Delta_t y_{i,j} \\
& + \left[\hat{T}_{i,j+\frac{1}{2}} \right] p_{j+1}^{n+1,k+1} \\
& + \left[\hat{D}_{i,j+\frac{1}{2}} \right] \Delta_t S_{g,j+1} \\
& + \left[\hat{A}_{o,j+\frac{1}{2}} \right] \Delta_t x_{i,j+1} + \left[\hat{A}_{g,j+\frac{1}{2}} \right] \Delta_t y_{i,j+1} \\
& = \frac{V_{pj}}{C_1 \Delta t} \Delta_t (x_i \rho_o S_o + y_i \rho_g S_g)_j, \quad 2 \leq i \leq N_c. \tag{4.4.25}
\end{aligned}$$

where

$$\hat{T}_{i,j+\frac{1}{2}} = \tilde{T}_{o,j+\frac{1}{2}}^{n+1,k} x_{i,j+1}^n + \tilde{T}_{g,j+\frac{1}{2}}^{n+1,k} y_{i,j+1}^n, \tag{4.4.26a}$$

$$\hat{D}_{i,j+\frac{1}{2}} = D_{o,j+\frac{1}{2}}^{n+1,k} x_{i,j+1}^n + D_{g,j+\frac{1}{2}}^{n+1,k} y_{i,j+1}^n, \tag{4.4.26b}$$

$$\hat{A}_{m,j-\frac{1}{2}} = \left[T_{m,j-\frac{1}{2}}^{n+1,k} (p_{j-1}^{n+1,k} - p_j^{n+1,k}) - D_{m,j-\frac{1}{2}}^{n+1,k} \delta_t S_{g,j} \right], \quad m = o, g, \quad (4.4.26c)$$

and

$$\hat{A}_{m,j+\frac{1}{2}} = \left[T_{m,j+\frac{1}{2}}^{n+1,k} (p_{j+1}^{n+1,k} - p_j^{n+1,k}) - D_{m,j+\frac{1}{2}}^{n+1,k} \delta_t S_{g,j+1} \right], \quad m = o, g. \quad (4.4.26d)$$

The right-hand side of Eq. 4.4.25 is expanded as follows:

$$\Delta_t(x_{i,m} \rho_m S_m)_j = S_{m,j}^n \Delta_t(\rho_m x_{i,m})_j + (\rho_m x_{i,m})_j^{n+1,k} \Delta_t S_{m,j}, \quad m = o, g. \quad (4.4.27a)$$

Since the first term in Eq. 4.4.27a contains the time variation of the primary and "equilibrium" variables $x_{i,m}$, Eq. 4.4.27a may further be expanded as

$$\begin{aligned} \Delta_t(x_{i,m} \rho_m S_m)_j &= S_{m,j}^n \left(x_{i,m,j}^n \Delta_t \rho_{m,j} + \rho_{m,j}^{n+1,k} \Delta_t x_{i,m,j} \right) \\ &\quad + (\rho_m x_{i,m})_j^{n+1,k} \Delta_t S_{m,j}, \quad m = o, g. \end{aligned} \quad (4.4.27b)$$

Similarly to the overall equation, Eq. 4.4.21, $\Delta_t \rho_o$ and $\Delta_t \rho_g$ appearing in Eq. 4.4.27b for $m = o$ and $m = g$, are replaced by Eqs. 4.4.17 and 4.4.18, respectively, thus, the term on the right-hand side of Eq. 4.4.25b becomes

$$\begin{aligned} \Delta_t(x_i \rho_o S_o + y_i \rho_g S_g)_j &= \left[[S_{g,j}^n (y_{i,j}^n G_{p,j} - x_{i,j}^n O_{p,j}) + x_{i,j}^n O_{p,j}] \Delta_t p_j \right. \\ &\quad + \sum_{l=2}^{N_c-1} [S_{g,j}^n (y_{i,j}^n G_{y_l,j} - x_{i,j}^n O_{y_l,j}) + x_{i,j}^n O_{y_l,j}] \Delta_t y_{l,j} \\ &\quad + S_{g,j}^n \rho_{g,j}^{n+1,k} \Delta_t y_{i,j} + \left(\rho_{o,j}^{n+1,k} - S_{g,j}^n \rho_{o,j}^{n+1,k} \right) \Delta_t x_{i,j} \\ &\quad \left. + [(\rho_g y_i)_j^{n+1,k} - (\rho_o x_i)_j^{n+1,k}] \Delta_t S_{g,j} \right]. \end{aligned} \quad (4.4.28)$$

Using Eq. 4.4.28 into the right-hand side of the flow equation, Eq. 4.4.25, and rearranging gives

$$\begin{aligned}
& \left[\hat{T}_{i,j-\frac{1}{2}} \right] p_{j-1}^{n+1,k+1} \\
& - \left[\hat{T}_{i,j-\frac{1}{2}} + \hat{T}_{i,j+\frac{1}{2}} + \frac{V_{pj}}{C_1 \Delta t} [S_{g,j}^n (y_{i,j}^n G_{p,j} - x_{i,j}^n O_{p,j}) + x_{i,j}^n O_{p,j}] \right] p_j^{n+1,k+1} \\
& - \left[\hat{D}_{i,j-\frac{1}{2}} + \frac{V_{pj}}{C_1 \Delta t} [(\rho_g y_i)^{n+1,k} - (\rho_o x_i)_j^{n+1,k}] \right] \Delta_t S_{g,j} \\
& + \left[\hat{A}_{o,j-\frac{1}{2}} - \frac{V_{pj}}{C_1 \Delta t} (\rho_{o,j}^{n+1,k} - S_{g,j}^n \rho_{o,j}^{n+1,k}) \right] \Delta_t x_{i,j} \\
& + \left[\hat{A}_{g,j-\frac{1}{2}} + \hat{A}_{g,j+\frac{1}{2}} - \frac{V_{pj}}{C_1 \Delta t} [S_{g,j}^n (y_{i,j}^n G_{y_i,j} - x_{i,j}^n O_{y_i,j} + \rho_{g,j}^{n+1,k}) + x_{i,j}^n O_{y_i,j}] \right] \Delta_t y_{i,j} \\
& - \frac{V_{pj}}{C_1 \Delta t} \sum_{\substack{l=2 \\ l \neq i}}^{N_c-1} [S_{g,j}^n (y_{i,j}^n G_{y_l,j} - x_{i,j}^n O_{y_l,j}) + x_{i,j}^n O_{y_l,j}] \Delta_t y_{l,j} \\
& + \left[\hat{T}_{i,j+\frac{1}{2}} \right] p_{j+1}^{n+1,k+1} \\
& + \left[\hat{D}_{i,j+\frac{1}{2}} \right] \Delta_t S_{g,j+1} \\
& + \left[\hat{A}_{o,j+\frac{1}{2}} \right] \Delta_t x_{i,j+1} \\
& + \left[\hat{A}_{g,j+\frac{1}{2}} \right] \Delta_t y_{i,j+1} \\
& = - \frac{V_{pj}}{C_1 \Delta t} [S_{g,j}^n (y_{i,j}^n G_{p,j} - x_{i,j}^n O_{p,j}) + x_{i,j}^n O_{p,j}] p_j^n, \quad 2 \leq i \leq N_c. \quad (4.4.29)
\end{aligned}$$

Since the primary variables $\{\Delta_t y_i\}_{i=2}^{N_c-1}$, will arise only in the flow equation of component i , $2 \leq i \leq N_c - 1$, the expansion of component i flow equation, for $2 \leq i \leq N_c - 1$ will differ from the expansion of the component N_c flow equation.

4.4.1.d Flow Equation of Component i , $2 \leq i \leq N_c - 1$

Following Eq. 4.4.6c, the "equilibrium" variables $\Delta_t x_i$, shown in Eq. 4.4.29 for $2 \leq i \leq N_c - 1$, are expressed in terms of the primary variables $p^{n+1,k+1}$ and $\{\Delta_t y_i\}_{i=2}^{N_c-1}$ so that the final form of the component flow equation, Eq. 4.4.29 is as follows

$$\begin{aligned}
& \left[\hat{T}_{i,j-\frac{1}{2}} \right] p_{j-1}^{n+1,k+1} \\
& - \left[\hat{T}_{i,j-\frac{1}{2}} + \hat{T}_{i,j+\frac{1}{2}} + \frac{V_{pj}}{C_1 \Delta t} (S_{g,j}^n (y_{i,j}^n G_{p,j} - x_{i,j}^n O_{p,j}) + x_{i,j}^n O_{p,j}) \right. \\
& \quad \left. - \left(\hat{A}_{o,j-\frac{1}{2}} - \frac{V_{pj}}{C_1 \Delta t} (\rho_{o,j}^{n+1,k} - S_{g,j}^n \rho_{o,j}^{n+1,k}) \right) \sum_{k=1}^{N_c} \hat{a}_{i-1,k,j} \hat{b}_{k,j} \right] p_j^{n+1,k+1} \\
& - \left[\hat{D}_{i,j-\frac{1}{2}} + \frac{V_{pj}}{C_1 \Delta t} ((\rho_g y_i)_j^{n+1,k} - (\rho_o x_i)_j^{n+1,k}) \right] \Delta_t S_{g,j} \\
& + \sum_{\substack{l=2 \\ l \neq i}}^{N_c-1} \left[\left(\hat{A}_{o,j-\frac{1}{2}} - \frac{V_{pj}}{C_1 \Delta t} (\rho_{o,j}^{n+1,k} - S_{g,j}^n \rho_{o,j}^{n+1,k}) \right) \sum_{k=1}^{N_c} \hat{a}_{i-1,k,j} \hat{c}_{k,l,j} \right. \\
& \quad \left. - \frac{V_{pj}}{C_1 \Delta t} (S_{g,j}^n (y_{i,j}^n G_{y_i,j} - x_{i,j}^n O_{y_i,j}) + x_{i,j}^n O_{y_i,j}) \right] \Delta_t y_{l,j} \\
& + \left[\left(\hat{A}_{o,j-\frac{1}{2}} - \frac{V_{pj}}{C_1 \Delta t} (\rho_{o,j}^{n+1,k} - S_{g,j}^n \rho_{o,j}^{n+1,k}) \right) \sum_{k=1}^{N_c} \hat{a}_{i-1,k,j} \hat{c}_{k,i,j} \right. \\
& \quad \left. + \hat{A}_{g,j-\frac{1}{2}} - \frac{V_{pj}}{C_1 \Delta t} (S_{g,j}^n (y_{i,j}^n G_{y_i,j} - x_{i,j}^n O_{y_i,j} + \rho_{g,j}) + x_{i,j}^n O_{y_i,j}) \right] \Delta_t y_{i,j} \\
& + \left[\hat{T}_{i,j+\frac{1}{2}} + \hat{A}_{o,j+\frac{1}{2}} \sum_{k=1}^{N_c} \hat{a}_{i-1,k,j+1} \hat{b}_{k,j+1} \right] p_{j+1}^{n+1,k+1} \\
& + \left[\hat{D}_{i,j+\frac{1}{2}} \right] \Delta_t S_{g,j+1} \\
& + \sum_{\substack{l=2 \\ l \neq i}}^{N_c-1} \left[\hat{A}_{o,j+\frac{1}{2}} \sum_{k=1}^{N_c} \hat{a}_{i-1,k,j+1} \hat{c}_{k,l,j+1} \right] \Delta_t y_{l,j+1} \\
& + \left[\left(\hat{A}_{g,j+\frac{1}{2}} + \hat{A}_{o,j+\frac{1}{2}} \sum_{k=1}^{N_c} \hat{a}_{i-1,k,j+1} \hat{c}_{k,i,j+1} \right) \right] \Delta_t y_{i,j+1} \\
& = \left[\left(\hat{A}_{o,j-\frac{1}{2}} - \frac{V_{pj}}{C_1 \Delta t} (\rho_{o,j}^{n+1,k} - S_{g,j}^n \rho_{o,j}^{n+1,k}) \right) \sum_{k=1}^{N_c} \hat{a}_{i-1,k,j} \hat{b}_{k,j} \right. \\
& \quad \left. - \frac{V_{pj}}{C_1 \Delta t} (S_{g,j}^n (y_{i,j}^n G_{p,j} - x_{i,j}^n O_{p,j}) + x_{i,j}^n O_{p,j}) \right] p_j^n
\end{aligned}$$

$$+ \left[\hat{A}_{o,j+\frac{1}{2}} \sum_{k=1}^{N_c} \hat{a}_{i-1,k,j+1} \hat{b}_{k,j+1} \right] p_{j+1}^n, \quad 2 \leq i \leq N_c - 1. \quad (4.4.30)$$

4.4.1.e Flow Equation of Component N_c

Similar to the component flow equation for $2 \leq i \leq N_c - 1$, Eq. 4.4.30, the component flow equation for $i = N_c$, Eq. 4.4.29, can be further expanded so that the terms $\Delta_t x_{N_c}$ and $\Delta_t y_{N_c}$ are written in terms of the primary variables $\Delta_t p$ and $\{\Delta_t y_i\}_{i=2}^{N_c-1}$. Thus, the final form of Eq. 4.4.29 for $i = N_c$ is given by

$$\begin{aligned} & \left[\hat{T}_{N_c, j-\frac{1}{2}} \right] p_{j-1}^{n+1, k+1} \\ & - \left[\hat{T}_{N_c, j-\frac{1}{2}} + \hat{T}_{N_c, j+\frac{1}{2}} + \frac{V_{pj}}{C_1 \Delta t} (S_{g,j}^n (y_{N_c,j}^n G_{p,j} - x_{N_c,j}^n O_{p,j}) + x_{N_c,j}^n O_{p,j}) \right. \\ & - \left(\hat{A}_{o, j-\frac{1}{2}} - \frac{V_{pj}}{C_1 \Delta t} (\rho_{o,j}^{n+1, k} - S_{g,j}^n \rho_{o,j}^{n+1, k}) \right) \sum_{k=1}^{N_c} \hat{a}_{N_c-1, k, j} \hat{b}_{k, j} \\ & - \left. \left(\hat{A}_{g, j-\frac{1}{2}} - \frac{V_{pj}}{C_1 \Delta t} S_{g,j}^n \rho_{g,j}^{n+1, k} \right) \sum_{k=1}^{N_c} \hat{a}_{N_c, k, j} \hat{b}_{k, j} \right] p_j^{n+1, k+1} \\ & - \left[\hat{D}_{N_c, j-\frac{1}{2}} + \frac{V_{pj}}{C_1 \Delta t} \left((\rho_g y_{N_c})_j^{n+1, k} - (\rho_o x_{N_c})_j^{n+1, k} \right) \right] \Delta_t S_{g, j} \\ & + \sum_{l=2}^{N_c-1} \left[\left(\hat{A}_{o, j-\frac{1}{2}} - \frac{V_{pj}}{C_1 \Delta t} (\rho_{o,j}^{n+1, k} - S_{g,j}^n \rho_{o,j}^{n+1, k}) \right) \sum_{k=1}^{N_c} \hat{a}_{N_c-1, k, j} \hat{c}_{k, l, j} \right. \\ & + \left. \hat{A}_{g, j-\frac{1}{2}} - \frac{V_{pj}}{C_1 \Delta t} (S_{g,j}^n (y_{N_c,j}^n G_{y_l, j} - x_{N_c,j}^n O_{y_l, j} + \rho_{g, j}) + x_{N_c,j}^n O_{y_l, j}) \right] \Delta_t y_{l, j} \\ & + \left[\hat{T}_{N_c, j+\frac{1}{2}} + \hat{A}_{o, j+\frac{1}{2}} \sum_{k=1}^{N_c} \hat{a}_{N_c-1, k, j+1} \hat{b}_{k, j+1} \right. \\ & + \left. \hat{A}_{g, j+\frac{1}{2}} \sum_{k=1}^{N_c} \hat{a}_{N_c, k, j+1} \hat{b}_{k, j+1} \right] p_{j+1}^{n+1, k+1} \\ & + \left[\hat{D}_{N_c, j+\frac{1}{2}} \right] \Delta_t S_{g, j+1} \\ & + \sum_{l=2}^{N_c-1} \left[\hat{A}_{o, j+\frac{1}{2}} \sum_{k=1}^{N_c} \hat{a}_{N_c-1, k, j+1} \hat{c}_{k, l, j+1} + \hat{A}_{g, j+\frac{1}{2}} \sum_{k=1}^{N_c} \hat{a}_{N_c, k, j+1} \hat{c}_{k, l, j+1} \right] \Delta_t y_{l, j+1} \end{aligned}$$

$$\begin{aligned}
&= \left[\left(\hat{A}_{o,j-\frac{1}{2}} - \frac{V_{pj}}{C_1 \Delta t} (\rho_{o,j}^{n+1,k} - S_{g,j}^n \rho_{o,j}^{n+1,k}) \right) \sum_{k=1}^{N_c} \hat{a}_{N_c-1,k,j} \hat{b}_{k,j} \right. \\
&\quad - \frac{V_{pj}}{C_1 \Delta t} S_{g,j}^n \rho_{g,j}^{n+1,k} \sum_{k=1}^{N_c} \hat{a}_{N_c,k,j} \hat{b}_{k,j} \\
&\quad \left. - \frac{V_{pj}}{C_1 \Delta t} (S_{g,j}^n (y_{N_c,j}^n G_{p,j} - x_{N_c,j}^n O_{p,j}) + x_{N_c,j}^n O_{p,j}) \right] p_j^n \\
&+ \left[\hat{A}_{o,j+\frac{1}{2}} \sum_{k=1}^{N_c} \hat{a}_{N_c-1,k,j+1} \hat{b}_{k,j+1} + \hat{A}_{g,j+\frac{1}{2}} \sum_{k=1}^{N_c} \hat{a}_{N_c,k,j+1} \hat{b}_{k,j+1} \right] p_{j+1}^n. \quad (4.4.31)
\end{aligned}$$

4.4.2 Binary Systems ($N_c = 2$)

We recall the set of unknowns, Q_j in a block j containing a two-phase binary mixture is defined as

$$Q_j = \{p, S_o, S_g, \{x_i\}_{i=1}^2, \{y_i\}_{i=1}^2\}_j^{n+1}.$$

We define the following subsets of Q_j :

$$\begin{cases} Q'_j = \{p, S_g\}_j^{n+1}; \\ Q''_j = \{x_2, y_2\}_j^{n+1} \end{cases}$$

The solution procedure is analogous to the multicomponent case. Here, we solve the overall mass balance equation (Eq. 4.1.15) and 1 component equation (Eq. 4.1.12) for the set of primary variables in Q'_j . However, the main difference lies in the fact that this set does not contain any mole fraction composition term. Moreover, an expansion of the phase fugacities yield a 2×2 matrix problem similar to Eq. 4.4.3 where the matrix M_j and the right-hand side vector \mathbf{B}_j respectively assume the following form

$$M_j = \begin{pmatrix} \left(\frac{\partial f_{1,L,j}}{\partial x_{2,j}} \right)^n & - \left(\frac{\partial f_{1,V,j}}{\partial y_{2,j}} \right)^n \\ \left(\frac{\partial f_{2,L,j}}{\partial x_{2,j}} \right)^n & - \left(\frac{\partial f_{2,V,j}}{\partial y_{2,j}} \right)^n \end{pmatrix} \quad (4.4.32a)$$

and

$$\mathbf{B}_j = \begin{pmatrix} - \left[\left(\frac{\partial f_{1,L,j}}{\partial p_j} \right)^n - \left(\frac{\partial f_{1,V,j}}{\partial p_j} \right)^n \right] \Delta_t p_j \\ - \left[\left(\frac{\partial f_{2,L,j}}{\partial p_j} \right)^n - \left(\frac{\partial f_{2,V,j}}{\partial p_j} \right)^n \right] \Delta_t p_j \end{pmatrix} \quad (4.4.32b)$$

We know that Eq. 4.4.3 explicitly relates the 2 variables $x_{2,j}$ and $y_{2,j}$ in Q'_j to the primary variable p_j in Q'_j . Thus, the solution of Eq. 4.4.3 is computed as follows

$$\Delta_t x_{2,j} = \left(\sum_{k=1}^2 \hat{a}_{i,k,j} \hat{b}_{k,j} \right) \Delta_t p_j, \quad (4.4.33a)$$

and

$$\Delta_t y_{2,j} = \left(\sum_{k=1}^2 \hat{a}_{2,k,j} \hat{b}_{k,j} \right) \Delta_t p_j, \quad (4.4.33b)$$

where $\hat{a}_{i,k,j}$ denotes the element in the i^{th} row and k^{th} column of the inverse of M_j , and where $\hat{b}_{k,j}$ is given by Eq. 4.4.6a. Note that Eqs. 4.4.33a and 4.4.33b are the analog equations of Eqs. 4.4.6c and 4.4.6d, respectively.

Using Eqs. 4.4.33a and 4.4.33b, and following the same procedure outlined for the multicomponent case, the overall mass balance equation, Eq. 4.4.21 and the component 2 flow equation, Eq. 4.4.31, reduce, respectively, to

$$\begin{aligned} & \left[\tilde{T}_{o,j-\frac{1}{2}}^{n+1,k} + \tilde{T}_{g,j-\frac{1}{2}}^{n+1,k} \right] p_j^{n+1,k+1} \\ & - \left[\tilde{T}_{o,j-\frac{1}{2}}^{n+1,k} + T_{g,j-\frac{1}{2}}^{n+1,k} + \tilde{T}_{o,j+\frac{1}{2}}^{n+1,k} + \tilde{T}_{g,j+\frac{1}{2}}^{n+1,k} \right. \\ & \quad \left. + \frac{V_{pj}}{C_1 \Delta t} (S_{g,j}^n (G_{p,j} - O_{p,j}) + O_{p,j}) \right] p_j^{n+1,k+1} \\ & - \left[D_{o,j-\frac{1}{2}}^{n+1,k} + D_{g,j-\frac{1}{2}}^{n+1,k} + \frac{V_{pj}}{C_1 \Delta t} (\rho_{g,j}^{n+1,k} - \rho_{o,j}^{n+1,k}) \right] \Delta_t S_{g,j} \\ & + \left[\tilde{T}_{o,j+\frac{1}{2}}^{n+1,k} + \tilde{T}_{g,j+\frac{1}{2}}^{n+1,k} \right] p_j^{n+1,k+1} \\ & + \left[D_{o,j+\frac{1}{2}}^{n+1,k} + D_{g,j+\frac{1}{2}}^{n+1,k} \right] \Delta_t S_{g,j+1} \\ & = - \frac{V_{pj}}{C_1 \Delta t} [S_{g,j}^n (G_{p,j} - O_{p,j}) + O_{p,j}] p_j^n, \end{aligned} \quad (4.4.34)$$

and

$$\begin{aligned}
& \left[\hat{T}_{2,j-\frac{1}{2}} \right] p_{j-1}^{n+1,k+1} \\
& - \left[\hat{T}_{2,j-\frac{1}{2}} + \hat{T}_{2,j+\frac{1}{2}} + \frac{V_{pj}}{C_1 \Delta t} (S_{g,j}^n (y_{2,j}^n G_{p,j} - x_{2,j}^n O_{p,j}) + x_{2,j}^n O_{p,j}) \right. \\
& \quad - \left(\hat{A}_{o,j-\frac{1}{2}} - \frac{V_{pj}}{C_1 \Delta t} (\rho_{o,j}^{n+1,k} - S_{g,j}^n \rho_{o,j}^{n+1,k}) \right) \sum_{k=1}^2 \hat{a}_{1,k,j} \hat{b}_{k,j} \\
& \quad \left. - \left(\hat{A}_{g,j-\frac{1}{2}} - \frac{V_{pj}}{C_1 \Delta t} S_{g,j}^n \rho_{g,j}^{n+1,k} \right) \sum_{k=1}^2 \hat{a}_{2,k,j} \hat{b}_{k,j} \right] p_j^{n+1,k+1} \\
& - \left[\hat{D}_{2,j-\frac{1}{2}} + \frac{V_{pj}}{C_1 \Delta t} ((\rho_g y_2)_j^{n+1,k} - (\rho_o x_2)_j^{n+1,k}) \right] \Delta_t S_{g,j} \\
& + \left[\hat{T}_{2,j+\frac{1}{2}} + \hat{A}_{o,j+\frac{1}{2}} \sum_{k=1}^2 \hat{a}_{1,k,j+1} \hat{b}_{k,j+1} + \hat{A}_{g,j+\frac{1}{2}} \sum_{k=1}^2 \hat{a}_{2,k,j+1} \hat{b}_{k,j+1} \right] p_{j+1}^{n+1,k+1} \\
& + \left[\hat{D}_{2,j+\frac{1}{2}} \right] \Delta_t S_{g,j+1} \\
& = \left[\left(\hat{A}_{o,j-\frac{1}{2}} - \frac{V_{pj}}{C_1 \Delta t} (\rho_{o,j}^{n+1,k} - S_{g,j}^n \rho_{o,j}^{n+1,k}) \right) \sum_{k=1}^2 \hat{a}_{1,k,j} \hat{b}_{k,j} \right. \\
& \quad - \frac{V_{pj}}{C_1 \Delta t} S_{g,j}^n \rho_{g,j}^{n+1,k} \sum_{k=1}^2 \hat{a}_{2,k,j} \hat{b}_{k,j} \\
& \quad \left. - \frac{V_{pj}}{C_1 \Delta t} (S_{g,j}^n (y_{2,j}^n G_{p,j} - x_{2,j}^n O_{p,j}) + x_{2,j}^n O_{p,j}) \right] p_j^n \\
& + \left[\hat{A}_{o,j+\frac{1}{2}} \sum_{k=1}^2 \hat{a}_{1,k,j+1} \hat{b}_{k,j+1} + \hat{A}_{g,j+\frac{1}{2}} \sum_{k=1}^2 \hat{a}_{2,k,j+1} \hat{b}_{k,j+1} \right] p_{j+1}^n. \tag{4.4.35}
\end{aligned}$$

4.5 Single-Phase Fluid with Varying Composition, $j \in N_{r3}$

Here, we discuss a technique developed to handle gridblocks of the reservoir that contain a single-phase fluid with varying composition. Single-phase with varying composition means the single-phase fluid composition is different than the original single-phase composition and during the flow process, may be mixed with a single-phase fluid of different composition. This situation occurs, for example, in isochronal testing when during a buildup period the two-phase mixture in a gridblock may collapse into a single-phase fluid of "varying composition" and during the following drawdown, may be mixed with a single-phase fluid of different composition. The technique developed for simulating this case can also be applied to complex processes such as gas cycling and miscible flooding.

We recall the set of all gridblocks containing only one phase where the composition of the phase may vary with time is denoted by N_{r3} . The component flow equations, for gridblock j , Eq. 4.1.12, (assuming one phase, $m = L$ or $m = V$ exists in the gridblock) are given by

$$\begin{aligned}
 & U_{j+\frac{1}{2}} \left[\left(\rho_o \frac{k_{ro}}{\mu_o} x_i + \rho_g \frac{k_{rg}}{\mu_g} y_i \right)_{j+1}^{n+1} (p_{j+1}^{n+1} - p_j^{n+1}) \right] \\
 & - U_{j-\frac{1}{2}} \left[\left(\frac{\rho_m}{\mu_m} x_{i,m} \right)_j^{n+1} (p_j^{n+1} - p_{j-1}^{n+1}) \right] \\
 & = \frac{V_{pj}}{C_1 \Delta t} \Delta_t (x_{i,m} \rho_m)_j, \quad 1 \leq i \leq N_c, \quad 2 \leq j \leq N_r - 1, \quad (4.5.1)
 \end{aligned}$$

and the overall mass balance equation, Eq. 4.1.15, reduces to

$$\begin{aligned}
 & U_{j+\frac{1}{2}} \left[\left(\rho_o \frac{k_{ro}}{\mu_o} + \rho_g \frac{k_{rg}}{\mu_g} \right)_{j+1}^{n+1} (p_{j+1}^{n+1} - p_j^{n+1}) \right] \\
 & - U_{j-\frac{1}{2}} \left[\left(\frac{\rho_m}{\mu_m} \right)_j^{n+1} (p_j^{n+1} - p_{j-1}^{n+1}) \right] \\
 & = \frac{V_{pj}}{C_1 \Delta t} \Delta_t \rho_{m,j}, \quad 1 \leq i \leq N_c, \quad 2 \leq j \leq N_r - 1. \quad (4.5.2)
 \end{aligned}$$

Note we allow the upstream block to contain a two-phase fluid, but assume that gridblock j contains only one phase. At the single-phase gridblock j , Eq. 4.5.1 represents N_c discrete mass balance equations, one for each hydrocarbon component. The unknowns at each such single-phase gridblock is given by Eq. 4.2.4.

$$Q_j = \{p_j, \{x_{i,m,j}\}_{i=1}^{N_c}\}, \quad j \in N_{r3}.$$

Eqs. 4.5.1, 4.5.2 and 4.1.16a or 4.1.16b constitute the system of N_c+1 equations solved to obtain the values of the $N_c + 1$ variables defined in the set Q_j . The inner boundary conditions are given by Eq. 4.1.19, where k_{rg} (or k_{ro}) is set to unity. The possible outer boundary conditions, Eqs. 3.2.11a or 4.1.23 - 4.1.24 remain unchanged. The saturation and the fugacity, Eqs. 4.1.17 and 4.1.18, are not applicable since the block j is single-phase. The only remaining equation is the mole fraction constraint for the phase considered, i.e.,

$$\sum_{i=1}^{N_c} x_{i,m,j}^{n+1} = 1. \quad (4.5.3)$$

These equations are still nonlinear and must be solved iteratively.

We define the following subset of Q_j :

$$Q'_j = \{p_j, \{x_{i,m,j}\}_{i=2}^{N_c}\}.$$

Eight cases of adjacent gridblock phase behavior are possible, but only four of them are treated since the other four are symmetric. The approach to these cases is essentially the same as for the single-phase and two-phase equations; i.e., nonlinearities are resolved as they arise and we will use the same techniques of linearization as for two-phase blocks to solve the overall mass balance equation, Eq. 4.5.2, and $N_c - 1$ component flow equations, Eq. 4.5.3. We outline the procedure below. The notation we will use is as follows: A block filled with single-phase gas with initial composition is labeled 1. A block filled with single-phase gas with

variable composition is labeled 2. Labels 3 and 4 respectively denote blocks containing a single-phase liquid with initial composition and with variable composition, respectively. A two-phase block is labeled 5.

4.5.1 Block $j \equiv 2$ and Block $j + 1 \equiv 1$

Here, the block of interest, gridblock j contains a single-phase fluid with varying composition and therefore, the unknowns for this block are p_j and $\{\Delta_t y_{i,j}\}_{i=2}^{N_c}$, whereas for block $j + 1$, only pressure, p_{j+1} is unknown.

4.5.1.a Overall Mass Balance Equation

Since adjacent blocks, j and $j + 1$ contain only one phase, the overall mass balance equation, Eq. 4.5.2, reduces to

$$\begin{aligned} & U_{j+\frac{1}{2}} \left[\left(\frac{\rho_g}{\mu_g} \right)_{j+1}^{n+1} (p_{j+1}^{n+1} - p_j^{n+1}) \right] \\ & - U_{j-\frac{1}{2}} \left[\left(\frac{\rho_g}{\mu_g} \right)_j^{n+1} (p_j^{n+1} - p_{j-1}^{n+1}) \right] \\ & = \frac{V_{pj}}{C_1 \Delta t} \Delta_t \rho_{g,j}, \quad 1 \leq i \leq N_c, \quad 2 \leq j \leq N_r - 1. \end{aligned} \quad (4.5.4a)$$

Furthermore, since gas phase density is function of pressure and composition, then $\Delta_t \rho_{g,j}$ is approximated by Eq. 4.4.16 so that Eq. 4.5.4a becomes

$$\begin{aligned} & \left[T_{g,j-\frac{1}{2}}^{n+1,k} \right] p_{j-1}^{n+1,k+1} \\ & - \left[T_{g,j-\frac{1}{2}}^{n+1,k} + T_{g,j+\frac{1}{2}}^{n+1,k} + \frac{V_{pj}}{C_1 \Delta t} \left(\left(\frac{\partial \rho_g}{\partial p} \right)_{\{y_i\}_{i=2}^{N_c}} \right)_j^{n+1,k} \right] p_j^{n+1,k+1} \\ & + \left[T_{g,j+\frac{1}{2}}^{n+1,k} \right] p_{j+1}^{n+1,k+1} \\ & - \frac{V_{pj}}{C_1 \Delta t} \sum_{l=2}^{N_c} \left(\left(\frac{\partial \rho_g}{\partial y_l} \right)_{y_{k,p}, k \neq 1, l} \right)_j^{n+1,k} \Delta_t y_{l,j} \end{aligned}$$

$$= -\frac{V_{pj}}{C_1 \Delta t} \left(\left(\frac{\partial \rho_g}{\partial p} \right)_{\{y_k\}_{k=2}^{N_c}} \right)_j^{n+1,k} p_j^n. \quad (4.5.4b)$$

4.5.1.b Component Flow Equations

Since block $j + 1$ contains only single-phase gas, Eq. 4.5.1 simplifies to

$$\begin{aligned} & U_{j+\frac{1}{2}} \left[\left(\frac{\rho_g}{\mu_g} y_i \right)_{j+1}^{n+1} (p_{j+1}^{n+1} - p_j^{n+1}) \right] \\ & - U_{j-\frac{1}{2}} \left[\left(\frac{\rho_g}{\mu_g} y_i \right)_j^{n+1} (p_j^{n+1} - p_{j-1}^{n+1}) \right] \\ & = \frac{V_{pj}}{C_1 \Delta t} \Delta_t (y_i \rho_g)_j, \quad 1 \leq i \leq N_c. \end{aligned} \quad (4.5.5a)$$

The right-hand side of Eq. 4.5.5a is expanded as

$$\Delta_t (y_i \rho_g) = y_i^n \Delta_t \rho_g + \rho_g^{n+1,k} \Delta_t y_i, \quad 1 \leq i \leq N_c. \quad (4.5.5b)$$

Using Eq. 4.5.5b, where $\Delta_t \rho_g$ is approximated by Eq. 4.4.16, into Eq. 4.5.5a gives

$$\begin{aligned} & \left[T_{g,j-\frac{1}{2}}^{n+1,k} y_{i,j}^n \right] p_{j-1}^{n+1,k+1} \\ & - \left[T_{g,j-\frac{1}{2}}^{n+1,k} y_{i,j}^n + T_{g,j+\frac{1}{2}}^{n+1,k} y_{i,j+1}^n + \frac{V_{pj}}{C_1 \Delta t} y_{i,j}^n \left(\left(\frac{\partial \rho_g}{\partial p} \right)_{\{y_k\}_{k=2}^{N_c}} \right)_j^{n+1,k} \right] p_j^{n+1,k+1} \\ & + \left[T_{g,j-\frac{1}{2}}^{n+1,k} (p_{j-1}^{n+1,k} - p_j^{n+1,k}) \right. \\ & \quad \left. - \frac{V_{pj}}{C_1 \Delta t} \left(\rho_{g,j}^{n+1,k} + \left(\left(\frac{\partial \rho_g}{\partial y_i} \right)_{\substack{y_{k,p} \\ k \neq 1,i}} \right)_j^{n+1,k} y_{i,j}^n \right) \right] \Delta_t y_{i,j} \\ & - \frac{V_{pj}}{C_1 \Delta t} y_{i,j}^n \sum_{\substack{l=2 \\ l \neq i}}^{N_c} \left(\left(\frac{\partial \rho_g}{\partial y_l} \right)_{\substack{y_{k,p} \\ k \neq 1,l}} \right)_j^{n+1,k} \Delta_t y_{l,j} \\ & + \left[T_{g,j+\frac{1}{2}}^{n+1,k} y_{i,j+1}^n \right] p_{j+1}^{n+1,k+1} \\ & = -\frac{V_{pj}}{C_1 \Delta t} y_{i,j}^n \left(\left(\frac{\partial \rho_g}{\partial p} \right)_{\{y_k\}_{k=2}^{N_c}} \right)_j^{n+1,k} p_j^n, \quad 2 \leq i \leq N_c. \end{aligned} \quad (4.5.5c)$$

Note that in Eq. 4.5.5c, $y_{i,j+1}$ is fixed and equal to the initial mole fraction composition.

Eqs. 4.5.4b and 4.5.5c are valid for the case where block $j \equiv 4$ and block $j+1 \equiv 3$. We only need to replace the subscript g by the subscript o in the density and transmissibility terms, and replace the gas mole fraction composition y_i by the liquid mole fraction composition x_i .

4.5.2 Block $j \equiv 2$ and Block $j+1 \equiv 5$

In block j , the unknowns j are p_j and $\{\Delta_t y_{i,j}\}_{i=2}^{N_c}$ since the block is filled with a single-phase fluid with varying composition. The upstream block contains a two-phase fluid, and therefore, the unknowns are p_{j+1} , $\Delta_t S_{g,j+1}$, $\{\Delta_t x_{i,j+1}\}_{i=2}^{N_c}$ and $\{\Delta_t y_{i,j+1}\}_{i=2}^{N_c}$.

4.5.2.a Overall Mass Balance Equation

Since Block $j+1$ contains a two-phase fluid, the overall mass balance equation must include a saturation term at that block as is shown in the following equation

$$\begin{aligned}
 & \left[T_{g,j-\frac{1}{2}}^{n+1,k} \right] p_{j-1}^{n+1,k+1} \\
 & - \left[T_{g,j-\frac{1}{2}}^{n+1,k} + \tilde{T}_{g,j+\frac{1}{2}}^{n+1,k} + \tilde{T}_{o,j+\frac{1}{2}}^{n+1,k} + \frac{V_{pj}}{C_1 \Delta t} \left(\left(\frac{\partial \rho_g}{\partial p} \right)_{\{y_i\}_{i=2}^{N_c}} \right)_j \right] p_j^{n+1,k+1} \\
 & - \frac{V_{pj}}{C_1 \Delta t} \sum_{l=2}^{N_c} \left(\left(\frac{\partial \rho_g}{\partial y_l} \right)_{y_{k,p}, k \neq l} \right)_j \Delta_t y_{l,j} \\
 & + \left[\tilde{T}_{o,j+\frac{1}{2}}^{n+1,k} + \tilde{T}_{g,j+\frac{1}{2}}^{n+1,k} \right] p_{j+1}^{n+1,k+1} \\
 & + (D_{o,j+\frac{1}{2}}^{n+1,k} + D_{g,j+\frac{1}{2}}^{n+1,k}) \Delta_t S_{g,j+1} \\
 & = - \frac{V_{pj}}{C_1 \Delta t} \left(\left(\frac{\partial \rho_g}{\partial p} \right)_{\{y_i\}_{i=2}^{N_c}} \right)_j p_j^n.
 \end{aligned} \tag{4.5.6}$$

where the right-hand side term expansion is analogous to Eq. 4.5.4b.

4.5.2.b Component Flow Equations

The component flow equations assume the following form

$$\begin{aligned}
& \left[T_{g,j-\frac{1}{2}}^{n+1,k} y_{i,j}^n \right] p_{j-1}^{n+1,k+1} \\
& - \left[T_{g,j-\frac{1}{2}}^{n+1,k} y_{i,j}^n + \hat{T}_{i,j+\frac{1}{2}}^{n+1,k} + \frac{V_{pj}}{C_1 \Delta t} y_{i,j}^n \left(\left(\frac{\partial \rho_g}{\partial p} \right)_{\{y_i\}_{i=2}^{N_c}} \right)_j^{n+1,k} \right] p_j^{n+1,k+1} \\
& + \left[T_{g,j-\frac{1}{2}}^{n+1,k} (p_{j-1}^{n+1,k} - p_j^{n+1,k}) \right. \\
& \quad \left. - \frac{V_{pj}}{C_1 \Delta t} \left(\rho_{g,j}^{n+1,k} + \left(\left(\frac{\partial \rho_g}{\partial y_i} \right)_{\substack{y_k,p \\ k \neq 1,i}} \right)_j^{n+1,k} y_{i,j}^n \right) \right] \Delta_t y_{i,j} \\
& + \left[\hat{T}_{i,j+\frac{1}{2}}^{n+1,k} \right] p_{j+1}^{n+1,k+1} \\
& + \left[\hat{D}_{i,j+\frac{1}{2}}^{n+1,k} \right] \Delta_t S_{g,j+1} \\
& + \left[\hat{A}_{o,j+\frac{1}{2}}^{n+1,k} \right] \Delta_t x_{i,j+1} \\
& + \left[\hat{A}_{g,j+\frac{1}{2}}^{n+1,k} \right] \Delta_t y_{i,j+1} \\
& = - \frac{V_{pj}}{C_1 \Delta t} y_{i,j}^n \left(\left(\frac{\partial \rho_g}{\partial p} \right)_{\{y_k\}_{k=2}^{N_c}} \right)_j^{n+1,k} p_j^n, \quad 2 \leq i \leq N_c. \tag{4.5.7}
\end{aligned}$$

Note that Eq. 4.5.7 includes saturation and mole fraction composition terms at the upstream block that contains a two-phase fluid, i.e., $\{\Delta_t x_{i,j+1}\}_{i=2}^{N_c}$ and $\Delta_t y_{N_c,j+1}$ are expressed in terms of the primary variables $\Delta_t p_{j+1}$ and $\{\Delta_t y_{l,j+1}\}_{l=2}^{N_c-1}$ via Eqs. 4.4.6c and 4.4.6d, i.e., for $2 \leq i \leq N_c - 1$, Eq. 4.5.7 becomes

$$\begin{aligned}
& \left[T_{g,j-\frac{1}{2}}^{n+1,k} y_{i,j}^n \right] p_{j-1}^{n+1,k+1} \\
& - \left[T_{g,j-\frac{1}{2}}^{n+1,k} y_{i,j}^n + \hat{T}_{i,j+\frac{1}{2}}^{n+1,k} + \frac{V_{pj}}{C_1 \Delta t} y_{i,j}^n \left(\left(\frac{\partial \rho_g}{\partial p} \right)_{\{y_i\}_{i=2}^{N_c}} \right)_j^{n+1,k} \right] p_j^{n+1,k+1}
\end{aligned}$$

$$\begin{aligned}
& + \left[T_{g,j-\frac{1}{2}}^{n+1,k} (p_{j-1}^{n+1,k} - p_j^{n+1,k}) \right. \\
& \quad \left. - \frac{V_{pj}}{C_1 \Delta t} \left(\rho_{g,j}^{n+1,k} + \left(\left(\frac{\partial \rho_g}{\partial y_i} \right)_{\substack{y_k,p \\ k \neq 1,i}} \right)_j^{n+1,k} y_{i,j}^n \right) \right] \Delta_t y_{i,j} \\
& + \left[\hat{T}_{i,j+\frac{1}{2}}^{n+1,k} \right] p_{j+1}^{n+1,k+1} \\
& + \left[\hat{D}_{i,j+\frac{1}{2}}^{n+1,k} \right] \Delta_t S_{g,j+1} \\
& + \sum_{\substack{l=2 \\ l \neq i}}^{N_c-1} \left[\hat{A}_{o,j+\frac{1}{2}} \sum_{k=1}^{N_c} \hat{a}_{i-1,k,j+1} \hat{c}_{k,l,j+1} \right] \Delta_t y_{l,j+1} \\
& + \left[\hat{A}_{g,j+\frac{1}{2}} + \hat{A}_{o,j+\frac{1}{2}} \sum_{k=1}^{N_c} \hat{a}_{i-1,k,j+1} \hat{c}_{k,i,j+1} \right] \Delta_t y_{i,j+1} \\
& = - \frac{V_{pj}}{C_1 \Delta t} y_{i,j}^n \left[\left(\left(\frac{\partial \rho_g}{\partial p} \right)_{\{y_k\}_{k=2}^{N_c}} \right)_j^{n+1,k} \right] p_j^n \\
& + \left[\hat{A}_{o,j+\frac{1}{2}} \sum_{k=1}^{N_c} \hat{a}_{i-1,k,j+1} \hat{b}_{k,j+1} \right] p_{j+1}^n, \quad 2 \leq i \leq N_c - 1, \quad (4.5.8a)
\end{aligned}$$

and for $i = N_c$, Eq. 4.5.7 becomes

$$\begin{aligned}
& \left[T_{g,j-\frac{1}{2}}^{n+1,k} y_{N_c,j}^n \right] p_{j-1}^{n+1,k+1} \\
& - \left[T_{g,j-\frac{1}{2}}^{n+1,k} y_{N_c,j}^n + \hat{T}_{N_c,j+\frac{1}{2}}^{n+1,k} + \frac{V_{pj}}{C_1 \Delta t} y_{N_c,j}^n \left(\left(\frac{\partial \rho_g}{\partial p} \right)_{\{y_i\}_{i=2}^{N_c}} \right)_j^{n+1,k} \right] p_j^{n+1,k+1} \\
& + \left[T_{g,j-\frac{1}{2}}^{n+1,k} (p_{j-1}^{n+1,k} - p_j^{n+1,k}) \right. \\
& \quad \left. - \frac{V_{pj}}{C_1 \Delta t} \left(\rho_{g,j}^{n+1,k} + \left(\left(\frac{\partial \rho_g}{\partial y_{N_c}} \right)_{\substack{y_k,p \\ k \neq 1,N_c}} \right)_j^{n+1,k} y_{N_c,j}^n \right) \right] \Delta_t y_{N_c,j} \\
& - \frac{V_{pj}}{C_1 \Delta t} y_{N_c,j}^n \sum_{\substack{l=2 \\ l \neq N_c}}^{N_c} \left(\left(\frac{\partial \rho_g}{\partial y_l} \right)_{\substack{y_k,p \\ k \neq 1,l}} \right)_j^{n+1,k} \Delta_t y_{l,j}
\end{aligned}$$

$$\begin{aligned}
& + \left[\hat{T}_{i,j+\frac{1}{2}}^{n+1,k} + \hat{A}_{o,j+\frac{1}{2}} \sum_{k=1}^{N_c} \hat{a}_{N_c-1,k,j+1} \hat{b}_{k,j+1} + \hat{A}_{g,j+\frac{1}{2}} \sum_{k=1}^{N_c} \hat{a}_{N_c,k,j+1} \hat{b}_{k,j+1} \right] p_{j+1}^{n+1,k+1} \\
& + \left[\hat{D}_{i,j+\frac{1}{2}}^{n+1,k} \right] \Delta_t S_{g,j+1} \\
& + \sum_{l=2}^{N_c-1} \left[\hat{A}_{o,j+\frac{1}{2}} \sum_{k=1}^{N_c} \hat{a}_{N_c-1,k,j+1} \hat{c}_{k,l,j+1} + \hat{A}_{g,j+\frac{1}{2}} \sum_{k=1}^{N_c} \hat{a}_{N_c,k,j+1} \hat{c}_{k,l,j+1} \right] \Delta_t y_{l,j+1} \\
& + \left[\hat{A}_{g,j+\frac{1}{2}} + \hat{A}_{o,j+\frac{1}{2}} \sum_{k=1}^{N_c} \hat{a}_{N_c-1,k,j+1} \hat{c}_{k,N_c,j+1} \right] \Delta_t y_{N_c,j+1} \\
& = -\frac{V_{pj}}{C_1 \Delta t} y_{N_c,j}^n \left[\left(\left(\frac{\partial \rho_g}{\partial p} \right)_{\{y_k\}_{k=2}^{N_c}} \right)_j^{n+1,k} \right] p_j^n \\
& + \left[\hat{A}_{o,j+\frac{1}{2}} \sum_{k=1}^{N_c} \hat{a}_{N_c-1,k,j+1} \hat{b}_{k,j+1} + \hat{A}_{g,j+\frac{1}{2}} \sum_{k=1}^{N_c} \hat{a}_{N_c,k,j+1} \hat{b}_{k,j+1} \right] p_{j+1}^n, \quad (4.5.8b)
\end{aligned}$$

where $\hat{A}_{o,j+\frac{1}{2}}$ and $\hat{A}_{g,j+\frac{1}{2}}$ are given by Eq. 4.4.26d.

For block $j \equiv 4$ and block $j+1 \equiv 5$, we still use Eq. 4.5.6. We also use Eqs. 4.5.8a and 4.5.8b provided we exchange the subscript g appearing at the downstream gridblock j density and transmissibility terms for the subscript o , and we replace all mole fraction composition terms x_i evaluated at the downstream block by y_i .

4.5.3 Block $j \equiv 2$ and Block $j+1 \equiv 2$

Here, we assume that both the upstream and downstream blocks contain single-phase fluids with varying and different compositions. The unknowns for both blocks are pressure and composition.

4.5.3.a Overall Mass Balance Equation

The overall mass balance equation is given by

$$\begin{aligned}
& \left[T_{g,j-\frac{1}{2}}^{n+1,k} \right] p_{j-1}^{n+1,k+1} \\
& - \left[T_{g,j-\frac{1}{2}}^{n+1,k} + T_{g,j+\frac{1}{2}}^{n+1,k} + \frac{V_{pj}}{C_1 \Delta t} \left(\left(\frac{\partial \rho_g}{\partial p} \right)_{\{y_i\}_{i=2}^{N_c}} \right)_j^{n+1,k} \right] p_j^{n+1,k+1}
\end{aligned}$$

$$\begin{aligned}
& -\frac{V_{pj}}{C_1 \Delta t} \sum_{l=2}^{N_c} \left(\left(\frac{\partial \rho_g}{\partial y_l} \right)_{y_{k,p}, p} \right)_j^{n+1,k} \Delta t y_{l,j} \\
& + \left[T_{g,j+\frac{1}{2}}^{n+1,k} \right] p_{j+1}^{n+1,k+1} \\
& = -\frac{V_{pj}}{C_1 \Delta t} \left(\left(\frac{\partial \rho_g}{\partial p} \right)_{\{y_i\}_{i=2}^{N_c}} \right)_j^{n+1,k} p_j^n, \quad (4.5.9)
\end{aligned}$$

4.5.3.b Component Flow Equations

The component flow equations include mole fraction compositions terms at the upstream and downstream blocks.

$$\begin{aligned}
& \left[T_{g,j-\frac{1}{2}}^{n+1,k} y_{i,j}^n \right] p_{j-1}^{n+1,k+1} \\
& - \left[T_{g,j-\frac{1}{2}}^{n+1,k} y_{i,j}^n + T_{g,j+\frac{1}{2}}^{n+1,k} y_{i,j+1}^n + \frac{V_{pj}}{C_1 \Delta t} \left(\left(\frac{\partial \rho_g}{\partial p} \right)_{\{y_i\}_{i=2}^{N_c}} \right)_j^{n+1,k} y_{i,j}^n \right] p_j^{n+1,k+1} \\
& + \left[T_{g,j-\frac{1}{2}}^{n+1,k} (p_{j-1}^{n+1,k} - p_j^{n+1,k}) \right. \\
& \quad \left. - \frac{V_{pj}}{C_1 \Delta t} \left(\rho_{g,j}^{n+1,k} + \left(\left(\frac{\partial \rho_g}{\partial y_i} \right)_{y_{k,p}, p} \right)_j^{n+1,k} y_{i,j}^n \right) \right] \Delta t y_{i,j} \\
& + \left[T_{g,j+\frac{1}{2}}^{n+1,k} y_{i,j+1}^n \right] p_{j+1}^{n+1,k+1} \\
& + \left[T_{g,j+\frac{1}{2}}^{n+1,k} (p_{j+1}^{n+1,k} - p_j^{n+1,k}) \right] \Delta t y_{i,j+1} \\
& = -\frac{V_{pj}}{C_1 \Delta t} y_{i,j}^n \left(\left(\frac{\partial \rho_g}{\partial p} \right)_{\{y_k\}_{k=2}^{N_c}} \right)_j^{n+1,k} p_j^n, \quad 2 \leq i \leq N_c. \quad (4.5.10)
\end{aligned}$$

Note that the expansion of the right-hand side of Eq. 4.5.10 is analogous to Eq. 4.5.5c. Eqs. 4.5.9 and 4.5.10 are valid for the case Block $j \equiv 4$ and block $j+1 \equiv 4$, provided we exchange x_i for y_i and the subscript g for the subscript o .

4.5.4 Block $j \equiv 2$ and Block $j + 1 \equiv 4$

Here, the adjacent blocks contain a single-phase gas with varying composition and a single-phase liquid with varying composition, respectively. The unknowns are pressure and composition for both blocks. (While we do not usually expect this case to occur in actual physical situations, this possibility is accounted for in our simulator.)

4.5.4.a Overall Mass Balance Equation

The overall mass balance equation is written as

$$\begin{aligned}
 & \left[T_{g,j-\frac{1}{2}}^{n+1,k} \right] p_{j-1}^{n+1,k+1} \\
 & - \left[T_{g,j-\frac{1}{2}}^{n+1,k} + T_{o,j+\frac{1}{2}}^{n+1,k} + \frac{V_{pj}}{C_1 \Delta t} \left(\left(\frac{\partial \rho_g}{\partial p} \right)_{\{y_i\}_{i=2}^{N_c}} \right)_j \right]^{n+1,k} p_j^{n+1,k+1} \\
 & - \frac{V_{pj}}{C_1 \Delta t} \sum_{l=2}^{N_c} \left(\left(\frac{\partial \rho_g}{\partial y_l} \right)_{\substack{y_{k,p} \\ k \neq 1,l}} \right)_j^{n+1,k} \Delta_t y_{l,j} \\
 & + \left[T_{o,j+\frac{1}{2}}^{n+1,k} \right] p_{j+1}^{n+1,k+1} \\
 & = - \frac{V_{pj}}{C_1 \Delta t} \left(\left(\frac{\partial \rho_g}{\partial p} \right)_{\{y_i\}_{i=2}^{N_c}} \right)_j^{n+1,k} p_j^n, \tag{4.5.11}
 \end{aligned}$$

4.5.4.b Component Flow Equations

The component flow equations include mole fraction compositions terms at the upstream and downstream blocks.

$$\begin{aligned}
 & \left[T_{g,j-\frac{1}{2}}^{n+1,k} y_{i,j}^n \right] p_{j-1}^{n+1,k+1} \\
 & - \left[T_{g,j-\frac{1}{2}}^{n+1,k} y_{i,j}^n + T_{o,j+\frac{1}{2}}^{n+1,k} x_{i,j+1}^n + \frac{V_{pj}}{C_1 \Delta t} \left(\left(\frac{\partial \rho_g}{\partial p} \right)_{\{y_i\}_{i=2}^{N_c}} \right)_j \right]^{n+1,k} y_{i,j}^n p_j^{n+1,k+1}
 \end{aligned}$$

$$\begin{aligned}
& + \left[T_{g,j-\frac{1}{2}}^{n+1,k} (p_{j-1}^{n+1,k} - p_j^{n+1,k}) \right. \\
& \quad \left. - \frac{V_{pj}}{C_1 \Delta t} \left(\rho_{g,j}^{n+1,k} + \left(\left(\frac{\partial \rho_g}{\partial y_i} \right)_{\substack{y_k,p \\ k \neq 1,i}} \right)_j^{n+1,k} y_{i,j}^n \right) \right] \Delta_t y_{i,j} \\
& + \left[T_{o,j+\frac{1}{2}}^{n+1,k} x_{i,j+1}^n \right] p_{j+1}^{n+1,k+1} \\
& + \left[T_{o,j+\frac{1}{2}}^{n+1,k} (p_{j+1}^{n+1,k} - p_j^{n+1,k}) \right] \Delta_t x_{i,j+1} \\
& = - \frac{V_{pj}}{C_1 \Delta t} y_{i,j}^n \left(\left(\frac{\partial \rho_g}{\partial p} \right)_{\{y_k\}_{k=2}^{N_c}} \right)_j^{n+1,k} p_j^n, \quad 2 \leq i \leq N_c. \tag{4.5.12}
\end{aligned}$$

Eqs. 4.5.11 and 4.5.12 are valid for the case block $j \equiv 4$ and block $j + 1 \equiv 2$, provided we exchange x_i for y_i and the supscript g for the supscript o .

$$\begin{pmatrix}
 * & * & * & * & * & * & * & * & * \\
 * & * & * & * & * & * & * & * & * \\
 * & * & * & * & * & * & * & * & * \\
 * & * & * & * & * & * & * & * & * \\
 * & * & * & * & * & * & * & * & * & * \\
 * & * & * & * & * & * & * & * & * & * \\
 * & * & * & * & * & * & * & * & * & * \\
 * & * & * & * & * & * & * & * & * & * \\
 & & & & * & * & * & * & * & * \\
 & & & & * & * & * & * & * & * \\
 & & & & * & * & * & * & * & * \\
 & & & & * & * & * & * & * & * \\
 & & & & & * & * & * & & \\
 & & & & & & * & * & * & \\
 & & & & & & & * & * & * \\
 & & & & & & & & * & * & * \\
 & & & & & & & & & * & * \\
 & & & & & & & & & & * & *
 \end{pmatrix} \quad (4.6.3)$$

where A_1 is a 5×4 submatrix, B_1 , A_2 , C_2 and C_3 are 4×4 submatrices, and the remaining submatrices are 1×1 . The vectors P_1 and P_2 contain pressure, saturation and 2 mole fraction composition terms, whereas the remaining P_i , ($3 \leq i \leq 10$), vectors contain only pressure.

We recall that to simulate a gas cycling process in a retrograde gas condensate reservoir, we must specify the outer boundary pressure and the mole fraction composition of the fluid flowing across the outer boundary. If the specified outer boundary pressure is equal to the reservoir initial pressure, then the gridblocks near the wellbore become two-phase as the pressure at these gridblocks drop, whereas the outer boundary gridblocks that initially contained a single-phase gas of fixed composition start mixing with single-phase gas of varying composition. During the infinite acting (transient flow) period, the single-phase gridblocks away from both boundaries remain at initial conditions. In the case where the two first gridblocks contain two phases and only the last outer boundary gridblock is mixing with a single-phase gas of varying composition, the matrix assumes the following form:

4.7 Automatic Time Step Selector

The time grid will be given by the following relation:

$$t^{n+1} = t^n + \Delta t^{n+1}, \quad (4.7.1)$$

where $t^0 = 0$ and Δt^{n+1} is to be specified. The model has the option of keeping the time step size constant or selecting it in accordance with the variations of the parameters. The purpose of adding a time step selector is to automatically select the time step size to avoid numerical instability, and to save the expense and effort in selecting a suitable time step size by trial and error. Also, significant computer time can often be saved by allowing the time step size to vary as the simulation proceeds.

The method of relative changes is employed for selecting the time step size. In this method, selected variables are allowed a certain change over one time step. In our implementation, pressure, saturation and overall mole fraction composition are chosen as the variables. The computational procedure is summarized below:

- (1) Input the initial time step size, $\Delta t_{init.}$, the maximum time step size, Δt_{max} , the maximum change in pressure, Δp_{fix} , the maximum change in saturation $\Delta S_{g,fix}$ the maximum change in overall composition Δz_{fix} and a safety factor such that $0 < factor \leq 0.95$.
- (2) Calculate the changes in these variables between the current time step $n + 1$ and previous time step n for each gridblock:

$$(\Delta p)_j = |p_j^{n+1} - p_j^n|, \quad 1 \leq j \leq N_r, \quad (4.7.2)$$

$$(\Delta S_g)_j = |S_{g,j}^{n+1} - S_{g,j}^n|, \quad 1 \leq j \leq N_r, \quad (4.7.3)$$

and

$$(\Delta z)_j = |(z_i^{n+1})_j - (z_i^n)_j|, \quad 1 \leq i \leq N_c, \quad 1 \leq j \leq N_r, \quad (4.7.4)$$

- (3) Calculate the maximum changes in these variables for all gridblocks:

$$\Delta p_{max} = \max_{1 \leq j \leq N_r} \{\Delta p\}_j, \quad (4.7.5)$$

$$\Delta S_{g,max} = \max_{1 \leq j \leq N_r} \{\Delta S_g\}_j, \quad (4.7.6)$$

$$\Delta z_{max} = \max_{\substack{1 \leq j \leq N_r \\ 1 \leq i \leq N_c}} \{\Delta z_i\}_j. \quad (4.7.7)$$

(4) Calculate Δt for the next time step using

$$\Delta t^{n+1} = \min\{\Delta t_p, \Delta t_{S_g}, \Delta t_z\}, \quad (4.7.8)$$

where

$$\Delta t_p = (factor) \Delta t^n \frac{\Delta p_{fix}}{\Delta p_{max}}, \quad (4.7.9)$$

$$\Delta t_{S_g} = (factor) \Delta t^n \frac{\Delta S_{g,fix}}{\Delta S_{g,max}}, \quad (4.7.10)$$

and

$$\Delta t_z = (factor) \Delta t^n \frac{\Delta z_{fix}}{\Delta z_{max}}, \quad (4.7.11)$$

(5) The new time step size is limited by

$$\Delta t_{min} \leq \Delta t^{n+1} \leq \Delta t_{max}, \quad (4.7.12)$$

where Δt_{min} and Δt_{max} are the minimum and maximum time step sizes defined as input parameters.

The model requires that convergence be achieved in at most the maximum number of iterations that is also defined as an input parameter. If convergence is not achieved in the maximum number of iterations, the program automatically restarts the time step with time step size equal to the old time step multiplied by the safety factor. Note that during boundary-dominated flow period, the time step size tends to increase since pressure, saturation and composition changes from time

step to time step tend to be small, and hence, the size of time step computed from Eqs. 4.7.9 - 4.7.11 would be large and increasing. In fact for steady-state flow (constant pressure and composition outer boundary), Eqs. 4.7.9 - 4.7.10 predict an infinite time step size. Also, our experience with the simulation of the depletion of gas systems (sealed outer boundary) indicates that the most accurate answers are obtained during boundary-dominated flow by using a constant time step size.

4.8 Appearance and Disappearance of a Phase

We consider three basic cases. The first two deal with the formation of a second phase in a gridblock which initially contains one phase. The third case deals with the situation where a phase disappears; i.e., a gridblock goes from two-phase to single-phase over an iteration or a time step.

4.8.1 Block $j \equiv 1, 3$

We assume that at initial conditions, block j contains only one phase and that the composition of that phase will not change unless a second phase develops in the gridblock. This situation will occur when the initial reservoir pressure is above the initial reservoir saturation pressure and the outer reservoir boundary is either no flow or constant pressure with constant composition identical to the initial reservoir fluid composition. During production, the saturation pressure of this gridblock will not change as long as the gridblock remains single-phase. In this case, the model checks for the appearance of a second phase in gridblock j at the end of each iteration. If the pressure, $p_j^{n+1,k+1}$, drops below the saturation pressure of the initial in-place phase, then block j is assumed to contain two phases. This criterion for the appearance of a second phase is sufficient.

4.8.2 Block $j \equiv 2, 4$

Here, we assume that the composition of the fluid in gridblock j can change even during the time period when the gridblock contains only one phase. This occurs because the single-phase fluid of gridblock j is mixed with single-phase fluid of different composition from an adjacent gridblock. This can happen during gas cycling (gas injection across the outer reservoir boundary in our model) or during pressure buildup, or in a drawdown following a buildup where blocks returned to single-phase during the buildup. In this case, the saturation pressure must be calculated for the in-place single-phase fluid at the end of each iteration using the latest available estimates of pressure and composition. (The procedure^{9,10} for estimating values for the mole fraction compositions of both phases at the computed

pressure, $p_j^{n+1,k+1}$, is normally conducted by flashing the initial in-place phase to that pressure). However, our model does obtain convergence by assuming the mole fraction composition of both phases, to be equal to the mole fraction composition of both phases at the saturation point, i.e., $\{x_{i,m,j}^{n+1,k} = x_{i,m,j}^{sat}\}_{i=1}^{N_c}$ for constant rate production. For the case when the reservoir is produced at a constant pressure with $(p_i - p_{wf}) > 200 \text{ psia}$, the model switches to a flash calculation procedure, if convergence is not attained. Furthermore, all parameters, as well as derivatives involving terms evaluated at the previous time step, when the newly appearing phase is absent, are estimated at the saturation point.

4.8.3 Disappearance of a Phase

We handle the case when a two-phase block becomes single-phase the same way as is advocated by Coats⁷ and Fussell and Fussell¹. The criterion they use is as follows: if a phase saturation at the end of an iteration is less than zero, set that phase saturation to zero, set the saturation of the remaining phase to unity, and continue.

4.9 Material Balance

The basic material balance equation is computed as follows

$$\frac{\sum_{j=1}^{N_r} [(\rho_o S_o + \rho_g S_g)_j^{n+1} - (\rho_o S_o + \rho_g S_g)_j^n] V_{p,j}}{q_t^{n+1} \Delta t^{n+1}}, \quad (4.9.1)$$

where q_t^{n+1} is the average total molar flow rate (*lbmoles/day*) occurring at the new time step $n + 1$.

The material balance is satisfied whenever the ratio given by Eq. 4.9.1 is equal to unity.

4.10 Summary of the Overall Computational Procedure of the Simulator

The overall solution scheme of our formulation follows a two-step procedure. First, for a two-phase block, pressure, saturation and $N_c - 2$ oil or gas mole fraction compositions are solved for implicitly using implicit pressure and phase composition dependent terms. Then following Eq. 4.4.3, the remaining $N_c + 2$ oil or gas mole fraction compositions are determined explicitly by simple matrix multiplication. Since none of the coefficients in the flow equations are evaluated explicitly, a set of nonlinear equations is formed. This feature results in a formulation that is iterative over a time step. The solution procedure over a time step can be summarized by the following steps:

Given the values of pressure, saturation, and phase mole fraction composition obtained at time level n , t^n , at all gridblocks,

- (1) Compute the $N_c \times N_c$ matrix M_j given by Eq. 4.4.5a for all two-phase gridblocks, and invert it. (For a reservoir at initial pressure, filled with a single-phase fluid, only one matrix M_j is computed during the initialization process using the partial derivatives computed at the initial reservoir saturation point. This matrix is associated with all the reservoir gridblocks.)
- (2) Set the time step size in accordance with the variations of the parameters as desired.
- (3) Update the fluid properties such as phase densities and viscosities via the phase package.
- (4) Construct the matrix problem in accordance with the phase configuration of each gridblock, i.e., use Eq. 4.3.5 when a block and the adjacent blocks contain a single-phase fluid with known composition so that only pressures for these blocks are the unknowns; use the N_c flow equations, Eqs. 4.4.21, 4.4.30 and 4.4.31 when a block contains a two-phase fluid; finally, if a block is filled with a single-phase fluid with variable compositions, then, depending on the phase configuration of the gridblock of interest and the upstream gridblock, allocate the appropriate equations, i.e., 4.5.4b, 4.5.5c, 4.5.6 - 4.5.8a - 4.5.8b, 4.5.9 - 4.5.10 or 4.5.12 - 4.5.12.

- (4) Solve the matrix problem, sort the solution vector for the appropriate parameters and check for convergence. If convergence is not attained, repeat step (3), else proceed.
- (5) Check whether the changes in the variables are acceptable. If results are acceptable, proceed to step (1), if not, repeat step (2).

CHAPTER V

MODEL VALIDATION AND DISCUSSION

All results considered are for one - dimensional radial flow to a completely penetrating well located at the center of a cylindrical reservoir.

5.1 Analytical Results

To ensure the validity of the model in the single-phase region, we use single-phase theoretical results for both constant rate and constant pressure production. We consider results for both transient and boundary-dominated flow. We also show results from our model match the multiphase flow analytical solution for steady-state flow in the entire drainage region. Here, we formulate the problem first considered by O'Dell and Miller⁴⁴ for cycling a gas condensate reservoir, and use analytical results presented by Jones⁴⁵.

5.1.1 Single-Phase Gas Flow

Throughout our consideration of the single-phase flow of a real gas, we present results in terms of the pseudopressure function $m(p)$ which is defined by

$$m(p) = \int_{p_b}^p \frac{2p'}{\mu(p')Z(p')} dp', \quad (5.1.1)$$

where p_b is an arbitrary reference pressure and Z is the gas deviation factor obtained by solving the appropriate cubic equation of state. The dimensionless wellbore pseudopressure drop and dimensionless time based on wellbore radius, respectively, are defined by

$$m_{wD} = \frac{0.00633\pi kh}{qTR} [m(p_i) - m(p_{wf})], \quad (5.1.2)$$

and

$$t_D = \frac{0.00633kt}{\phi\mu_i c_i r_w^2}, \quad (5.1.3)$$

where q represents the gas flow rate in lbmoles/day, R is the universal gas constant, c the fluid compressibility and μ the viscosity obtained from our PVT package. In Eq. 5.1.3 the viscosity-compressibility product is evaluated at initial conditions.

5.1.1.a Transient Single-Phase Gas Flow

Wattenbarger and Ramey⁴⁶ show that during transient flow, the dimensionless wellbore pseudopressure drop is given by

$$m_{wD} = \frac{1}{2}(\ln t_D + 0.80907) + s, \quad (5.1.4)$$

where s is the skin factor.

For production at a constant flowing bottomhole pressure, p_{wf} , Bratvold⁴⁷ has verified that for the transient flow, we have

$$\frac{1}{q_D} \approx \frac{1}{2}(\ln t_D + 0.80907) + s, \quad (5.1.5)$$

where

$$q_D = \frac{q(t)TR}{0.00633\pi kh[m(p_i) - m(p_{wf})]} \quad (5.1.6)$$

Note that in Eq. 5.1.4 the rate is constant and p_{wf} is a function of time, whereas, in Eq. 5.1.5, q is time-dependent and p_{wf} is constant. Eq. 5.1.4 is highly accurate for $t_D > 10^2$ and Eq. 5.1.5 is accurate for $t_D > 10^3$.

5.1.1.b Boundary-Dominated Single-Phase Gas Flow

We verify the accuracy of our model results for pseudosteady state flow by using numerical results developed by Al-Hussainy et al.⁴⁸ For constant rate production with the pressure at the outer boundary held constant at p_e , steady-state flow is achieved. Then, the wellbore pseudopressure drop is given by

$$\frac{0.00633\pi kh}{qTR} [m(p_e) - m(p_{wf})] = \ln \frac{r_e}{r_w} - \frac{1}{2} + s, \quad (5.1.7)$$

and

$$\frac{0.00633\pi kh}{qTR} [m(\bar{p}) - m(p_{wf})] = \ln \frac{r_e}{r_w} - \frac{3}{4} + s \quad (5.1.8)$$

where r_e is the radius of the cylindrical reservoir, p_e is the pressure at the outer boundary and \bar{p} is the average reservoir pressure. Ding⁴⁹ reports that Eqs. 5.1.7 and 5.1.8 are accurate to within 1% for $t_{AD} \geq 0.1$, where t_{AD} is the dimensionless time based on drainage area, defined by

$$t_{AD} = \frac{0.00633kt}{\phi(\mu c)_i A}. \quad (5.1.9)$$

Here, c represents the fluid compressibility obtained via the PVT package at the initial pressure and composition, and A is the cylindrical drainage area given by

$$A = \pi(r_e^2 - r_w^2). \quad (5.1.10)$$

Ding⁴⁹ and Reynolds et al.⁵⁰ developed a method for correlating the dimensionless wellbore pseudopressure drop with the liquid flow dimensionless wellbore pressure drop during boundary-dominated flow; this method provides us with another equation to test our model. Reynolds et al.⁴⁹ show that the dimensionless wellbore pseudopressure drop can be approximated by

$$m_{wD} = 2\pi\hat{t}_{AD} + \ln \left(\frac{r_e}{r_w} \right) - \frac{3}{4} + s, \quad (5.1.11)$$

for $t_{AD} \geq 0.08$. Here, \hat{t}_{AD} is defined as

$$\hat{t}_{AD} = \frac{0.00633kt}{\phi(\bar{\mu}\bar{c})A}. \quad (5.1.12)$$

In Eq. 5.1.12, the product $\bar{\mu}\bar{c}$ represents the fluid viscosity-compressibility product evaluated at an average reservoir pressure, \bar{p} .

5.1.2 The Steady-State Model Problem

We recall that the compositional form of partial differential equations governing the flow of a oil and gas in a porous medium are given by

$$0.00633 \frac{1}{r} \frac{\partial}{\partial r} \left[rk \left(\rho_o \frac{k_{ro}}{\mu_o} x_i + \rho_g \frac{k_{rg}}{\mu_g} y_i \right) \frac{\partial p}{\partial r} \right] = \phi \frac{\partial}{\partial t} (\rho_o S_o x_i + \rho_g S_g y_i), 1 \leq i \leq N_c, \quad (5.1.13)$$

for $r_w < r < r_e$ and $t > 0$, under the constraints

$$\sum_{i=1}^{N_c} x_i = 1, \quad (5.1.14a)$$

$$\sum_{i=1}^{N_c} y_i = 1 \quad (5.1.14b)$$

and

$$S_o + S_g = 1. \quad (5.1.15)$$

The thermodynamic equilibrium at any point in the reservoir is expressed by

$$f_{i,L} = f_{i,V}. \quad (5.1.16)$$

For steady-state flow to prevail in the reservoir, pressure, saturation and mole fraction composition must be independent of time. This implies that the right-hand side of Eq. 5.1.13 must be zero so that Eq. 5.1.13 reduces to the following equation

:

$$\frac{1}{r} \frac{d}{dr} \left[rk \left(\rho_o \frac{k_{ro}}{\mu_o} x_i + \rho_g \frac{k_{rg}}{\mu_g} y_i \right) \frac{dp}{dr} \right] = 0, \quad 1 \leq i \leq N_c. \quad (5.1.17)$$

The saturation, mole fraction and fugacity constraints, Eqs. 5.1.14 - 5.1.16 still apply. For the constant rate production, the inner boundary condition is given by

$$q_t = 0.00633(2\pi r_w h) \left[\left(\rho_o \frac{k_{ro}}{\mu_o} + \rho_g \frac{k_{rg}}{\mu_g} \right) \left(\frac{dp}{dr} \right) \right]_{r=r_w}, \quad t > 0. \quad (5.1.18)$$

The outer boundary conditions which ultimately yield steady-state flow during the boundary-dominated flow period are given by the following equations:

$$p(r_e, t) = p_e \quad (5.1.19)$$

and

$$z_{i,e} = y_{i,I}, \quad (5.1.20)$$

where $\{z_{i,e}\}_{i=1}^{N_c}$ denotes the fixed composition at the outer boundary and $\{y_{i,I}\}_{i=1}^{N_c}$ may either be the initial composition of the in-place gas or any other fixed composition of an injected gas; p_e represents the fixed pressure at the outer boundary. Eqs. 5.1.17 - 5.1.20 represent the formulation of the steady-state model problem. If we hold p_e at p_i , the initial pressure, or at any pressure greater than p_{dew} , the dew point pressure of the initial in-place gas, then the model problem given by Eqs. 5.1.17 - 5.1.20 is equivalent to the model first considered by O'Dell and Miller⁴⁴ for cycling a gas condensate reservoir.

To begin the investigation of the nature of the solution to Eqs. 5.1.17 - 5.1.20, we note that $p_e > p_{dew}$ implies that part of the reservoir is subject to single-phase flow and part of the reservoir contains a two-phase fluid. We cannot at this point say if both phases are mobile over the entire two-phase region. Following the work of Jones⁴⁵, we integrate Eq. 5.1.13 over r to obtain

$$\left[rk \left(\rho_o \frac{k_{ro}}{\mu_o} x_i + \rho_g \frac{k_{rg}}{\mu_g} y_i \right) \frac{dp}{dr} \right] = C_i, \quad 1 \leq i \leq N_c. \quad (5.1.21)$$

Here C_i is a constant dependent on the flowing component. Summing up Eq. 5.1.21 over all i , we obtain

$$\left[rk \left(\rho_o \frac{k_{ro}}{\mu_o} + \rho_g \frac{k_{rg}}{\mu_g} \right) \frac{dp}{dr} \right] = C, \quad (5.1.22)$$

where

$$C = \sum_{i=1}^{N_c} C_i. \quad (5.1.23)$$

Dividing Eq. 5.1.21 by Eq. 5.1.22 and rearranging gives

$$\frac{\rho_o \frac{k_{ro}}{\mu_o}}{\rho_o \frac{k_{ro}}{\mu_o} + \rho_g \frac{k_{rg}}{\mu_g}} x_i + \frac{\rho_g \frac{k_{rg}}{\mu_g}}{\rho_o \frac{k_{ro}}{\mu_o} + \rho_g \frac{k_{rg}}{\mu_g}} y_i = \tilde{C}_i \quad (5.1.24)$$

where

$$\tilde{C}_i = \frac{C_i}{C}. \quad (5.1.25)$$

Note that the coefficients of the mole fractions x_i and y_i are the analytical expressions for the fraction of the total moles flowing in the liquid phase and the fraction of the total moles flowing in the vapor phase, respectively. Thus, the left-hand side of Eq. 5.1.24 represents the mole fraction of component i in the flowing fluid. Since we assume only gas exists, applying Eq. 5.1.24 at $r = r_e$ gives

$$\tilde{C}_i = z_{i,e} = y_{i,I}, \quad 1 \leq i \leq N_c. \quad (5.1.26)$$

where the second equality of Eq. 5.1.26 follows from Eq. 5.1.20. Eqs. 5.1.24 and 5.1.26 indicate that the overall composition of the flowing fluid at any point r is the composition of the injected fluid.

We can rewrite Eq. 5.1.24 as

$$L(r)x_i + V(r)y_i = z_{i,e}, \quad (5.1.27)$$

where $L(r)$ and $V(r)$ are defined as follows

$$L(r) = \frac{\rho_o \frac{k_{ro}}{\mu_o}}{\rho_o \frac{k_{ro}}{\mu_o} + \rho_g \frac{k_{rg}}{\mu_g}} \quad (5.1.28)$$

and

$$V(r) = \frac{\rho_g \frac{k_{rg}}{\mu_g}}{\rho_o \frac{k_{ro}}{\mu_o} + \rho_g \frac{k_{rg}}{\mu_g}}. \quad (5.1.29)$$

Summing Eq. 5.1.27 over all i gives

$$L(r) + V(r) = 1 \quad (5.1.30)$$

The steady-state solution must satisfy Eq. 5.1.27 and the constraints given by Eqs. 5.1.14 and 5.1.16. We see that Eqs. 5.1.14, 5.1.16, 5.1.27 and 5.1.30 form a system of equations which is equivalent to the single-cell separation (flash) equations at the cell pressure $p(r)$. Hence, $L(r)$, $V(r)$, $\{x_i\}_{i=1}^{N_c}$ and $\{y_i\}_{i=1}^{N_c}$ satisfy the flash equations at any r ⁴⁵.

Dividing Eq. 5.1.28 by Eq. 5.1.29, we have

$$\frac{L(r)}{V(r)} = \frac{\rho_o \frac{k_{ro}}{\mu_o}}{\rho_g \frac{k_{rg}}{\mu_g}}. \quad (5.1.31)$$

As shown in Ref. 45, an expression for the relative permeability ratio can be obtained by rearranging Eq. 5.1.31 as

$$\frac{k_{ro}}{k_{rg}} = \frac{L(r)\mu_o\rho_g}{V(r)\mu_g\rho_o} = \frac{L(r)\mu_o Z_o}{V(r)\mu_g Z_g}, \quad (5.1.32)$$

where Z_o and Z_g are the compressibility factors for the oil and gas phase, respectively. If the pressure profile is known, Eq. 5.1.32 can readily be used to obtain the saturation profile by interpolating in a k_{ro}/k_{rg} versus S_g curve constructed from the relative permeability curves.

In Eq. 5.1.32, k_{ro} remains nonnegative as long $L(r)$ is nonnegative. Since $L(r)$ is given by the flash calculations and, hence, is greater than zero if $p(r) < p_{dew}$, then wherever two phases coexist, both are mobile as pointed out in Ref. 45. This yields a discontinuity in the saturation distribution at $p(r_{dew}) = p_{dew}$ with an oil saturation greater than the critical oil saturation in the region $r < r_{dew}$ and an oil saturation equal to zero in the region $r > r_{dew}$.

If $p(r)$ is known, the above results would allow us to compute the parameters in the set $\{S_o, S_g, L, V, \{x_i\}_{i=1}^{N_c}, \{y_i\}_{i=1}^{N_c}\}_r$. The equation which forms a constraint on all the distributions simultaneously, including the pressure distribution, is expressed by the following pseudopressure transformation,

$$m(p) = \int_{p_b}^p \left(\rho_o \frac{k_{ro}}{\mu_o} + \rho_g \frac{k_{rg}}{\mu_g} \right) dp', \quad (5.1.33)$$

where p_b is some base pressure. Eq. 5.1.33 can be evaluated since phase densities, phase viscosities and relative permeabilities can be established once pressure is known. Differentiating Eq. 5.1.33 with respect to r gives

$$\frac{dm(p)}{dr} = \left(\rho_o \frac{k_{ro}}{\mu_o} + \rho_g \frac{k_{rg}}{\mu_g} \right) \frac{dp}{dr}. \quad (5.1.34)$$

Summing Eq. 5.1.17 over all i and substituting Eq. 5.1.34 in the resulting equation yields

$$\frac{1}{r} \frac{d}{dr} \left(r \frac{dm(p)}{dr} \right) = 0. \quad (5.1.35a)$$

Similarly, substituting Eq. 5.1.34 into Eq. 5.1.18 gives

$$0.00633 \frac{2\pi kh}{q_t} \left(r \frac{dm(p)}{dr} \right)_{r_w} = 1. \quad (5.1.35b)$$

We define the dimensionless pseudopressure drop by

$$m_D(p) = 0.00633 \frac{2\pi kh}{q_t} [m(p_i) - m(p)]. \quad (5.1.36)$$

Using Eq. 5.1.36 in Eqs. 5.1.35a and 5.1.35b gives

$$\frac{1}{r} \frac{d}{dr} \left(r \frac{dm_D(p)}{dr} \right) = 0, \quad (5.1.37)$$

and

$$\left(r \frac{dm_D(p)}{dr} \right)_{r_w} = -1. \quad (5.1.38)$$

The outer boundary condition, Eq. 5.1.19, can also be expressed in terms of the dimensionless pseudopressure drop as

$$m_D(r_e) = 0.00633 \frac{2\pi kh}{qt} \int_{p_e}^{p_i} \left(\rho_o \frac{k_{ro}}{\mu_o} + \rho_g \frac{k_{rg}}{\mu_g} \right) dp'. \quad (5.1.39)$$

If we hold p_e at p_i , then the right-hand side of Eq. 5.1.39 is zero, and Eqs. 5.1.37 - 5.1.39 can be solved by simple integration to yield the radial distribution of the dimensionless pseudopressure drop, i.e.,

$$m_D [p(r)] = -\ln \left(\frac{r}{r_e} \right). \quad (5.1.40)$$

The steady-state model results are summarized as follows :

- (i) The composition of the moving fluid at any point of the reservoir is the composition of the injected fluid at $r = r_e$.
- (ii) The number of moles of liquid flowing, L , the number of moles of vapor flowing, V , the mole fractions in the liquid phase, $\{x_i\}_{i=1}^{N_c}$, and the mole fractions in the vapor phase, $\{y_i\}_{i=1}^{N_c}$, satisfy the flash equations.
- (iii) Saturations at any point of the reservoir can be computed from Eq. 5.1.32 by interpolation of input relative permeability curves.
- (iv) Two phases are mobile over any region of the reservoir where they coexist.
- (v) The dimensionless pseudopressure drop, Eq. 5.1.36, follows the standard steady-state single-phase liquid flow equation, Eq. 5.1.40.

The most practical way to achieve steady-state flow is to start the model at time zero and deplete the reservoir through the transient flow regime into steady-state, either at a constant rate or a constant pressure. The duplication of the five steady-state results listed above is the criterion we use to further establish the accuracy of the model for two-phase flow.

5.2 Fluid and Rock Properties

5.2.1 Description of Fluids Used

The mixtures considered in this work are gas condensate, volatile oil and black-oil. Table 5.1 contains the summary of the fluid properties of a binary volatile oil, whereas Table 5.2 depicts the characteristics of the binary retrograde gas condensate. Table 5.3 documents the initial compositions of five ternary systems considered and Tables 5.4 and 5.5, respectively, show 14-component and 17-component mixtures. Each of the ternary systems is a pseudo-mixture consisting of three components: methane, n-butane and n-decane. The first three mixtures are typical gas condensates with widely different phase behavior characteristics. The main difference between these mixtures is in their richness. Mix 1 is a lean gas condensate mixture, having 4.5% maximum liquid dropout obtained from a constant composition expansion process (CCE). Mix 2 is a richer gas condensate mixture that yields a maximum volume percent of 7% during a CCE process. Mix 3 is a heavy gas condensate mixture with a CCE maximum liquid dropout of 12.5%. The volatile oil and black-oil are referred to as Mix 4 and Mix 5, respectively. The ternary systems compositions are taken from the experimental data presented by Reamer, Sage, and Lacey.⁵¹ Fig. 5.1 presents the constant composition expansion data for the three gas condensate fluid mixtures where mole fraction of the liquid is plotted as a function of pressure. Fig. 5.2 presents similar data for the volatile and black-oil mixtures.

The Zudkevitch-Joffe-Redlich-Kwong¹⁶ equation of state is used for all the ternary systems shown in Table 5.3. The binary interaction parameters are all set to zero except $k_{1,2} = 0.024$ and $k_{2,3} = 0.025$. For this EOS, the van der Waals coefficients are unique functions of temperature and are set to $\Omega_{a,2} = 0.40982$, $\Omega_{b,2} = 0.0805$, $\Omega_{a,3} = 0.45$, $\Omega_{b,3} = 0.07312$, for $T = 740$ °R and $\Omega_{a,2} = 0.4154$, $\Omega_{b,2} = 0.0759$, $\Omega_{a,3} = 0.4583$, $\Omega_{b,3} = 0.07279$, for $T = 620$ °R. $\Omega_{a,1} = 0.4251$ and $\Omega_{b,1} = 0.0859$ for both values of temperature. The saturation pressures and compositions are shown in Table 5.3.

TABLE 5.1

Summary of the Binary Volatile Oil Data

MIXTURE : C_1/C_6

EOS: Peng-Robinson

System Temperature	($^{\circ}R$)	600.
Initial Methane Mole Fraction	(-)	0.60
Bubble Point Pressure	($psia$)	2567
Methane Gas Mole Fraction at Bubble Point	(-)	0.930
Binary Interaction Parameter $k_{1,2}$	(-)	0.040

TABLE 5.2

Summary of the Binary Gas Condensate Data

MIXTURE : C_1/C_{10} EOS: Zudkevitch-Joffe-Redlich-Kwong

System Temperature	(°R)	800.
Initial Methane Mole Fraction	(-)	0.90
Dew Point Pressure	(<i>psia</i>)	4613
Methane Liquid Mole Fraction at Dew Point	(-)	0.784
Binary Interaction Parameter $k_{1,2}$	(-)	0.025
$\Omega_{a,1}$	(-)	0.42510
$\Omega_{a,2}$	(-)	0.45000
$\Omega_{b,1}$	(-)	0.08590
$\Omega_{b,2}$	(-)	0.07312

TABLE 5.3

Saturation Point Properties for the Ternary System

 $C_1/n - C_4/n - C_{10}$

Zudkevitch-Joffe-Redlich-Kwong EOS

Mixture	T ($^{\circ}R$)	Liquid		Vapor	
		C_4	C_{10}	C_4	C_{10}
Mix 1 $p_{dew} = 3969.7 \text{ psia}$ $\%L_{max} = 4.5$	620	0.03618	0.24854	0.01800	0.02590
Mix 2 $p_{dew} = 3106.9 \text{ psia}$ $\%L_{max} = 7.0$	740	0.16350	0.24294	0.11305	0.04752
Mix 3 $p_{dew} = 4189.6 \text{ psia}$ $\%L_{max} = 12.5$	740	0.03906	0.21429	0.02998	0.07374
Mix 4 (Volatile Oil) $p_b = 3173.0 \text{ psia}$	620	0.15200	0.22800	0.06789	0.01682
Mix 5 (Black Oil) $p_b = 2328.2 \text{ psia}$	620	0.0700	0.43600	0.02125	0.00613

TABLE 5.4

Composition and Characterization of 14 - Component Reservoir Oil

MIX 6 : $N_2 - CO_2/C_1 - C_{10+}$

Peng-Robinson EOS

 $T = 684 \text{ } ^\circ R, p_b = 3085 \text{ } psia$

Component	Mole (%)	Density (g/cm^3)	Molecular Weight
N_2	0.102		
CO_2	0.208		
C_1	52.006		
C_2	4.754		
C_3	2.393		
iC_4	0.455		
nC_4	0.979		
iC_5	0.427		
nC_5	0.598		
150 BP	1.112	0.6660	85.53
250 BP	2.579	0.7606	89.84
300 BP	3.041	0.7712	103.88
350 BP	3.029	0.7832	117.59
450 BP	28.317	0.8594	285.22

TABLE 5.5

**Composition and Characterization of
17-Component Retrograde Gas Condensate
Mix 7 : $N_2 - CO_2/C_1 - C_{15+}$
Schmidt-Wenzel EOS**

$$T = 623 \text{ } ^\circ R, p_{dew} = 3646.9 \text{ } \textit{psia}$$

Component	Mole (%)	Density (g/cm^3)	Molecular Weight
N_2	0.65		
CO_2	0.40		
C_1	75.45		
C_2	7.13		
C_3	3.87		
iC_4	1.02		
nC_4	2.17		
iC_5	0.92		
nC_5	1.07		
150 BP	1.47	0.6793	89
200 BP	1.10	0.7175	98
250 BP	0.68	0.7396	110
300 BP	0.46	0.7535	121
350 BP	0.77	0.7621	131
400 BP	0.77	0.7742	144
450 BP	1.24	0.7852	165
475 BP	0.83	0.7621	216

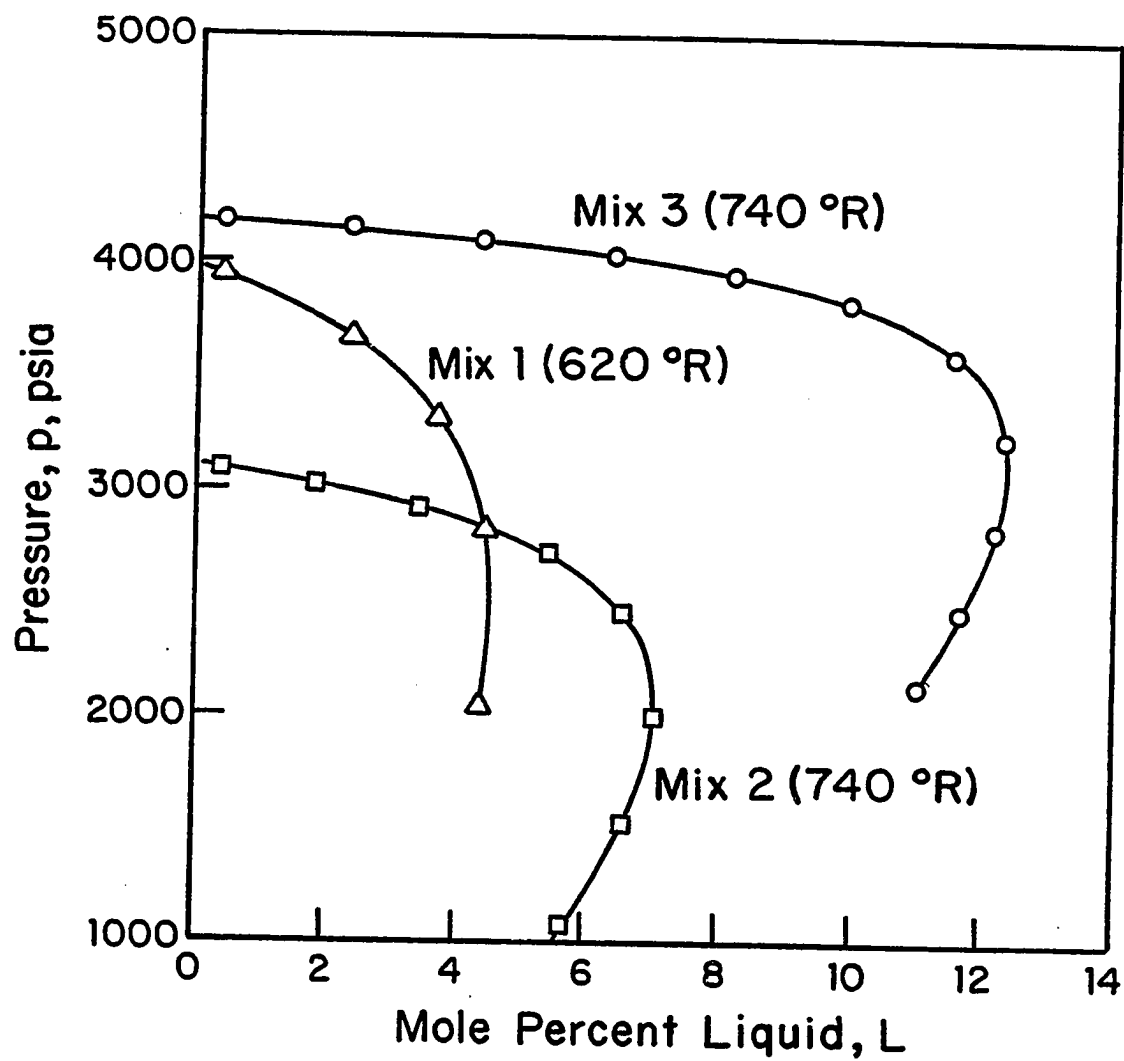


Fig. 5.1 - Constant composition expansion data; retrograde gas condensate, ternary systems.

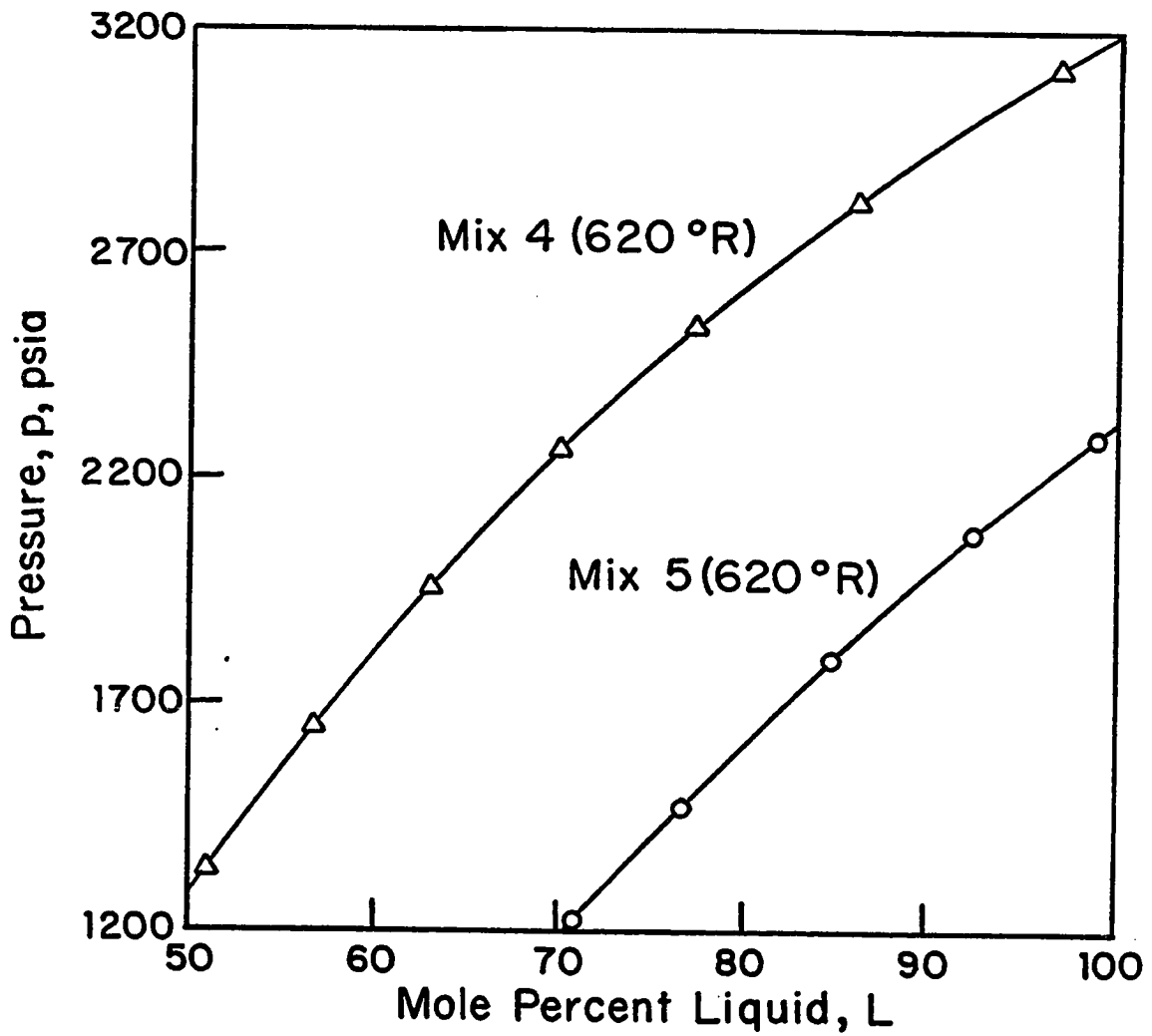


Fig. 5.2 - Constant composition expansion data; volatile and black-oil, ternary systems.

Mix 6 and Mix 7 are shown in Table 5.4 and an Table 5.5, respectively. Table 5.4 shows the composition and characterization of the 14-component volatile oil system. The Peng-Robinson¹⁷ equation of state predicts a bubble point pressure of 3085 psia at $T = 684$ °R. The last multicomponent mixture considered, Mix 7, is a retrograde gas condensate 17-component system presented in Table 5.5. We used the Schmidt-Wenzel²² (SW) EOS to model its phase behavior. The binary interaction coefficients for the SW EOS between various binary pairs must be determined to make accurate predictions. Firoozabadi *et al.*⁵² observed that the interaction parameters between methane and light hydrocarbons up to C_5 could be assumed to be equal to zero, while a good approximation for the interaction coefficients between methane and heavy hydrocarbon from $n-C_6$ to $n-C_{20}$ is 0.035. Hydrocarbon/ CO_2 and hydrocarbon/ N_2 interaction coefficients are about 0.15 and 0.12, respectively. The SW EOS predicts a dew point pressure of 3646.9 psia at $T = 623$ °R for Mix 7.

The properties of the C_{6+} fractions shown in Table 5.4 and Table 5.5 are obtained as follows. The molecular weights and specific gravities are obtained from Katz and Firoozabadi⁵³. The boiling points and the specific gravities are used to obtain the Watson characterization factors which in turn will be used to generate the Pitzer acentric factors in accordance with the Kesler and Lee⁵⁴ correlations. The critical properties are also estimated from the same correlations.

5.2.2 Rock Properties Description

Three sets of relative permeability data are considered in this work. Set 1 is extracted from the study of Kniazeff and Naville⁵; the critical oil saturation, $S_{o,c}$ for this data set is 0.50. Set 1 pertains to the imbibition process of oil displacing gas and is used to simulate responses of gas condensate reservoirs. Fig. 5.3 depicts this set. Relative permeability data of Set 2 and Set 3 pertain to the drainage process of gas displacing oil. These data sets are used to simulate responses of volatile oil and black oil systems. Set 2 is extracted from the study of Raghavan⁵⁵; the critical gas saturation, $S_{g,c}$, for this data set is 0.07. Set 3 is taken from the study of Bøe

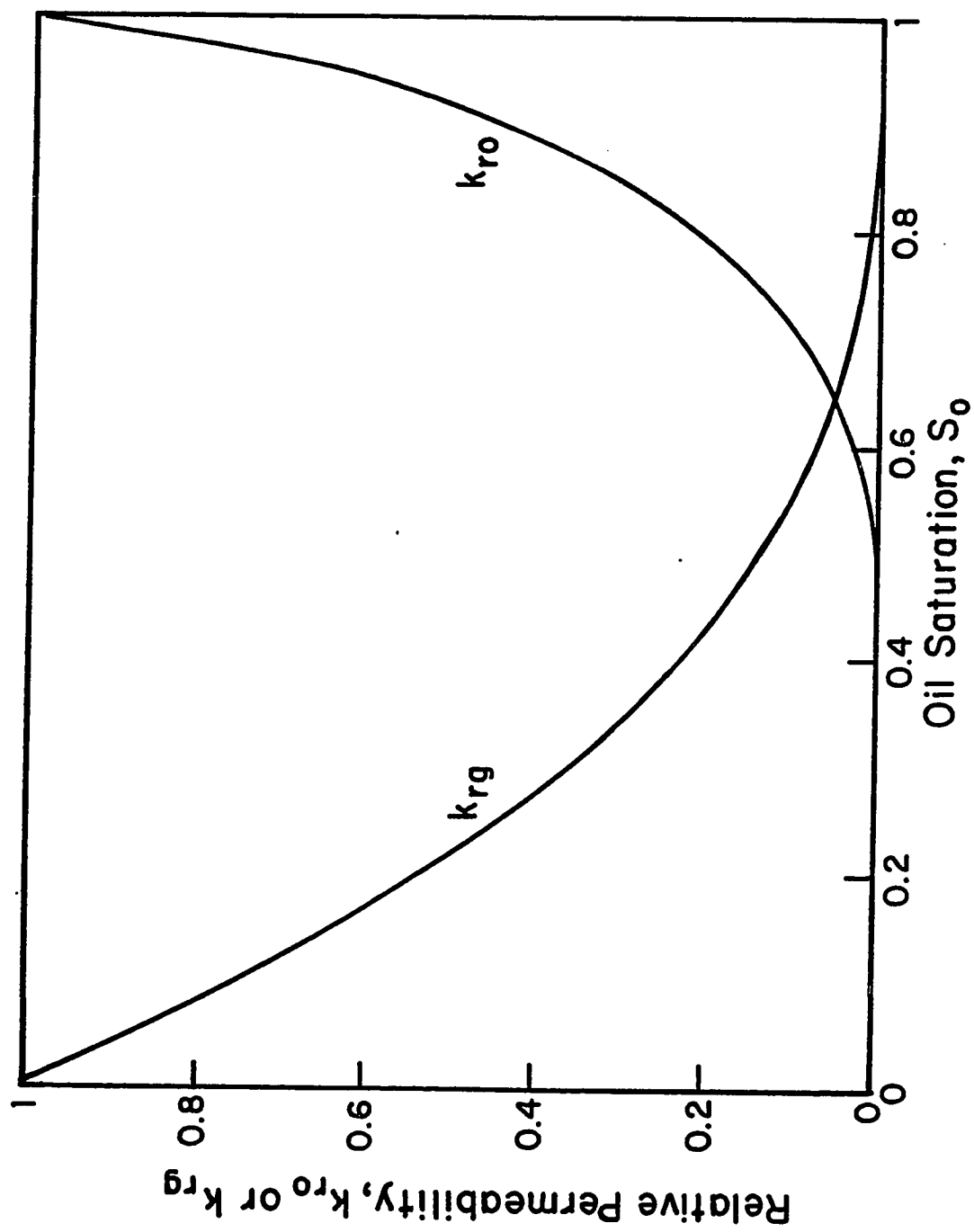


Fig. 5.3 - Relative permeability data;
Set 1, imbibition.

et al.⁵⁶; the critical gas saturation for this data set is 0. Fig. 5.4 presents these two sets of relative permeability data.

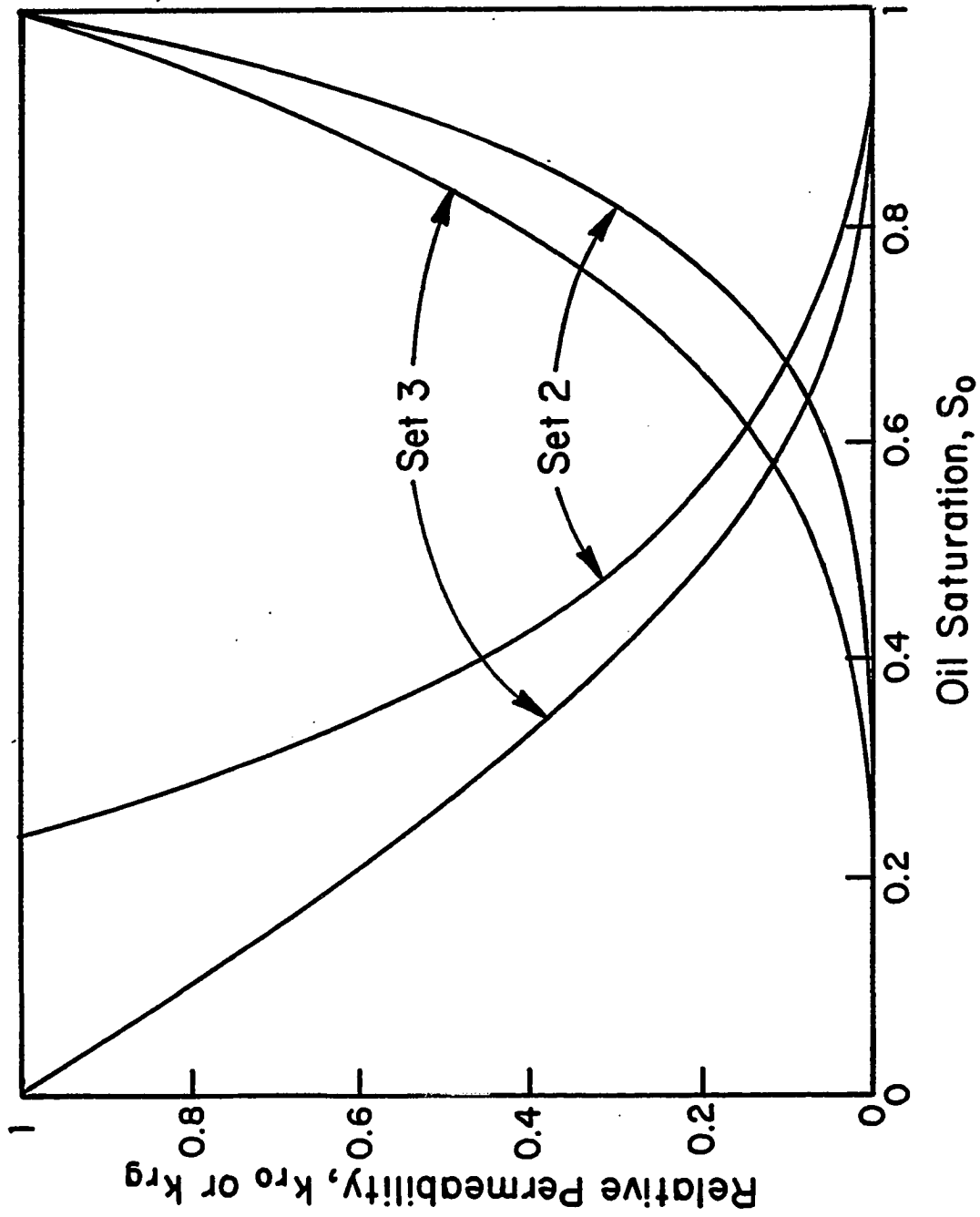


Fig. 5.4 - Relative permeability data; Sets 2 and 3, drainage.

5.3 Single-Phase Flow Results

All the runs were conducted for a reservoir with the same geometric properties. Table 5.6 shows the parameters used. Tables 5.1 and 5.2, respectively, give the PVT properties used for volatile oil and gas condensate cases considered. The Peng-Robinson equation of state is used to simulate the volatile oil, whereas the Zudkevitch - Joffe - Redlich - Kwong EOS is used for the gas condensate case.

5.3.1 Single-Phase Gas

In this subsection, we considered the binary gas mixture described in Table 5.2 which has a dew point pressure of 4613 psia. We simulated a drawdown test with an initial pressure equal to 6000 psia so that, throughout the flow period considered, only single-phase gas exists within the reservoir. Fig. 5.5 shows a plot of the dimensionless wellbore pseudopressure drop versus dimensionless time obtained for constant rate production. Results for $s = 0$ and $s = 5$ are presented. In Fig. 5.5 (as well as in Fig. 5.6 through Fig. 5.10) results obtained from our simulator are shown by square data points and theoretical results (Eqs. 5.1.4, 5.1.5, and 5.1.11) are shown as solid lines. As shown in Fig. 5.5, the model results agree with those predicted by the theory, i.e., Eq. 5.1.4, very well.

The constant pressure production results for transient flow are illustrated in Fig. 5.6, and again, the simulator results are in good agreement with the theoretical result, Eq. 5.1.5.

During boundary-dominated flow, the accuracy of our model is verified using the constant rate production analysis mentioned above. As shown in Fig. 5.7, the simulator results are in close agreement between the theoretical correlation, Eq. 5.1.11.

5.3.2 Single-Phase Oil

For the volatile oil of Table 5.1 the Peng-Robinson equation of state predicts a bubble point pressure equal to 2567 psia. For the case considered, the drawdown period starts at an initial pressure of 4000 psia and the wellbore pressure remains

TABLE 5.6

Summary of Input Reservoir Data

Single-Phase and Binary Systems

Reservoir Extent Radius, r_e	(<i>ft</i>)	660.0
Absolute Reservoir Permeability, k	(<i>md</i>)	10.0
Porosity, ϕ	(-)	0.3
Formation Thickness, h	(<i>ft</i>)	15.5
Wellbore Radius, r_w	(<i>ft</i>)	0.33

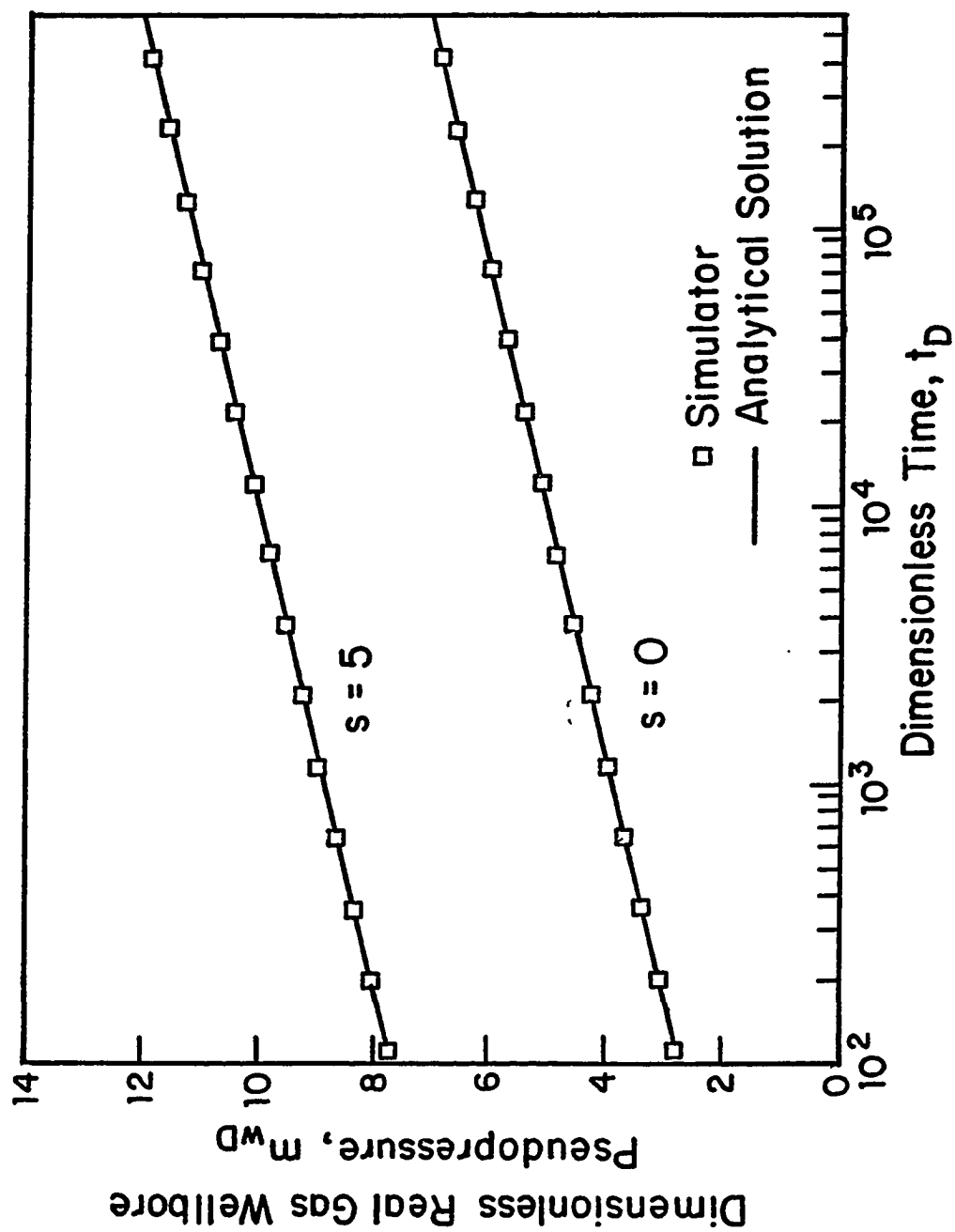


Fig. 5.5 - Single-phase gas; constant rate production: transient flow.

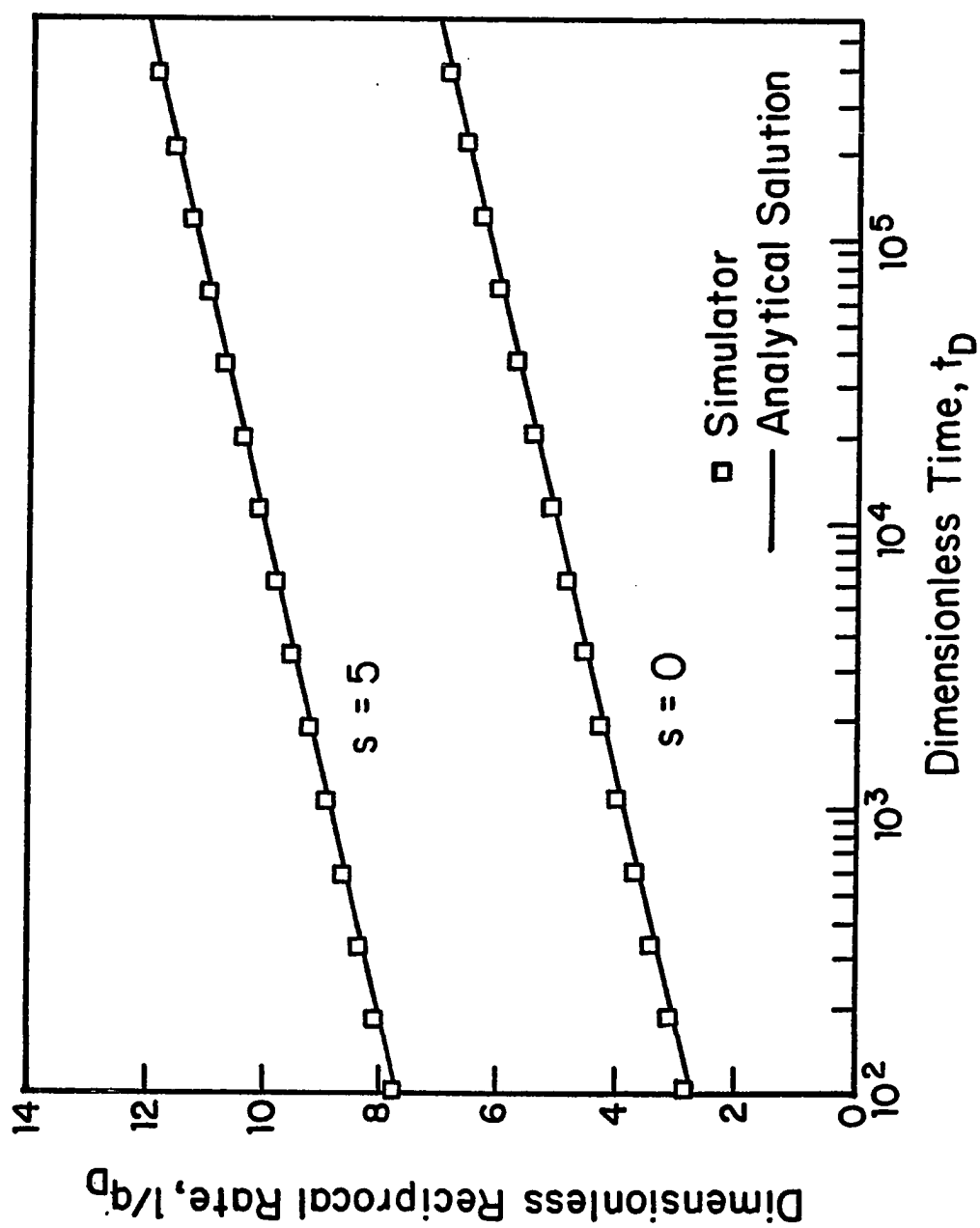


Fig. 5.6 - Single-phase gas; constant pressure production; transient flow.

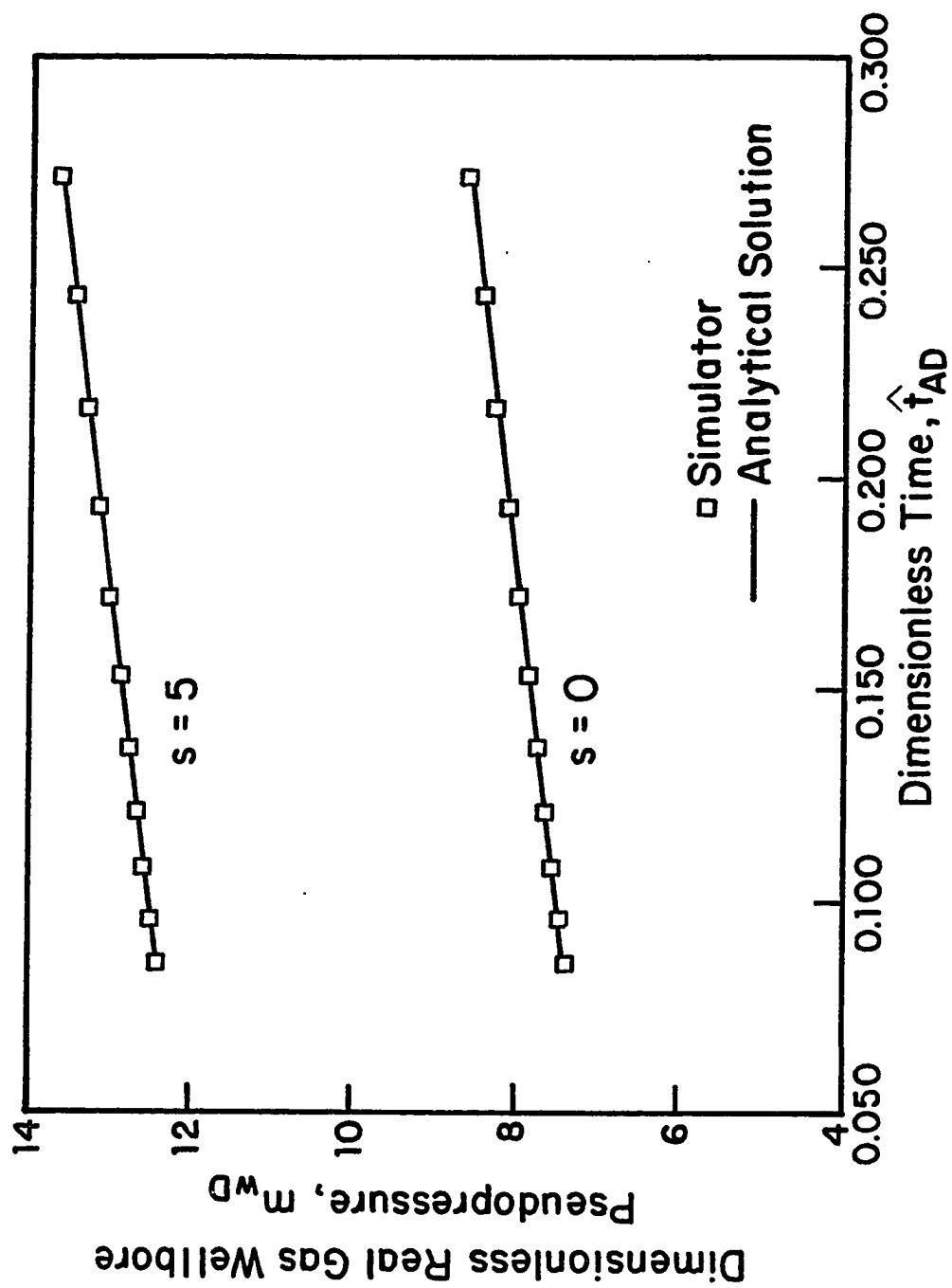


Fig. 5.7 - Single-phase gas; constant rate production: boundary-dominated flow.

above the bubble point pressure for the times considered. Since this mix is highly volatile, i.e., the density (or oil formation volume factor) varies substantially with pressure, we present results in terms of pseudopressure in order to account for the variations in PVT properties. For the oil case, the pseudopressure function $m(p)$ is constructed from Eq. 5.1.1 with the compressibility factor, Z , and viscosity, μ , corresponding to the liquid phase.

Fig. 5.8 shows plots of the dimensionless wellbore pseudopressure drop versus dimensionless time obtained from the simulator during the transient flow period for constant rate production. Note results are presented for two cases, $s = 0$ and $s = 5$. Fig. 5.9 is a similar plot for production at a constant flowing wellbore pressure. The influence of the boundary effects for a constant rate production case are exhibited in Fig. 5.10 where the simulator results are compared to Eq. 5.1.11. Note in all cases, the solution obtained from the simulator is in excellent agreement with the expected theoretical equations.

These cases illustrate the validity of our model in the single-phase region. Next, we discuss some of the results obtained for multiphase flow.

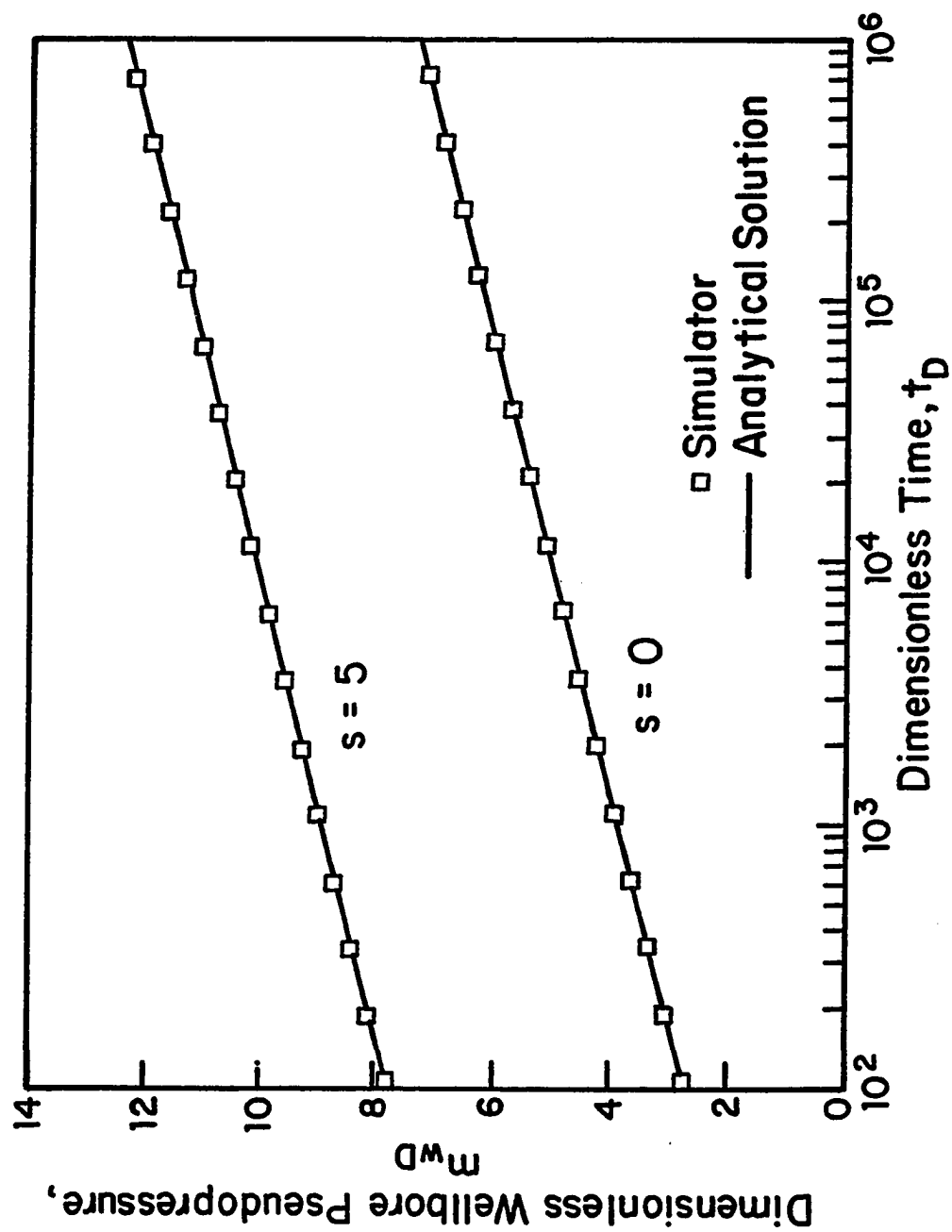


Fig. 5.8 - Single-phase oil; constant rate production: transient flow.

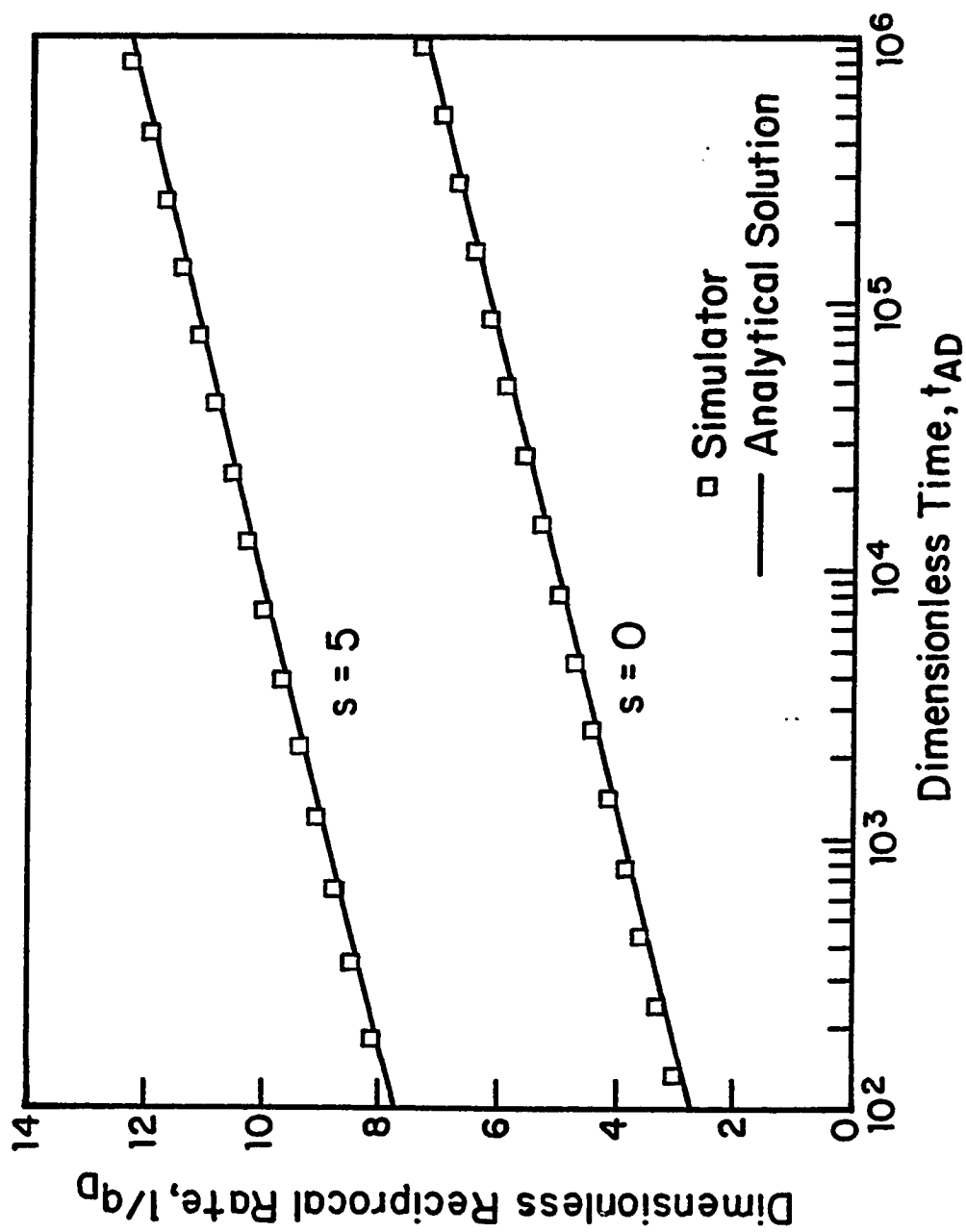


Fig. 5.9 - Single-phase oil; constant pressure production: transient flow.

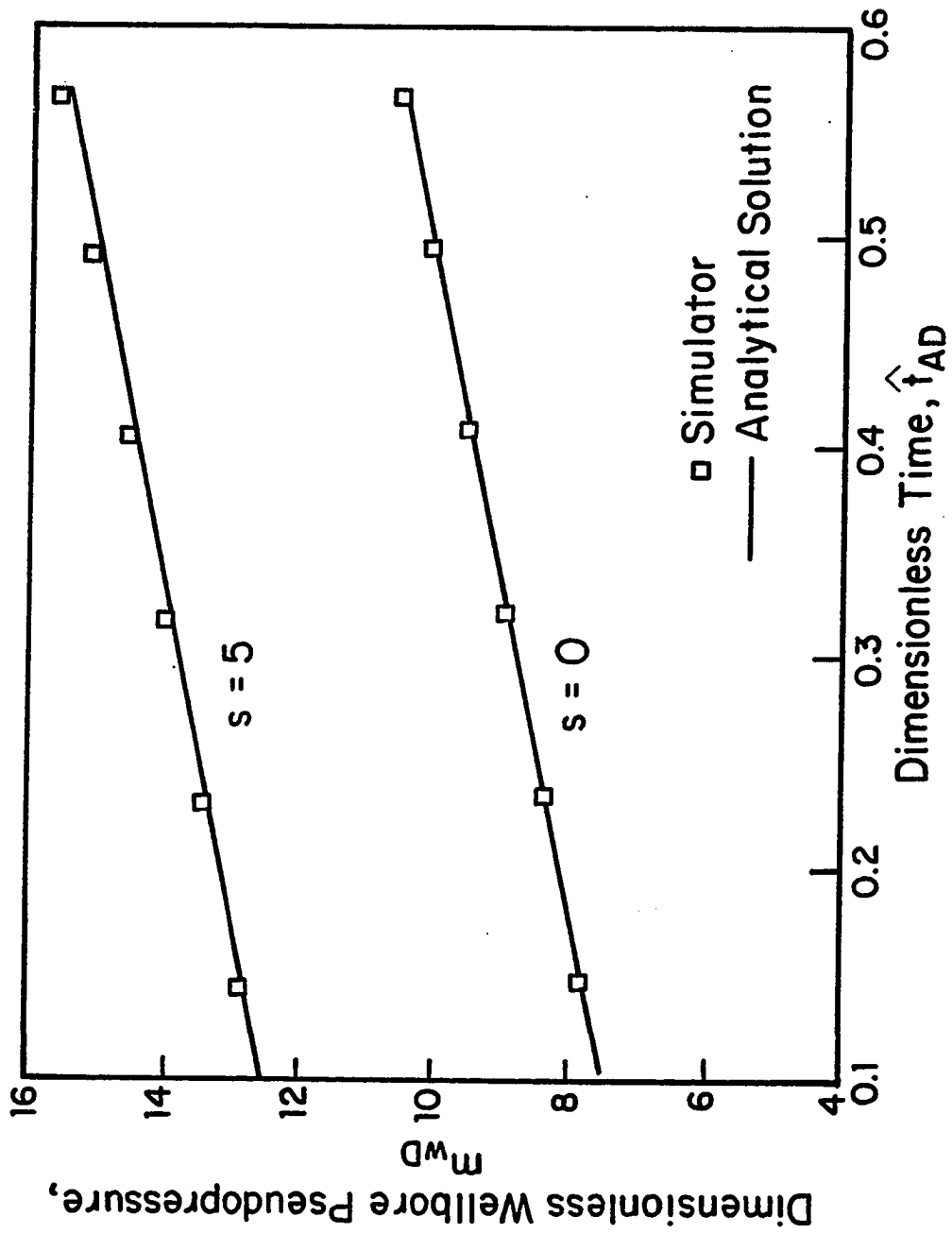


Fig. 5.10 - Single-phase oil; constant rate production: boundary-dominated flow.

5.4 Two-Phase Flow Results

The reservoir parameters used for both binary systems considered are shown in Table 5.6, whereas Table 5.7 represents the data used for all gas condensate reservoirs containing more than two components. Tables 5.8 and 5.9 show the parameters used for the volatile oil reservoir and for the black-oil reservoir, respectively.

5.4.1 Boltzmann Variable as a Correlating Parameter

In this section, we show that simulator values of dependent variables (pressure, saturation and mole fractions) obtained under two-phase flow conditions can be correlated in terms of Boltzmann variable r^2/t , or equivalently in terms of the inverse Boltzmann variable t/r^2 , during the infinite-acting (transient flow) period. In these results, we use a sufficiently large external reservoir radius, r_e , such that all variables in the gridblocks near the outer boundary remain approximately at initial conditions during the time period considered. In plotting each dependent variable in terms of t/r^2 , we plot all values of the variable obtained at each time step and at each simulator gridblock. Since the Boltzmann variable does not apply at early times^{57,58}, we will see that the correlation of dependent variables is not perfect at early times.

5.4.1.a Binary Systems

For the gas condensate reservoir, we consider drawdown results obtained with initial pressure of about 3 psia above the initial reservoir dew-point pressure, so the initial gas saturation is $S_{g,i} = 1$. The reservoir is produced at $q = 7500$ lbmoles/day for a total time of $t = 0.5$ day. Fifty geometrically spaced⁴¹ radial gridblocks were used with the reservoir parameters shown in Table 5.6. At the end of production, all grid blocks except the 3 outermost gridblocks are in two-phase flow. Fig. 5.11 shows a plot of simulator values of $p(r, t)$ versus t/r^2 . Note that the results show that pressure can be correlated in terms of the inverse Boltzmann variable, t/r^2 . Figs. 5.12 and 5.13 show that S_g and the overall mole fraction of component 1, z_1 , can also be correlated in terms of the Boltzmann variable. These results illustrate

TABLE 5.7

Summary of Input Reservoir Data

Retrograde Gas Condensate

Reservoir Extent Radius, r_e	(<i>ft</i>)	2000.0
Absolute Reservoir Permeability, k	(<i>md</i>)	5.0
Porosity, ϕ	(-)	0.20
Formation Thickness, h	(<i>ft</i>)	40.0
Wellbore Radius, r_w	(<i>ft</i>)	0.25

TABLE 5.8

Summary of Input Reservoir Data

Volatile Oil

Reservoir Extent Radius, r_e	(<i>ft</i>)	2000.0
Absolute Reservoir Permeability, k	(<i>md</i>)	10.0
Porosity, ϕ	(-)	0.20
Formation Thickness, h	(<i>ft</i>)	40.0
Wellbore Radius, r_w	(<i>ft</i>)	0.25

TABLE 5.9

Summary of Input Reservoir Data

Black-Oil

Reservoir Extent Radius, r_e	(<i>ft</i>)	1000.0
Absolute Reservoir Permeability, k	(<i>md</i>)	10.0
Porosity, ϕ	(-)	0.30
Formation Thickness, h	(<i>ft</i>)	20.0
Wellbore Radius, r_w	(<i>ft</i>)	0.50

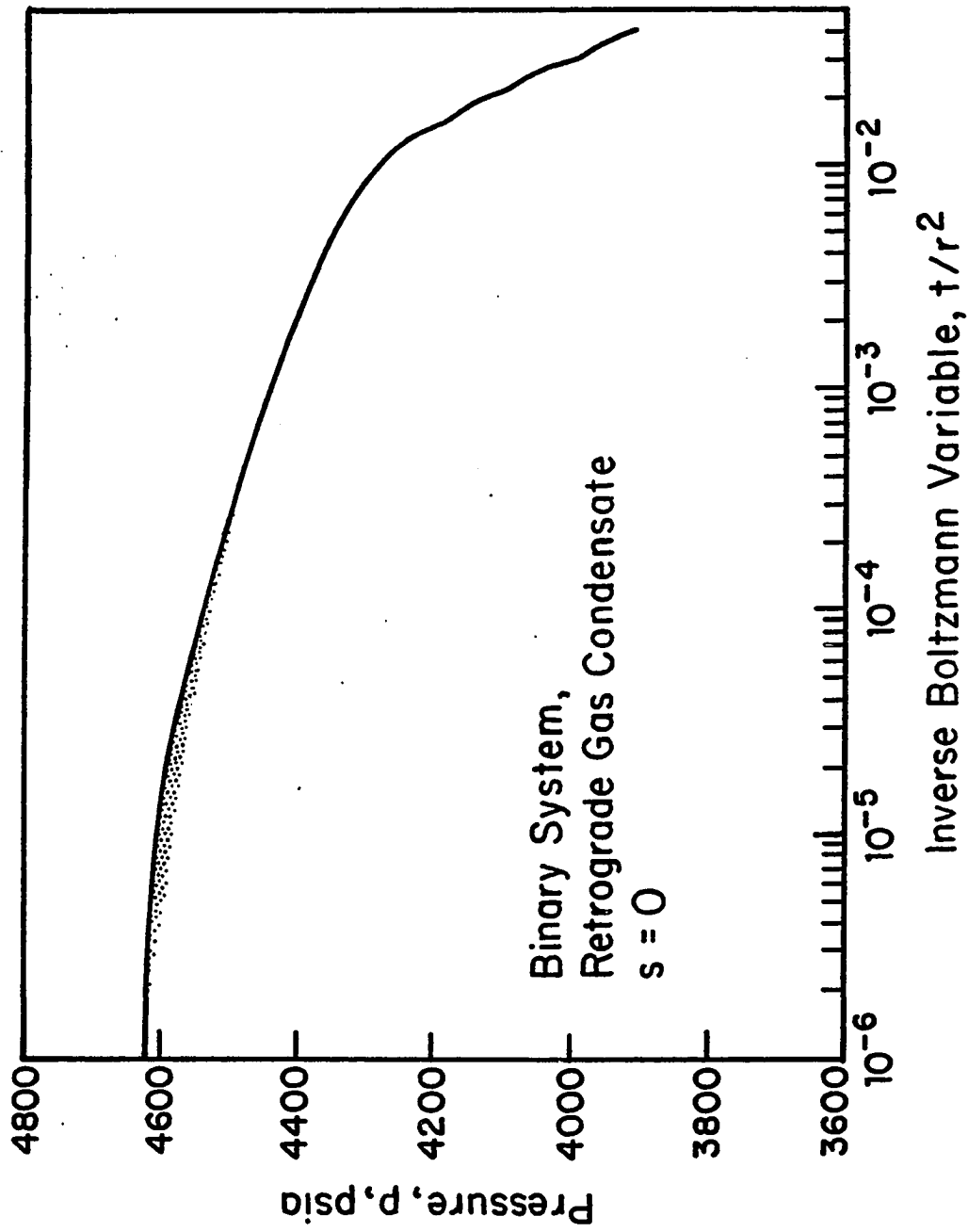


Fig. 5.11 - Correlation of pressure in terms of inverse Boltzmann variable.

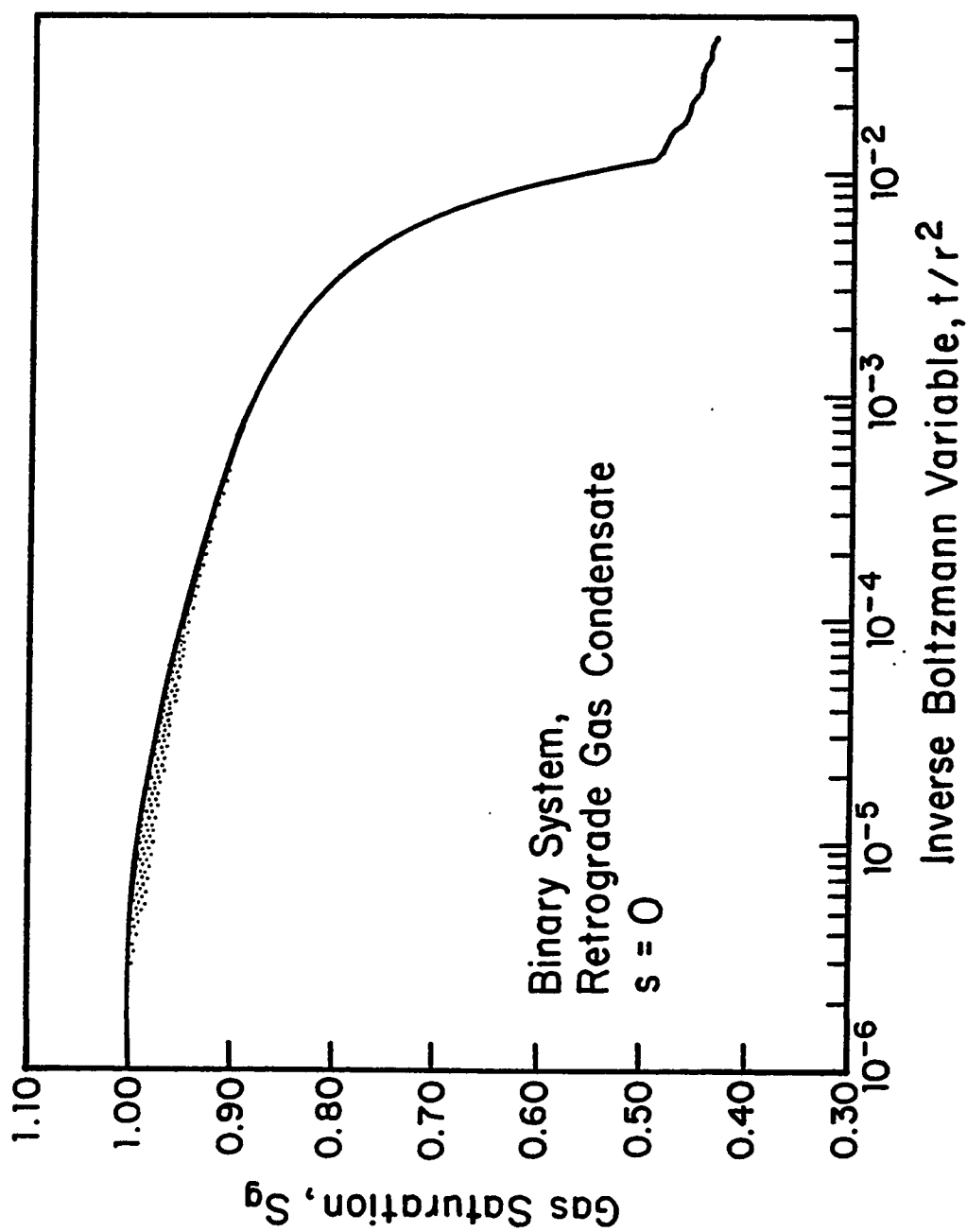


Fig. 5.12 - Correlation of gas saturation in terms of inverse Boltzmann variable.

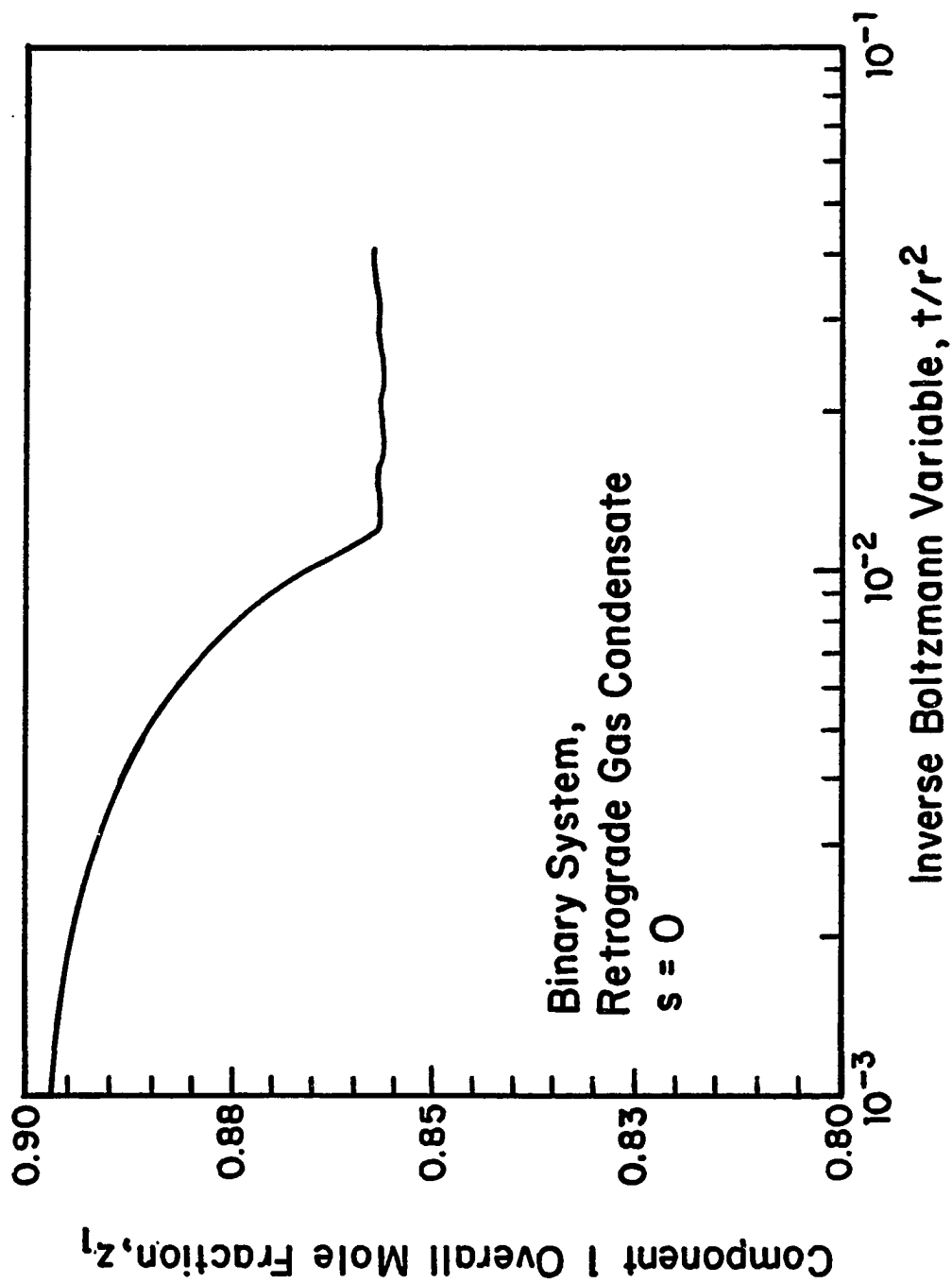


Fig. 5.13 - Correlation of composition in terms of inverse Boltzmann variable.

that gas saturation and fluid compositions may be considered to be a functions of pressure. The results shown in Fig. 5.14 represent a plot of the (S_g, p) values obtained at each grid block at each time step. The results show during transient flow, S_g is a function of pressure.

5.4.1.b Ternary Systems

In all cases considered in this subsection, we used one hundred, geometrically-spaced⁶, radial gridblocks.

For the gas condensate reservoir, we considered drawdown results obtained for two types of mixtures, Mix 1 and Mix 3, and for the volatile oil reservoir, Mix 4 is used in simulating a drawdown behavior.

The dew point pressure of Mix 1 is 3969.7 psia. The results were obtained with an initial reservoir pressure of 4200 psia. Fig. 5.15 shows a plot of simulator values of $S_g(r, t)$ versus t/r^2 and illustrates that gas saturation can be correlated in terms of the Boltzmann variable. Note that our model can handle sharp saturation fronts. Fig. 5.16 shows that the pressure also can be correlated in terms of the inverse Boltzmann variable, t/r^2 .

The last ternary gas condensate mixture, Mix 3, is the heaviest of all three mixtures (12% maximum liquid dropout during a CCE). This type of mixture typically causes convergence difficulties. Nghiem¹⁹ observes that for certain fluids, there exist some regions in some reservoirs where one observes severe oscillations in the solution from iterate to iterate. These problems occur during pressure decline across a bubble point of an oil reservoir or a dew point of a gas condensate reservoir. For the gas condensate case, during an iteration, the liquid dropped out as pressure declines below the saturation point affects the whole numerical scheme in such a way that the pressure increases during the subsequent iteration, and all of liquid goes back into solution. This process keeps repeating and the scheme does not converge. According to Nghiem¹⁹, this problem was first reported by Mansoori¹⁸ and then by Coats⁵⁹ for fully-implicit simulators, however, our simulator did not experience this instability. Figs. 5.17 through 5.22 demonstrate the behavior and consistency

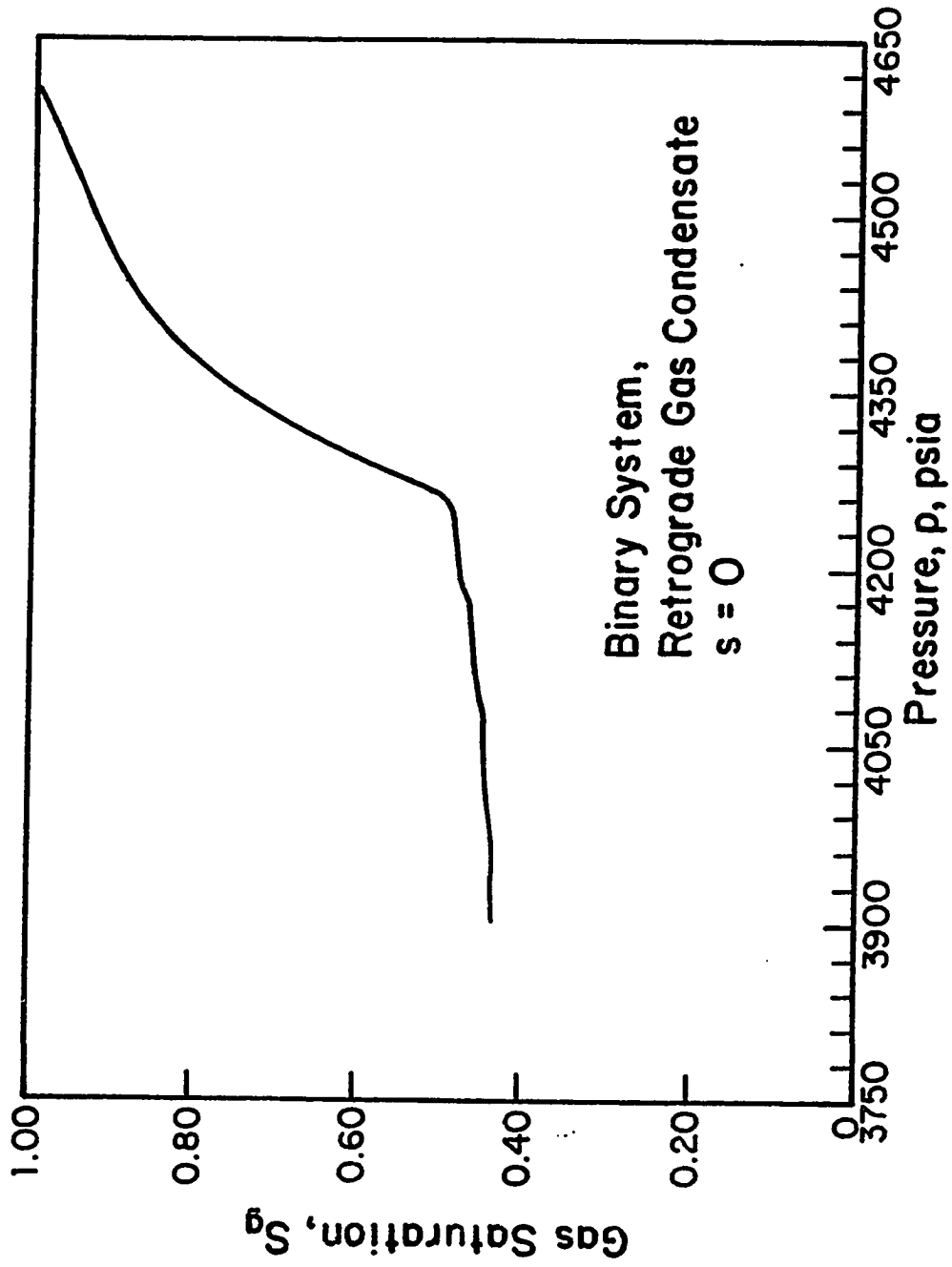


Fig. 5.14 - Plot of gas saturation as function of pressure.

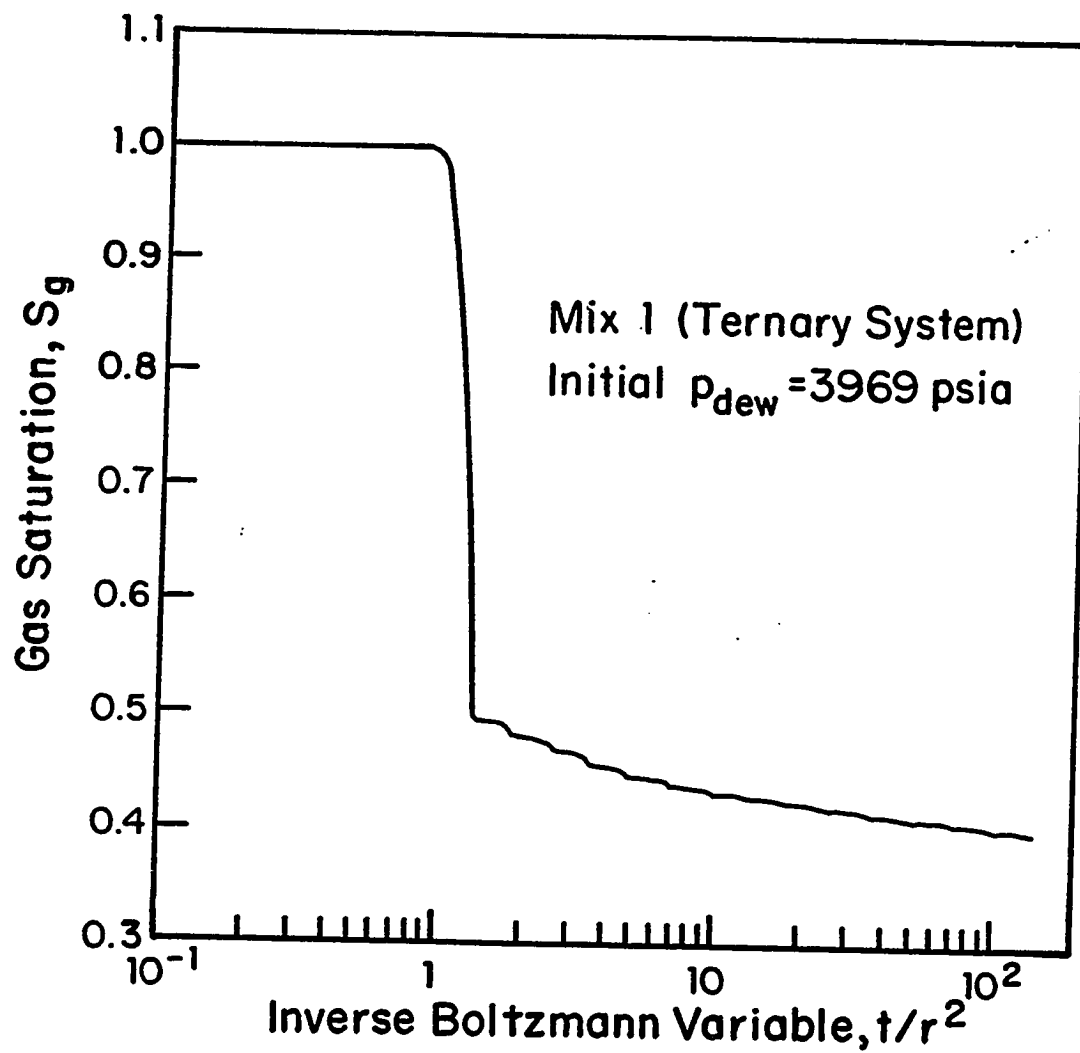


Fig. 5.15 - Correlation of gas saturation in terms of inverse Boltzmann variable; retrograde gas condensate, ternary system, $s = 0$.

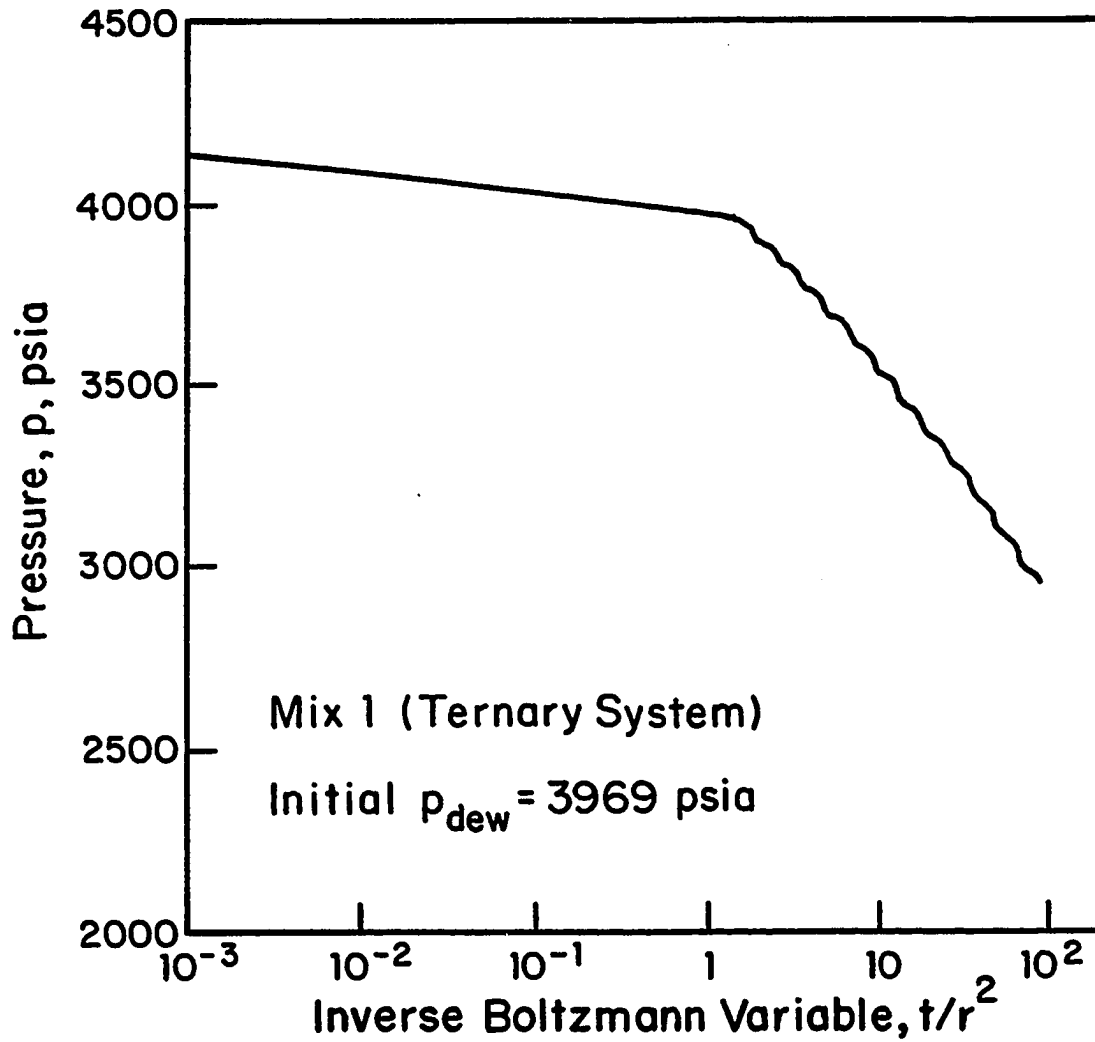


Fig. 5.16 - Correlation of pressure in terms of inverse Boltzmann variable; retrograde gas condensate, ternary system, $s = 0$.

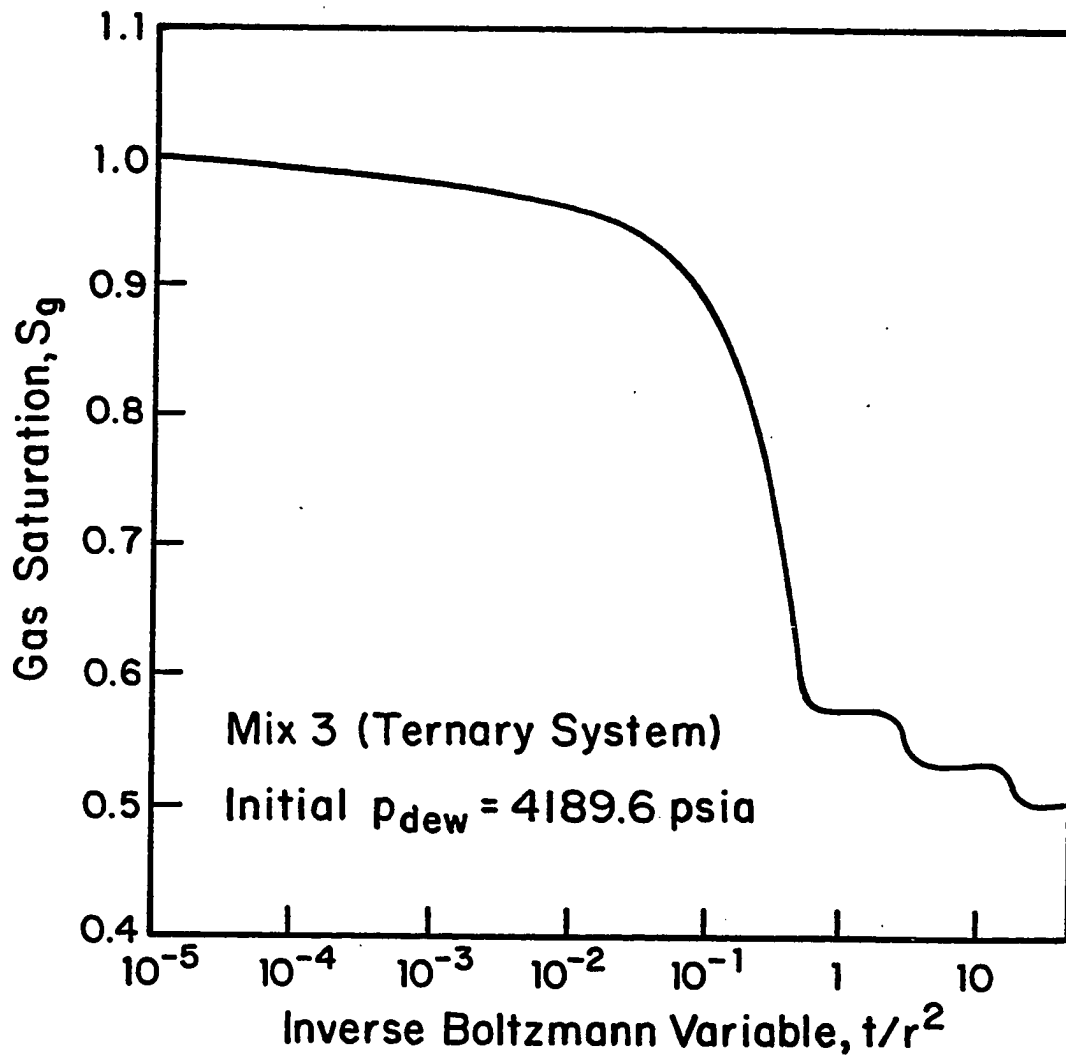


Fig. 5.17 - Correlation of gas saturation in terms of inverse Boltzmann variable; retrograde gas condensate, ternary system, $s = 0$.

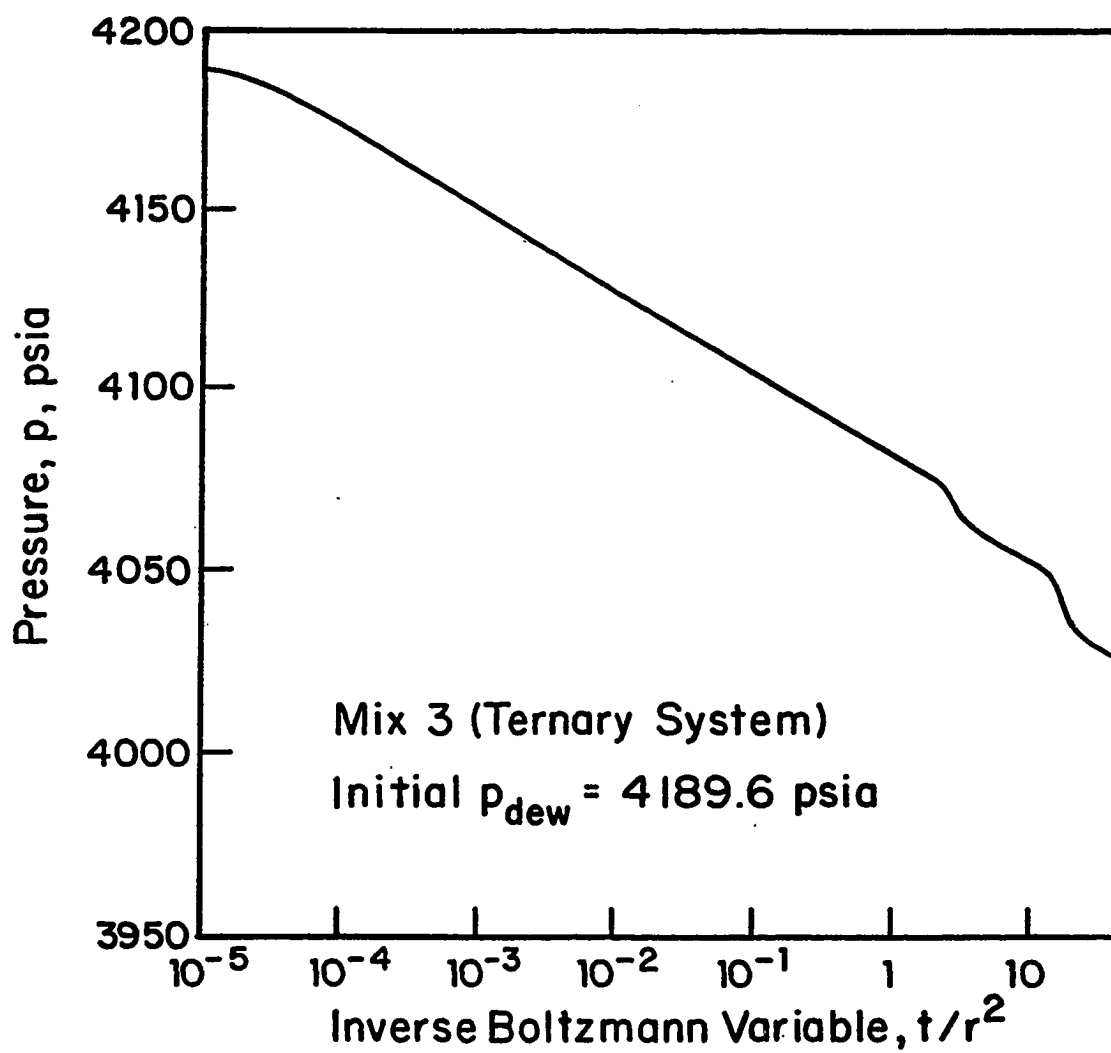


Fig. 5.18 - Correlation of pressure in terms of inverse Boltzmann variable; retrograde gas condensate, ternary system, $s = 0$.

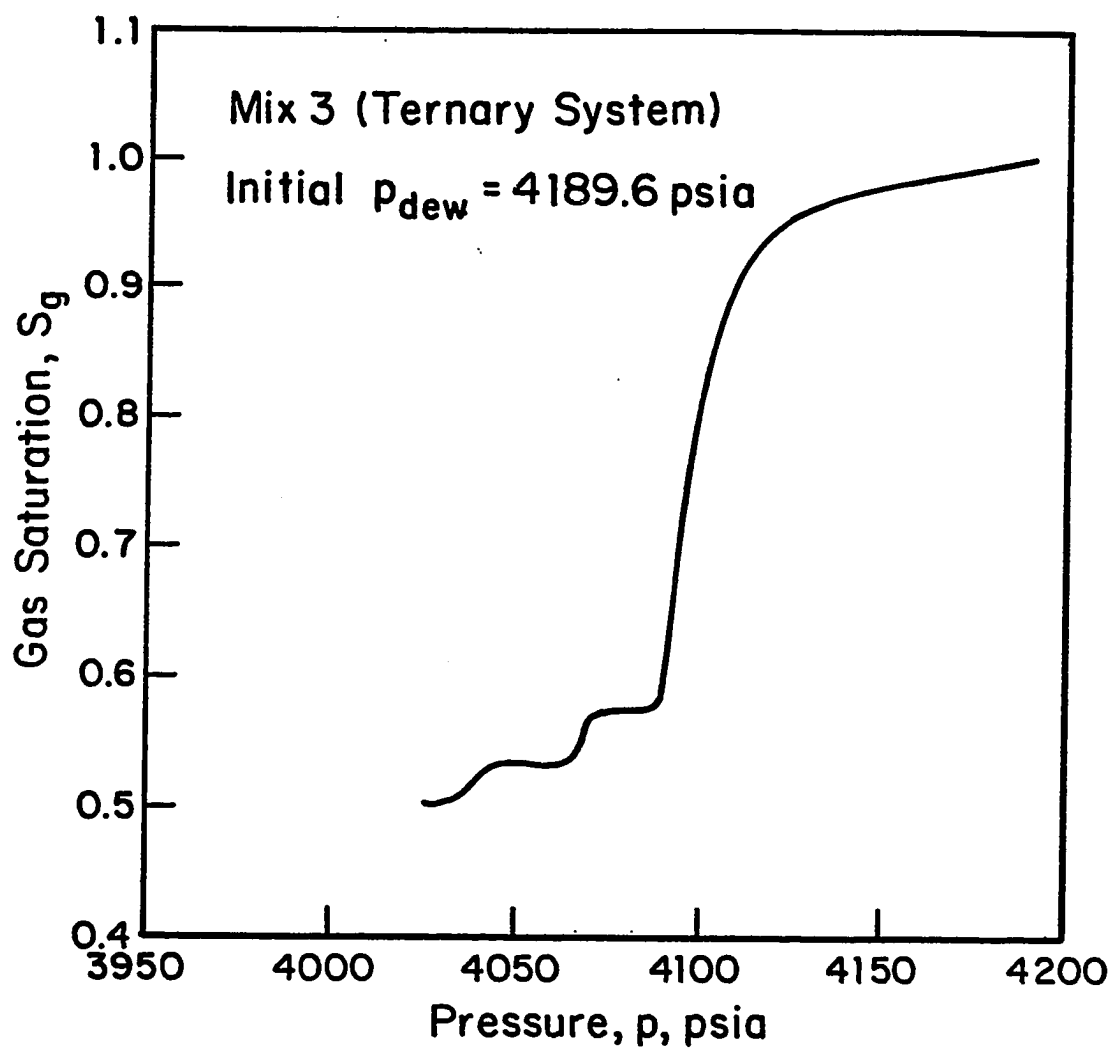


Fig. 5.19 - Plot of gas saturation as function of pressure; retrograde gas condensate, ternary system, $s = 0$.

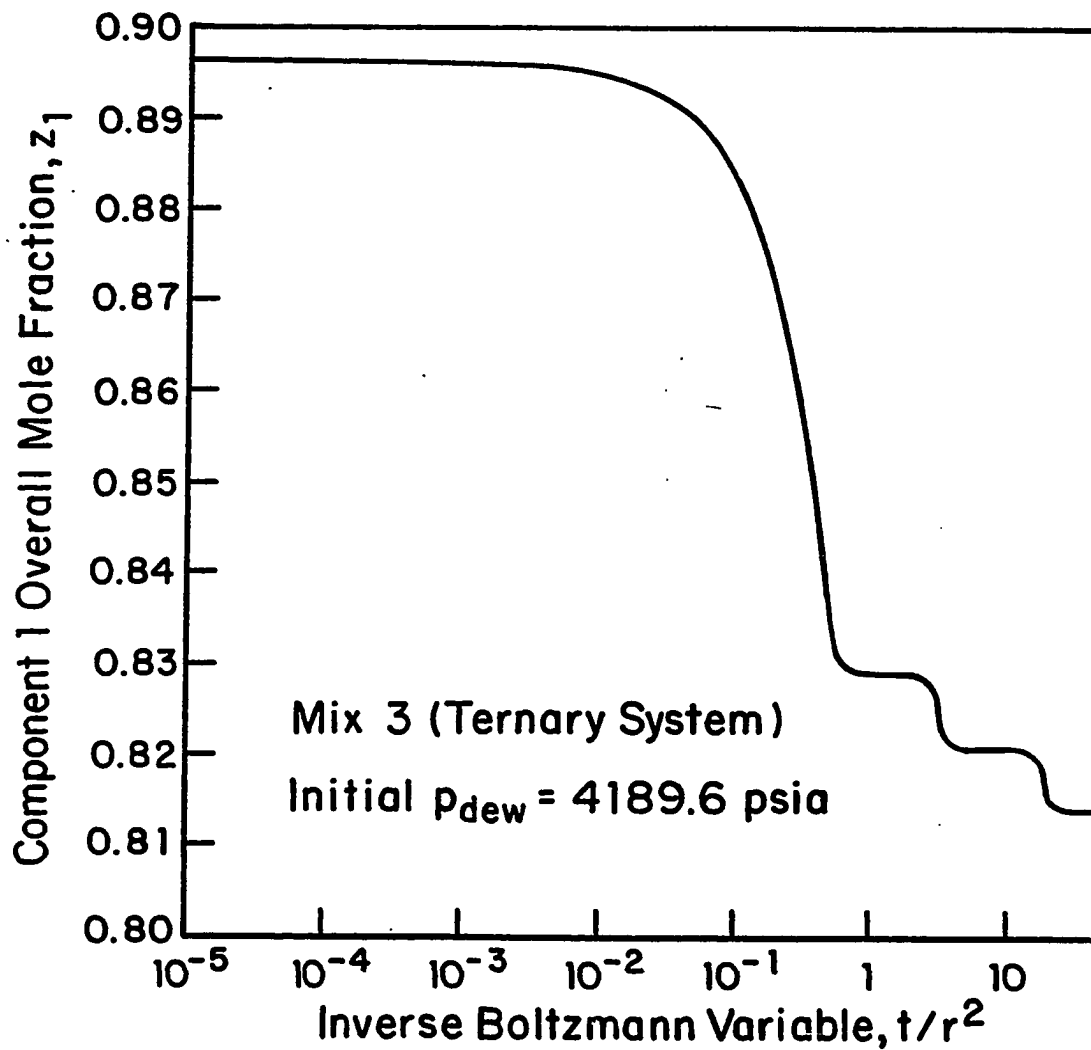


Fig. 5.20 - Correlation of composition in terms of inverse Boltzmann variable; retrograde gas condensate, ternary system, $s = 0$.

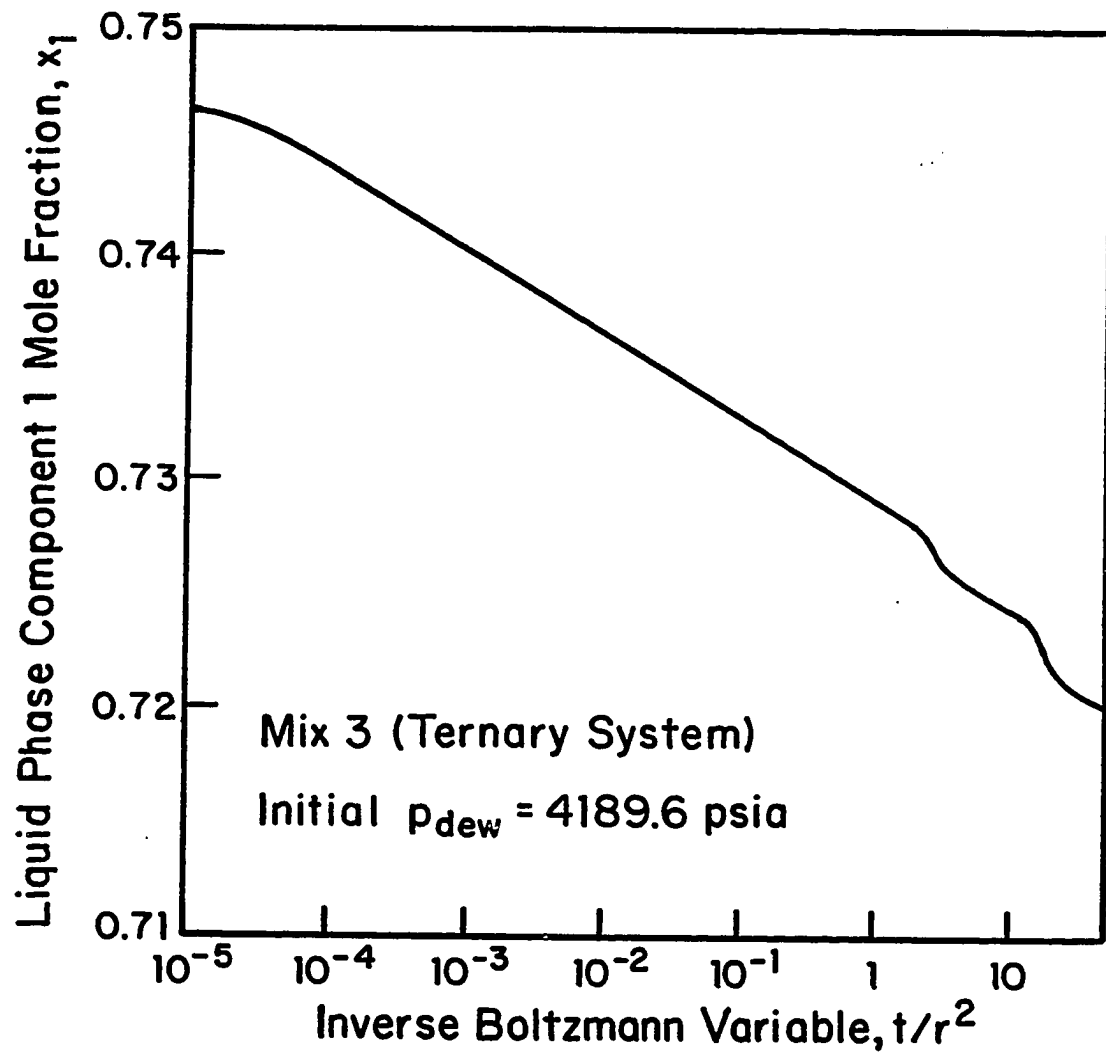


Fig. 5.21 - Correlation of liquid composition in terms of inverse Boltzmann variable; retrograde gas condensate, ternary system, $s = 0$.

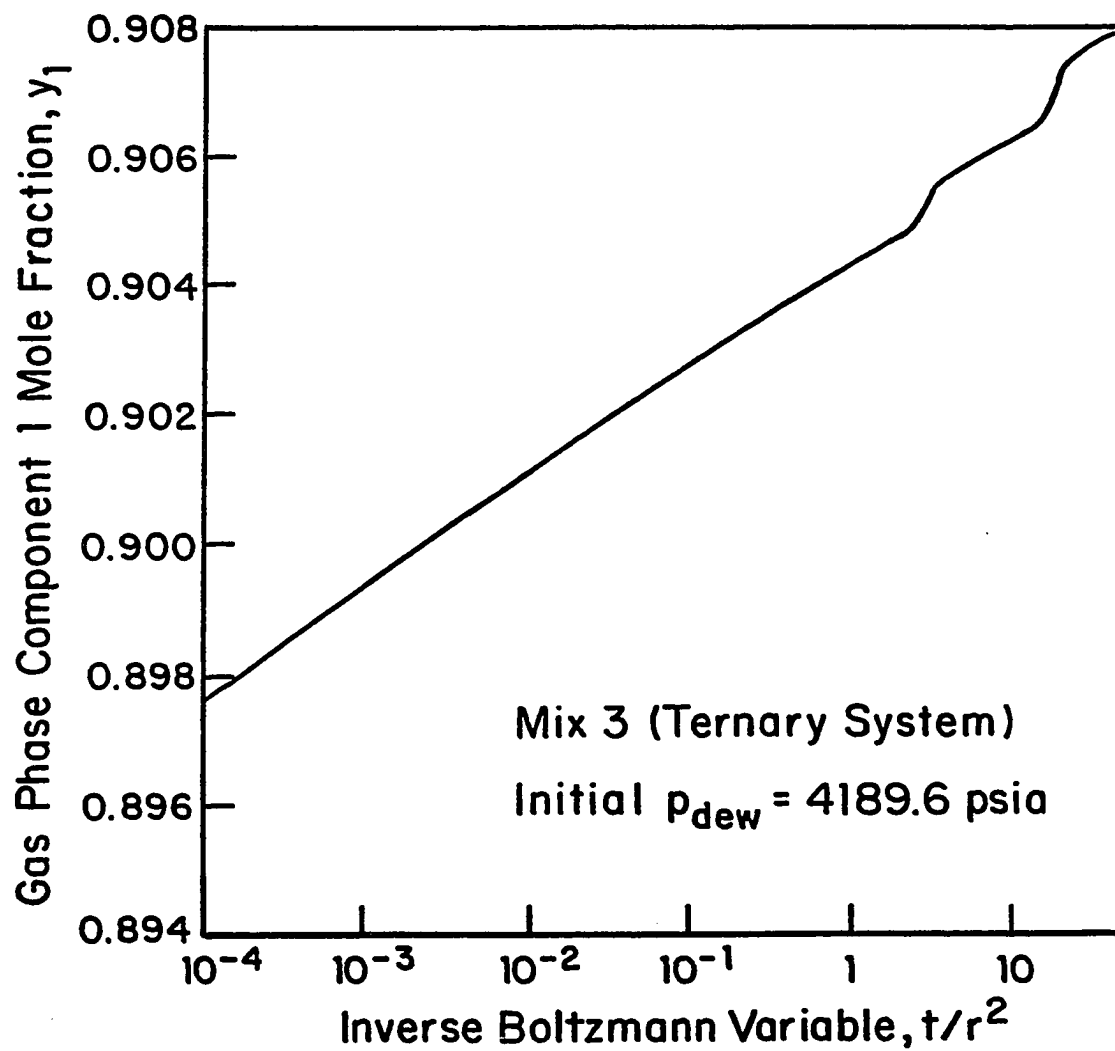


Fig. 5.22 - Correlation of gas composition in terms of inverse Boltzmann variable; retrograde gas condensate, ternary system, $s = 0$.

of the results obtained. The dew point pressure of Mix 3 is 4189.6 psia. The draw-down run was conducted with an initial reservoir pressure of about 1 psia above the saturation pressure. Fig. 5.17 shows a plot of $S_g(r, t)$ versus t/r^2 which indicates a perfect correlation of saturation in terms of the inverse Boltzmann variable. Fig. 5.18 illustrates the correlation of pressure in terms of the inverse Boltzmann variable. The results presented in Fig. 5.19 represent a plot of the (S_g, p) values obtained at each gridblock at each time step and shows that gas saturation may be considered to be a unique function of pressure. Finally, Figs. 5.20 - 5.22 show the correlation of the in-situ overall, liquid and gas mole fractions of methane in terms of the inverse Boltzmann variable. These results illustrate that gas saturation and fluid compositions may be considered to be functions of pressure. Note that the in-situ overall mole fraction composition is based on phase densities, saturations and compositions, i.e.,

$$z_i = \rho_o S_o x_i + \rho_g S_g y_i. \quad (5.4.1)$$

Mix 4 is a volatile oil with a bubble point pressure of 3173 psia. The initial reservoir pressure is about 2 psia above the saturation pressure. Similar to the gas condensate cases, all dependent variables correlate in terms of the inverse Boltzmann variable as is illustrated in Figs. 5.23, 5.24 and 5.26 - 5.28. Fig. 5.25 presents the (S_g, p) values obtained at each gridblock at each time step.

5.4.1.c 14-Component Volatile System

We extended the testing of the new formulation by running the model for more complex mixtures. Mix 6 is a volatile oil containing CO_2 and N_2 . Our simulator handled the mixture reasonably well, i.e., as the pressure declined below the saturation pressure of 3085 psia, the pressure and gas saturation correlated in terms of the inverse Boltzmann variable as shown in Fig. 5.29.

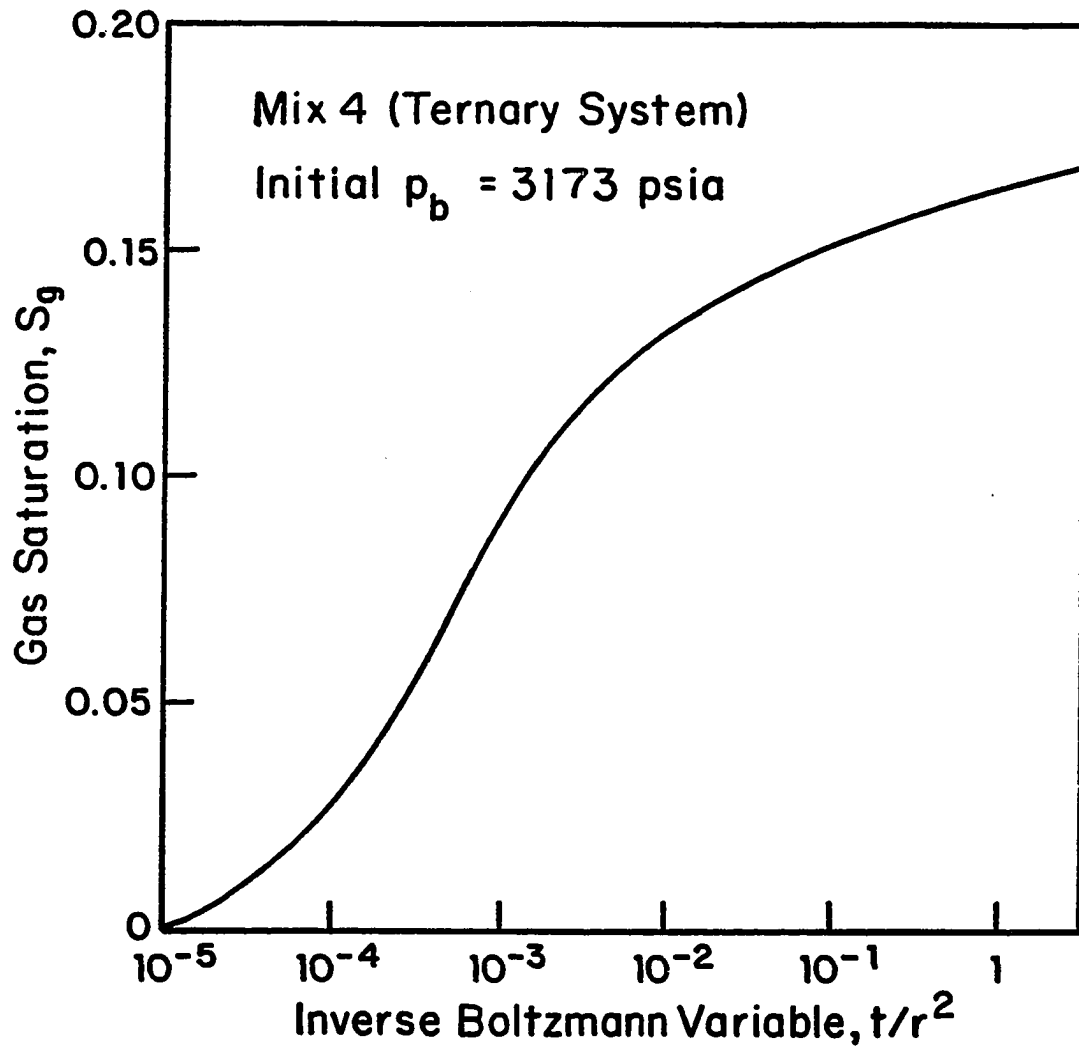


Fig. 5.23 - Correlation of gas saturation in terms of inverse Boltzmann variable; volatile oil, ternary system, $s = 0$.

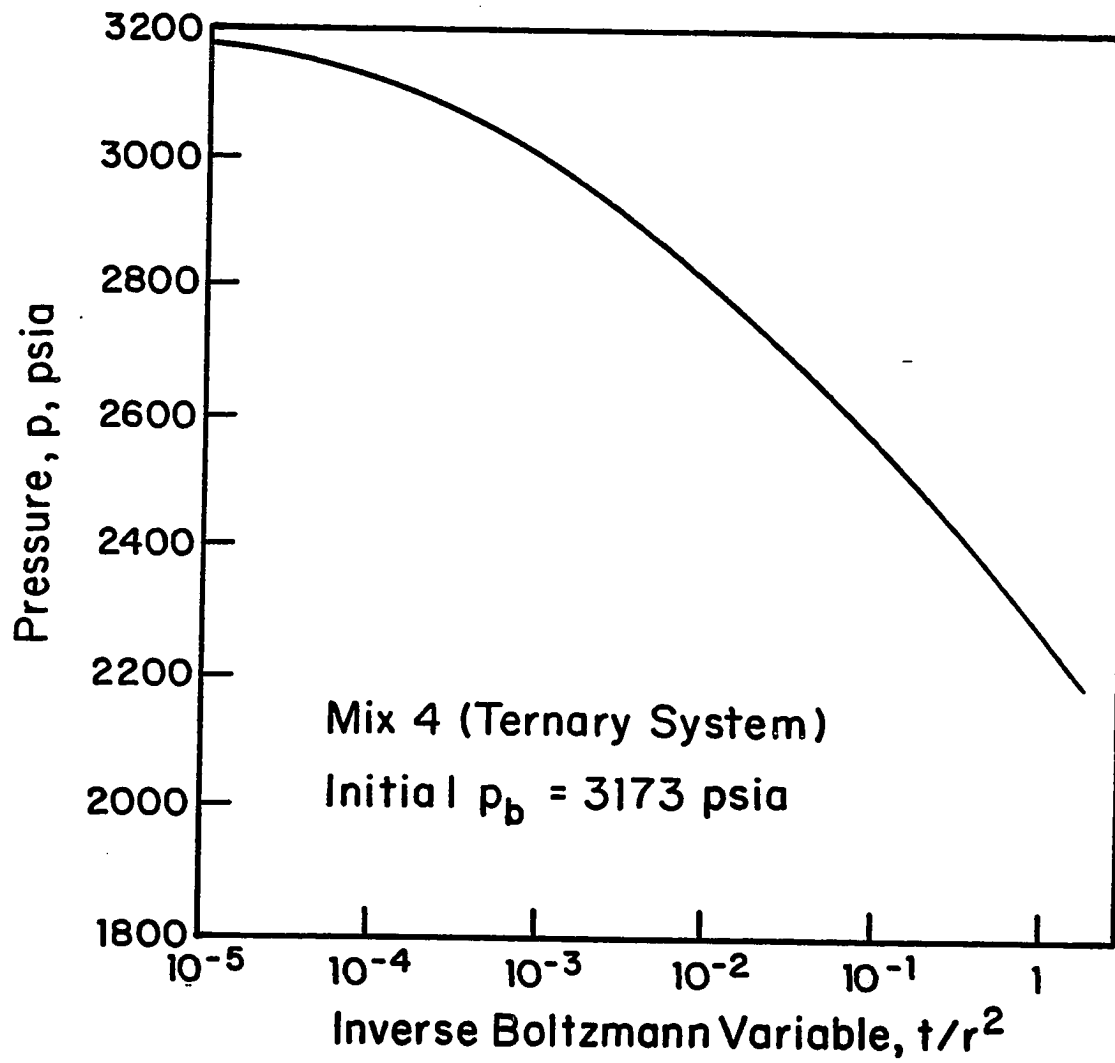


Fig. 5.24 - Correlation of pressure in terms of inverse Boltzmann variable; volatile oil, ternary system, $s = 0$.

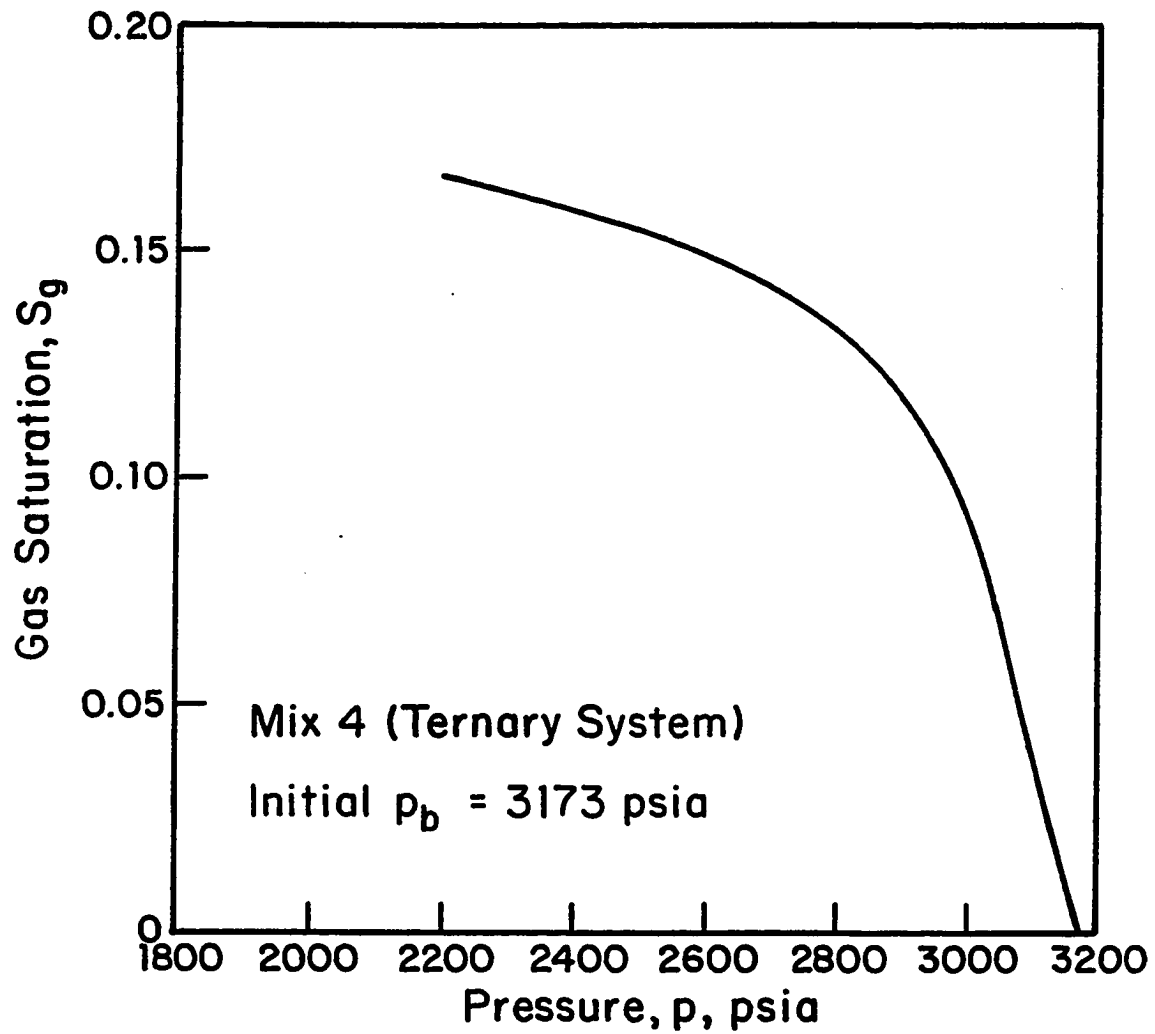


Fig. 5.25 - Plot of gas saturation as function of pressure; volatile oil, ternary system, $s = 0$.

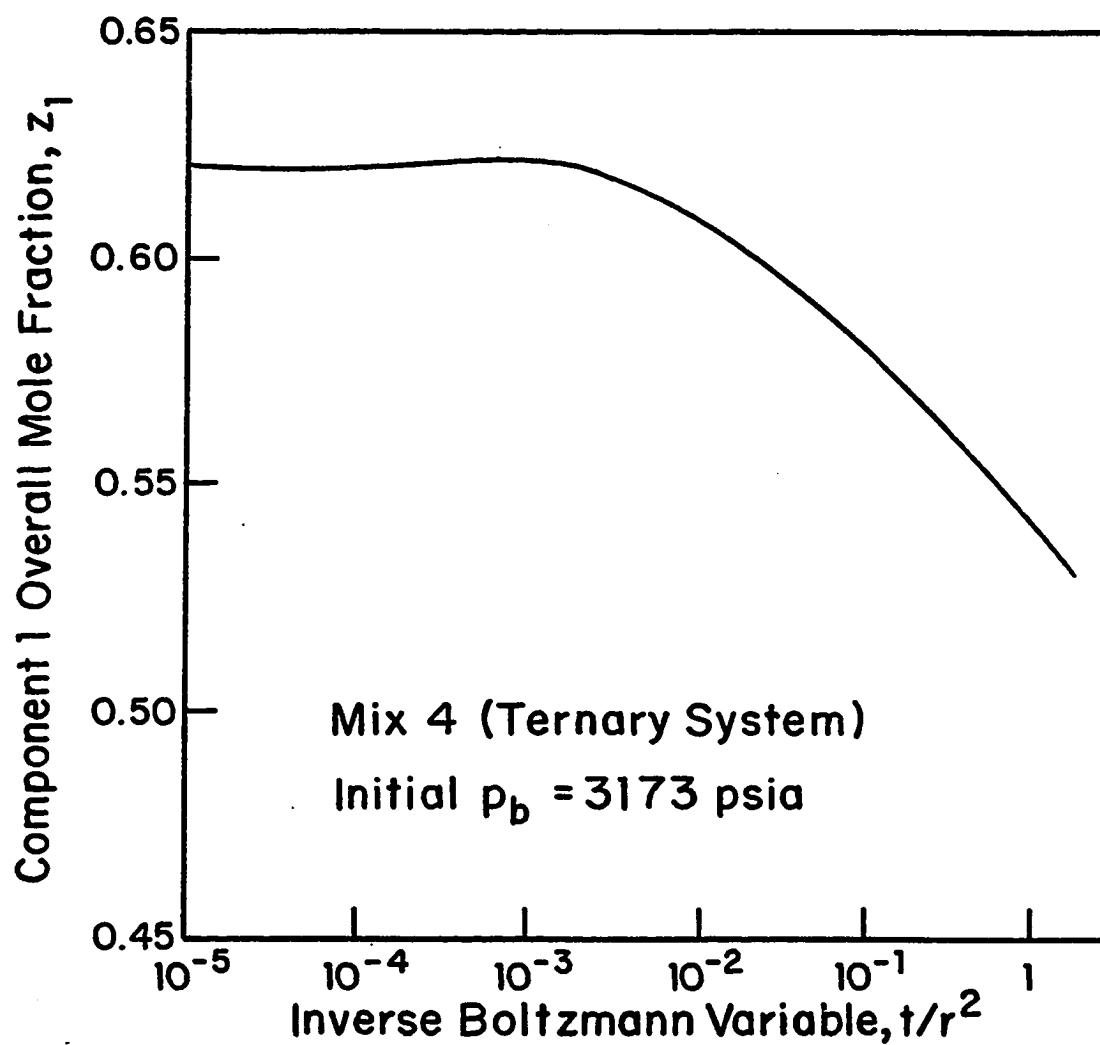


Fig. 5.26 - Correlation of composition in terms of inverse Boltzmann variable; volatile oil, ternary system, $s = 0$.

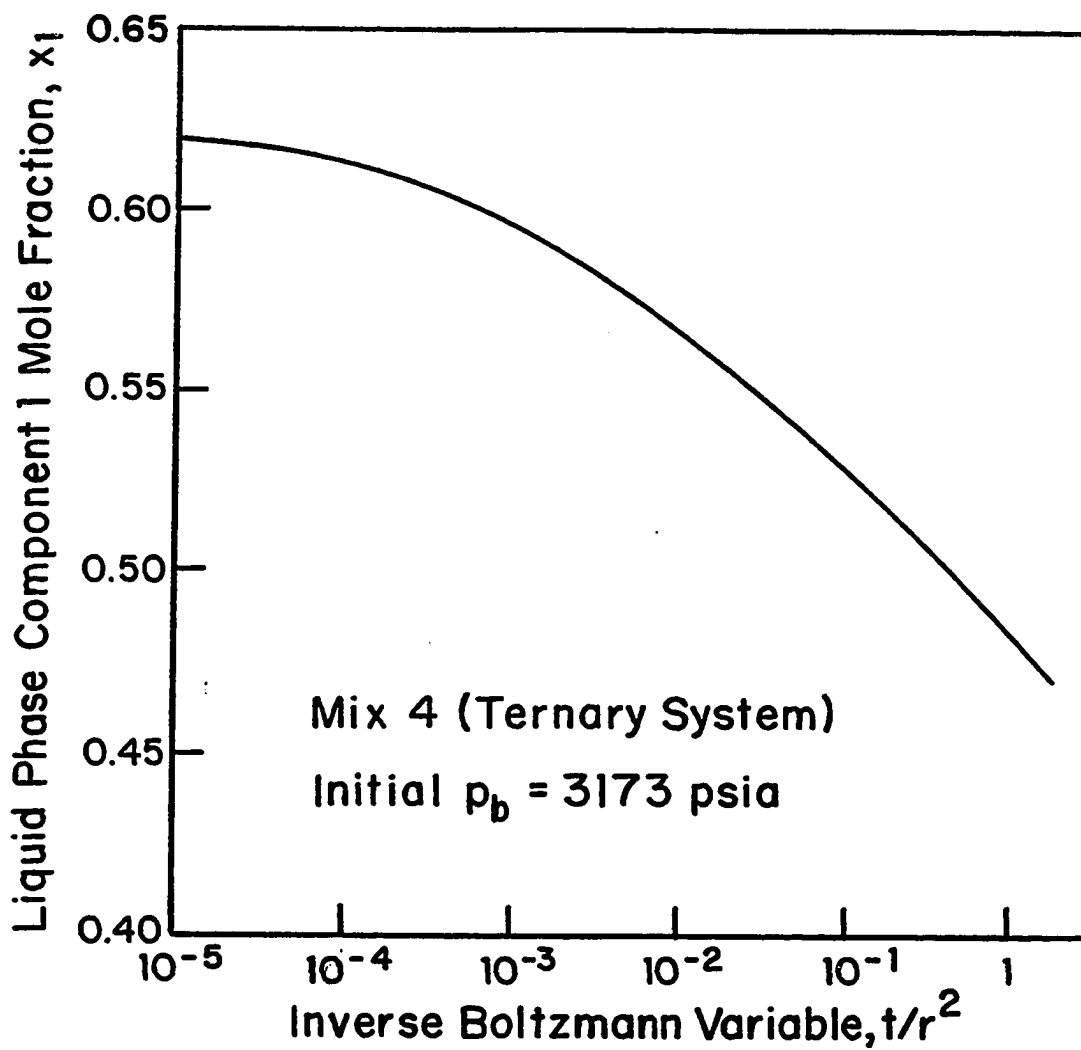


Fig. 5.27 - Correlation of liquid composition in terms of inverse Boltzmann variable; volatile oil, ternary system, $s = 0$.

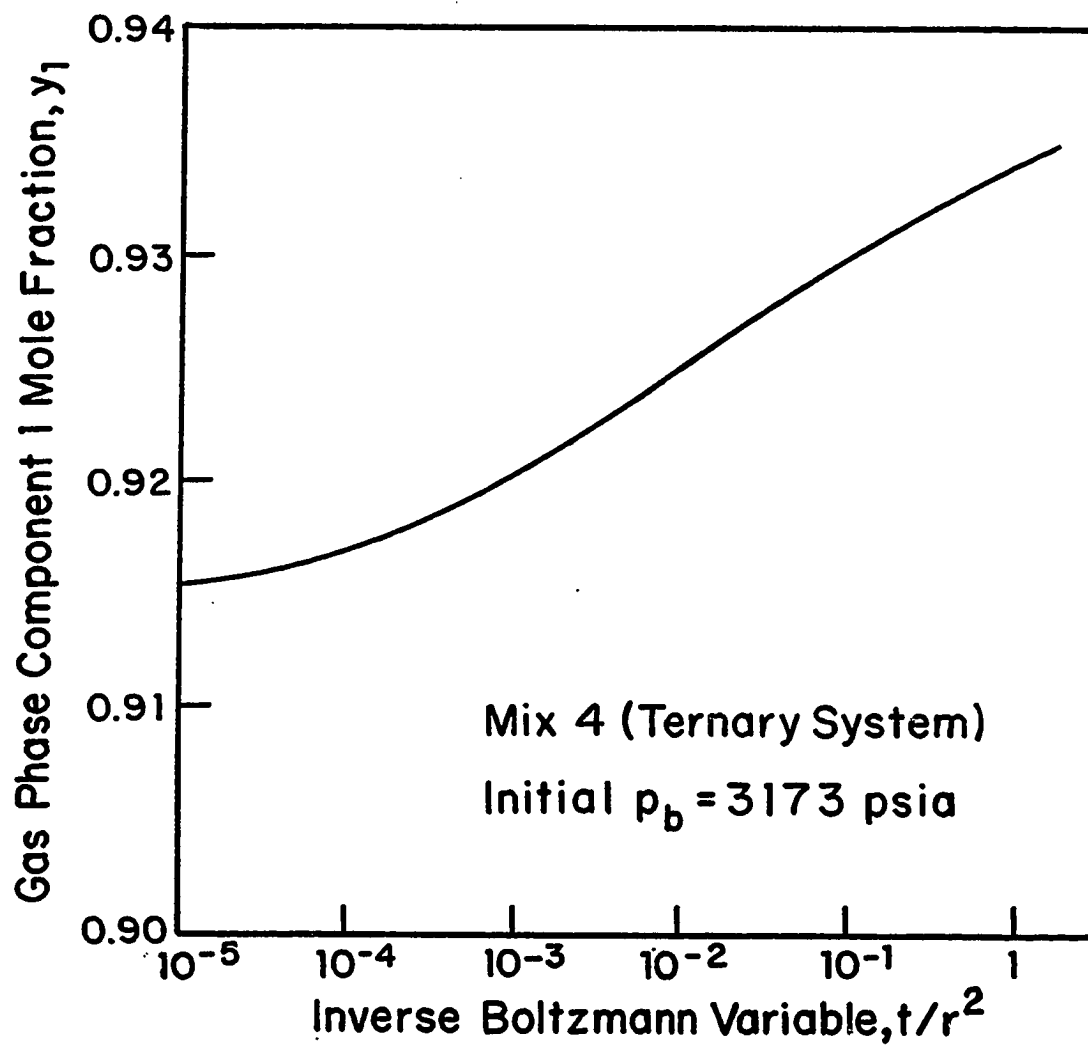


Fig. 5.28 - Correlation of gas composition in terms of inverse Boltzmann variable; volatile oil, ternary system, $s = 0$.

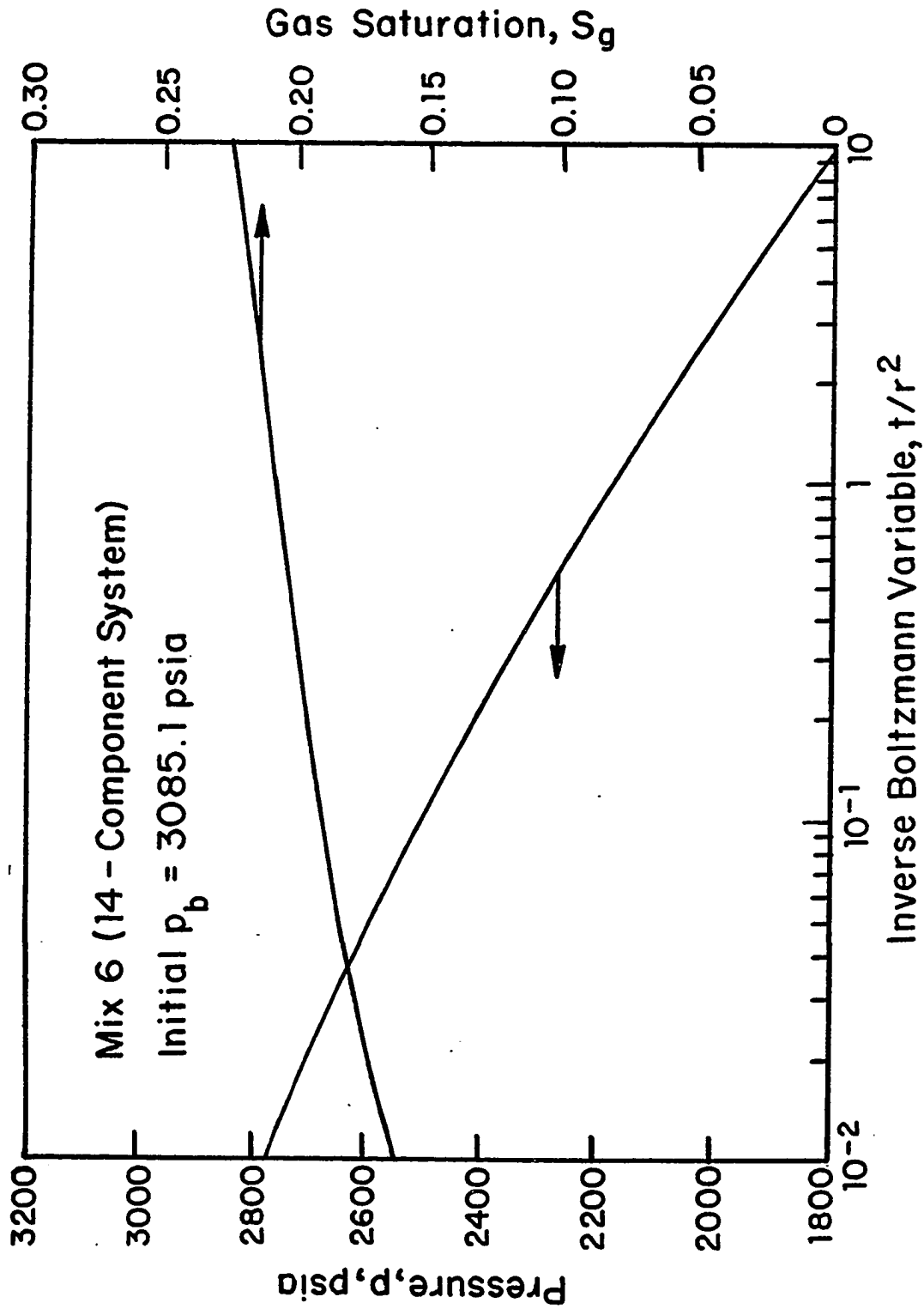


Fig. 5.29 - Correlation of pressure and gas saturation in terms of inverse Boltzmann variable; volatile oil, $s = 0$.

5.4.1.d 17-component Gas Condensate System

We also satisfactorily simulated a fluid flow for a complex 17-component gas condensate mixture (Mix 7) with a dew point pressure of 3646.9 psia. A reservoir with an initial pressure equal to the dew point pressure was produced at a rate of 7500 lbmoles/day for a 1 day period. As shown in Fig. 5.30, gridblock pressures and saturations correlated in terms of the inverse Boltzmann variable.

Although not shown in this work, mole fraction composition for Mix 6 (14-component) and Mix 7 (17-component) fluids also correlated in terms of the inverse Boltzmann variable.

5.4.2 Steady-State

The reservoir is initially filled with a single-phase fluid characterized by Mix 2 and Table 5.10 shows the reservoir data used for the steady-state run. The overall composition of the fluid injected at the outer boundary is set equal to the overall composition of the initial fluid in-place. Fig. 5.31 is a semilog plot of the overall mole fraction composition at the first gridblock divided by the overall mole fraction composition of the initial in-place gas, $\{z_i(r_1)/z_{i,e}\}_{i=1}^{N_c}$, versus dimensionless time, t_D . Data for the mole fractions of methane, n-butane and n-decane in Mix 2 are shown. For the system parameters used here, steady-state starts at approximately $t_D = 2.5 \times 10^7$.

At early times, we see in Fig. 5.31 that the sandface overall mole fractions differ from the mole fractions of the in-place gas. After the onset of steady-state, the ratio of mole fractions is essentially unity. Although not shown in this work, similar results hold for all radial locations. This plot clearly indicates that the simulator results reproduce the first characteristic of the steady-state model problem.

The semilog plot of in-place mole fractions in the liquid phase versus dimensionless radial distance, r_D , is shown in Fig. 5.32. The data in this figure pertains to times beyond the start of the steady-state flow. The mole fractions have been normalized by dividing by the values of the mole fractions at the dew point pressure. The solid lines are the data obtained from flash calculations, whereas the circular

TABLE 5.10

Summary of Input Reservoir Data

Steady-State and Gas Cycling Runs

Reservoir Extent Radius, r_e	(<i>ft</i>)	100.0
Absolute Reservoir Permeability, k	(<i>md</i>)	5.0
Porosity, ϕ	(-)	0.20
Formation Thickness, h	(<i>ft</i>)	40.0
Wellbore Radius, r_w	(<i>ft</i>)	0.25

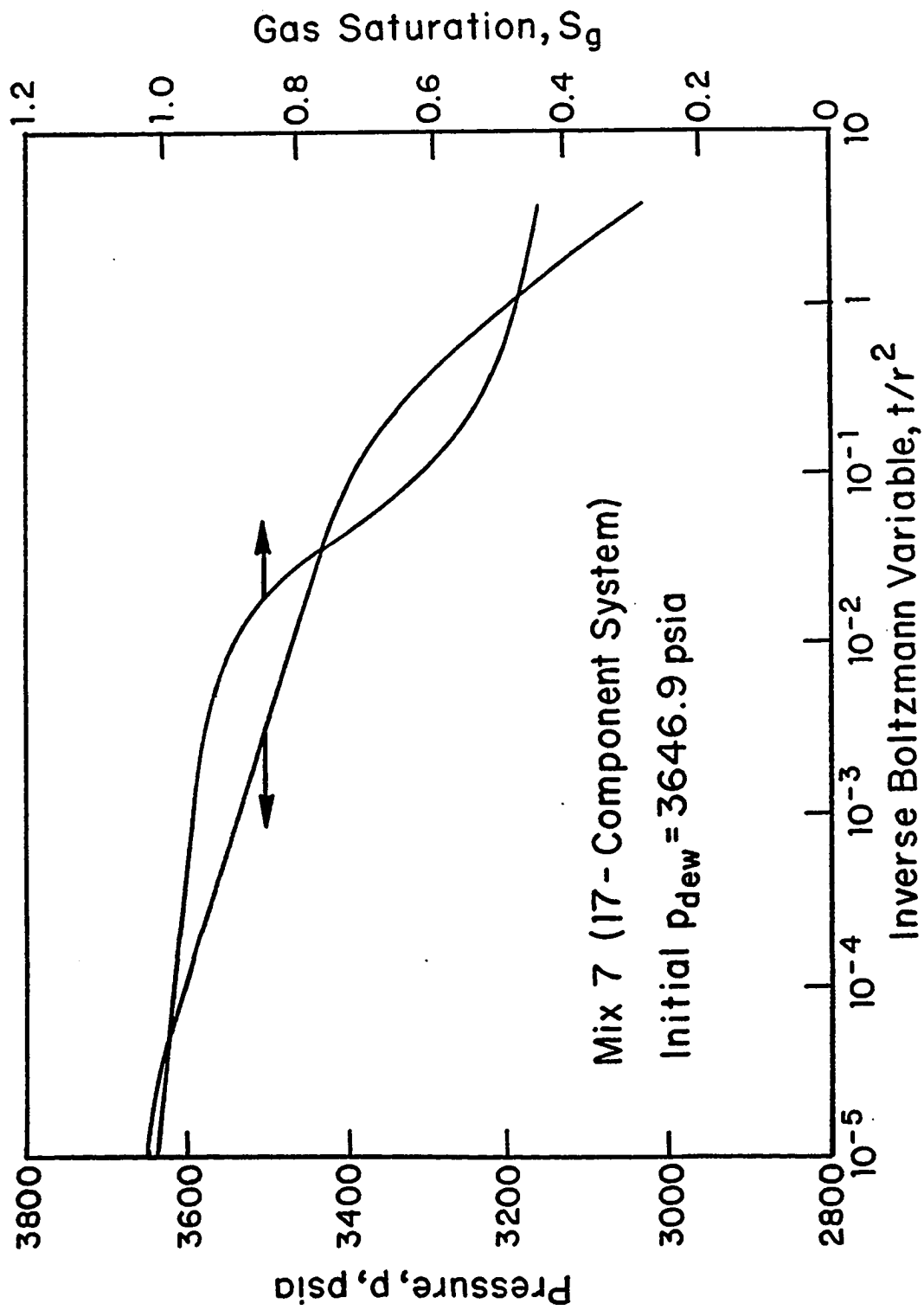


Fig. 5.30 - Correlation of pressure and gas saturation in terms of inverse Boltzmann variable; retrograde gas condensate, $s = 0$.

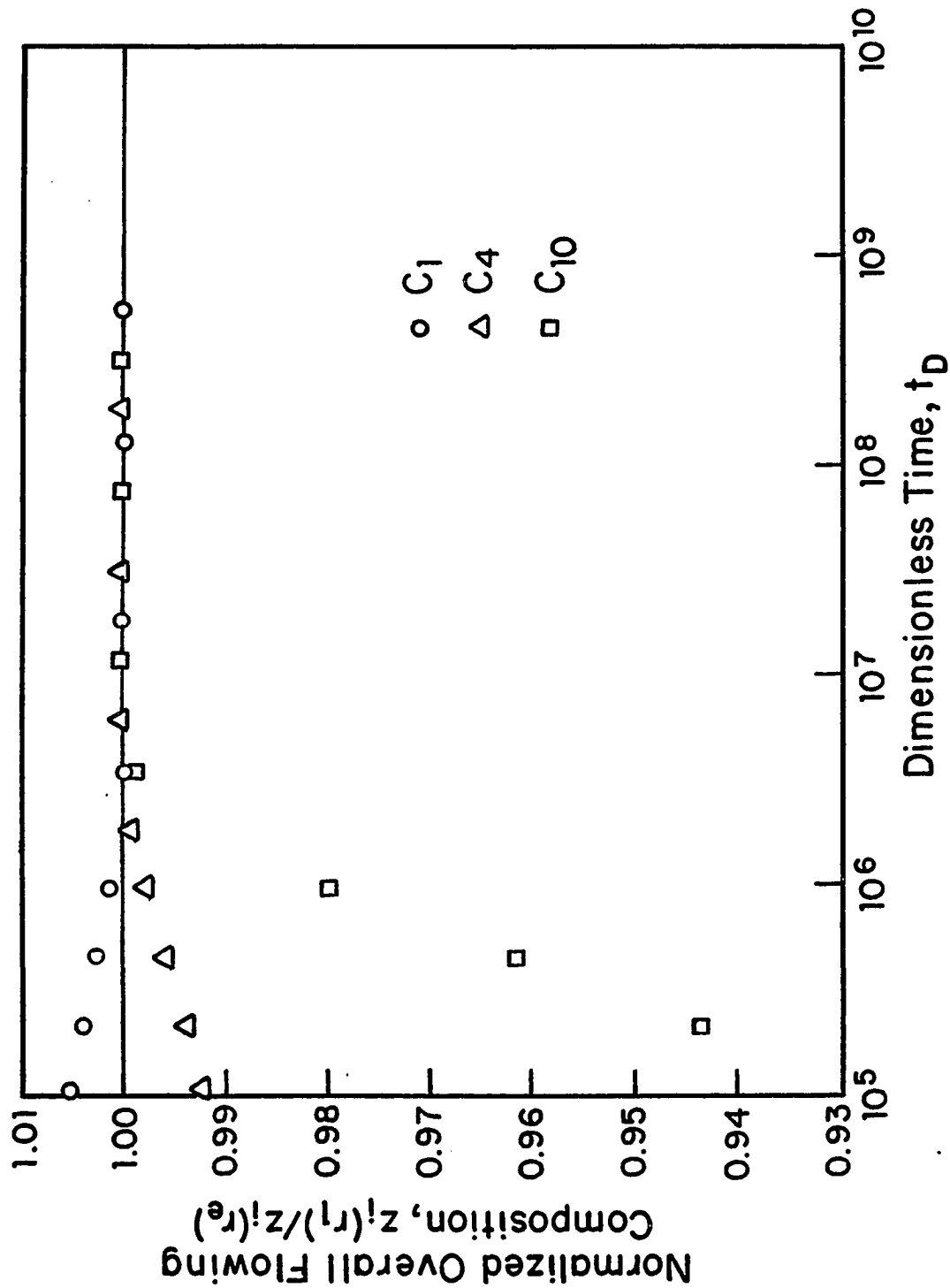


Fig. 5.31 - Comparison of simulator results with steady-state theory predictions; overall flowing mole fractions.

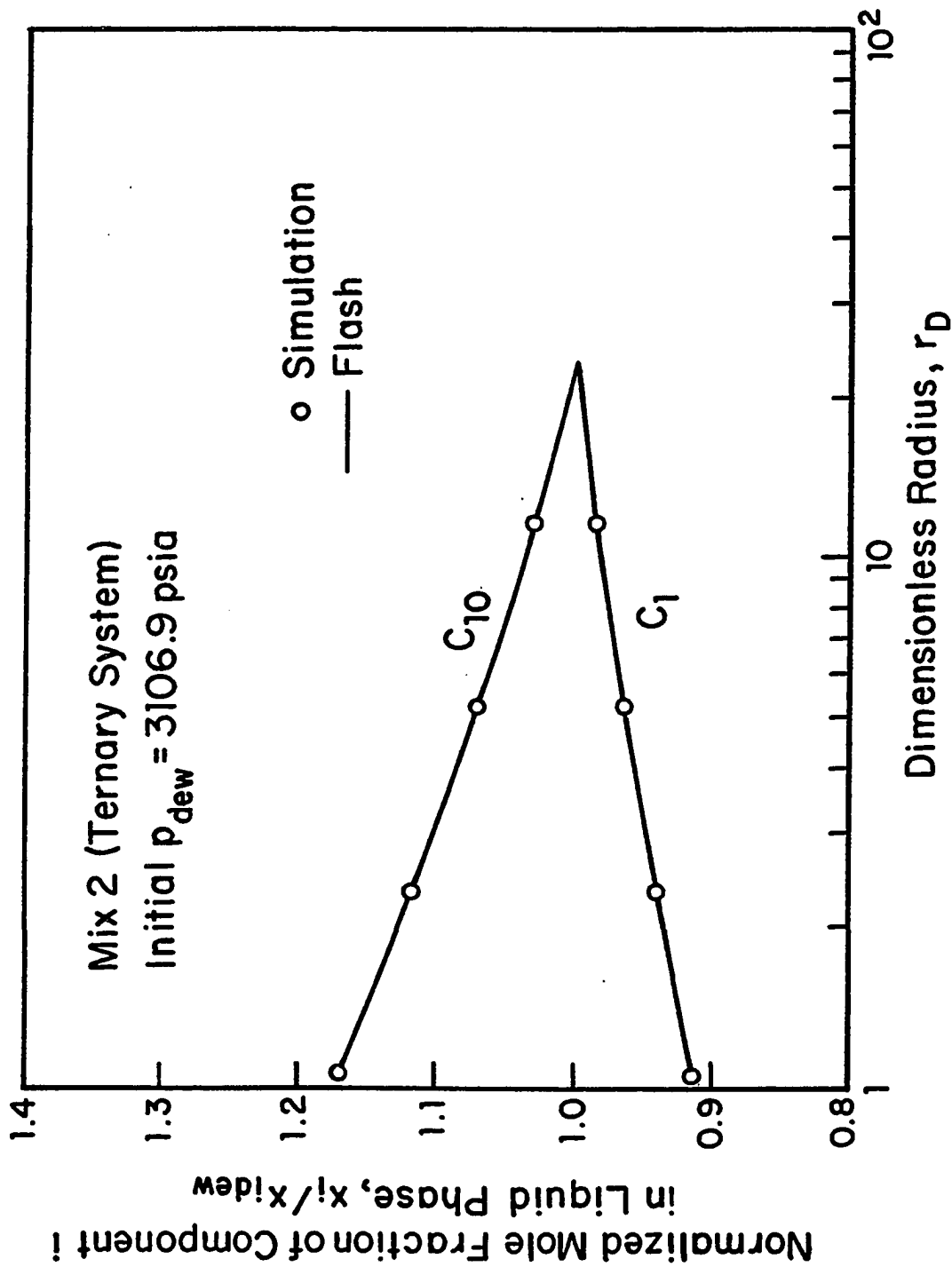


Fig. 5.32 - Comparison of simulator results with steady-state theory predictions; liquid phase mole fractions.

data points represent the simulator predictions for Mix 2. We see that the mole fractions computed by the model and those computed from flash data are in excellent agreement. Similarly, the oil saturation predicted by Eq. 5.1.32 are matched by the simulator output almost perfectly, as is shown in Fig. 5.33. The error in the mole fractions is essentially zero, while the model saturations differ from those computed from Eq. 5.1.32 by less than 0.3%. Note that there is a discontinuity in the oil saturation with magnitude greater than $S_{oc} = 0.30$ for $p < p_{dew}$ ($r_D < 25$) and $S_o = 0$ for $p > p_{dew}$ ($r_D > 25$).

Fig. 5.34 is a semilog plot of the dimensionless pseudopressure drop, $m_D(r_D)$, defined by Eq. 5.1.36, versus dimensionless radial distance, r_D . Again, results are for times beyond the onset of steady-state. The radial extent of the two-phase zone is shown in the figure. The solid line with slope -2.303 is a plot of Eq. 5.1.40. The match between the simulator $m_D(r_D)$ and that given by Eq. 5.1.40 is excellent.

We have shown that the model reproduces the five characteristics of the steady-state model problem.

5.4.3 Comparison with the Fully-Implicit Model (Coats Approach)

Mix 2 and Mix 5 are used to compare results from our model and the fully-implicit model based on Coats procedure. The fully-implicit used is the one developed by Jones⁴⁵.

5.4.3.a Constant Rate Production

The reservoir is filled with single-phase retrograde gas condensate characterized by Mix 2. The initial reservoir saturation pressure is 3106.9 psia. The runs were conducted with an initial pressure of about 3 psia above the dew point, for a total simulation time of 1.0 day with an initial time step size of 10^{-3} days. In Fig. 5.35, as well as in Figs. 5.36 through 5.38, results obtained from our simulator are shown by a solid curve and results obtained from the fully-implicit model are shown by circular points. Fig. 5.35 is a plot a flowing bottomhole pressure versus time and Fig. 5.36 presents a plot of the sandface gas saturation versus time. Gas and liquid

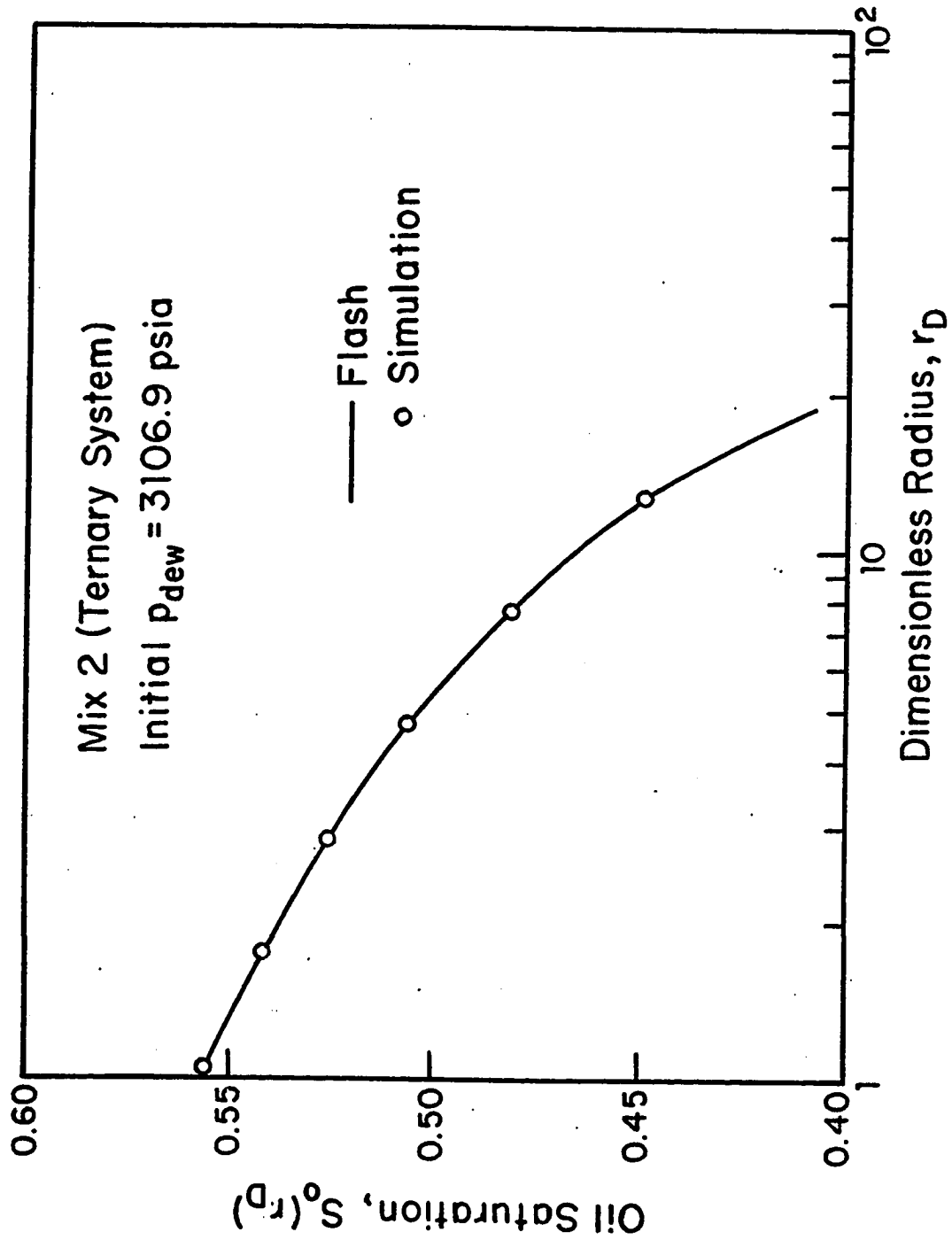


Fig. 5.33 - Comparison of simulator results with steady-state theory predictions; gas saturation.

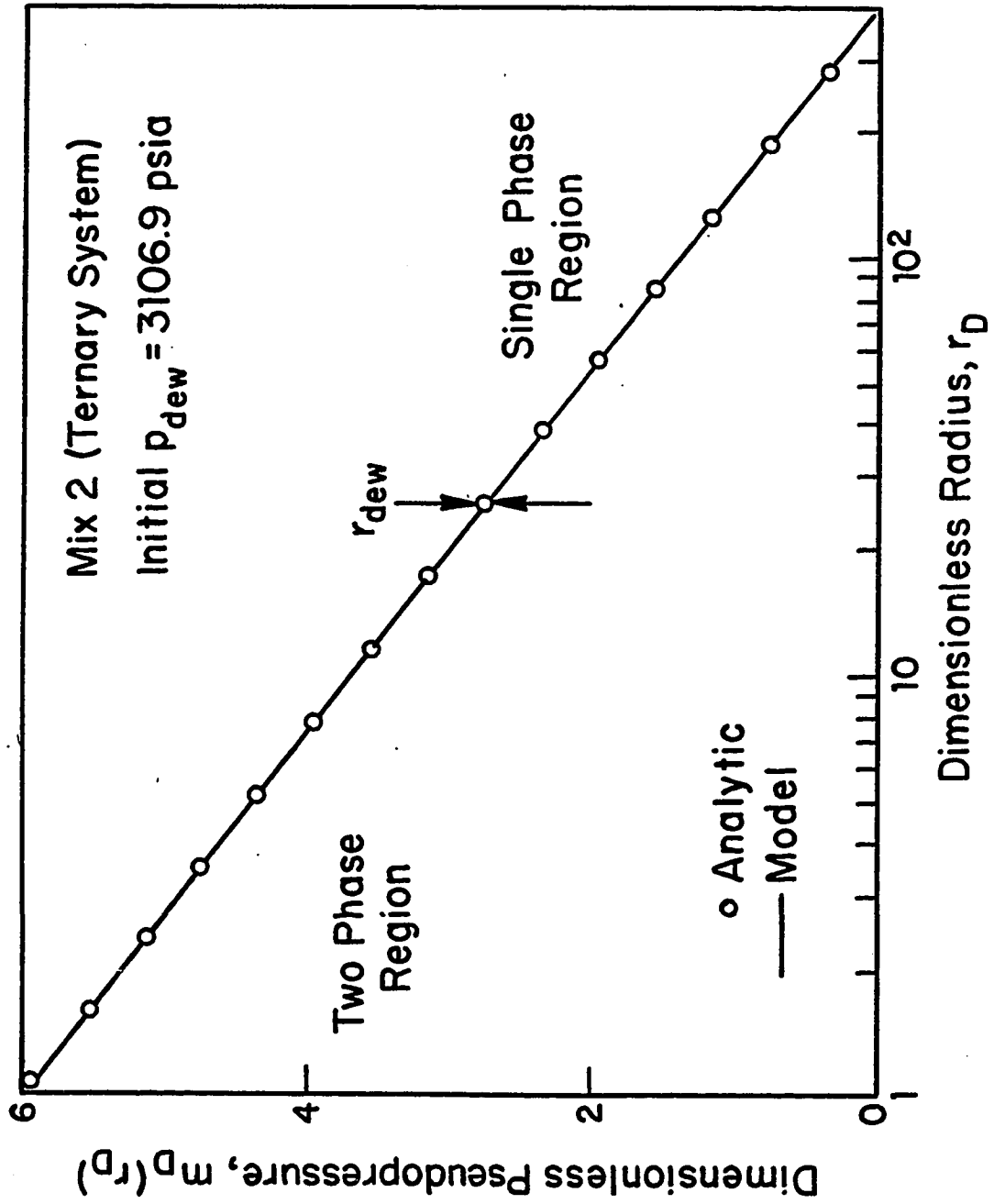


Fig. 5.34 - Comparison of simulator results with steady-state theory predictions; pseudopressure drop distribution.

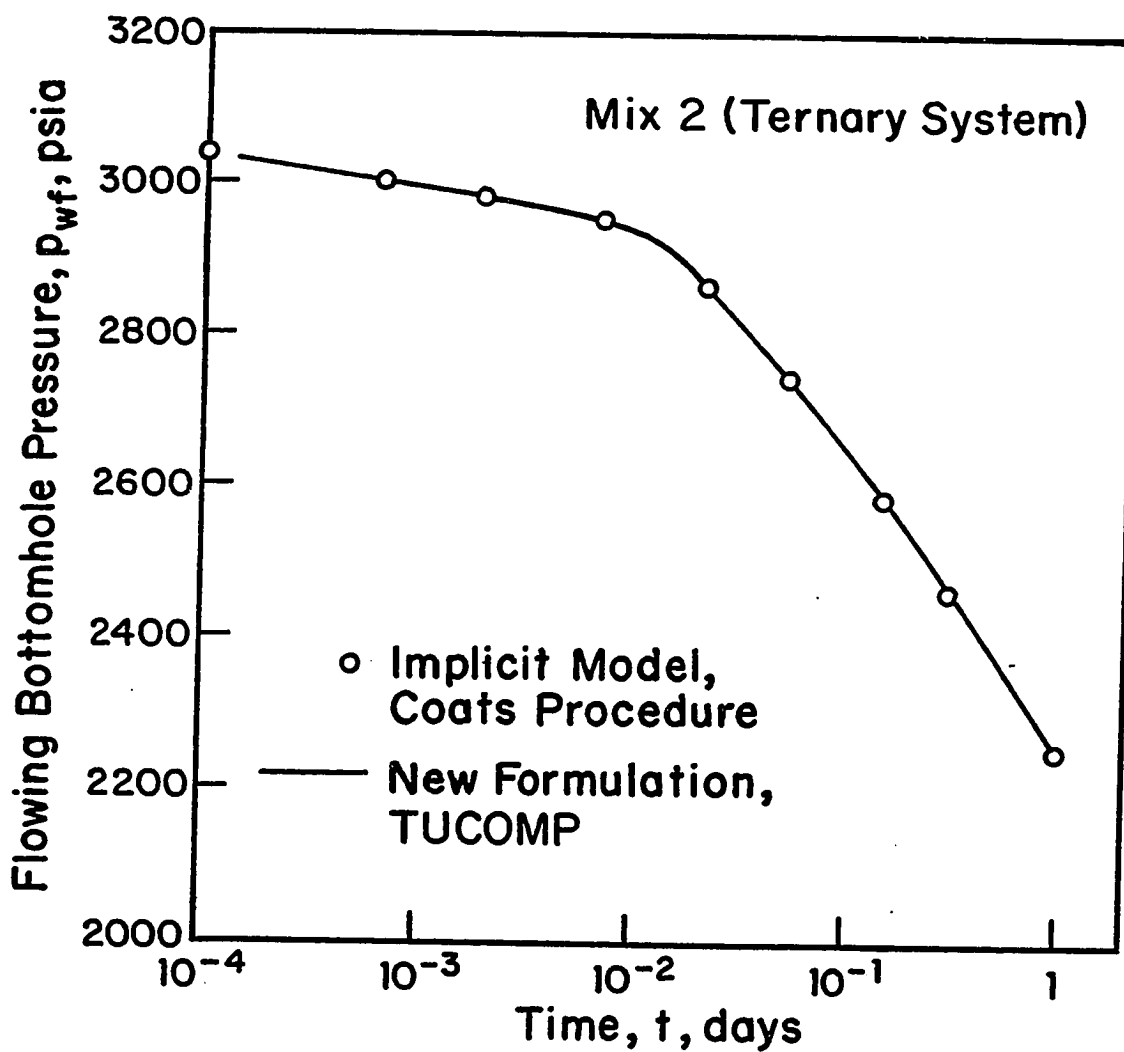


Fig. 5.35 - Comparison of implicit model and new formulation pressure results; retrograde gas condensate, $s = 0$.

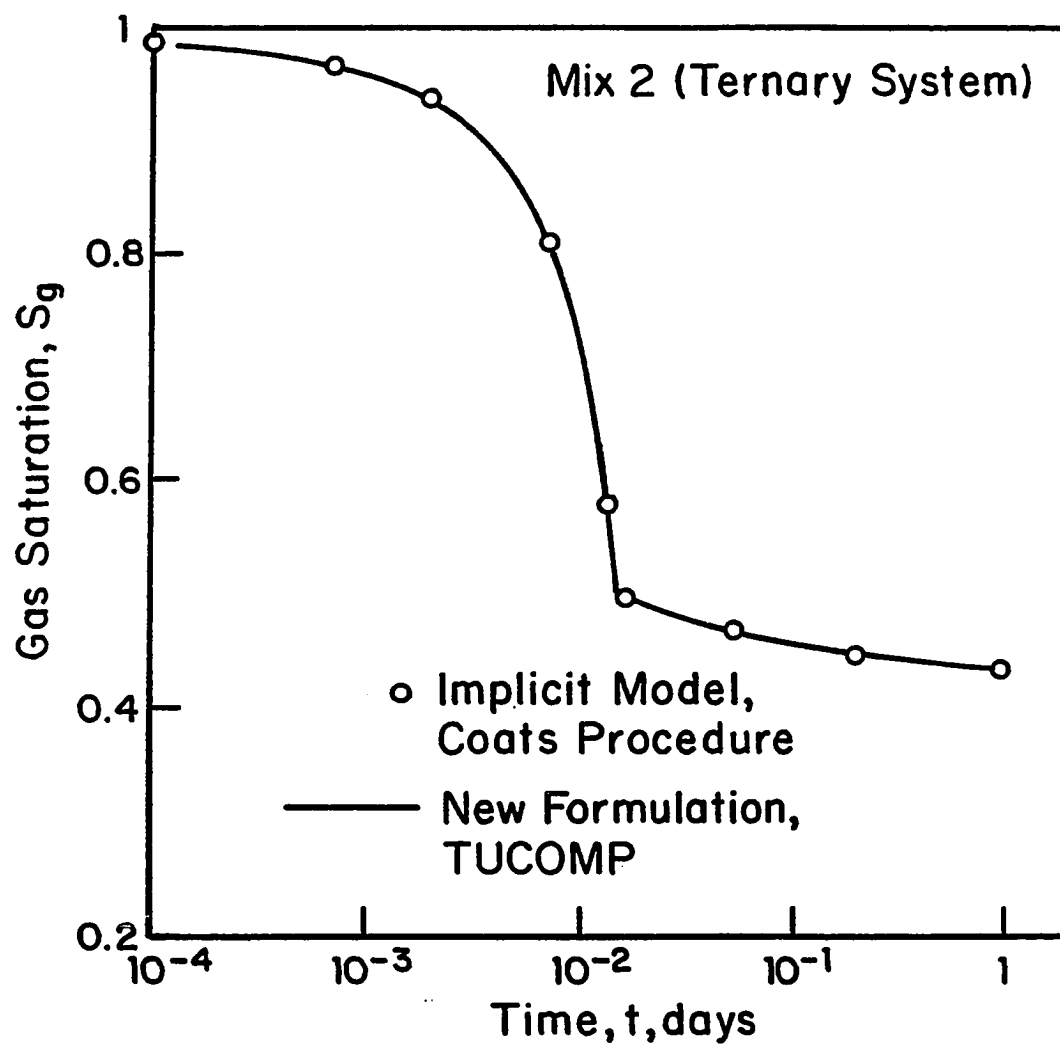


Fig. 5.36 - Comparison of implicit model and new formulation saturation results; retrograde gas condensate, $s = 0$.

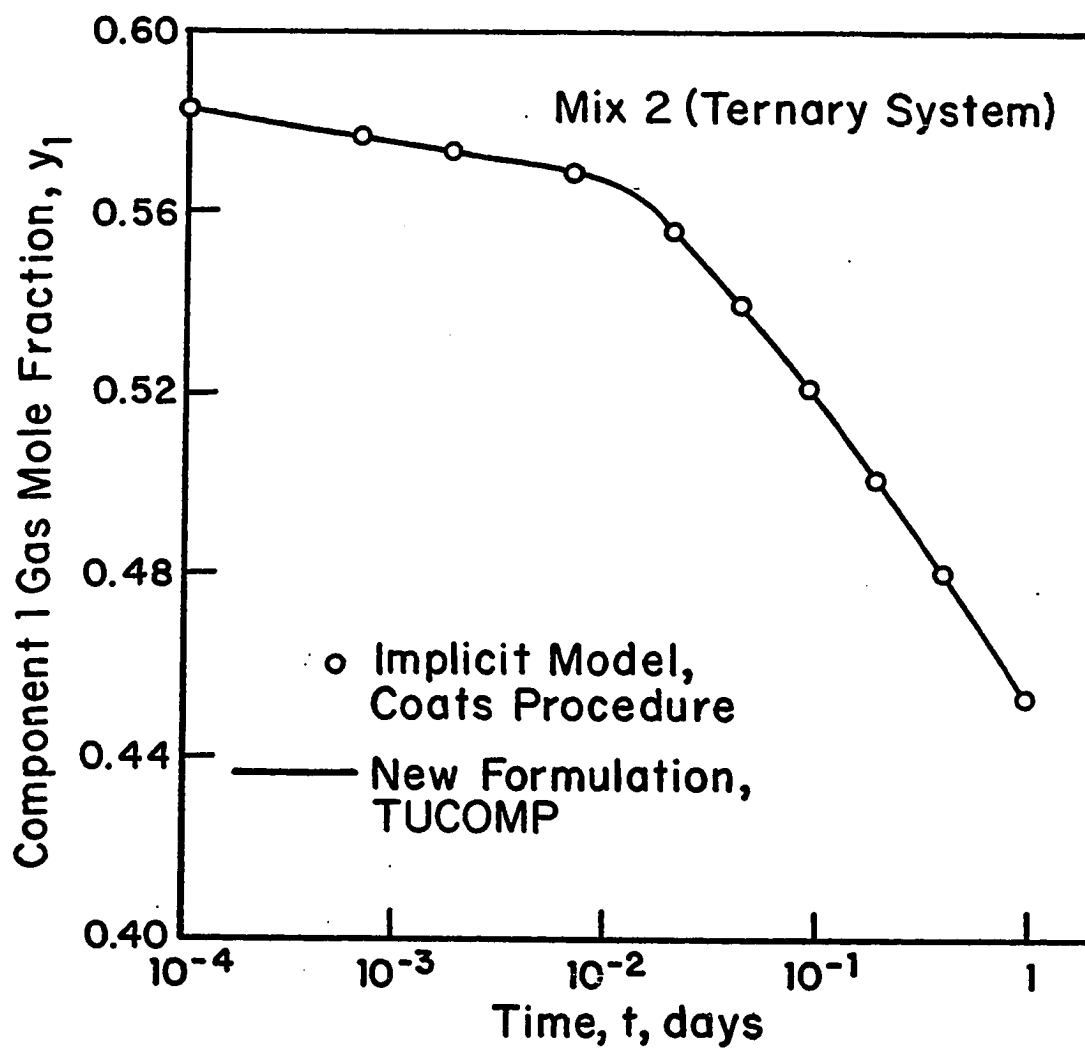


Fig. 5.37 - Comparison of implicit model and new formulation gas composition results; retrograde gas condensate, $s = 0$.

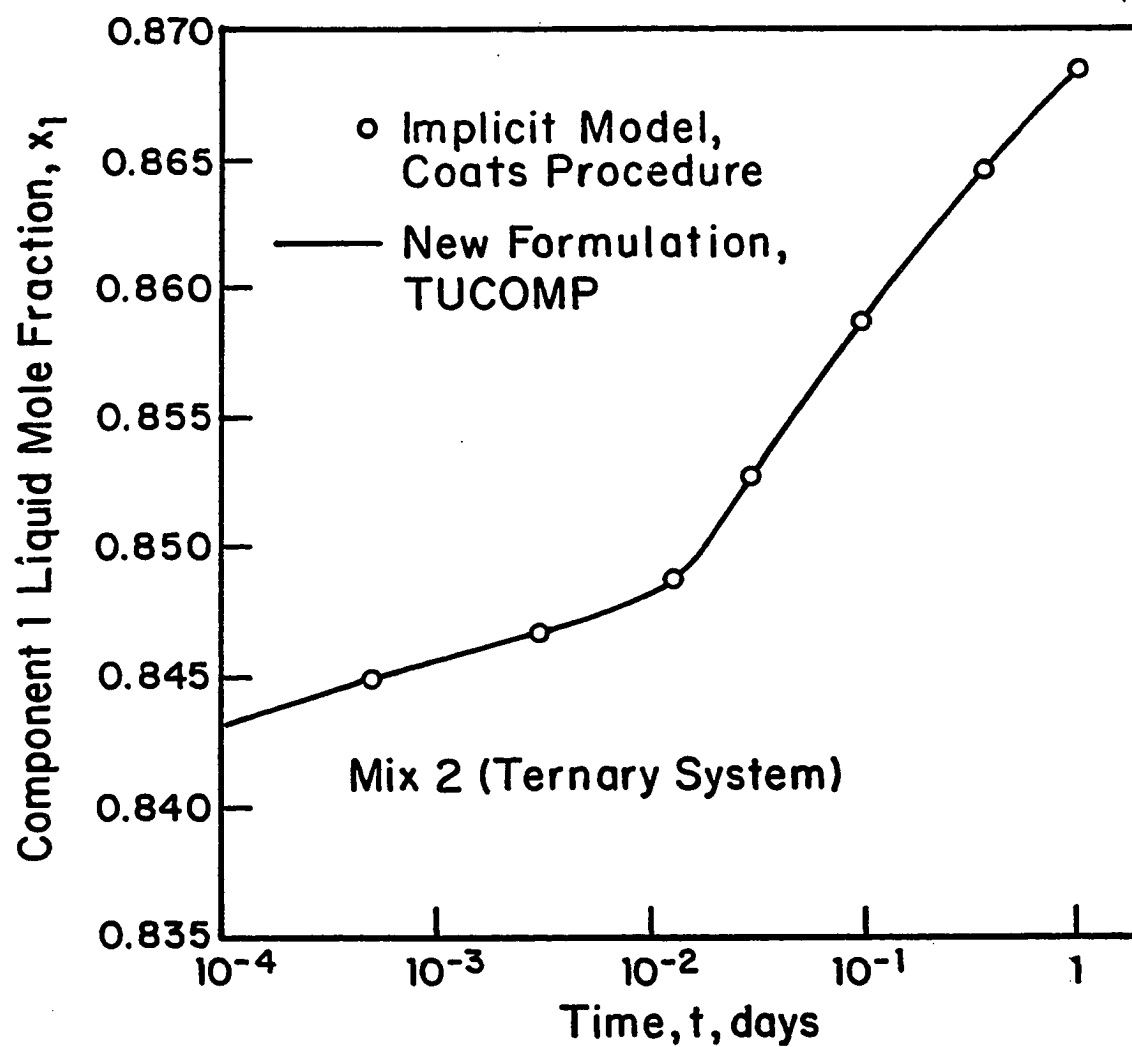


Fig. 5.38 - Comparison of implicit model and new formulation liquid composition results; retrograde gas condensate, $s = 0$.

phase mole fractions compositions of methane versus time are illustrated in Figs. 5.37 and 5.38, respectively. All figures clearly demonstrate that results from both models agree very well.

The CPU times used by both models are shown in Fig. 5.39 for a constant time step size with $\Delta t = 10^{-3}$ days. Fig. 5.40 shows results for a case where time steps are selected automatically based on a maximum change in saturation of 2% over the time step. In Figs. 5.39 and 5.40, the CPU time is plotted versus simulation time. CPU time for our model result is represented by a solid curve, whereas, the fully-implicit model result is shown by a dashed curve. Both figures clearly demonstrate that the new formulation is on the order of 5 times faster than the fully-implicit method. Finally, the CPU time per time step per gridblock is 0.0366 for the fully implicit and 0.00833 for our model.

5.4.3.b Constant Pressure Production

The last ternary mixture simulation run was performed for a black-oil (Mix 5) with a bubble point pressure of 2328 psia. A reservoir with an initial reservoir pressure of about 2 psia above the bubble point was produced for 10 days at a constant flowing bottom hole pressure of 1850 psia. Figs. 5.41 and 5.42 compare our model results with those obtained from the fully-implicit model. Our results are represented by solid curves, whereas the fully-implicit simulator results are shown by circular data points. In Fig. 5.41, first gridblock pressure and saturation are plotted versus time and in Fig. 5.42, total molar rate and reservoir average pressure are plotted versus time. Both figures illustrate the excellent agreement between the results of both models.

5.4.4 Other Results

As discussed previously, our simulator avoids flash calculations by use of the expansions of the fugacities to solve for composition. Since the expansions of both phase fugacities are equated every time step and not the actual fugacities, we can further check the validity of these expansions by computing the actual difference

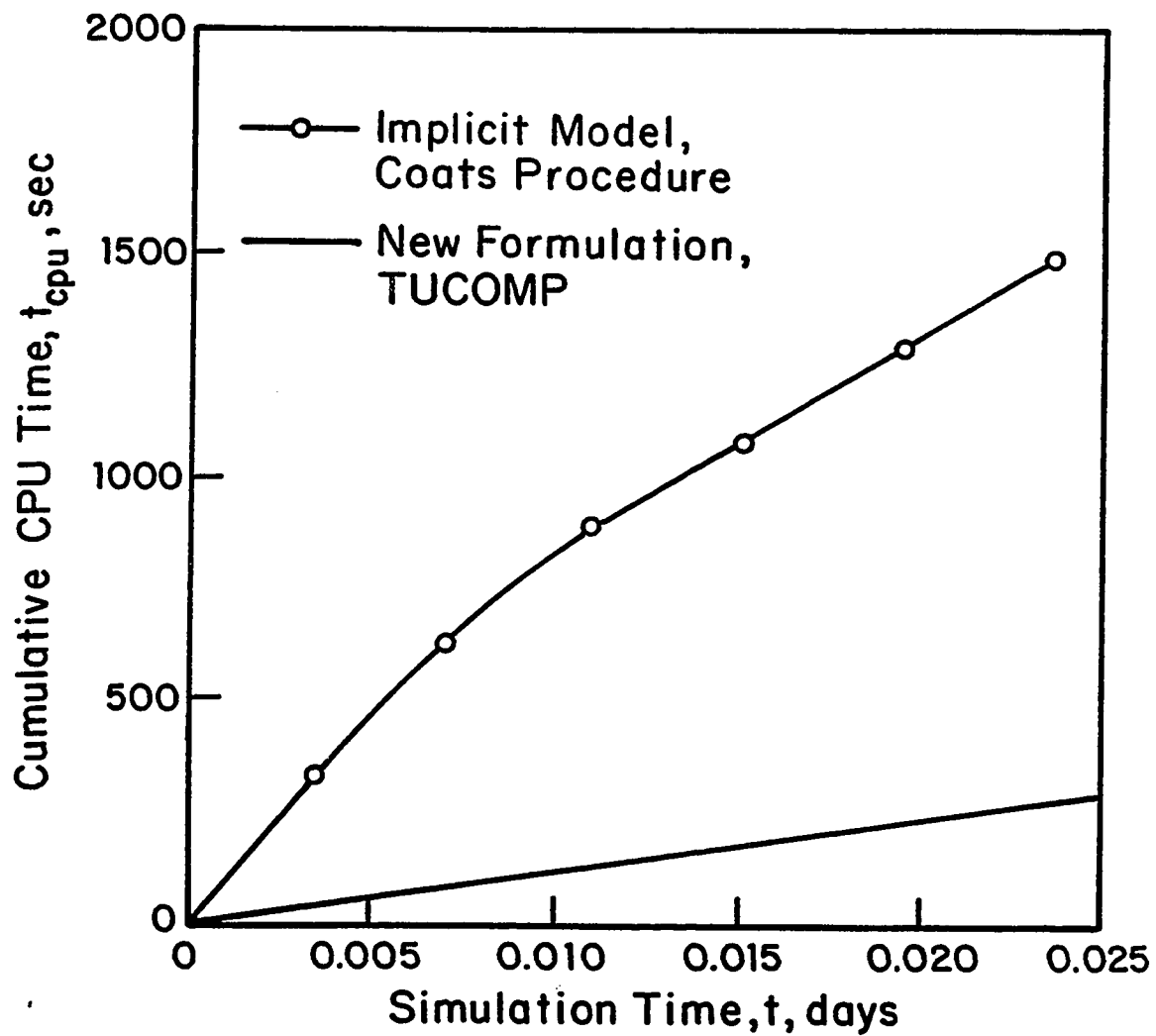


Fig. 5.39 - Comparison of CPU time used by implicit and new formulation models; constant time step, $\Delta t = 10^{-3}$ days.

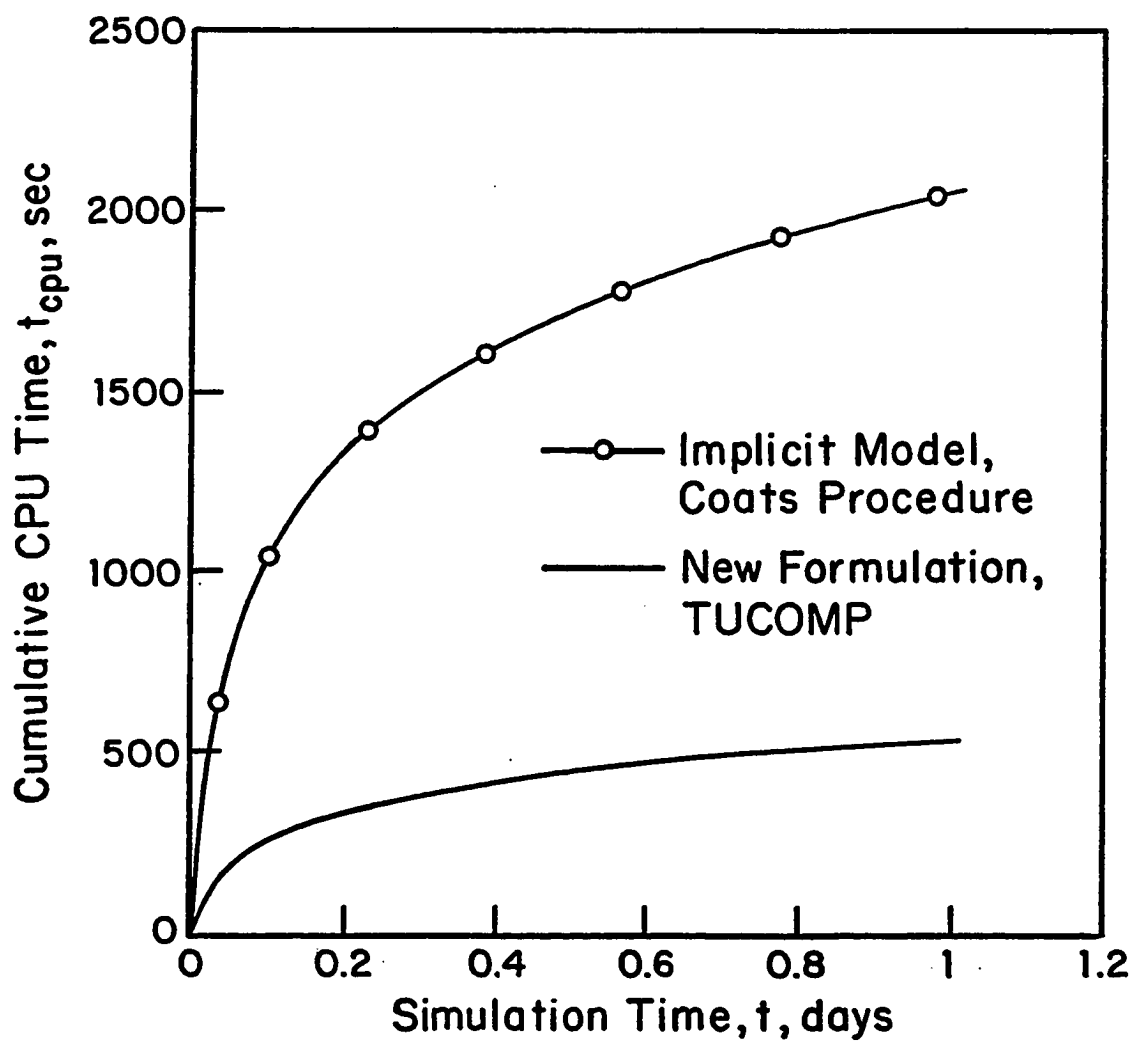


Fig. 5.40 - Comparison of CPU time used by implicit and new formulation models; automatic time step selection.

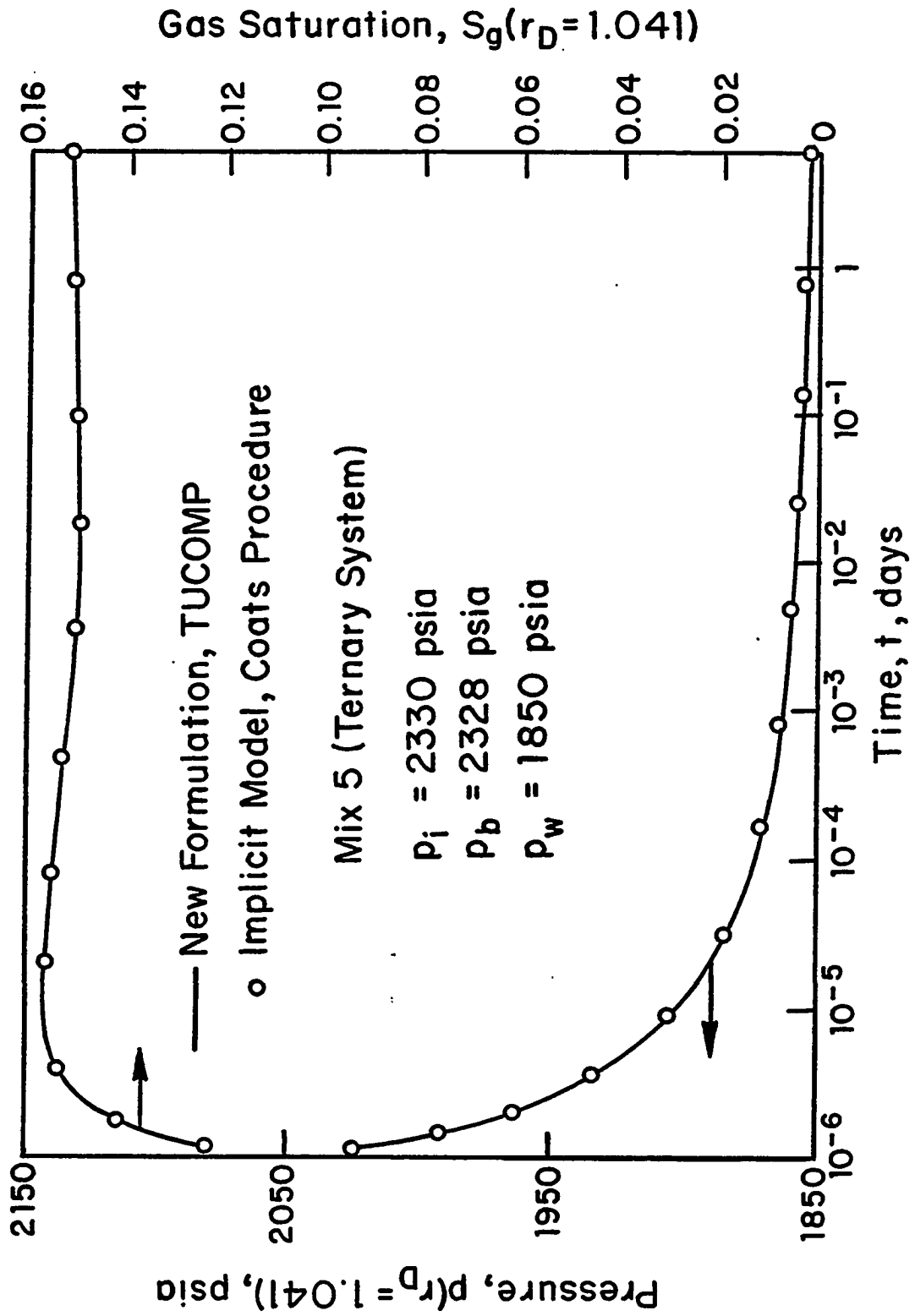


Fig. 5.41 - Comparison of implicit and new formulation models results; black oil constant rate, $s = 0$.

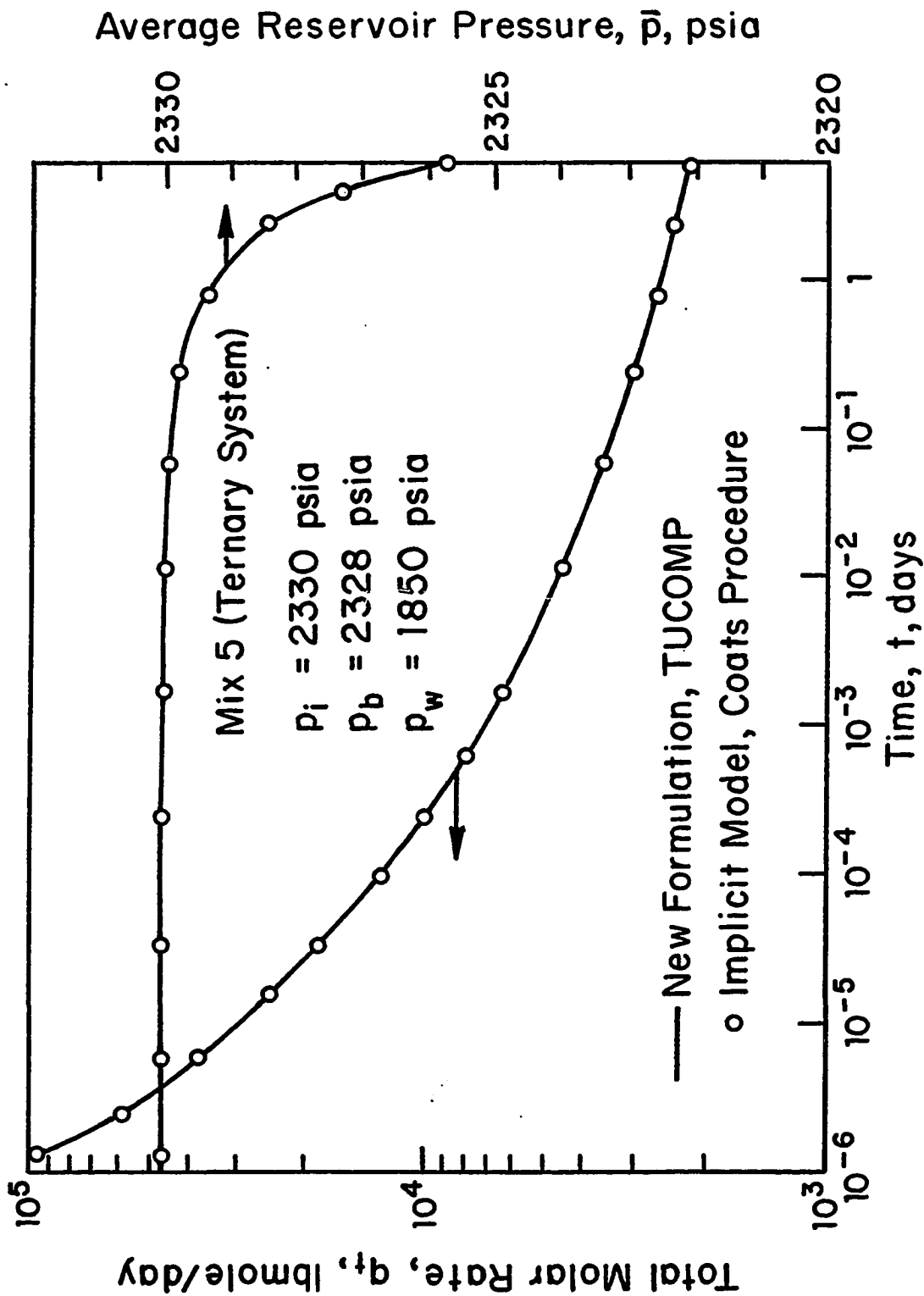


Fig. 5.42 - Comparison of implicit and new formulation models results; black oil constant flowing bottomhole pressure, $s = 0$.

between fugacities for each component in each phase. Table 5.11 shows the range of values of $\sum_i \left(\frac{f_{i,L}}{f_{i,V}} - 1 \right)^2$ computed every 10 time steps. These results indicate that regardless of the pressure or composition differential between states, the actual phase equilibrium, as expected by minimizing the Gibbs free energy, is achieved at equilibrium. Furthermore, we checked our model accuracy by taking a gridblock pressure, and overall mole fractions composition at time t and performing a flash calculation with our phase package to determine gas and liquid compositions as well as liquid dropout or the amount of gas released. Note that L , the number of moles of liquid per number of moles of mixture computed in the simulator is based on saturation and density as it is shown in Eq. 5.4.1, i.e., $L = \rho_o S_o / (\rho_o S_o + \rho_g S_g)$. Table 5.12 shows that the simulator results for Mix 2 are in excellent agreement with those obtained by performing a flash calculation using our PVT package.

Although not shown in this work, flash calculations were performed for all mixtures, and the results were similar to those of Table 5.12 which were obtained with Mix 2.

5.4.5 Isochronal Tests

We ran the model for two types of fluid mixtures. The first test pertains to Mix 2, and Set 2 relative permeability data, whereas the second test uses Mix 4 and Set 3 relative permeability data. Tables 5.13 and 5.14 depict the reservoir and rate schedules data for test 1 and 2, respectively.

5.4.5.a Test 1

The reservoir pressure is initially at 3150 psia, which is approximately 43 psia above the dew point pressure. A thick skin zone exists around the well, $r_s = 1.5$ feet, with a skin factor of $s = 7$. Details of the reservoir data are presented in Table 5.13. This isochronal test assumes a time period between for each drawdown and buildup period of about 0.2 days. There are four flow rates selected for this test with the sequence of 10000, 7500, 5000, 2500 lbmoles/day.

TABLE 5.11

L_2 Norm Square Error on Fugacities for 17-Component Mixture

Time Step Number	$\sum_i \left(\frac{f_{i,L}}{f_{i,V}} - 1 \right)^2$
10	2.32×10^{-7}
20	1.02×10^{-7}
30	2.41×10^{-7}
40	1.03×10^{-6}
50	7.01×10^{-6}
60	9.31×10^{-6}
70	1.05×10^{-5}
80	6.06×10^{-6}
90	8.64×10^{-6}
100	5.54×10^{-6}
1000	4.32×10^{-6}

TABLE 5.12

Comparison of Simulator and Phase Package Results

MIX 2: Retrograde Gas Condensate

P (<i>psia</i>)	z_i	Liquid Dropout		K-Values	
		Model	Flash	Model	Flash
3039	0.83920138	0.015	0.015	1.449	1.449
	0.11310125			0.677	0.677
	0.04769737			0.177	0.177
2701	0.68664664	0.511	0.511	1.636	1.636
	0.14367021			0.621	0.621
	0.16968315			0.112	0.112
2123	0.58455555	0.640	0.641	2.052	2.053
	0.15922037			0.568	0.568
	0.25622408			0.058	0.058

TABLE 5.13

Isochronal Test 1

Reservoir Data

Reservoir Extent Radius, r_e	(<i>ft</i>)	2000.0
Absolute Reservoir Permeability, k	(<i>md</i>)	5.0
Porosity, ϕ	(-)	0.2
Formation Thickness, h	(<i>ft</i>)	40.0
Wellbore Radius, r_w	(<i>ft</i>)	0.25

Rate Schedule

Flowing Time, t_i ,	(<i>hr</i>)	4.8
Shut-in Time, Δt_i ,	(<i>hr</i>)	4.8
Flow Rate 1, q_1 ,	(<i>lbmoles/day</i>)	10000
Flow Rate 2, q_2 ,	(<i>lbmoles/day</i>)	7500
Flow Rate 3, q_3 ,	(<i>lbmoles/day</i>)	5000
Flow Rate 4, q_4 ,	(<i>lbmoles/day</i>)	2500

TABLE 5.14

Isochronal Test 2

Reservoir Data

Reservoir Extent Radius, r_e	(<i>ft</i>)	2000.0
Absolute Reservoir Permeability, k	(<i>md</i>)	5.0
Porosity, ϕ	(-)	0.2
Formation Thickness, h	(<i>ft</i>)	40.0
Wellbore Radius, r_w	(<i>ft</i>)	0.25

Rate Schedule

Flowing Time, t_i ,	(<i>hr</i>)	4.8
Shut-in Time, Δt_i ,	(<i>hr</i>)	4.8
Flow Rate 1, q_1 ,	(<i>lbmoles/day</i>)	2500
Flow Rate 2, q_2 ,	(<i>lbmoles/day</i>)	5000
Flow Rate 3, q_3 ,	(<i>lbmoles/day</i>)	7500
Flow Rate 4, q_4 ,	(<i>lbmoles/day</i>)	10000

Fig. 5.43 presents the gas saturation changes at the well as a function of the well flowing pressure for the entire isochronal test. As noted in this figure, there are three shut-in periods during the test, which are represented by the dashed curves and depicted by *bu1* to *bu3*. Results for the four flow periods are plotted as the solid curves and denoted as *dd1* to *dd4*. Results in this figure also show the behavior of the sandface gas saturation is similar to that of a black-oil fluid. The gas phase dissolves in the liquid phase rather than the liquid phase revaporizing as the pressure increases during the buildup periods. This type of behavior is expected as it was reported in Ref. 60, where the in-place fluid critical temperature is evaluated and shown to be subcritical for the fluid in the vicinity of the well. Here, we can see the effect of the large flow rate imposed during the first flow period dictates the magnitude of saturation in the near-well region. Although not shown here, the size of the two-phase zone is significant at the end of the first flow period and has exceeded the radius of the skin zone. This zone grows more slowly for the subsequent flow periods due to the lower flow rates.

5.4.5.b Test 2

The initial reservoir pressure is 4200 psia. The rate sequence is 2500, 5000, 7500 and 10000 lbmoles/day. The skin factor used in this simulation is zero. The isochronal flowing and shut-in times are 0.1 days per period. The reservoir data and rate schedule are documented in Table 5.14. Fig. 5.44 presents a plot of gas saturation, S_g , versus pressure, p , obtained at the sandface. The dashed curves depict the responses obtained during the buildup periods and are denoted as *bu1* to *bu3*. The solid curves are for the flowing periods and are marked as *dd1* to *dd4*. Again, we observe that the gas phase is dissolved into the liquid phase during the shut-in periods and that the sandface gas saturation increases somewhat with subsequent drawdowns.

The preceding effects demonstrate the model's capability for handling the presence of black-oil and gas condensate in the same reservoir. In fact, this case shows the numerical complexity in the formulation as some blocks containing single-phase

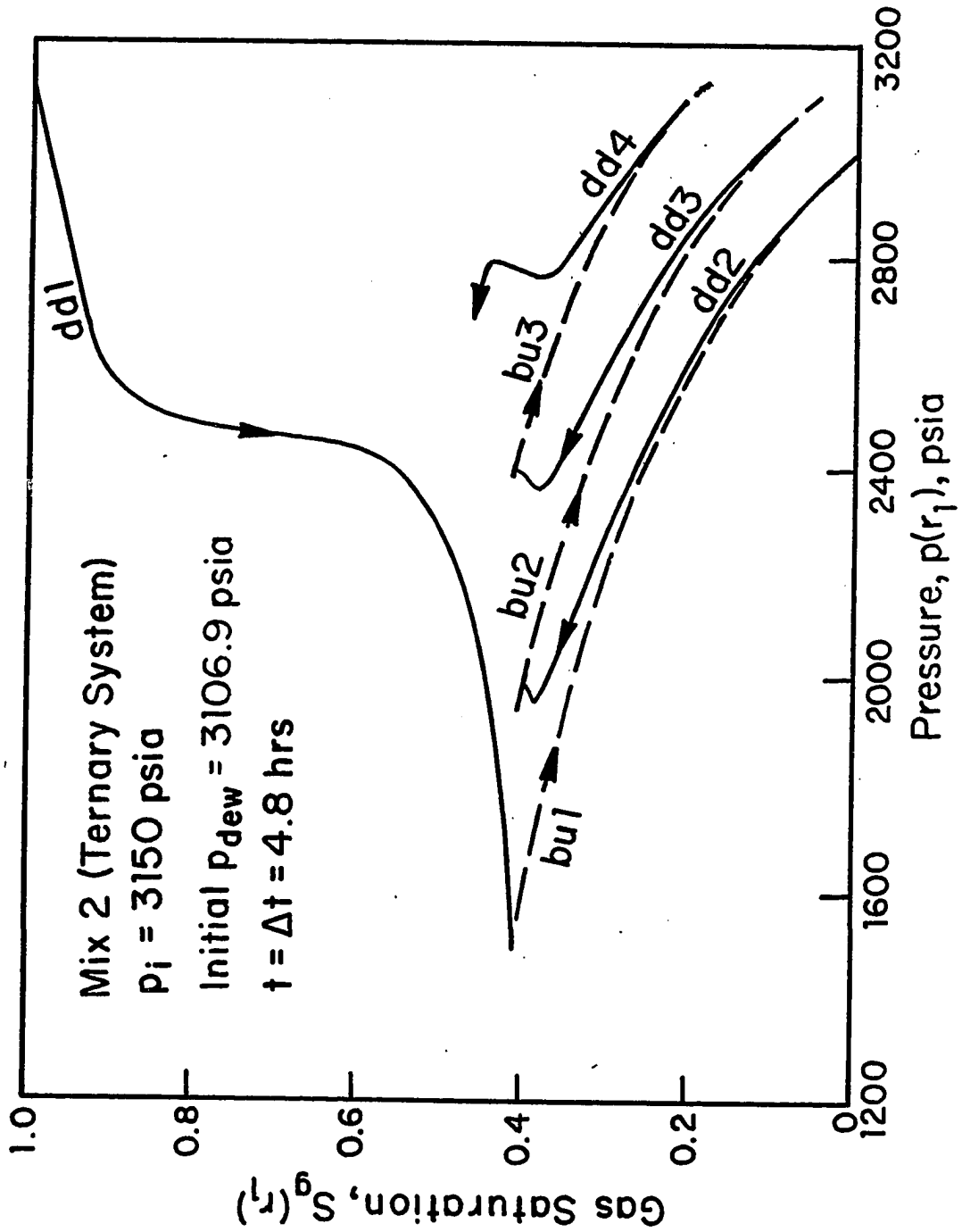


Fig. 5.43 - Variation in sandface saturation during an isochronal test; retrograde gas condensate, $s = 7$, $r_{sD} = 6.03$.

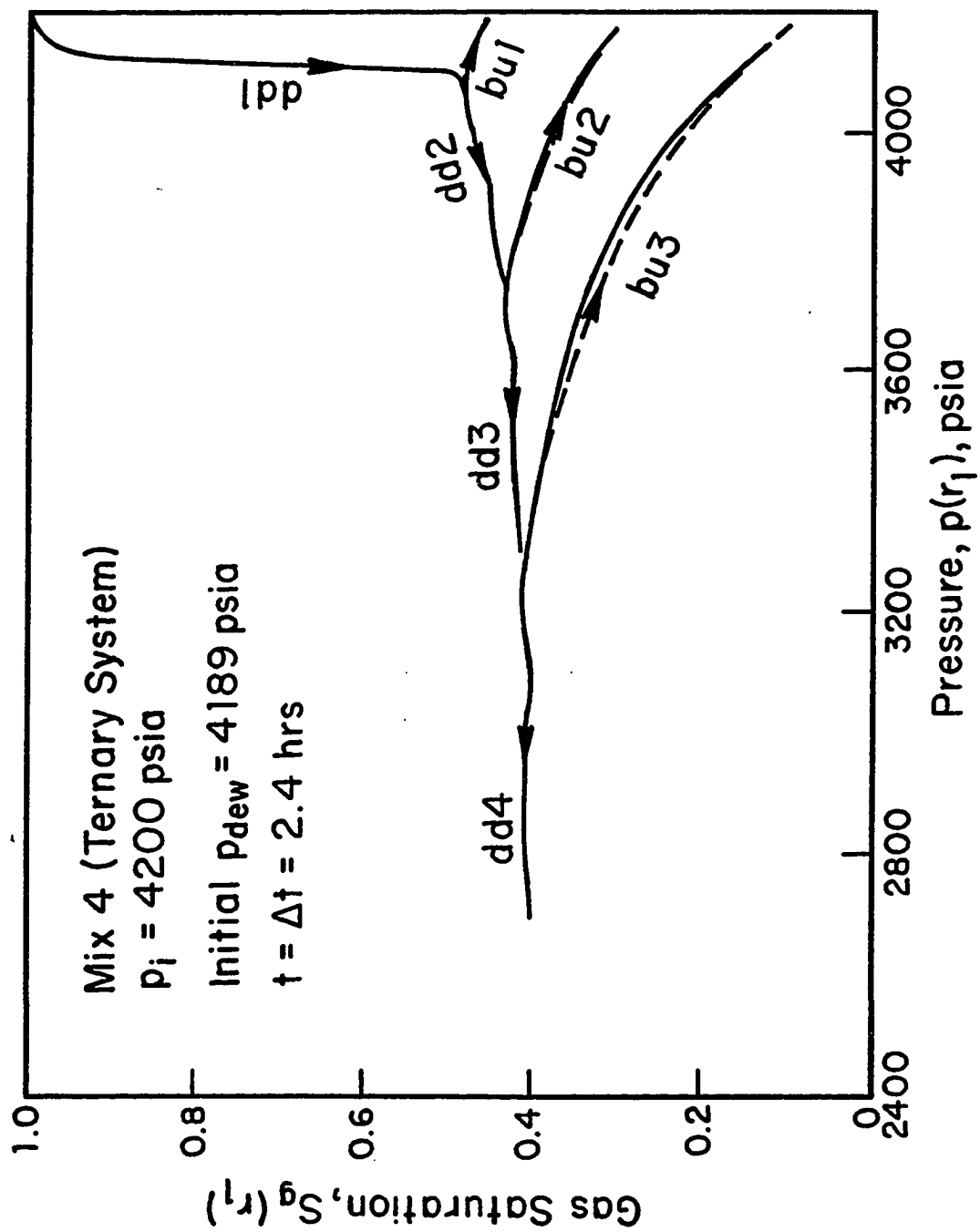


Fig. 5.44 - Variation in sandface saturation during an isochronal test; retrograde gas condensate, $s = 0$.

oil are adjacent to other ones filled with a two-phase fluid which in turn are coupled with single-phase gas blocks that may or may not be of different compositions than the initial composition. The model screens the reservoir for the phase configuration of all blocks and treats them accordingly as is stipulated in the formulation.

5.4.6 Gas Cycling

The gas cycling problem is applied to a reservoir whose data is shown in Table 5.10. The reservoir is initially filled with a single-phase fluid characterized by Mix 2 and the reservoir pressure prior to injection is 3150 *psia*. A high pressure (i.e., 4150 *psia*) injection of pure methane is conducted at the outer boundary, whereas at the producing well 7500 *lbmoles* of fluid is being delivered each day. At the start of the run, the model treats all gridblocks as single-phase gridblocks with changing composition since a foreign gas composition is in contact with the in-place fluid. At early times, the region in the vicinity of the producing well is affected by condensate accumulation due to falling pressure. The dew point pressure dictates how fast and how far the liquid zone advances inside the reservoir. Fig. 5.45 shows the sandface oil saturation and pressure behaviors as functions of injection time. As the injection front advances into the reservoir, the liquid starts revaporizing as is shown by the oil saturation profile in Fig. 5.45. Fig. 5.46 indicates the increase in methane concentration and disappearance of butane. Although not shown in this work, at late times steady-state prevails as predicted by the theory, and the whole reservoir becomes filled with dry gas.

In summary, we have shown that the new numerical solution procedure formulated yields a stable accurate algorithm. In fact, the formulation of the procedure (Chapter IV) and the examples presented here suggest that the method achieves the level of robustness of fully-implicit models based on Coats scheme in substantially less CPU time than is required by a fully-implicit model.

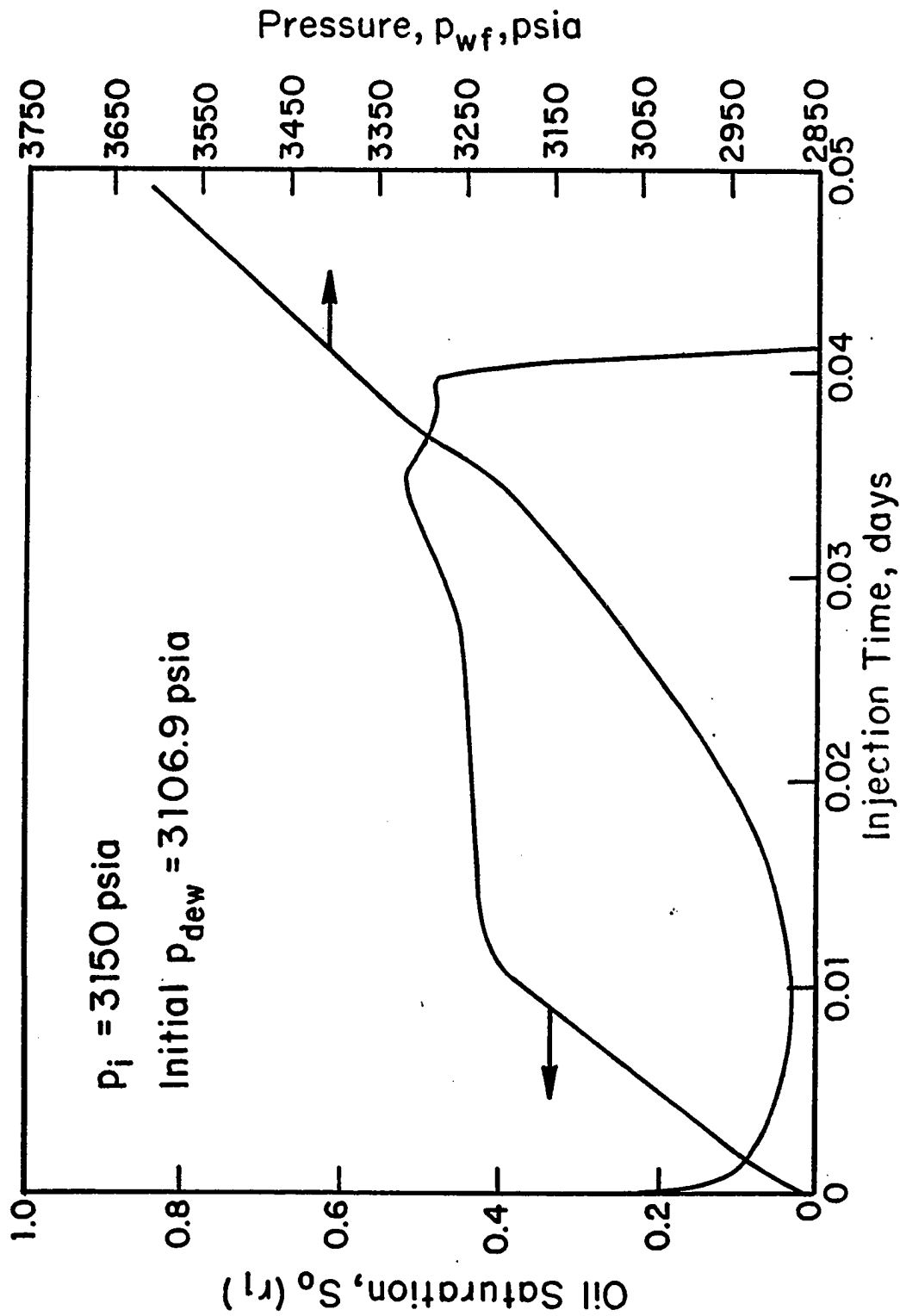


Fig. 5.45 - Sandface pressure and saturation profiles during gas cycling; retrograde gas condensate, ternary system.

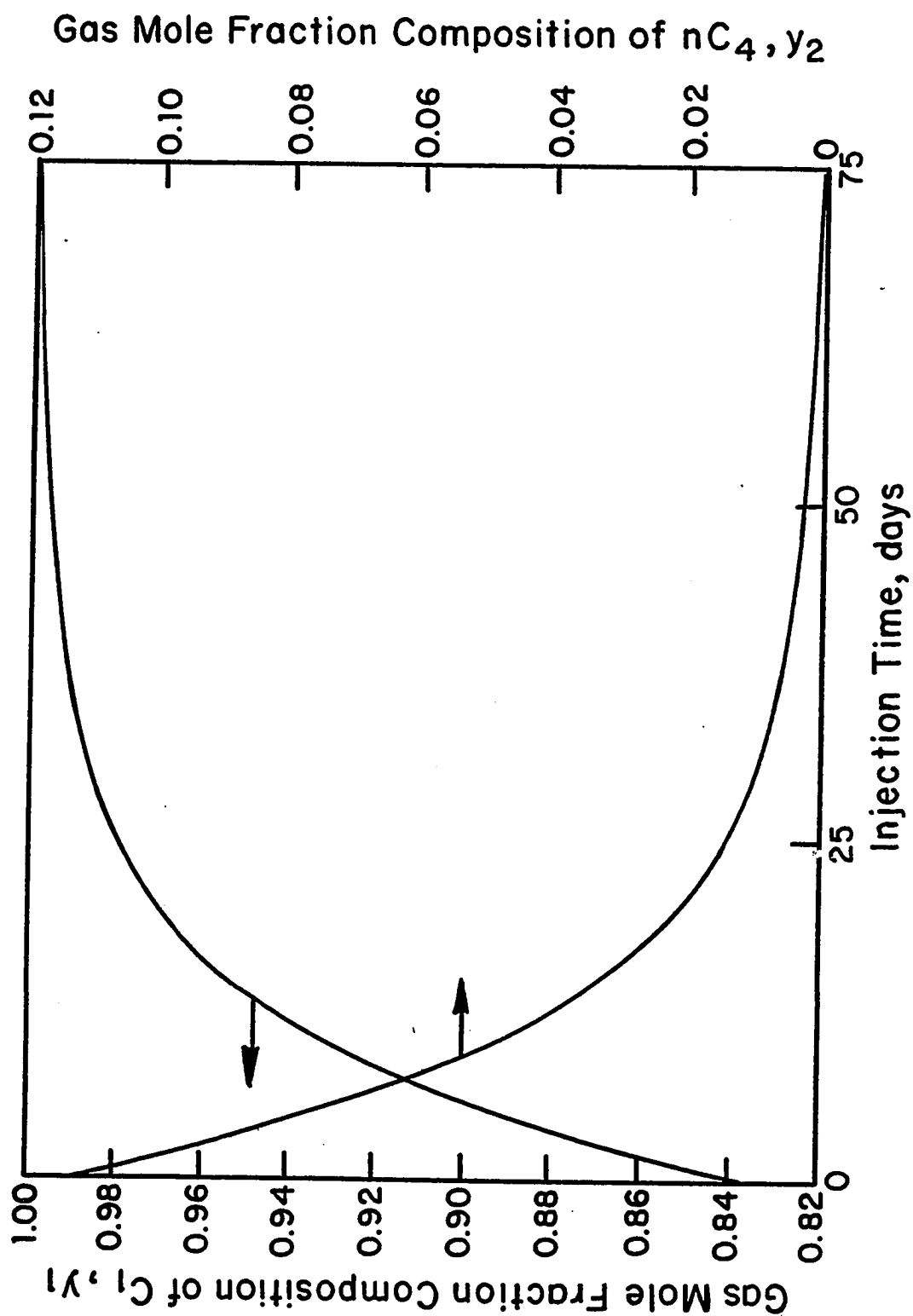


Fig. 5.46 - Sandface gas composition profiles during gas cycling; retrograde gas condensate, ternary system.

CHAPTER VI

CONCLUSIONS

In this work, we presented a new, computationally efficient approach to the simulation of flow of a multicomponent hydrocarbon mixture in an isothermal petroleum reservoir. In common with all models of this type, our formulation is based on the simultaneous solution of individual hydrocarbon species mass conservation equations. Interphase mass transfer of the various species is modeled by assuming that at every "point" in the reservoir where two hydrocarbon phases coexist, instantaneous thermodynamic equilibrium between the phases is achieved.

Phase behavior and fluid properties are described using a generalized equation of state which degenerates to any of five EOS's commonly used in the petroleum industry. In addition to the major contribution of this work, (i.e., the development of an efficient compositional reservoir simulator), a secondary contribution is a thorough review of equations of state for Petroleum Engineers, along with a detailed description (with all necessary working equations) for the construction of a phase package for modeling petroleum fluid PVT properties.

Although our formulation is completely general (i.e., it can be applied to simulate flow in multidimensional reservoirs), in this work, the method was applied to one-dimensional radial flow. The governing component mass conservation partial differential equations were approximated using standard, fully-implicit finite differences. The major innovation of this work is a method of **directly incorporating the thermodynamic equilibrium equations into the species conservation**

equations, so that mass conservation and phase equilibrium are satisfied simultaneously. Unlike conventional fully-implicit simulators, our formulation does not employ Newton's method; instead, we employ a semi-implicit approach similar to that of Letkman and Ridings for Beta-models. As a result, for an N_c component hydrocarbon fluid reservoir, we never solve more than N_c equations per reservoir gridblock in our matrix solution. We further enhance the efficiency of our model by solving the minimum number of equations required to accurately describe flow at each reservoir gridblock. Thus, we solve the full N_c equations for every gridblock where two phases coexist, or where mixing of a single phase with varying composition occurs; however, in gridblocks containing a single phase with fixed (known) composition, we solve only one mass conservation equation for gridblock pressure. This approach leads to smaller matrix problems (and therefore reduced execution times) in systems containing a large number of hydrocarbon components. The resulting formulation is extremely fast, robust and accurate. (Comparisons with an available conventional fully-implicit, compositional simulator indicate model execution times of up to five times faster than the conventional model on identical test problems.)

In the following, we summarize the contributions of this work in the areas of phase behavior modeling and compositional reservoir simulation.

6.1 PVT Package

The major contribution of the first part of this work is that it collects and synthesizes all information vital to writing a robust PVT package based on a generalized equation of state that degenerates to any of five widely used equations of state (Redlich-Kwong, Zudkevitch-Joffe-Redlich-Kwong, Soave-Redlich-Kwong and Schmidt-Wenzel). We have provided analytical expressions for evaluation of the partial derivatives used in Newton-Raphson iteration for phase behavior calculations for five equations of state. Procedures for determining saturation points (both upper and lower) at a given temperature have been delineated. Further, details on

a simple method (based on the successive substitution solution procedure) for determining whether the system temperature is above or below the mixture critical temperature (without actually determining the critical temperature) were provided. We have successfully applied the successive substitution procedure to all five equations of state discussed in this work. The Baker and Luks³³ approach to provide initial guesses for the MVNR scheme was successfully applied to subcritical and supercritical lower dew points using all five equations of state.

In summary, this first part facilitates the design and implementation of a robust commercial quality hydrocarbon PVT package.

6.2 Reservoir Model

In this work, we presented the difference equations for a new fully-implicit compositional reservoir simulator with PVT properties modeled using a generalized equation of state. Unlike conventional compositional simulators, our model does not employ Newton-Raphson iteration for the solution of the flow equations; rather it is based on a generalized Letkman-Ridings⁴³ linearization approach.

As in conventional simulators, the thermodynamic phase equilibrium constraint is imposed by equating fugacities of each component in each phase. The current model expands fugacities at the current time level as a first order Taylor's series about known values at the old time level (when the phases were at equilibrium). This allows us to explicitly incorporate the thermodynamic equilibrium equations into the discrete flow equations by elimination of $N_c - 1$ mole fraction compositions, which greatly enhances the speed and robustness of the model.

We carefully detailed the logic involved in modeling conditions at each gridblock based on using the minimum number of equations for accurate flow description. The number of equations solved at a particular gridblock varies between one equation, for a single-phase fluid with fixed (known) compositions, and N_c equations, for blocks containing two phases or a single-phase fluid with varying composition. Note that in the latter case, the thermodynamic equilibrium constraint is not applicable. This new approach results in a matrix problem where only the gridblock parameters

that are varying over a time step are being solved for. Note that binary systems constitute a special case, and we detailed procedures on their treatment.

We validated our model by matching simulation results with a published steady-state analytical solution. Further, during the transient period, we confirmed that all dependent variables (i.e., pressure, saturation and individual mole fraction compositions) are unique functions of the Boltzmann variable, r^2/t , in a homogeneous reservoir.

Comparison with an available fully-implicit simulator based on Coats⁷ procedure, showed that, for typical problems, a speedup in execution times of 500% may be obtained without any loss of accuracy.

We successfully applied the model to a wide variety of mixtures (ranging from binary systems to 17-component complex mixtures containing non-hydrocarbon components (N_2 and CO_2)). Simulation runs included primary depletion of retrograde gas condensate and volatile oil reservoirs, during which sequences of draw-down are interspersed by buildups to simulate isochronal tests. We also simulated dry gas injection for gas cycling of a retrograde gas condensate reservoir. Simulation of these processes serve as severe tests to the model robustness, since at any particular time it is possible for the reservoir to exhibit fluid behavior varying from black oil to retrograde gas condensate depending on the location in the reservoir.

While our simulator is one-dimensional, it appears to be clear that the underlying ideas (Letkman-Ridings⁴³ approach coupled and solved simultaneously with the thermodynamic equilibrium equations) should extend directly to multi-dimensional problems.

NOMENCLATURE

- a - Attraction parameter in the van der Waals EOS for pure compounds.
- a_c - Attraction parameter in the Redlich-Kwong EOS, Eq. 2.2.10.
- a_i - Attraction parameter of component i , Eq. 2.2.36.
- $a_{i,m}$ - Mixing parameter defined in Eq. C2.
- a_m - Attraction parameter in the generalized EOS for either phase (Liquid or Vapor).
- $a_{c,i}$ - Attraction parameter in the Redlich-Kwong EOS for component i , Eq. 2.2.34.
- \hat{a} - Matrix element, Eq. 4.4.6c.
- A - Cubic equation coefficient, Eq. 2.2.13;
Drainage area, Eq. 5.1.10.
- A_m - Cubic equation coefficient relative to either phase (Liquid or Vapor), Eq. 2.2.44.
- $\hat{A}_{m,j}$ - Matrix element of either phase (Liquid or Vapor), Eq. 4.4.26a.
- $\hat{A}_{o,j}$ - Matrix element of the oil phase, Eq. 4.4.26a.
- $\hat{A}_{g,j}$ - Matrix element of the gas phase, Eq. 4.4.26a.
- $A(t)$ - Amount of quantity at time t , Eq. 3.1.1.
- b - Repulsion parameter in the van der Waals EOS for pure compounds.
- b_i - Repulsion parameter of component i , Eq. 2.2.35.
- $b_{i,m}$ - Mixing parameter defined in Eq. C1.
- b_m - Repulsion parameter in the generalized EOS for either phase (Liquid or Vapor).
- \hat{b} - Vector element, Eq. 4.4.6a.

B	-	Cubic equation coefficient, Eq. 2.2.14
B_j	-	Equilibrium equation vector at gridblock j , Eq. 4.4.3.
B_m	-	Cubic equation coefficient relative to either phase (Liquid or Vapor), Eq. 2.2.45.
c_i	-	Initial fluid compressibility, $1/psia$.
\bar{c}	-	Average compressibility, $1/psia$.
\hat{c}	-	Vector element, Eq. 4.4.6b.
C	-	Concentration of a quantity, Eq. 3.1.1.
C_i	-	Concentration of component i , Eq. 3.1.10; Constant defined in Eq. 5.1.21.
\tilde{C}_i	-	Constant defined in Eq. 5.1.26.
C_1	-	Unit Conversion constant.
$D_{m,j+\frac{1}{2}}$	-	Derivative term of either phase (Liquid or Vapor), Eq. 4.4.10a.
$D_{o,j+\frac{1}{2}}$	-	Derivative term of the oil phase (Liquid or Vapor), Eq. 4.4.10a.
$D_{g,j+\frac{1}{2}}$	-	Derivative term of the gas phase (Liquid or Vapor), Eq. 4.4.10a.
$\hat{D}_{i,j+\frac{1}{2}}$	-	Derivative term of component i , Eq. 4.4.26b.
E	-	Error vector, Eq. 2.6.6
<i>factor</i>	-	Safety factor.
$f_{i,m}$	-	Fugacity of component i in either phase (Liquid or Vapor).
$f_{i,L}$	-	Fugacity of component i in the liquid phase.
$f_{i,V}$	-	Fugacity of component i in the vapor phase.
F	-	Flux through a surface.
F_i	-	Flux of component i .
F_m	-	Mass flux of either phase (Liquid or Vapor).
F_i	-	Ratio of both fugacities of component i .
G_p	-	Sum defined in Eq. 4.4.20a.
G_v	-	Sum defined in Eq. 4.4.20b.
h	-	Total reservoir thickness, <i>ft</i> .
J	-	Jacobian.
k	-	Parameter in the Schmidt and Wenzel EOS, Eq. 2.2.28a;

	-	Permeability, <i>md</i> .
k_j	-	Permeability at gridblock <i>j</i> .
k_{rm}	-	Relative permeability of either phase (Liquid or Vapor).
k_{ro}	-	Relative permeability of the oil phase.
k_{rg}	-	Relative permeability of the gas phase.
$k_{i,j}$	-	Binary interaction parameter.
k_s	-	Skin zone permeability, <i>md</i> .
K_i	-	<i>K</i> - value of component <i>i</i> .
K_l	-	Largest root of Eq. 2.5.3.
K_s	-	Smallest root of Eq. 2.5.3.
<i>L</i>	-	Number of moles of liquid per mole of fluid mixture.
$m(p)$	-	Real gas pseudopressure function, $psia^2/cp$.
m_D	-	Dimensionless pseudopressure function.
m_{wD}	-	Dimensionless wellbore pseudopressure drop.
M_i	-	Molecular weight of component <i>i</i> .
M_j	-	Equilibrium equation matrix, Eq. 4.4.3.
M_o	-	Mean molecular weight of the oil phase.
M_g	-	Mean molecular weight of the gas phase.
n_r	-	Radial component of the outer normal vector.
n_s	-	Number of skin blocks.
n_θ	-	Angular component of the outer normal vector.
n_z	-	Vertical component of the outer normal vector.
N_c	-	Number of components in a mixture.
N_{cI}	-	Number of components in a mixture of injected fluid.
$N_{i,m}$	-	Number of moles of component <i>i</i> in either phase (Liquid or Vapor).
N_r	-	Number of radial blocks.
<i>O</i>	-	Error order.
O_p	-	Sum defined in Eq. 4.4.19a.
O_y	-	Sum defined in Eq. 4.4.19b.
<i>p</i>	-	System pressure, <i>psia</i> .

\bar{p}	-	Average reservoir pressure.
p_b	-	Bubble point pressure, <i>psia</i> .
p_c	-	Critical pressure, <i>psia</i> .
$p_{c,i}$	-	Critical pressure of component <i>i</i> , <i>psia</i> .
p_{dew}	-	Dew point pressure, <i>psia</i> .
p_e	-	Outer boundary pressure, <i>psia</i> .
p_i	-	Initial reservoir pressure, <i>psia</i> .
p_r	-	Reduced pressure.
p_{vp}	-	Vapor pressure, <i>psia</i> .
$p_{vp,i}$	-	Vapor pressure of component <i>i</i> .
$p_{vp,r}$	-	Reduced vapor pressure.
p_{wf}	-	Flowing bottomhole pressure, <i>psia</i> .
P	-	Solution vector, Eqs. 4.3.12 and 4.6.1.
Q	-	Rate, units per unit time per unit volume; Set of unknowns, Eq. 4.2.1.
Q_j	-	Set of unknowns at gridblock <i>j</i> .
q_D	-	Dimensionless rate.
q_t	-	Total molar rate, <i>lbmoles/day</i> .
r	-	Radial distance, <i>ft</i> .
r_e	-	Reservoir radius, <i>ft</i> .
r_j	-	Radial distance of gridblock <i>j</i> .
r_s	-	Skin zone radius.
r_w	-	Wellbore radius, <i>ft</i> .
R	-	Universal gas constant.
R	-	Solution Vector in the MVNR method, Eq. 2.6.7; Right-hand side vector, Eqs. 4.3.11 and 4.6.1.
s	-	Skin factor.
S	-	Surface area.
S_m	-	Saturation of either phase (Liquid or Vapor).
S_g	-	Gas saturation.

S_o	-	Oil saturation.
t	-	Time, <i>days</i> .
t_{AD}	-	Dimensionless time based on drainage area.
\hat{t}_{AD}	-	Dimensionless time based on drainage area and average viscosity-compressibility product.
t_D	-	Dimensionless time.
T	-	System temperature, degree Rankine.
T_b	-	Boiling temperature, °R.
T_{br}	-	Reduced boiling temperature.
T_c	-	Critical temperature, degree Rankine.
$T_{c,i}$	-	Critical temperature of component i , degree Rankine.
T_r	-	Reduced temperature.
$T_{m,j+\frac{1}{2}}$	-	Transmissibility of either phase (liquid or Vapor) at gridblock j , Eq. 4.3.6a.
$T_{o,j+\frac{1}{2}}$	-	Transmissibility of the liquid phase at gridblock j , Eq. 4.3.6a.
$T_{m,j+\frac{1}{2}}$	-	Transmissibility of the gas phase at gridblock j , Eq. 4.3.6a.
$\tilde{T}_{m,j+\frac{1}{2}}$	-	Transmissibility of either phase (liquid or Vapor) at gridblock j , Eq. 4.3.10a.
$\tilde{T}_{o,j+\frac{1}{2}}$	-	Transmissibility of the oil phase at gridblock j , Eq. 4.3.10a.
$\tilde{T}_{g,j+\frac{1}{2}}$	-	Transmissibility of the gas phase at gridblock j , Eq. 4.3.10a.
$\hat{T}_{i,j+\frac{1}{2}}$	-	Transmissibility term of component i at gridblock j
$u_{i,m}$	-	Parameter used in differentiation, Eq. C3.
U	-	Parameter in the Schmidt-Wenzel EOS.
$U_{j+\frac{1}{2}}$	-	Finite difference constant, Eq. 4.1.13a.
v_m	-	Velocity of either phase (Liquid or Vapor), $RB/(ft^2 - day)$.

- v_o - Velocity of the liquid phase, $RB/(ft^2 - day)$.
- v_g - Velocity of the gas phase, $RB/(ft^2 - day)$.
- $v_{m,r}$ - Radial component of the velocity of either phase (Liquid or Vapor).
- $v_{m,\theta}$ - Angular component of the velocity of either phase (Liquid or Vapor).
- $v_{m,z}$ - Vertical component of the velocity of either phase (Liquid or Vapor).
- V - Volume, ft^3 .
- V_m - Volume in either phase (Liquid or Vapor), ft^3 .
- V_p - Total pore volume, ft^3 .
- $V_{p,j}$ - Pore volume of gridblock j , ft^3 .
- V^* - Ideal gas volume, ft^3 .
- V - Number of moles of vapor per mole of fluid mixture.
- V_c - Critical volume, ft^3 .
- $V_{c,i}$ - Critical volume of component i , ft^3 .
- $w_{i,m}$ - Parameter used in differentiation, Eq. C4.
- W - Parameter in the Schmidt-Wenzel EOS.
- x_i - Mole fraction composition of component i in the liquid phase.
- $x_{i,m}$ - Mole fraction composition of component i in either phase (Liquid or Vapor).
- X_j - Vector in the equilibrium equation, Eq. 4.4.3.
- y_i - Mole fraction composition of component i in the vapor phase.
- $y_{i,I}$ - Mole fraction composition of component i of the injected fluid.
- z_i - Overall mole fraction composition of component i .
- $z_{i,e}$ - Overall mole fraction composition of component i at the outer boundary.
- z' - Direction in which gravity acts.
- Z - Compressibility factor.
- Z_c - Critical Compressibility factor.

- Z_m - Compressibility factor of either phase (Liquid or Vapor).
 Z_i^* - Compressibility factor of component i saturated liquid at $p_{sat,i}$ and T .
 $Z_{i,L}$ - Compressibility factor of component i .
in the liquid phase.

Subscripts

- a - Relative to the parameter a .
 avg - Average value.
 b - Relative to the parameter b ;
At bubble point.
 c - Critical property.
 dew - At dew point.
 D - Dimensionless.
 e - External boundary.
 fix - Fixed value.
 g - Gas.
 i - Initial conditions;
Component number.
 I - Injection.
 j - Gridblock number.
 k - Component number.
 l - Component number.
 L - Liquid phase.
 m - Phase, liquid or vapor.
 max - Maximum value.
 min - Minimum value.
 mix - Mixture.
 ns - Relative to the skin blocks.
 o - Oil.
 p - Relative to pressure;

		Relative to pore volume.
r	-	Reduced property. Radial direction.
s	-	Skin zone.
sat	-	Saturation point.
sc	-	Standard conditions.
S_g	-	Relative to gas saturation.
t	-	Total; Time.
vp	-	At vapor point.
V	-	Vapor.
w	-	Wellbore.
wD	-	Wellbore dimensionless.
wf	-	Flowing at wellbore.
y	-	Relative to gas phase composition.
z	-	Relative to overall composition.

Superscripts

o	-	Property evaluated at the vapor pressure.
k	-	Iteration level.
n	-	Time level.
t	-	Transpose.
$*$	-	Ideal gas property. Equilibrium point.
-1		Inverse.

Greek notation

α	-	Equation of state parameter, Eq. 2.2.12; mesh expansion factor, Eq. 4.1.4.
α_i	-	Equation of state parameter of component i , Eq. 2.2.42.

β_c	-	Parameter in the Schmidt-Wenzel EOS, Eq. 2.2.30b.
δ_t	-	Time difference operator.
$\delta_{i,j}$	-	Kronecker delta.
Δ	-	Difference operator.
Δ_r	-	Difference operator in the r -direction.
Δ_t	-	Time difference operator.
ϵ	-	Error tolerance.
ϕ	-	Porosity.
γ_m	-	Specific weight of the fluid of either phase (Liquid or Vapor).
γ_o	-	Specific weight of the fluid of the liquid phase.
γ_g	-	Specific weight of the fluid of the gas phase.
Γ	-	Function defined in Eq. 2.5.3
$\lambda_{t,i}$	-	Total phase mobility of component i , Eq. 4.1.11b.
μ	-	Viscosity, cp .
$\bar{\mu}$	-	Average viscosity, cp .
μ_i	-	Initial viscosity, cp .
μ_m	-	Viscosity of either phase (Liquid or Vapor), cp .
μ_o	-	Oil phase viscosity, cp .
μ_g	-	Gas phase viscosity, cp .
μ_m^*	-	Low pressure viscosity of either phase (Liquid or Vapor), cp .
ω	-	Acentric factor.
ω_i	-	Acentric factor of component i .
ω_{mix}	-	Mixture acentric factor, Eq. 2.2.54.
Ω_a	-	van der Waals coefficient relative to a .
$\Omega_{a,i}$	-	van der Waals coefficient of component i relative to a .
Ω_b	-	van der Waals coefficient relative to b .
$\Omega_{b,i}$	-	van der Waals coefficient of component i relative to b .
ψ	-	Function used in EOS, Eq. 2.2.9.
$\psi_{i,m}$	-	Fugacity coefficient of component i in either phase (Liquid or Vapor).

- $\psi_{c,i}$ - Critical fugacity coefficient of component i , Eq. A5.
- $\psi_{i,L}$ - Fugacity coefficient of component i in the liquid phase.
- $\psi_{i,V}$ - Fugacity coefficient of component i in the vapor phase.
- ρ_m - Mass density of either phase (Liquid or Vapor), lbm/ft^3 .
- ρ_o - Mass density of the liquid phase, lbm/ft^3 .
- ρ_g - Density of the gas phase, lbm/ft^3 .
- ρ - Molar density, $lbmole/ft^3$.
- ρ_m - Molar density of either phase (Liquid or Vapor), $lbmoles/ft^3$.
- ρ_o - Oil phase molar density, $lbmoles/ft^3$.
- ρ_g - Gas phase molar density, $lbmoles/ft^3$.
- $\rho_{c,m}$ - Pseudocritical molar density of either phase (Liquid or Vapor), $lbmoles/ft^3$, Eq. 2.7.7.
- $\rho_{r,m}$ - Reduced molar density of either phase (Liquid or Vapor), $lbmoles/ft^3$, Eq. 2.7.5.
- τ_i - Parameter in the viscosity correlation, Eq. 2.7.1.
- ξ - Mixture parameter viscosity, Eq. 2.7.4.
- ξ_c - Parameter in the Schmidt-Wenzel EOS, Eq. 2.2.31.

REFERENCES

1. Fussell, L.T., and Fussell, D.D., "An Iterative Technique for Compositional Reservoir Models," SPEJ (Aug. 1979) 211-220.
2. Price, H.S. and Donohue, D.A.T.: "Isothermal Displacement With Interphase Mass Transfer," SPEJ, (June 1967) 205-320; Trans., AIME 240.
3. Roebuck, I.F. Jr., Henderson, G.E., Douglas, Jim Jr. and Ford, W.T.: "The Compositional Reservoir Simulator: Case I - The Linear Model," SPEJ (March 1969) 115-130; Trans., AIME, 246.
4. Culham, W.E., Farouq Ali, S.M. and Stahl, C.D.: "Experimental and Numerical Simulation of Two-Phase Flow With Interphase Mass Transfer in One and Two Dimensions," SPEJ (Sept. 1969) 323-337; Trans., AIME, 246.
5. Kniazeff, V.J. and Naville, S.A.: "Two-Phase Flow of Volatile Hydrocarbons," SPEJ (March 1965) 37-44; Trans., AIME, 234.
6. Nolen, J.S.: "Numerical Simulation of Compositional Phenomena in Petroleum Reservoirs," Reprint Series No 11 - Numerical Simulation, SPEJ, Dallas (1965) 269-284.
7. Coats, Keith H.: "An Equation of State Compositional Model," SPEJ (Oct. 1980) 363-376.
8. Nghiem, L.X., Fong, D.K. and Aziz K.: "Compositional Modeling With an Equation of State," SPEJ (Dec. 1981) 687-698.
9. Young, L.C. and Stephenson, R.E.: "A Generalized Compositional Approach for Reservoir Simulation," SPEJ (Oct. 1983) 727-742.

10. Thele, K.J., Lake L.W. and Sepehrnoori, K.: "A Comparison of Three Equation of State Compositional Simulators," paper SPE 12245 presented at the 1983 Reservoir Simulation Symposium, San Francisco, Nov. 15-18.
11. Acs, G., Doleschall, S. and Farkas E.: "General Purpose Compositional Model," SPEJ (Aug. 1985) 543-553.
12. Watts, J.W.: "A Compositional Formulation of the Pressure and Saturation Equations," SPERE (1986) 1, No 3, 243-252.
13. Spillette, A.G., Hillstad, J.G. and Stone, H.L.: "A High-Stability Sequential Solution Approach to Reservoir Simulation," paper SPE 4542 presented at the 48th Annual Fall Meeting of the Society of Petroleum Engineering of AIME, Las Vegas, NV, Sept. 30 - Oct. 3, 1973.
14. Chien, M.C.H., Lee, S.T. and Chen, W.H.: "A New Fully Implicit Compositional Simulator," paper SPE 13385 presented at the 8th SPE Symposium on Reservoir Simulation of the Society of Petroleum Engineers, Dallas, Tx, Feb. 1-4, 1987.
15. Collins, D.A., Nghiem, L.X. and Li, Y.K.: "An Efficient Approach to Adaptive-Implicit Compositional Simulation With an Equation of State," paper SPE 15133 presented at the 56th Annual California Regional Meeting of the Society of Petroleum Engineers, Oakland, CA, April 2-4, 1986.
16. Zudkevitch, D. and Joffe, J.: "Correlation and Prediction of Vapor-Liquid Equilibria with the Redlich-Kwong Equation of State," AIChE Journal (Jan. 1970) 112-119.
17. Peng, Ding-Yu and Robinson, D.B.: "A New Two-Constant Equation of State," *Ind. Eng. Chem. Fund.* (1976) 59-64.
18. Mansoori, J.: "Discussion of Compositional Modeling With an Equation of State," SPEJ (March 1982), 22, No 2, 202-203
19. Nghiem, L.X.: "Author's Reply to Discussion of Compositional Modeling With an Equation of State," SPEJ (March 1982) 22, No 2, 204

20. Redlich, O. and Kwong, J.N.S.: "On the Thermodynamics of Solutions. V — An Equation of State. Fugacities of Gaseous Solutions," *Chemical Reviews*, Vol. 44, 52–63.
21. Soave, G.: "Equilibrium Constants from a Modified Redlich–Kwong Equation of State," *Chemical Engineering Science*, 1972, Vol. 27, 1197–1203.
22. Schmidt, G. and Wenzel, H.: "A Modified Van Der Waals Type Equation of State," *Chem. Eng. Science*, Vol. 35, 1503–1512.
23. Nghiem, L.X., Aziz, K. and Li, Y.K.: "A Robust Iterative Method for Flash Calculations Using the Soave–Redlich–Kwong or the Peng–Robinson Equation of State," *SPEJ* (June 1983) 521–530.
24. Fussell, D.D. and Yanosik, J.L.: "An Iterative Sequence for Phase–Equilibria Calculations Incorporating the Redlich–Kwong Equation of State," *SPEJ* (June 1978) 173–182.
25. Lohrenz, J., Bray, B.G. and Clark, C.R.: "Calculating Viscosities of Reservoir Fluids From Their Compositions," *JPT* (Oct. 1964) 1171–1176.
26. Jossi, J.A., Stiel, L.I. and Thodos, G.: "The Viscosity of Pure Substances in the Dense Gaseous and Liquid Phases," *AIChE Journal* (March 1962), Vol. 8, No. 1, 59–62.
27. Herning, F. and Zipperer, L. : " Calculation of the Viscosity of Technical Gas Mixtures from the Viscosity of Individual Gases," *Gas u. Wasserfach*, (1936) 79, No. 39, 69.
28. Stiel, L. I. and Thodos, George,: " The Viscosity of Nonpolar Gases at Normal Pressure," *AICHE J.*, (1962) 8, 59.
29. Walas, S.: *Phase Equilibria in Chemical Engineering*, Butterworth (ed.), Butterworth Publishers (1985).
30. Modell, M. and Reid, R.: *Thermodynamics and its applications*, Prentice Hall (2ed.), Prentice Hall, Inc. (1983).
31. Yarborough, L., : "Applications of a Generalized Equation of State to Petroleum Reservoir Fluids."in: *Equations of State in Engineering, Advances in*

- Chemistry Series*, 182, K. C. Chao and Robert L. Robison, ed., American Chemical Society, Washington, DC, (1979), 385-435.
32. Reid, R.C., Prausnitz, J.M. and Sherwood, T.K.: *The Properties of Gases and Liquids*, 3rd Edition Mc-Graw Hill 1977, New -York.
 33. Baker, Lee E. and Luks, K. D., :“ Critical Point and Saturation Pressure Calculations for Multipoint systems,” SPEJ (Dec. 1980) 15-24.
 34. Firoozabadi, Abbas : Reservoir - Fluid Phase Behavior and Volumetric Prediction With Equation of State., JPT (April 1988) 397-406.
 35. Abramowitz, M. and Stegun, I.: *Handbook Of Mathematical Functions*, Dover (ed.), Dover Publications, Inc., New - York (1970)
 36. Hong,C.:“Lumped-Component Characterization of Crude Oils for Compositional Simulation,” SPE DOE 10691 241-245
 37. Powell, M. J. D.:“A Hybrid Method for Nonlinear Equations,” *Numerical Methods for Nonlinear Algebraic Equations*, T. Rabinowitz (ed.), Gordon and Breach, London (1970).
 38. Powell, M. J. D.:“A Fortran Subroutine for Solving Systems of Nonlinear Algebraic Equations,” *Numerical Methods for Nonlinear Algebraic Equations*, T. Rabinowitz (ed.), Gordon and Breach, London (1970).
 39. Leverett, M.C. and Lewis, W.B.: “Steady Flow of Gas-Oil-Water Mixtures through Unconsolidated Sands,” (1941) Trans., AIME.
 40. Hawkins, M.F., Jr., “A Note on the skin Effect,” 356-357, Trans. AIME 207.
 41. Coats, K.H., “Geothermal Reservoir Modeling,” paper SPE 6892 presented at the 52nd Annual Technical Conference and Exhibition of the SPE of AIME, Denver, Colorado, Oct. 9-12, 1977.
 42. Aziz, K. and Settari, A., Petroleum Reservoir Simulation, Applied Science Publishers, Ltd., 1979, London.
 43. Letkman J.P. and Ridings, R.L.:“A Numerical Coning Model,” SPEJ (Dec. 1970) 418-424
 44. O'Dell, H.G. and Miller, R.N., “Successfully Cycling a Low Permeability, High Yield Gas Condensate Reservoir,” JPT (Jan. 1967) 41-44.

45. Jones J.R., *Computation and Analysis of Single Well Responses for Gas Condensate Systems*, Ph.D Dissertation, The University of Tulsa, 1985.
46. Wattenbarger, R. and Ramey, H. J., Jr.: "Gas Well Testing With Turbulence, Damage and Wellbore Storage", JPT (Aug. 1968) 877-887.
47. Bratvold, R. B.: *A Simulation Study of Gas Wells Under Radial Flow Conditions*, M.S. Thesis, University of Tulsa, Tulsa, OK (1986)
48. Al-Hussainy, R., Ramey, H. J., and Crawford, P. B.: "The Flow of Real Gases Through Porous Media", JPT (May 1966) 624-636.
49. Ding, W.: *Well Testing in Gas Reservoirs*, M.S Thesis, University of Tulsa, Tulsa, OK (1986).
50. Reynolds, A. C., Bratvold, R. B., and Ding, W.: "Semilog Analysis of Gas Well Drawdown and Buildup Data", SPEFE (Dec. 1987) 657-670.
51. Reamer, H.H., Sage, B.H., and Lacey, W.N.: "Phase Equilibria in Hydrocarbon Systems," *Ind. and Eng. Chem.* (June 1951), Vol. 43, No 46, 1436-1444.
52. Firoozabadi, A., Nutakki, R., Wong, T.W. and Aziz, K.: "EOS Predictions of Compressibility and Phase Behavior in Systems Containing Water, Hydrocarbons, and CO₂," SPE Reservoir Engineering, May 1988, 673-684.
53. Katz, D.L. and Firoozabadi, A.: "Predicting Phase Behavior of Condensate and Crude Oil Systems Using Methane Interaction Coefficients," JPT (Nov. 1978), Vol. 30, 1649-1655.
54. Kesler, M.G. and Lee, B.I.: "Improved Predictions of Enthalpy Fractions, " Hydrocarbon Processing (March 1976) 153-158.
55. Raghavan, R.: "Well Test Analysis: Wells producing by Solution Gas Drive," SPEJ (Aug. 1976) 196-208.
56. Bøe, A., Skjæveland, S.M., and Whitson, C.H.: "Two Phase Pressure Test Analysis," paper SPE 10224 presented at the 1981 SPE Annual Technical Conference and Exhibition, San Antonio, Oct. 5-7.
57. Serra, K., Peres, A. and Reynolds, A.C.: "Well Test Analysis for Solution-Gas-Drive Reservoirs: Part I; Determination of Relative and Absolute Permeabilities", paper SPE 17020, to appear SPEFE (June 1990)

58. Thompson L.G. and Vo D.T.: "Drawdown Well Test Analysis for Multicomponent Hydrocarbon Systems". presented at the 1988 SPE Annual Technical Conference and Exhibition, Houston, Oct. 2-5.
59. Coats, K.H.: "Reservoir Simulation: A general Model Formulation and Associated Physical/Numerical Sources of Instability," *Boundary and Interior Layers, Computational and Asymptotic Methods*, J.J.H. Miller (ed.), Boole Press, Dublin (1980).
60. Vo, D.T., Jones, J.R., and Raghavan, R., " Performance Predictions for Gas Condensate Reservoirs," paper SPE 16984 presented at the 1987 SPE annual Technical Conference and Exhibition, Dallas, Sept. 27 - 30.

APPENDIX A

REIDEL'S VAPOR PRESSURE EQUATION

Reidel's equation for computing the vapor pressure is given by

$$p_{vp} = \exp \left(A - \frac{B}{T_r} + C \log T_r + DT_r^6 \right), \quad (A1)$$

where p_c is in atmospheres, all temperatures are in $^{\circ}R$, and,

$$T_{br} = \frac{T_b}{T_c}, \quad (A2)$$

$$T_r = \frac{T}{T_c}, \quad (A3)$$

$$\psi_b = -35 + \left(\frac{36}{T_{br}} \right) + 42 \log(T_{br}) - T_{br}^6, \quad (A4)$$

$$\alpha = \frac{(315\psi_b) + \log(p_c)}{(.0838\psi_b) - \log(T_{br})}, \quad (A5)$$

$$Q = .0838(3.758 - \alpha), \quad (A6)$$

$$A = -35Q, \quad (A7)$$

$$B = -36Q, \quad (A8)$$

$$C = 42Q + \alpha, \quad (A9)$$

and

$$D = -Q, \quad (A10)$$

where T_b denotes the boiling temperature.

APPENDIX B

COATS' METHOD FOR Ω_a AND Ω_b (ZJRK EOS)

We present the method reported by Coats⁷ to evaluate the van der Waals coefficients relative to the ZJRK EOS.

The coefficients are evaluated for each individual component depending on whether the system temperature is above or below the critical temperature of the particular component.

Case (1) $T < T_{c,i}$

The two equations

$$f_{i,L} = f_{i,V} \quad (B1)$$

and

$$Z_{i,L} = Z_i^* \quad (B2)$$

are solved for $\Omega_{a,i}$ and $\Omega_{b,i}$ using the Newton-Raphson method for each component. Here, Z_i^* is the compressibility factor of the saturated liquid of component i at pure component saturation pressure and system temperature. Coats recommends the use of Reidel's vapor pressure equation to obtain the saturation pressure and Gunn and Yamada's method to evaluate liquid densities, and thus the Z_i^* 's.

Case (2) $T = T_{c,i}$

$\Omega_{a,i}$ and $\Omega_{b,i}$ are determined from the two following equations

$$\psi_{i,L} = \psi_{c,i} \quad (B3)$$

and

$$Z_{i,L} = Z_{c,i}, \quad (B4)$$

where $\psi_{i,L} = f_{i,L}/p$ is the fugacity coefficient evaluated from the pure component i ZJRK EOS, and $Z_{i,L}$ is the liquid compressibility factor obtained from the corresponding cubic equation. Here, $Z_{c,i}$ is the component i critical deviation factor which is tabulated, and $\psi_{c,i}$ is the critical fugacity coefficient determined by

$$\log \psi_{c,i} = -0.1754 - 0.0361\omega_i. \quad (B5)$$

Again, we use Newton-Raphson method to solve both equations above.

Case (3) $T > T_{c,i}$

We use the values $\Omega_{a,i}$ and $\Omega_{b,i}$, obtained from case (2), as suggested by Zudkevitch and Joffe.

APPENDIX C

EVALUATION OF PARTIAL DERIVATIVES

We present the derivatives of the partial fugacities with respect to the various variables for each iteration. We will perform the differentiation on the generalized fugacity equation that apply to all five equations of state with the appropriate parameters.

First we define the following:

$$b_{i,m} = \frac{b_i}{b_m} = \frac{1}{B_m} \frac{\Omega_{b,i} p T_{c,i}}{T p_{c,i}}, \quad (C1)$$

$$a_{i,m} = \frac{1}{A_m} \sum_{l=1}^{N_c} x_{l,m} \left[(1 - k_{i,l}) \sqrt{\frac{\Omega_{a,i} \Omega_{a,l} \alpha_i \alpha_l (T_{c,i} T_{c,l})^n}{(p_{c,i} p_{c,l}) T^n}} p \right], \quad (C2)$$

$$u_{i,m} = \frac{A_m}{B_m \sqrt{U^2 - 4W}} \left(b_{i,m} - a_{i,m} + 3 \frac{U + 2}{U^2 - 4W} \frac{b_i^{0.7}}{\sum_{k=1}^{N_c} x_{k,m} b_k^{0.7}} (\omega_i - \omega) \right) \quad (C3)$$

and

$$w_{i,m} = \left[\left(1 - \frac{1}{Z_m - B_m} \right) \frac{3(\omega_i - \omega)}{U^2 - 4W} \frac{b_i^{0.7}}{\sum_{k=1}^{N_c} x_{k,m} b_k^{0.7}} \right] \times (2Z_m + UZ_m + 2WB_m + UB_m), \quad (C4)$$

where $m = \text{Liquid or Vapor}$

$p - x$ or $p - y$ iteration

We will develop the derivative of the partial fugacity with respect to pressure for component i in phase m .

$$\begin{aligned} \frac{\partial f_{i,m}}{\partial p} &= \frac{f_{i,m}}{p} + f_{i,m} \frac{\partial}{\partial p} [b_{i,m} (Z_m - 1)] - \frac{f_{i,m}}{Z_m - B_m} \frac{\partial}{\partial p} (Z_m - B_m) \\ &+ f_{i,m} \frac{\partial}{\partial p} \left[u_{i,m} \ln \left(\frac{2Z_m + UB_m + B_m \sqrt{U^2 - 4W}}{2Z_m + UB_m - B_m \sqrt{U^2 - 4W}} \right) \right] \\ &+ f_{i,m} \frac{\partial w_{i,m}}{\partial p} \end{aligned} \quad (C5)$$

$$\frac{\partial}{\partial p} [b_{i,m} (Z_m - 1)] = b_{i,m} \frac{\partial Z_m}{\partial p} \quad (C6)$$

$$\frac{\partial Z_m}{\partial p} = \frac{\partial Z_m}{\partial A_m} \frac{\partial A_m}{\partial p} + \frac{\partial Z_m}{\partial B_m} \frac{\partial B_m}{\partial p} \quad (C7)$$

Differentiating the cubic equation with respect to A_m and B_m , we get

$$\frac{\partial Z_m}{\partial A_m} = \frac{(B_m - Z_m)}{3Z_m^2 - 2(B_m + 1 - UB_m)Z_m + (WB_m^2 - UB_m^2 - UB_m + A_m)} \quad (C8)$$

$$\frac{\partial Z_m}{\partial B_m} = \frac{Z_m^2(1 - U) - (2WB_m - 2UB_m - U) + (3WB_m^2 + 2WB_m + A_m)}{3Z_m^2 - 2(B_m + 1 - UB_m)Z_m + (WB_m^2 - UB_m^2 - UB_m + A_m)} \quad (C9)$$

Note that U and W are functions of composition and not of pressure so that they are not affected by this differentiation process.

$$\begin{aligned} \frac{\partial}{\partial p} \left[u_{i,m} \ln \left(\frac{2Z_m + UB_m + B_m \sqrt{U^2 - 4W}}{2Z_m + UB_m - B_m \sqrt{U^2 - 4W}} \right) \right] &= \\ &u_{i,m} \frac{\partial}{\partial p} \left[\ln \left(\frac{2Z_m + UB_m + B_m \sqrt{U^2 - 4W}}{2Z_m + UB_m - B_m \sqrt{U^2 - 4W}} \right) \right] \\ &+ \ln \left(\frac{2Z_m + UB_m + B_m \sqrt{U^2 - 4W}}{2Z_m + UB_m - B_m \sqrt{U^2 - 4W}} \right) \frac{\partial u_{i,m}}{\partial p} \end{aligned} \quad (C10)$$

$$\begin{aligned} \frac{\partial}{\partial p} \left[\ln \left(\frac{2Z_m + UB_m + B_m \sqrt{U^2 - 4W}}{2Z_m + UB_m - B_m \sqrt{U^2 - 4W}} \right) \right] &= \frac{2 \frac{\partial Z_m}{\partial p} + \frac{\partial B_m}{\partial p} (U + \sqrt{U^2 - 4W})}{2Z_m + UB_m + B_m \sqrt{U^2 - 4W}} \\ &- \frac{2 \frac{\partial Z_m}{\partial p} + \frac{\partial B_m}{\partial p} (U - \sqrt{U^2 - 4W})}{2Z_m + UB_m - B_m \sqrt{U^2 - 4W}} \end{aligned} \quad (C11)$$

$$\frac{\partial u_{i,m}}{\partial p} = u_{i,m} \frac{B_m}{A_m} \frac{\partial \left(\frac{A_m}{B_m} \right)}{\partial p} \quad (C12)$$

$$\frac{\partial \left(\frac{A_m}{B_m} \right)}{\partial p} = \frac{1}{B_m} \frac{\partial A_m}{\partial p} - \frac{A_m}{B_m^2} \frac{\partial B_m}{\partial p} \quad (C13)$$

$$\frac{\partial A_m}{\partial p} = \frac{A_m}{p} \quad (C14)$$

$$\frac{\partial B_m}{\partial p} = \frac{B_m}{p} \quad (C15)$$

Note that the following equations would be needed only for the SW EOS since $\omega_i - \omega = 0$ for the other cases.

$$\begin{aligned} \frac{\partial w_{i,m}}{\partial p} = & \frac{1}{(Z_m - B_m)^2} \frac{\partial}{\partial p} (Z_m - B_m) \left[\frac{3(\omega_i - \omega)}{U^2 - 4W} \frac{b_i^{0.7}}{\sum_{k=1}^{N_c} x_{k,m} b_k^{0.7}} \right] \\ & \times (2Z_m + UZ_m + 2WB_m + UB_m) \\ & - \left[\left(1 - \frac{1}{Z_m - B_m} \right) \frac{3(\omega_i - \omega)}{U^2 - 4W} \frac{b_i^{0.7}}{\sum_{k=1}^{N_c} x_{k,m} b_k^{0.7}} \right] \\ & \times \left[(U + 2) \frac{\partial Z_m}{\partial p} + (2W + U) \frac{\partial B_m}{\partial p} \right] \quad (C16) \end{aligned}$$

All the equations derived above define the variation of the partial fugacity of both phases with respect to pressure, which appears in the Jacobian matrices of both the $p-x$ and the $p-y$ iterations. The partial derivative of the partial fugacity of vapor with respect to the gas mole fraction composition which appears in the $p-x$ iteration Jacobian is the same as the one developed below for the $L-x$ iteration.

L - x iteration

$$\frac{\partial f_{i,v}}{\partial y_j} = \frac{f_{i,v}}{y_j} \delta_{i,j} + f_{i,v} \frac{\partial}{\partial y_j} [b_{i,v} (Z_V - 1)] - \frac{f_{i,v}}{Z_V - B_V} \frac{\partial}{\partial y_j} (Z_V - B_V)$$

$$\begin{aligned}
& + f_{i,v} \frac{\partial}{\partial y_j} \left[u_{i,v} \ln \left(\frac{2Z_V + UB_V + B_V \sqrt{U^2 - 4W}}{2Z_V + UB_V - B_V \sqrt{U^2 - 4W}} \right) \right] \\
& + f_{i,v} \frac{\partial w_{i,v}}{\partial y_j}
\end{aligned} \tag{C17}$$

$$\frac{\partial}{\partial y_j} [b_{i,v} (Z_V - 1)] = -(Z_V - 1) b_{i,v} b_{j,v} + b_{i,v} \frac{\partial Z_V}{\partial y_j} \tag{C18}$$

where

$$\frac{\partial b_{i,v}}{\partial y_j} = -b_{i,v} b_{j,v} \tag{C19}$$

Here Z_V is a function of A_V , B_V , U and W , which in turn are all functions of the composition. Thus

$$\frac{\partial Z_V}{\partial y_j} = \frac{\partial Z_V}{\partial A_V} \frac{\partial A_V}{\partial y_j} + \frac{\partial Z_V}{\partial B_V} \frac{\partial B_V}{\partial y_j} + \frac{\partial Z_V}{\partial U} \frac{\partial U}{\partial y_j} + \frac{\partial Z_V}{\partial W} \frac{\partial W}{\partial y_j} \tag{C20}$$

$\frac{\partial Z_V}{\partial A_V}$ and $\frac{\partial Z_V}{\partial B_V}$ are given by Eqs. C8 and C9 respectively.

$$\frac{\partial B_V}{\partial y_j} = \frac{\Omega_{b,j} p T_{c,j}}{T p_{c,j}} \tag{C21}$$

$$\frac{\partial A_V}{\partial y_j} = 2 \sum_{l=1}^{N_c} y_l \left[(1 - k_{j,l}) \sqrt{\frac{\Omega_{a,j} \Omega_{a,l} \alpha_j \alpha_l (T_{c,j} T_{c,l})^n}{(p_{c,j} p_{c,l}) T^n}} p \right] \tag{C22}$$

Now, the following expressions are only needed for the SW EOS. They are obtained from the cubic equation

$$\frac{\partial Z_V}{\partial U} = \frac{-B_V Z_V^2 + (2B_V^2 + B_V) Z_V - (B_V^3 + B_V^2)}{3Z_V^2 - 2(B_V + 1 - UB_V) Z_V + (WB_V^2 - UB_V^2 - UB_V + A_V)} \tag{C23}$$

Since $U + W = 1$ (combination of Eqs. 2.2.26 and 2.2.27), then

$$\frac{\partial Z_V}{\partial W} = -\frac{\partial Z_V}{\partial U} \tag{C24}$$

Recalling that $U = 1 + 3\omega$, and that

$$\omega_{mix} = \frac{\sum_{i=1}^{N_c} \omega_i x_{i,m} b_i^{0.7}}{\sum_{i=1}^{N_c} x_{i,m} b_i^{0.7}}$$

Then

$$\frac{\partial U}{\partial y_j} = 3 \left[\frac{b_j^{0.7} \left(\omega_j \sum_{i=1}^{N_c} y_i b_i^{0.7} - \sum_{i=1}^{N_c} \omega_i y_i b_i^{0.7} \right)}{\left(\sum_{i=1}^{N_c} y_i b_i^{0.7} \right)^2} \right] \quad (C25)$$

Again, we have

$$\frac{\partial W}{\partial y_j} = -\frac{\partial U}{\partial y_j} \quad (C26)$$

$$\begin{aligned} \frac{\partial}{\partial y_j} \left[u_{i,m} \ln \left(\frac{2Z_V + UB_V + B_V \sqrt{U^2 - 4W}}{2Z_V + UB_V - B_V \sqrt{U^2 - 4W}} \right) \right] = \\ u_{i,m} \frac{\partial}{\partial y_j} \left[\ln \left(\frac{2Z_V + UB_V + B_V \sqrt{U^2 - 4W}}{2Z_V + UB_V - B_V \sqrt{U^2 - 4W}} \right) \right] \\ + \ln \left(\frac{2Z_V + UB_V + B_V \sqrt{U^2 - 4W}}{2Z_V + UB_V - B_V \sqrt{U^2 - 4W}} \right) \frac{\partial u_{i,m}}{\partial y_j} \quad (C27) \end{aligned}$$

$$\begin{aligned} \frac{\partial}{\partial y_j} \left[\ln \left(\frac{2Z_V + UB_V + B_V \sqrt{U^2 - 4W}}{2Z_V + UB_V - B_V \sqrt{U^2 - 4W}} \right) \right] = \\ \frac{2 \frac{\partial Z_V}{\partial y_j} + (U + \sqrt{U^2 - 4W}) \frac{\partial B_V}{\partial y_j} + B_V \left[\frac{\partial U}{\partial y_j} + \frac{U \frac{\partial U}{\partial y_j} - 2 \frac{\partial W}{\partial y_j}}{\sqrt{U^2 - 4W}} \right]}{2Z_V + UB_V + B_V \sqrt{U^2 - 4W}} \\ - \frac{2 \frac{\partial Z_V}{\partial y_j} + (U + \sqrt{U^2 - 4W}) \frac{\partial B_V}{\partial y_j} + B_V \left[\frac{\partial U}{\partial y_j} - \frac{U \frac{\partial U}{\partial y_j} - 2 \frac{\partial W}{\partial y_j}}{\sqrt{U^2 - 4W}} \right]}{2Z_V + UB_V - B_V \sqrt{U^2 - 4W}} \quad (C28) \end{aligned}$$

Finally, To evaluate $\frac{\partial u_{i,v}}{\partial y_j}$ and $\frac{\partial w_{i,v}}{\partial y_j}$, we will need to apply the product rule to the derivatives of the parameters developed and to the following,

$$\frac{\partial a_{i,v}}{\partial y_j} = -\frac{a_{i,v}}{A_V} \frac{\partial A_V}{\partial y_j} + \frac{1}{A_V} \left[(1 - k_{i,j}) \sqrt{\frac{\Omega_{a,i} \Omega_{a,j} \alpha_i \alpha_j (T_{c,i} T_{c,j})^n}{(p_{c,i} p_{c,j}) T^n}} \right] \quad (C29)$$

All these expressions allow us to find $\frac{\partial f_{i,V}}{\partial y_j}$ for the L-x and the p-y iterations. now we will evaluate $\frac{\partial f_{i,L}}{\partial x_j}$ needed for the L-x and the p-x iterations. We remind the reader that here the x_j is one of the iteration variables and thus the differentiation is slightly different.

$$\begin{aligned} \frac{\partial f_{i,L}}{\partial x_i} = & \frac{f_{i,L}}{x_j} \left\{ \begin{array}{ll} -1, & \text{if } i = 1 \\ \delta_{i,j}, & \text{if } i \neq 1 \end{array} \right\} + f_{i,L} \frac{\partial}{\partial x_j} [b_{i,L} (Z_V - 1)] - \frac{f_{i,L}}{Z_V - B_V} \frac{\partial}{\partial x_j} (Z_V - B_V) \\ & + f_{i,L} \frac{\partial}{\partial x_j} \left[u_{i,L} \ln \left(\frac{2Z_V + UB_V + B_V \sqrt{U^2 - 4W}}{2Z_V + UB_V - B_V \sqrt{U^2 - 4W}} \right) \right] \\ & + f_{i,L} \frac{\partial w_{i,L}}{\partial x_j} \end{aligned} \quad (C30)$$

The differentiation process of the equation above is exactly the same as for $\frac{\partial f_{i,V}}{\partial y_j}$ except for the following modifications due to the fact that x_j is an iteration variable:

$$\frac{\partial b_{i,V}}{\partial y_j} = b_{i,V} b_{1,V} - b_{i,V} b_{j,V} \quad (C31)$$

The deviation factors derivatives are the same as those evaluated above. $\frac{\partial B_V}{\partial x_j}$, $\frac{\partial A_V}{\partial x_j}$, $\frac{\partial U}{\partial x_j}$ and $\frac{\partial a_{i,L}}{\partial x_j}$ are modified as

$$\frac{\partial B_L}{\partial x_j} = \frac{\Omega_{b,j} p T_{c,j}}{T_{p,c,j}} - \frac{\Omega_{b,1} p T_{c,j}}{T_{p,c,j}} \quad (C32)$$

$$\begin{aligned} \frac{\partial A_L}{\partial x_j} = & 2 \sum_{l=1}^{N_c} x_l \left[(1 - k_{j,l}) \sqrt{\frac{\Omega_{a,j} \Omega_{a,l} \alpha_j \alpha_l (T_{c,j} T_{c,l})^n}{(p_{c,j} p_{c,l}) T^n}} p \right] \\ & - 2 \sum_{l=1}^{N_c} x_l \left[(1 - k_{1,l}) \sqrt{\frac{\Omega_{a,1} \Omega_{a,l} \alpha_1 \alpha_l (T_{c,1} T_{c,l})^n}{(p_{c,1} p_{c,l}) T^n}} p \right] \end{aligned} \quad (C33)$$

$$\frac{\partial U}{\partial x_j} = 3 \left[\frac{(\omega_j b_j^{0.7} - \omega_1 b_1^{0.7}) \sum_{i=1}^{N_c} x_i b_i^{0.7} - (b_j^{0.7} - b_1^{0.7}) \sum_{i=1}^{N_c} \omega_i x_i b_i^{0.7}}{\left(\sum_{i=1}^{N_c} x_i b_i^{0.7} \right)^2} \right] \quad (C34)$$

$$\begin{aligned}
\frac{\partial a_{i,L}}{\partial x_j} = & \frac{1}{A_L} \left[(1 - k_{i,j}) \sqrt{\frac{\Omega_{a,i} \Omega_{a,j} \alpha_i \alpha_j (T_{c,i} T_{c,j})^n}{(p_{c,i} p_{c,j}) T^n}} p \right] \\
& - \frac{1}{A_L} \left[(1 - k_{1,j}) \sqrt{\frac{\Omega_{a,1} \Omega_{a,j} \alpha_1 \alpha_j (T_{c,1} T_{c,j})^n}{(p_{c,1} p_{c,j}) T^n}} p \right] \\
& - \frac{a_{i,L}}{A_L} \frac{\partial A_L}{\partial x_j}
\end{aligned} \tag{C35}$$

All these expressions do apply to the $V - y$ iteration, provided we replace V by L , x_j by y_j and vice-versa.

APPENDIX D

PHASE DENSITY AND DENSITY DERIVATIVES

Liquid and Vapor phase densities in $lbmoles/ft^3$ are calculated from the engineering equation of state

$$\rho_m = \frac{p}{Z_m RT}, \quad m = L, V, \quad (D1)$$

where p is the system pressure, T the system temperature, R the universal gas constant and Z_m represents the phase deviation factor, solution of the cubic equation, with the coefficients calculated using the mole fraction composition of the phase.

Derivatives of phase densities are calculated analytically from the engineering equation of state. Thus, for phase m , we have

$$\frac{\partial \rho_m}{\partial p} = \frac{1}{Z_m RT} \left(1 - \frac{p}{Z_m} \frac{\partial Z_m}{\partial p} \right), \quad (D2)$$

with

$$\frac{\partial Z_m}{\partial p} = \frac{\partial Z_m}{\partial A_m} \frac{\partial A_m}{\partial p} + \frac{\partial Z_m}{\partial B_m} \frac{\partial B_m}{\partial p}, \quad (D3)$$

where expressions for all the derivatives on the right-hand side of Eq. D3 for a generalized equation of state are presented in Appendix C. Similarly,

$$\frac{\partial \rho_m}{\partial x_{i,m}} = -\frac{p}{Z_m^2 RT} \frac{\partial Z_m}{\partial x_{i,m}}, \quad 2 \leq i \leq N_c, \quad (D4)$$

with

$$\frac{\partial Z_m}{\partial x_{i,m}} = \frac{\partial Z_m}{\partial A_m} \frac{\partial A_m}{\partial x_{i,m}} + \frac{\partial Z_m}{\partial B_m} \frac{\partial B_m}{\partial x_{i,m}}, \quad 2 \leq i \leq N_c, \quad (D5)$$

where again all needed derivatives are presented in Appendix C.

APPENDIX E

EXAMPLE RUN

Reservoir Extent Radius, r_e	(<i>ft</i>)	100.0
Absolute Reservoir Permeability, k	(<i>md</i>)	5.0
Porosity, ϕ	(-)	0.20
Formation Thickness, h	(<i>ft</i>)	40.0
Wellbore Radius, r_w	(<i>ft</i>)	0.25
Initial Reservoir Pressure, p_i	(<i>psia</i>)	3150
Injection Pressure, p_e	(<i>psia</i>)	3150
Production Rate, q	(<i>lbmoles/day</i>)	10000
Initial Composition,		Mix 2
Injection Composition,		Mix 2

3.11082E+03	1.00000E+00	0.00000E+00	8.39424E-01	8.39424E-01
3.12596E+03	1.00000E+00	0.00000E+00	8.39423E-01	8.39423E-01
3.13758E+03	1.00000E+00	0.00000E+00	8.39422E-01	8.39422E-01
3.14497E+03	1.00000E+00	0.00000E+00	8.39421E-01	8.39421E-01
3.14854E+03	1.00000E+00	0.00000E+00	8.39420E-01	8.39420E-01
3.14972E+03	1.00000E+00	0.00000E+00	8.39420E-01	8.39420E-01
3.14997E+03	1.00000E+00	0.00000E+00	8.39420E-01	8.39420E-01
3.15000E+03	1.00000E+00	0.00000E+00	8.39420E-01	8.39420E-01
3.15000E+03	1.00000E+00	0.00000E+00	8.39420E-01	8.39420E-01
3.15000E+03	1.00000E+00	0.00000E+00	8.39420E-01	8.39420E-01
3.15000E+03	1.00000E+00	0.00000E+00	8.39420E-01	8.39420E-01
3.15000E+03	1.00000E+00	0.00000E+00	8.39420E-01	8.39420E-01
3.15000E+03	1.00000E+00	0.00000E+00	8.39420E-01	8.39420E-01
3.15000E+03	1.00000E+00	0.00000E+00	8.39420E-01	8.39420E-01
3.15000E+03	1.00000E+00	0.00000E+00	8.39420E-01	8.39420E-01
3.15000E+03	1.00000E+00	0.00000E+00	8.39420E-01	8.39420E-01

TIME (days) = 2.01441E-05
 TIME STEP SIZE (days) = 8.25691E-06
 INITIAL RESERVOIR PRESSURE (psia) = 3.15000E+03
 INJECTION PRESSURE (psia) = 3.15000E+03
 WELLBORE PRESSURE (psia) = 3.04849E+03
 AVERAGE RESERVOIR PRESSURE (psia) = 3.14999E+03

RESERVOIR PROPERTIES DISTRIBUTION

*****	*****	*****	*****	*****
PRESSURE	GAS SATURATION	MOLES OF LIQUID	GAS MOLE FRAC.	OVERALL MOLE FRAC.
psia			C1	C1
*****	*****	*****	*****	*****
3.05943E+03	9.89676E-01	1.16650E-02	8.42090E-01	8.39094E-01
3.07939E+03	9.94048E-01	6.70147E-03	8.40997E-01	8.39306E-01
3.09802E+03	9.98082E-01	2.15289E-03	8.39939E-01	8.39405E-01
3.11475E+03	1.00000E+00	0.00000E+00	8.39424E-01	8.39424E-01
3.12891E+03	1.00000E+00	0.00000E+00	8.39423E-01	8.39423E-01
3.13949E+03	1.00000E+00	0.00000E+00	8.39422E-01	8.39422E-01
3.14595E+03	1.00000E+00	0.00000E+00	8.39421E-01	8.39421E-01

3.15000E+03	1.00000E+00	0.00000E+00	8.39420E-01	8.39420E-01
3.15000E+03	1.00000E+00	0.00000E+00	8.39420E-01	8.39420E-01
3.15000E+03	1.00000E+00	0.00000E+00	8.39420E-01	8.39420E-01
3.15000E+03	1.00000E+00	0.00000E+00	8.39420E-01	8.39420E-01
3.15000E+03	1.00000E+00	0.00000E+00	8.39420E-01	8.39420E-01
3.15000E+03	1.00000E+00	0.00000E+00	8.39420E-01	8.39420E-01
3.15000E+03	1.00000E+00	0.00000E+00	8.39420E-01	8.39420E-01
3.15000E+03	1.00000E+00	0.00000E+00	8.39420E-01	8.39420E-01

TIME (days) = 5.30485E-05
 TIME STEP SIZE (days) = 1.99826E-05
 INITIAL RESERVOIR PRESSURE (psia) = 3.15000E+03
 INJECTION PRESSURE (psia) = 3.15000E+03
 WELLBORE PRESSURE (psia) = 3.01906E+03
 AVERAGE RESERVOIR PRESSURE (psia) = 3.14998E+03

RESERVOIR PROPERTIES DISTRIBUTION

3.03019E+03	9.82656E-01	1.96948E-02	8.43631E-01	8.38440E-01
3.05085E+03	9.87725E-01	1.38902E-02	8.42552E-01	8.38957E-01
3.07079E+03	9.92180E-01	8.1851E-03	8.41472E-01	8.39230E-01
3.08969E+03	9.96262E-01	4.20097E-03	8.40416E-01	8.39366E-01
3.10698E+03	1.00000E+00	0.00000E+00	8.39425E-01	8.39425E-01
3.12227E+03	1.00000E+00	0.00000E+00	8.39424E-01	8.39424E-01
3.13459E+03	1.00000E+00	0.00000E+00	8.39422E-01	8.39422E-01
3.14309E+03	1.00000E+00	0.00000E+00	8.39421E-01	8.39421E-01
3.14770E+03	1.00000E+00	0.00000E+00	8.39421E-01	8.39421E-01
3.14948E+03	1.00000E+00	0.00000E+00	8.39420E-01	8.39420E-01
3.14993E+03	1.00000E+00	0.00000E+00	8.39420E-01	8.39420E-01
3.14999E+03	1.00000E+00	0.00000E+00	8.39420E-01	8.39420E-01
3.15000E+03	1.00000E+00	0.00000E+00	8.39420E-01	8.39420E-01
3.15000E+03	1.00000E+00	0.00000E+00	8.39420E-01	8.39420E-01
3.15000E+03	1.00000E+00	0.00000E+00	8.39420E-01	8.39420E-01
3.15000E+03	1.00000E+00	0.00000E+00	8.39420E-01	8.39420E-01
3.15000E+03	1.00000E+00	0.00000E+00	8.39420E-01	8.39420E-01

 PRESSURE Psia

 GAS SATURATION MOLES OF LIQUID GAS MOLE FRAC. OVERALL MOLE FRAC.

 Ci Ci

 PRESSURE psia

 GAS SATURATION MOLES OF LIQUID GAS MOLE FRAC. OVERALL MOLE FRAC.
 C1 C1 C1

2.97043E+03	9.59022E-01	4.69362E-02	8.46561E-01	8.33569E-01
2.99234E+03	9.70184E-01	3.40572E-02	8.45520E-01	8.36257E-01
3.01368E+03	9.77916E-01	2.51438E-02	8.44468E-01	8.37749E-01
3.03452E+03	9.83778E-01	1.84069E-02	8.43405E-01	8.38572E-01
3.05481E+03	9.88642E-01	1.28414E-02	8.42341E-01	8.39026E-01
3.07436E+03	9.92959E-01	7.93526E-03	8.41275E-01	8.39263E-01
3.09281E+03	9.96956E-01	3.42005E-03	8.40238E-01	8.39386E-01
3.10962E+03	1.00000E+00	0.00000E+00	8.39425E-01	8.39425E-01
3.12435E+03	1.00000E+00	0.00000E+00	8.39424E-01	8.39424E-01
3.13606E+03	1.00000E+00	0.00000E+00	8.39422E-01	8.39422E-01
3.14395E+03	1.00000E+00	0.00000E+00	8.39421E-01	8.39421E-01
3.14808E+03	1.00000E+00	0.00000E+00	8.39420E-01	8.39420E-01
3.14960E+03	1.00000E+00	0.00000E+00	8.39420E-01	8.39420E-01
3.14995E+03	1.00000E+00	0.00000E+00	8.39420E-01	8.39420E-01
3.15000E+03	1.00000E+00	0.00000E+00	8.39420E-01	8.39420E-01
3.15000E+03	1.00000E+00	0.00000E+00	8.39420E-01	8.39420E-01
3.15000E+03	1.00000E+00	0.00000E+00	8.39420E-01	8.39420E-01
3.15000E+03	1.00000E+00	0.00000E+00	8.39420E-01	8.39420E-01
3.15000E+03	1.00000E+00	0.00000E+00	8.39420E-01	8.39420E-01

TIME (days) = 4.64359E-04
 TIME STEP SIZE (days) = 1.57508E-04
 INITIAL RESERVOIR PRESSURE (psia) = 3.15000E+03
 INJECTION PRESSURE (psia) = 3.15000E+03
 WELLBORE PRESSURE (psia) = 2.94283E+03
 AVERAGE RESERVOIR PRESSURE (psia) = 3.14985E+03

RESERVOIR PROPERTIES DISTRIBUTION

 PRESSURE psia

 GAS SATURATION MOLES OF LIQUID GAS MOLE FRAC. OVERALL MOLE FRAC.
 C1 C1 C1

3.15000E+03 1.00000E+00 0.00000E+00 8.39420E-01 8.39420E-01

TIME (days) = 2.39324E-03
 TIME STEP SIZE (days) = 4.41956E-04
 INITIAL RESERVOIR PRESSURE (psia) = 3.15000E+03
 INJECTION PRESSURE (psia) = 3.15000E+03
 WELLBORE PRESSURE (psia) = 2.86679E+03
 AVERAGE RESERVOIR PRESSURE (psia) = 3.14922E+03

RESERVOIR PROPERTIES DISTRIBUTION

```

*****
PRESSURE          GAS SATURATION    MOLES OF LIQUID    GAS MOLE FRAC.    OVERALL MOLE FRAC.
psia
*****
2.88509E+03      8.26479E-01      1.97754E-01      8.50303E-01      7.91934E-01
2.91285E+03      8.94545E-01      1.20931E-01      8.49134E-01      8.14155E-01
2.93750E+03      9.31579E-01      7.85534E-02      8.48055E-01      8.25750E-01
2.96060E+03      9.53203E-01      5.36600E-02      8.47008E-01      8.32040E-01
2.98276E+03      9.66126E-01      3.87361E-02      8.45982E-01      8.35359E-01
3.00430E+03      9.75035E-01      2.84667E-02      8.44928E-01      8.37261E-01
3.02534E+03      9.81482E-01      2.10446E-02      8.43873E-01      8.38305E-01
3.04588E+03      9.86652E-01      1.51173E-02      8.42808E-01      8.38878E-01
3.06579E+03      9.91147E-01      9.99145E-03      8.41741E-01      8.39189E-01
3.08481E+03      9.95264E-01      5.32761E-03      8.40689E-01      8.39351E-01
3.10248E+03      9.99060E-01      1.05448E-03      8.39682E-01      8.39422E-01
3.11825E+03      1.00000E+00      0.00000E+00      8.39425E-01      8.39425E-01
3.13147E+03      1.00000E+00      0.00000E+00      8.39423E-01      8.39423E-01
3.14117E+03      1.00000E+00      0.00000E+00      8.39422E-01      8.39422E-01
3.14687E+03      1.00000E+00      0.00000E+00      8.39421E-01      8.39421E-01
3.14926E+03      1.00000E+00      0.00000E+00      8.39420E-01      8.39420E-01
3.14989E+03      1.00000E+00      0.00000E+00      8.39420E-01      8.39420E-01
3.14999E+03      1.00000E+00      0.00000E+00      8.39420E-01      8.39420E-01
3.15000E+03      1.00000E+00      0.00000E+00      8.39420E-01      8.39420E-01
3.15000E+03      1.00000E+00      0.00000E+00      8.39420E-01      8.39420E-01
*****
    
```

TIME (days) = 2.82259E-03
 TIME STEP SIZE (days) = 4.29350E-04

INITIAL RESERVOIR PRESSURE (psia) = 3.15000E+03
 INJECTION PRESSURE (psia) = 3.15000E+03
 WELLBORE PRESSURE (psia) = 2.85600E+03
 AVERAGE RESERVOIR PRESSURE (psia) = 3.14908E+03

RESERVOIR PROPERTIES DISTRIBUTION

```

*****
PRESSURE          GAS SATURATION    MOLES OF LIQUID    GAS MOLE FRAC.    OVERALL MOLE FRAC.
psia
*****
2.87627E+03      7.98518E-01      2.28886E-01      8.50663E-01      7.82678E-01
2.90535E+03      8.80011E-01      1.37465E-01      8.49453E-01      8.09471E-01
2.93064E+03      9.23429E-01      8.79157E-02      8.48357E-01      8.23264E-01
2.95408E+03      9.48390E-01      5.92122E-02      8.47305E-01      8.30705E-01
2.97647E+03      9.62999E-01      4.23469E-02      8.46279E-01      8.34608E-01
2.99817E+03      9.72881E-01      3.09514E-02      8.45227E-01      8.36849E-01
3.01935E+03      9.79841E-01      2.29325E-02      8.44176E-01      8.38077E-01
3.04004E+03      9.85283E-01      1.66834E-02      8.43113E-01      8.38754E-01
3.06016E+03      9.89925E-01      1.13822E-02      8.42045E-01      8.39123E-01
3.07948E+03      9.94131E-01      6.60844E-03      8.40985E-01      8.39318E-01
3.09761E+03      9.98032E-01      2.20873E-03      8.39962E-01      8.39414E-01
3.11397E+03      1.00000E+00      0.00000E+00      8.39425E-01      8.39425E-01
3.12806E+03      1.00000E+00      0.00000E+00      8.39424E-01      8.39424E-01
3.13888E+03      1.00000E+00      0.00000E+00      8.39422E-01      8.39422E-01
3.14571E+03      1.00000E+00      0.00000E+00      8.39421E-01      8.39421E-01
3.14888E+03      1.00000E+00      0.00000E+00      8.39420E-01      8.39420E-01
3.14982E+03      1.00000E+00      0.00000E+00      8.39420E-01      8.39420E-01
3.14998E+03      1.00000E+00      0.00000E+00      8.39420E-01      8.39420E-01
3.15000E+03      1.00000E+00      0.00000E+00      8.39420E-01      8.39420E-01
3.15000E+03      1.00000E+00      0.00000E+00      8.39420E-01      8.39420E-01
*****

```

TIME (days) = 3.24008E-03
 TIME STEP SIZE (days) = 4.17496E-04
 INITIAL RESERVOIR PRESSURE (psia) = 3.15000E+03
 INJECTION PRESSURE (psia) = 3.15000E+03
 WELLBORE PRESSURE (psia) = 2.84594E+03
 AVERAGE RESERVOIR PRESSURE (psia) = 3.14894E+03

PRESSURE psia	GAS SATURATION	MOLES OF LIQUID	GAS MOLE FRAC. C1	OVERALL MOLE FRAC. C1
2.86109E+03	7.42608E-01	2.90338E-01	8.51273E-01	7.64106E-01
2.89310E+03	8.51962E-01	1.69193E-01	8.49966E-01	8.00315E-01
2.91967E+03	9.08074E-01	1.05509E-01	8.48834E-01	8.18470E-01
2.94374E+03	9.39503E-01	6.94555E-02	8.47771E-01	8.28143E-01
2.96654E+03	9.57359E-01	4.88581E-02	8.46742E-01	8.33170E-01
2.98851E+03	9.69115E-01	3.52990E-02	8.45692E-01	8.36062E-01
3.00991E+03	9.77063E-01	2.61321E-02	8.44646E-01	8.37641E-01
3.03082E+03	9.83034E-01	1.92633E-02	8.43587E-01	8.38514E-01
3.05122E+03	9.87954E-01	1.36298E-02	8.42521E-01	8.38994E-01
3.07093E+03	9.92315E-01	8.66587E-03	8.41456E-01	8.39252E-01
3.08966E+03	9.96344E-01	4.10915E-03	8.40413E-01	8.39386E-01
3.10687E+03	9.99991E-01	9.83961E-06	8.39428E-01	8.39426E-01
3.12218E+03	1.00000E+00	0.00000E+00	8.39424E-01	8.39424E-01
3.13465E+03	1.00000E+00	0.00000E+00	8.39423E-01	8.39423E-01
3.14331E+03	1.00000E+00	0.00000E+00	8.39421E-01	8.39421E-01
3.14794E+03	1.00000E+00	0.00000E+00	8.39420E-01	8.39420E-01
3.14960E+03	1.00000E+00	0.00000E+00	8.39420E-01	8.39420E-01
3.14996E+03	1.00000E+00	0.00000E+00	8.39420E-01	8.39420E-01
3.15000E+03	1.00000E+00	0.00000E+00	8.39420E-01	8.39420E-01
3.15000E+03	1.00000E+00	0.00000E+00	8.39420E-01	8.39420E-01

TIME (days) = 4.03730E-03
 TIME STEP SIZE (days) = 3.92174E-04
 INITIAL RESERVOIR PRESSURE (psia) = 3.15000E+03
 INJECTION PRESSURE (psia) = 3.15000E+03
 WELLBORE PRESSURE (psia) = 2.82658E+03
 AVERAGE RESERVOIR PRESSURE (psia) = 3.14868E+03

RESERVOIR PROPERTIES DISTRIBUTION

PRESSURE psia	GAS SATURATION	MOLES OF LIQUID	GAS MOLE FRAC. C1	OVERALL MOLE FRAC. C1
2.85448E+03	7.14711E-01	3.20588E-01	8.51534E-01	7.54841E-01

3.00282E+03	9.74761E-01	2.87860E-02	8.44993E-01	8.37232E-01
3.02390E+03	9.81237E-01	2.13278E-02	8.43939E-01	8.38288E-01
3.04449E+03	9.86426E-01	1.53766E-02	8.42874E-01	8.38871E-01
3.06449E+03	9.90934E-01	1.02350E-02	8.41805E-01	8.39188E-01
3.08363E+03	9.95063E-01	5.55463E-03	8.40751E-01	8.39355E-01
3.10149E+03	9.98861E-01	1.27801E-03	8.39739E-01	8.39423E-01
3.11746E+03	1.00000E+00	0.00000E+00	8.39425E-01	8.39425E-01
3.13097E+03	1.00000E+00	0.00000E+00	8.39424E-01	8.39424E-01
3.14098E+03	1.00000E+00	0.00000E+00	8.39422E-01	8.39422E-01
3.14689E+03	1.00000E+00	0.00000E+00	8.39421E-01	8.39421E-01
3.14931E+03	1.00000E+00	0.00000E+00	8.39420E-01	8.39420E-01
3.14991E+03	1.00000E+00	0.00000E+00	8.39420E-01	8.39420E-01
3.14999E+03	1.00000E+00	0.00000E+00	8.39420E-01	8.39420E-01
3.15000E+03	1.00000E+00	0.00000E+00	8.39420E-01	8.39420E-01

TIME (days) = 4.78786E-03
 TIME STEP SIZE (days) = 3.69632E-04
 INITIAL RESERVOIR PRESSURE (psia) = 3.15000E+03
 INJECTION PRESSURE (psia) = 3.15000E+03
 WELBORE PRESSURE (psia) = 2.80707E+03
 AVERAGE RESERVOIR PRESSURE (psia) = 3.14843E+03

RESERVOIR PROPERTIES DISTRIBUTION

*****	*****	*****	*****	*****
PRESSURE	GAS SATURATION	MOLES OF LIQUID	GAS MOLE FRAC.	OVERALL MOLE FRAC.
psia			C1	C1
*****	*****	*****	*****	*****
2.84241E+03	6.58666E-01	3.80521E-01	8.52004E-01	7.36274E-01
2.87914E+03	8.12110E-01	2.13831E-01	8.50539E-01	7.87157E-01
2.90759E+03	8.86977E-01	1.29576E-01	8.49350E-01	8.11725E-01
2.93256E+03	9.27600E-01	8.31491E-02	8.48265E-01	8.24568E-01
2.95590E+03	9.50022E-01	5.73233E-02	8.47229E-01	8.31174E-01
2.97820E+03	9.64401E-01	4.07433E-02	8.46180E-01	8.34972E-01
2.99986E+03	9.73733E-01	2.99717E-02	8.45138E-01	8.37036E-01
3.02101E+03	9.80452E-01	2.22309E-02	8.44084E-01	8.38180E-01
3.04167E+03	9.85770E-01	1.61278E-02	8.43021E-01	8.38813E-01
3.06176E+03	9.90346E-01	1.09038E-02	8.41952E-01	8.39157E-01
3.08105E+03	9.94516E-01	6.17297E-03	8.40895E-01	8.39340E-01

3.14896E+03 1.00000E+00 0.00000E+00 8.39420E-01 8.39420E-01
 3.14985E+03 1.00000E+00 0.00000E+00 8.39420E-01 8.39420E-01
 3.14999E+03 1.00000E+00 0.00000E+00 8.39420E-01 8.39420E-01
 3.15000E+03 1.00000E+00 0.00000E+00 8.39420E-01 8.39420E-01

TIME (days) = 5.49224E-03
 TIME STEP SIZE (days) = 3.46356E-04
 INITIAL RESERVOIR PRESSURE (psia) = 3.15000E+03
 INJECTION PRESSURE (psia) = 3.15000E+03
 WELLBORE PRESSURE (psia) = 2.78554E+03
 AVERAGE RESERVOIR PRESSURE (psia) = 3.14820E+03

RESERVOIR PROPERTIES DISTRIBUTION

```

*****
PRESSURE          GAS SATURATION    MOLES OF LIQUID    GAS MOLE FRAC.    OVERALL MOLE FRAC.
psia
*****
2.83135E+03      6.02335E-01      4.39625E-01      8.52427E-01      7.17708E-01
2.87160E+03      7.86870E-01      2.41825E-01      8.50843E-01      7.78779E-01
2.90128E+03      8.73973E-01      1.44346E-01      8.49615E-01      8.07509E-01
2.92682E+03      9.20411E-01      9.14037E-02      8.48516E-01      8.22353E-01
2.95047E+03      9.45673E-01      6.23363E-02      8.47475E-01      8.29942E-01
2.97297E+03      9.61679E-01      4.38871E-02      8.46424E-01      8.34302E-01
2.99476E+03      9.71868E-01      3.21242E-02      8.45384E-01      8.36665E-01
3.01602E+03      9.79051E-01      2.38434E-02      8.44334E-01      8.37975E-01
3.03681E+03      9.84616E-01      1.74500E-02      8.43272E-01      8.38700E-01
3.05705E+03      9.89322E-01      1.20703E-02      8.42204E-01      8.39097E-01
3.07655E+03      9.93566E-01      7.24861E-03      8.41143E-01      8.39310E-01
3.09496E+03      9.97489E-01      2.82019E-03      8.40112E-01      8.39411E-01
3.11170E+03      1.00000E+00      0.00000E+00      8.39426E-01      8.39426E-01
3.12631E+03      1.00000E+00      0.00000E+00      8.39424E-01      8.39424E-01
3.13778E+03      1.00000E+00      0.00000E+00      8.39423E-01      8.39423E-01
3.14524E+03      1.00000E+00      0.00000E+00      8.39421E-01      8.39421E-01
3.14877E+03      1.00000E+00      0.00000E+00      8.39420E-01      8.39420E-01
3.14981E+03      1.00000E+00      0.00000E+00      8.39420E-01      8.39420E-01
3.14998E+03      1.00000E+00      0.00000E+00      8.39420E-01      8.39420E-01
3.15000E+03      1.00000E+00      0.00000E+00      8.39420E-01      8.39420E-01
*****
    
```

TIME (days) = 5.82880E-03
 TIME STEP SIZE (days) = 3.36551E-04
 INITIAL RESERVOIR PRESSURE (psia) = 3.15000E+03
 INJECTION PRESSURE (psia) = 3.15000E+03
 WELLBORE PRESSURE (psia) = 2.77368E+03
 AVERAGE RESERVOIR PRESSURE (psia) = 3.14809E+03

RESERVOIR PROPERTIES DISTRIBUTION

```

*****
PRESSURE          GAS SATURATION    MOLES OF LIQUID    GAS MOLE FRAC.    OVERALL MOLE FRAC.
      psia          *****          *****          *****          *****
*****          C1          C1          C1          C1
2.82606E+03      5.74039E-01      4.68884E-01      8.52628E-01      7.08427E-01
2.86817E+03      7.74585E-01      2.55373E-01      8.50981E-01      7.74695E-01
2.89847E+03      8.67740E-01      1.51407E-01      8.49732E-01      8.05476E-01
2.92430E+03      9.17001E-01      9.53146E-02      8.48625E-01      8.21291E-01
2.94809E+03      9.43629E-01      6.46927E-02      8.47582E-01      8.29353E-01
2.97068E+03      9.60414E-01      4.53487E-02      8.46531E-01      8.33982E-01
2.99253E+03      9.71013E-01      3.31116E-02      8.45491E-01      8.36488E-01
3.01384E+03      9.78418E-01      2.45723E-02      8.44442E-01      8.37877E-01
3.03468E+03      9.84101E-01      1.80398E-02      8.43382E-01      8.38646E-01
3.05499E+03      9.88870E-01      1.25856E-02      8.42314E-01      8.39068E-01
3.07458E+03      9.93148E-01      7.72179E-03      8.41252E-01      8.39295E-01
3.09312E+03      9.97101E-01      3.25646E-03      8.40217E-01      8.39405E-01
3.11005E+03      1.00000E+00      0.00000E+00      8.39426E-01      8.39426E-01
3.12495E+03      1.00000E+00      0.00000E+00      8.39425E-01      8.39425E-01
3.13680E+03      1.00000E+00      0.00000E+00      8.39423E-01      8.39423E-01
3.14469E+03      1.00000E+00      0.00000E+00      8.39421E-01      8.39421E-01
3.14857E+03      1.00000E+00      0.00000E+00      8.39420E-01      8.39420E-01
3.14977E+03      1.00000E+00      0.00000E+00      8.39420E-01      8.39420E-01
3.14998E+03      1.00000E+00      0.00000E+00      8.39420E-01      8.39420E-01
3.15000E+03      1.00000E+00      0.00000E+00      8.39420E-01      8.39420E-01
  
```

TIME (days) = 6.15515E-03
 TIME STEP SIZE (days) = 3.26356E-04
 INITIAL RESERVOIR PRESSURE (psia) = 3.15000E+03
 INJECTION PRESSURE (psia) = 3.15000E+03

WELLBORE PRESSURE (psia) = 2.76001E+03
AVERAGE RESERVOIR PRESSURE (psia) = 3.14799E+03

RESERVOIR PROPERTIES DISTRIBUTION

```

*****
PRESSURE          GAS SATURATION    MOLES OF LIQUID    GAS MOLE FRAC.    OVERALL MOLE FRAC.
  psia
*****
2.82082E+03      5.45620E-01      4.97982E-01      8.52825E-01      6.99133E-01
2.86491E+03      7.62517E-01      2.68632E-01      8.51111E-01      7.70680E-01
2.89586E+03      8.61679E-01      1.58262E-01      8.49841E-01      8.03493E-01
2.92196E+03      9.13706E-01      9.90999E-02      8.48726E-01      8.20260E-01
2.94590E+03      9.41663E-01      6.69578E-02      8.47680E-01      8.28781E-01
2.96857E+03      9.59205E-01      4.67447E-02      8.46628E-01      8.33672E-01
2.99048E+03      9.70203E-01      3.40476E-02      8.45589E-01      8.36316E-01
3.01184E+03      9.77824E-01      2.52574E-02      8.44541E-01      8.37782E-01
3.03273E+03      9.83622E-01      1.85895E-02      8.43482E-01      8.38594E-01
3.05309E+03      9.88451E-01      1.30630E-02      8.42415E-01      8.39040E-01
3.07276E+03      9.92762E-01      8.15886E-03      8.41351E-01      8.39281E-01
3.09141E+03      9.96741E-01      3.66156E-03      8.40313E-01      8.39399E-01
3.10852E+03      1.00000E+00      0.00000E+00      8.39426E-01      8.39426E-01
3.12367E+03      1.00000E+00      0.00000E+00      8.39425E-01      8.39425E-01
3.13586E+03      1.00000E+00      0.00000E+00      8.39423E-01      8.39423E-01
3.14415E+03      1.00000E+00      0.00000E+00      8.39421E-01      8.39421E-01
3.14836E+03      1.00000E+00      0.00000E+00      8.39420E-01      8.39420E-01
3.14973E+03      1.00000E+00      0.00000E+00      8.39420E-01      8.39420E-01
3.14998E+03      1.00000E+00      0.00000E+00      8.39420E-01      8.39420E-01
3.15000E+03      1.00000E+00      0.00000E+00      8.39420E-01      8.39420E-01

```

```

TIME (days) = 6.47118E-03
TIME STEP SIZE (days) = 3.16033E-04
INITIAL RESERVOIR PRESSURE (psia) = 3.15000E+03
INJECTION PRESSURE (psia) = 3.15000E+03
WELLBORE PRESSURE (psia) = 2.74493E+03
AVERAGE RESERVOIR PRESSURE (psia) = 3.14788E+03

```

RESERVOIR PROPERTIES DISTRIBUTION

```

*****
PRESSURE          GAS SATURATION    MOLES OF LIQUID    GAS MOLE FRAC.    OVERALL MOLE FRAC.
      psia          C1          C1          C1          C1
*****
2.81558E+03      5.17078E-01      5.26919E-01      8.53020E-01      6.89826E-01
2.86183E+03      7.50674E-01      2.81594E-01      8.51233E-01      7.66739E-01
2.89342E+03      8.55789E-01      1.64912E-01      8.49942E-01      8.01561E-01
2.91980E+03      9.10524E-01      1.02735E-01      8.48819E-01      8.19258E-01
2.94387E+03      9.39773E-01      6.91345E-02      8.47771E-01      8.28227E-01
2.96663E+03      9.58050E-01      4.80786E-02      8.46718E-01      8.33371E-01
2.98859E+03      9.69434E-01      3.49358E-02      8.45679E-01      8.36150E-01
3.00999E+03      9.77264E-01      2.59025E-02      8.44632E-01      8.37690E-01
3.03092E+03      9.83175E-01      1.91033E-02      8.43574E-01      8.38543E-01
3.05133E+03      9.88063E-01      1.35066E-02      8.42507E-01      8.39013E-01
3.07107E+03      9.92406E-01      8.56360E-03      8.41443E-01      8.39267E-01
3.08983E+03      9.96407E-01      4.03859E-03      8.40402E-01      8.39393E-01
3.10709E+03      1.00000E+00      0.00000E+00      8.39427E-01      8.39427E-01
3.12246E+03      1.00000E+00      0.00000E+00      8.39425E-01      8.39425E-01
3.13497E+03      1.00000E+00      0.00000E+00      8.39423E-01      8.39423E-01
3.14363E+03      1.00000E+00      0.00000E+00      8.39421E-01      8.39421E-01
3.14815E+03      1.00000E+00      0.00000E+00      8.39420E-01      8.39420E-01
3.14968E+03      1.00000E+00      0.00000E+00      8.39420E-01      8.39420E-01
3.14997E+03      1.00000E+00      0.00000E+00      8.39420E-01      8.39420E-01
3.15000E+03      1.00000E+00      0.00000E+00      8.39420E-01      8.39420E-01

```

```

TIME (days) = 6.62399E-03
TIME STEP SIZE (days) = 1.52803E-04
INITIAL RESERVOIR PRESSURE (psia) = 3.15000E+03
INJECTION PRESSURE (psia) = 3.15000E+03
WELLBORE PRESSURE (psia) = 2.73634E+03
AVERAGE RESERVOIR PRESSURE (psia) = 3.14783E+03

```

RESERVOIR PROPERTIES DISTRIBUTION

```

*****
PRESSURE          GAS SATURATION    MOLES OF LIQUID    GAS MOLE FRAC.    OVERALL MOLE FRAC.
      psia          C1          C1          C1          C1
*****

```

2.81310E+03	5.03060E-01	5.41019E-01	8.53112E-01	6.85273E-01
2.86034E+03	7.44914E-01	2.87882E-01	8.51292E-01	7.64821E-01
2.89226E+03	8.52938E-01	1.68128E-01	8.49990E-01	8.00624E-01
2.91877E+03	9.08988E-01	1.04493E-01	8.48863E-01	8.18773E-01
2.94291E+03	9.38863E-01	7.01826E-02	8.47813E-01	8.27959E-01
2.96571E+03	9.57495E-01	4.87192E-02	8.46760E-01	8.33226E-01
2.98770E+03	9.69066E-01	3.53608E-02	8.45722E-01	8.36069E-01
3.00912E+03	9.76998E-01	2.62097E-02	8.44675E-01	8.37645E-01
3.03007E+03	9.82963E-01	1.93469E-02	8.43617E-01	8.38518E-01
3.05051E+03	9.87880E-01	1.37159E-02	8.42550E-01	8.38999E-01
3.07028E+03	9.92238E-01	8.75350E-03	8.41486E-01	8.39259E-01
3.08910E+03	9.96252E-01	4.21336E-03	8.40443E-01	8.39389E-01
3.10647E+03	9.99908E-01	1.03364E-04	8.39452E-01	8.39426E-01
3.12190E+03	1.00000E+00	0.00000E+00	8.39425E-01	8.39425E-01
3.13455E+03	1.00000E+00	0.00000E+00	8.39423E-01	8.39423E-01
3.14337E+03	1.00000E+00	0.00000E+00	8.39421E-01	8.39421E-01
3.14805E+03	1.00000E+00	0.00000E+00	8.39420E-01	8.39420E-01
3.14966E+03	1.00000E+00	0.00000E+00	8.39420E-01	8.39420E-01
3.14997E+03	1.00000E+00	0.00000E+00	8.39420E-01	8.39420E-01
3.15000E+03	1.00000E+00	0.00000E+00	8.39420E-01	8.39420E-01

TIME (days) = 6.92601E-03
 TIME STEP SIZE (days) = 3.02020E-04
 INITIAL RESERVOIR PRESSURE (psia) = 3.15000E+03
 INJECTION PRESSURE (psia) = 3.15000E+03
 WELBORE PRESSURE (psia) = 2.72746E+03
 AVERAGE RESERVOIR PRESSURE (psia) = 3.14773E+03

RESERVOIR PROPERTIES DISTRIBUTION

2.80829E+03	4.93074E-01	5.51193E-01	8.53290E-01	6.81746E-01
2.85761E+03	7.33381E-01	3.00428E-01	8.51399E-01	7.60988E-01
2.89013E+03	8.47288E-01	1.74490E-01	8.50078E-01	7.98765E-01

3.14999E+03 1.00000E+00 0.00000E+00 8.39420E-01 8.39420E-01
 3.14999E+03 1.00000E+00 0.00000E+00 8.39420E-01 8.39420E-01

TIME (days) = 9.63545E-03
 TIME STEP SIZE (days) = 6.45608E-04
 INITIAL RESERVOIR PRESSURE (psia) = 3.15000E+03
 INJECTION PRESSURE (psia) = 3.15000E+03
 WELBORE PRESSURE (psia) = 2.67038E+03
 AVERAGE RESERVOIR PRESSURE (psia) = 3.14685E+03

RESERVOIR PROPERTIES DISTRIBUTION

 PRESSURE psia

 GAS SATURATION

 MOLES OF LIQUID

 GAS MOLE FRAC.

 OVERALL MOLE FRAC.

 C1

2.75474E+03	4.84726E-01	5.62518E-01	8.55205E-01	6.73944E-01
2.83430E+03	6.21121E-01	4.20073E-01	8.52304E-01	7.23841E-01
2.87338E+03	7.95216E-01	2.32615E-01	8.50761E-01	7.81532E-01
2.90257E+03	8.78864E-01	1.38822E-01	8.49551E-01	8.09096E-01
2.92803E+03	9.21425E-01	9.02155E-02	8.48469E-01	8.22659E-01
2.95156E+03	9.47159E-01	6.06429E-02	8.47405E-01	8.30371E-01
2.97400E+03	9.62430E-01	4.30226E-02	8.46367E-01	8.34494E-01
2.99575E+03	9.72371E-01	3.15454E-02	8.45327E-01	8.36772E-01
3.01698E+03	9.79420E-01	2.34199E-02	8.44277E-01	8.38037E-01
3.03774E+03	9.84912E-01	1.71107E-02	8.43216E-01	8.38737E-01
3.05796E+03	9.89576E-01	1.17810E-02	8.42151E-01	8.39121E-01
3.07743E+03	9.93775E-01	7.01185E-03	8.41093E-01	8.39321E-01
3.09580E+03	9.97666E-01	2.62095E-03	8.40065E-01	8.39413E-01
3.11248E+03	1.00000E+00	0.00000E+00	8.39426E-01	8.39426E-01
3.12700E+03	1.00000E+00	0.00000E+00	8.39424E-01	8.39424E-01
3.13834E+03	1.00000E+00	0.00000E+00	8.39422E-01	8.39422E-01
3.14560E+03	1.00000E+00	0.00000E+00	8.39421E-01	8.39421E-01
3.14893E+03	1.00000E+00	0.00000E+00	8.39420E-01	8.39420E-01
3.14985E+03	1.00000E+00	0.00000E+00	8.39420E-01	8.39420E-01
3.14999E+03	1.00000E+00	0.00000E+00	8.39420E-01	8.39420E-01

TIME (days) = 1.02610E-02

TIME STEP SIZE (days) = 6.25552E-04
 INITIAL RESERVOIR PRESSURE (psia) = 3.15000E+03
 INJECTION PRESSURE (psia) = 3.15000E+03
 WELLBORE PRESSURE (psia) = 2.65274E+03
 AVERAGE RESERVOIR PRESSURE (psia) = 3.14665E+03

RESERVOIR PROPERTIES DISTRIBUTION

 PRESSURE psia

 GAS SATURATION MOLES OF LIQUID GAS MOLE FRAC. OVERALL MOLE FRAC.
 C1 C1

2.73791E+03	4.82984E-01	5.65217E-01	8.55780E-01	6.71710E-01
2.82905E+03	5.92915E-01	4.49423E-01	8.52504E-01	7.14574E-01
2.86988E+03	7.82844E-01	2.46292E-01	8.50901E-01	7.77421E-01
2.89969E+03	8.72584E-01	1.45945E-01	8.49672E-01	8.07052E-01
2.92543E+03	9.17865E-01	9.42976E-02	8.48582E-01	8.21551E-01
2.94912E+03	9.45089E-01	6.30287E-02	8.47515E-01	8.29778E-01
2.97165E+03	9.61133E-01	4.45200E-02	8.46477E-01	8.34167E-01
2.99346E+03	9.71494E-01	3.25585E-02	8.45438E-01	8.36592E-01
3.01474E+03	9.78769E-01	2.41693E-02	8.44389E-01	8.37937E-01
3.03555E+03	9.84383E-01	1.77180E-02	8.43329E-01	8.38682E-01
3.05583E+03	9.89109E-01	1.23129E-02	8.42264E-01	8.39091E-01
3.07539E+03	9.93343E-01	7.50118E-03	8.41205E-01	8.39306E-01
3.09389E+03	9.97265E-01	3.07177E-03	8.40173E-01	8.39408E-01
3.11077E+03	1.00000E+00	0.00000E+00	8.39426E-01	8.39426E-01
3.12559E+03	1.00000E+00	0.00000E+00	8.39424E-01	8.39424E-01
3.13732E+03	1.00000E+00	0.00000E+00	8.39422E-01	8.39422E-01
3.14504E+03	1.00000E+00	0.00000E+00	8.39421E-01	8.39421E-01
3.14873E+03	1.00000E+00	0.00000E+00	8.39420E-01	8.39420E-01
3.14981E+03	1.00000E+00	0.00000E+00	8.39420E-01	8.39420E-01
3.14999E+03	1.00000E+00	0.00000E+00	8.39420E-01	8.39420E-01

TIME (days) = 1.08685E-02
 TIME STEP SIZE (days) = 6.07548E-04
 INITIAL RESERVOIR PRESSURE (psia) = 3.15000E+03
 INJECTION PRESSURE (psia) = 3.15000E+03
 WELLBORE PRESSURE (psia) = 2.63304E+03
 AVERAGE RESERVOIR PRESSURE (psia) = 3.14645E+03

RESERVOIR PROPERTIES DISTRIBUTION

```

*****
PRESSURE          GAS SATURATION    MOLES OF LIQUID    GAS MOLE FRAC.    OVERALL MOLE FRAC.
  psia
*****
2.71916E+03      4.81012E-01      5.68261E-01      8.56407E-01      6.69182E-01
2.82386E+03      5.64575E-01      4.78628E-01      8.52700E-01      7.05291E-01
2.86658E+03      7.70678E-01      2.59691E-01      8.51034E-01      7.73375E-01
2.89700E+03      8.66467E-01      1.52872E-01      8.49784E-01      8.05053E-01
2.92303E+03      9.14419E-01      9.82445E-02      8.48686E-01      8.20473E-01
2.94686E+03      9.43097E-01      6.53242E-02      8.47616E-01      8.29202E-01
2.96948E+03      9.59893E-01      4.59517E-02      8.46578E-01      8.33851E-01
2.99134E+03      9.70661E-01      3.35196E-02      8.45539E-01      8.36416E-01
3.01267E+03      9.78158E-01      2.48741E-02      8.44491E-01      8.37839E-01
3.03353E+03      9.83889E-01      1.82846E-02      8.43433E-01      8.38629E-01
3.05387E+03      9.88677E-01      1.28059E-02      8.42368E-01      8.39063E-01
3.07351E+03      9.92944E-01      7.95334E-03      8.41308E-01      8.39291E-01
3.09213E+03      9.96893E-01      3.49050E-03      8.40273E-01      8.39402E-01
3.10919E+03      1.00000E+00      0.00000E+00      8.39426E-01      8.39426E-01
3.12427E+03      1.00000E+00      0.00000E+00      8.39425E-01      8.39425E-01
3.13636E+03      1.00000E+00      0.00000E+00      8.39423E-01      8.39423E-01
3.14449E+03      1.00000E+00      0.00000E+00      8.39421E-01      8.39421E-01
3.14852E+03      1.00000E+00      0.00000E+00      8.39420E-01      8.39420E-01
3.14977E+03      1.00000E+00      0.00000E+00      8.39420E-01      8.39420E-01
3.14998E+03      1.00000E+00      0.00000E+00      8.39420E-01      8.39420E-01

```

```

TIME (days) = 1.14575E-02
TIME STEP SIZE (days) = 5.88991E-04
INITIAL RESERVOIR PRESSURE (psia) = 3.15000E+03
INJECTION PRESSURE (psia) = 3.15000E+03
WELLBORE PRESSURE (psia) = 2.61002E+03
AVERAGE RESERVOIR PRESSURE (psia) = 3.14625E+03

```

RESERVOIR PROPERTIES DISTRIBUTION

```

*****
PRESSURE          GAS SATURATION    MOLES OF LIQUID    GAS MOLE FRAC.    OVERALL MOLE FRAC.
psia
*****
2.69727E+03      4.78725E-01      5.71810E-01      8.57120E-01      6.66195E-01
2.81870E+03      5.36107E-01      5.07676E-01      8.52893E-01      6.95994E-01
2.86344E+03      7.58728E-01      2.72802E-01      8.51158E-01      7.69399E-01
2.89450E+03      8.60515E-01      1.59601E-01      8.49888E-01      8.03103E-01
2.92082E+03      9.11089E-01      1.02057E-01      8.48781E-01      8.19425E-01
2.94477E+03      9.41181E-01      6.75316E-02      8.47709E-01      8.28641E-01
2.96748E+03      9.58708E-01      4.73206E-02      8.46670E-01      8.33543E-01
2.98940E+03      9.69871E-01      3.44319E-02      8.45631E-01      8.36246E-01
3.01077E+03      9.77582E-01      2.55377E-02      8.44585E-01      8.37745E-01
3.03167E+03      9.83428E-01      1.88139E-02      8.43527E-01      8.38576E-01
3.05206E+03      9.88276E-01      1.32638E-02      8.42463E-01      8.39034E-01
3.07177E+03      9.92575E-01      8.37181E-03      8.41403E-01      8.39276E-01
3.09050E+03      9.96548E-01      3.87983E-03      8.40364E-01      8.39395E-01
3.10771E+03      1.00000E+00      0.00000E+00      8.39426E-01      8.39426E-01
3.12302E+03      1.00000E+00      0.00000E+00      8.39424E-01      8.39424E-01
3.13543E+03      1.00000E+00      0.00000E+00      8.39422E-01      8.39422E-01
3.14395E+03      1.00000E+00      0.00000E+00      8.39421E-01      8.39421E-01
3.14831E+03      1.00000E+00      0.00000E+00      8.39420E-01      8.39420E-01
3.14973E+03      1.00000E+00      0.00000E+00      8.39420E-01      8.39420E-01
3.14998E+03      1.00000E+00      0.00000E+00      8.39420E-01      8.39420E-01

```

```

TIME (days) = 1.19537E-02
TIME STEP SIZE (days) = 4.96130E-04
INITIAL RESERVOIR PRESSURE (psia) = 3.15000E+03
INJECTION PRESSURE (psia) = 3.15000E+03
WELLBORE PRESSURE (psia) = 2.58682E+03
AVERAGE RESERVOIR PRESSURE (psia) = 3.14609E+03

```

RESERVOIR PROPERTIES DISTRIBUTION

```

*****
PRESSURE          GAS SATURATION    MOLES OF LIQUID    GAS MOLE FRAC.    OVERALL MOLE FRAC.
psia
*****

```


3.04900E+03	9.87593E-01	1.40440E-02	8.42624E-01	8.38983E-01
3.06884E+03	9.91952E-01	9.07893E-03	8.41562E-01	8.39249E-01
3.08777E+03	9.95969E-01	4.53265E-03	8.40517E-01	8.39382E-01
3.10532E+03	9.99667E-01	3.72911E-04	8.39517E-01	8.39425E-01
3.12090E+03	1.00000E+00	0.00000E+00	8.39424E-01	8.39422E-01
3.13381E+03	1.00000E+00	0.00000E+00	8.39422E-01	8.39421E-01
3.14296E+03	1.00000E+00	0.00000E+00	8.39421E-01	8.39420E-01
3.14790E+03	1.00000E+00	0.00000E+00	8.39420E-01	8.39420E-01
3.14963E+03	1.00000E+00	0.00000E+00	8.39420E-01	8.39420E-01
3.14997E+03	1.00000E+00	0.00000E+00	8.39420E-01	8.39420E-01

TIME (days) = 1.33148E-02
 TIME STEP SIZE (days) = 7.93347E-04
 INITIAL RESERVOIR PRESSURE (psia) = 3.15000E+03
 INJECTION PRESSURE (psia) = 3.15000E+03
 WELLBORE PRESSURE (psia) = 2.55242E+03
 AVERAGE RESERVOIR PRESSURE (psia) = 3.14565E+03

RESERVOIR PROPERTIES DISTRIBUTION

*****	*****	*****	*****	*****
PRESSURE	GAS SATURATION	MOLES OF LIQUID	GAS MOLE FRAC.	OVERALL MOLE FRAC.
psia			C1	C1
*****	*****	*****	*****	*****
2.64590E+03	4.66622E-01	5.06739E-01	8.58716E-01	6.56754E-01
2.80211E+03	4.90125E-01	5.54457E-01	8.53506E-01	6.80246E-01
2.85410E+03	7.19971E-01	3.14975E-01	8.51526E-01	7.56510E-01
2.88723E+03	8.41590E-01	1.80920E-01	8.50187E-01	7.96875E-01
2.91447E+03	9.00641E-01	1.13996E-01	8.49052E-01	8.16108E-01
2.93885E+03	9.35231E-01	7.43808E-02	8.47971E-01	8.26874E-01
2.96181E+03	9.55071E-01	5.15186E-02	8.46929E-01	8.32574E-01
2.98390E+03	9.67483E-01	3.71893E-02	8.45892E-01	8.35710E-01
3.00539E+03	9.75871E-01	2.75094E-02	8.44848E-01	8.37447E-01
3.02641E+03	9.82082E-01	2.03596E-02	8.43794E-01	8.38412E-01
3.04694E+03	9.87123E-01	1.45813E-02	8.42731E-01	8.38945E-01
3.06686E+03	9.91526E-01	9.56203E-03	8.41669E-01	8.39229E-01
3.08591E+03	9.95573E-01	4.97909E-03	8.40620E-01	8.39372E-01
3.10364E+03	9.99314E-01	7.69189E-04	8.39613E-01	8.39424E-01
3.11943E+03	1.00000E+00	0.00000E+00	8.39423E-01	8.39423E-01

TIME (days) = 1.58335E-02
 TIME STEP SIZE (days) = 1.24004E-03
 INITIAL RESERVOIR PRESSURE (psia) = 3.15000E+03
 INJECTION PRESSURE (psia) = 3.15000E+03
 WELLBORE PRESSURE (psia) = 2.52283E+03
 AVERAGE RESERVOIR PRESSURE (psia) = 3.14484E+03

RESERVOIR PROPERTIES DISTRIBUTION

***** PRESSURE psia *****	***** GAS SATURATION *****	***** MOLES OF LIQUID *****	***** GAS MOLE FRAC. C1 *****	***** OVERALL MOLE FRAC. C1 *****
2.61782E+03	4.64230E-01	5.90784E-01	8.59545E-01	6.52883E-01
2.77660E+03	4.86949E-01	5.59057E-01	8.54428E-01	6.76793E-01
2.84231E+03	6.63934E-01	3.74990E-01	8.51985E-01	7.37941E-01
2.87860E+03	8.15356E-01	2.10268E-01	8.50539E-01	7.88196E-01
2.90707E+03	8.86499E-01	1.30103E-01	8.49367E-01	8.11563E-01
2.93206E+03	9.27316E-01	8.34777E-02	8.48270E-01	8.24472E-01
2.95537E+03	9.50328E-01	5.69896E-02	8.47223E-01	8.31264E-01
2.97766E+03	9.64443E-01	4.06994E-02	8.46186E-01	8.34987E-01
2.99931E+03	9.73755E-01	2.99497E-02	8.45145E-01	8.37047E-01
3.02046E+03	9.80465E-01	2.22185E-02	8.44094E-01	8.38191E-01
3.04114E+03	9.85770E-01	1.61289E-02	8.43034E-01	8.38824E-01
3.06125E+03	9.90312E-01	1.09428E-02	8.41971E-01	8.39165E-01
3.08058E+03	9.94440E-01	6.25876E-03	8.40917E-01	8.39340E-01
3.09873E+03	9.98282E-01	1.92802E-03	8.39896E-01	8.39418E-01
3.11510E+03	1.00000E+00	0.00000E+00	8.39424E-01	8.39424E-01
3.12917E+03	1.00000E+00	0.00000E+00	8.39422E-01	8.39422E-01
3.13989E+03	1.00000E+00	0.00000E+00	8.39421E-01	8.39421E-01
3.14644E+03	1.00000E+00	0.00000E+00	8.39420E-01	8.39420E-01
3.14922E+03	1.00000E+00	0.00000E+00	8.39420E-01	8.39420E-01
3.14992E+03	1.00000E+00	0.00000E+00	8.39421E-01	8.39421E-01

TIME (days) = 1.70351E-02
 TIME STEP SIZE (days) = 1.20156E-03
 INITIAL RESERVOIR PRESSURE (psia) = 3.15000E+03

INJECTION PRESSURE (psia) = 3.15000E+03
 WELLBORE PRESSURE (psia) = 2.50670E+03
 AVERAGE RESERVOIR PRESSURE (psia) = 3.14445E+03

RESERVOIR PROPERTIES DISTRIBUTION

```

*****
PRESSURE          GAS SATURATION    MOLES OF LIQUID    GAS MOLE FRAC.    OVERALL MOLE FRAC.
psia
*****
3.60226E+03      4.63443E-01      5.92509E-01      8.59992E-01      6.50895E-01
2.76224E+03      4.85539E-01      5.61277E-01      8.54933E-01      6.74942E-01
2.83669E+03      6.35780E-01      4.04725E-01      8.52201E-01      7.28640E-01
2.87474E+03      8.02619E-01      2.24435E-01      8.50695E-01      7.83969E-01
2.90385E+03      8.79745E-01      1.37776E-01      8.49503E-01      8.09375E-01
2.92912E+03      9.23580E-01      8.77673E-02      8.48398E-01      8.23322E-01
2.95259E+03      9.48113E-01      5.95439E-02      8.47349E-01      8.30638E-01
2.97498E+03      9.63042E-01      4.23169E-02      8.46311E-01      8.34643E-01
2.99670E+03      9.72796E-01      3.10565E-02      8.45272E-01      8.36856E-01
3.01791E+03      9.79745E-01      2.30472E-02      8.44222E-01      8.38086E-01
3.03864E+03      9.85177E-01      1.68086E-02      8.43164E-01      8.38767E-01
3.05883E+03      9.89785E-01      1.15433E-02      8.42101E-01      8.39135E-01
3.07827E+03      9.93950E-01      6.81375E-03      8.41045E-01      8.39325E-01
3.09658E+03      9.97830E-01      2.43583E-03      8.40018E-01      8.39414E-01
3.11319E+03      1.00000E+00      0.00000E+00      8.39424E-01      8.39422E-01
3.12761E+03      1.00000E+00      0.00000E+00      8.39422E-01      8.39422E-01
3.13879E+03      1.00000E+00      0.00000E+00      8.39421E-01      8.39421E-01
3.14587E+03      1.00000E+00      0.00000E+00      8.39420E-01      8.39420E-01
3.14903E+03      1.00000E+00      0.00000E+00      8.39420E-01      8.39420E-01
3.14990E+03      1.00000E+00      0.00000E+00      8.39421E-01      8.39421E-01
*****

```

TIME (days) = 1.81977E-02
 TIME STEP SIZE (days) = 1.16265E-03
 INITIAL RESERVOIR PRESSURE (psia) = 3.15000E+03
 INJECTION PRESSURE (psia) = 3.15000E+03
 WELLBORE PRESSURE (psia) = 2.48881E+03
 AVERAGE RESERVOIR PRESSURE (psia) = 3.14408E+03

RESERVOIR PROPERTIES DISTRIBUTION

```

*****
PRESSURE          GAS SATURATION    MOLES OF LIQUID    GAS MOLE FRAC.    OVERALL MOLE FRAC.
      psia
*****
2.58505E+03      4.62514E-01      5.94483E-01      8.60477E-01      6.48656E-01
2.74645E+03      4.83919E-01      5.63793E-01      8.55479E-01      6.72862E-01
2.83136E+03      6.07622E-01      4.34175E-01      8.52405E-01      7.19370E-01
2.87113E+03      7.90139E-01      2.38263E-01      8.50841E-01      7.79822E-01
2.90087E+03      8.73196E-01      1.45202E-01      8.49628E-01      8.07245E-01
2.92644E+03      9.19983E-01      9.18933E-02      8.48515E-01      8.22207E-01
2.95005E+03      9.45993E-01      6.19874E-02      8.47463E-01      8.30033E-01
2.97254E+03      9.61712E-01      4.38529E-02      8.46425E-01      8.34310E-01
2.99432E+03      9.71893E-01      3.20981E-02      8.45386E-01      8.36672E-01
3.01558E+03      9.79074E-01      2.38195E-02      8.44338E-01      8.37984E-01
3.03636E+03      9.84629E-01      1.74365E-02      8.43281E-01      8.38711E-01
3.05662E+03      9.89301E-01      1.20945E-02      8.42219E-01      8.39105E-01
3.07615E+03      9.93501E-01      7.32162E-03      8.41162E-01      8.39309E-01
3.09461E+03      9.97415E-01      2.90305E-03      8.40131E-01      8.39409E-01
3.11142E+03      1.00000E+00      0.00000E+00      8.39424E-01      8.39423E-01
3.12615E+03      1.00000E+00      0.00000E+00      8.39423E-01      8.39421E-01
3.13775E+03      1.00000E+00      0.00000E+00      8.39421E-01      8.39420E-01
3.14530E+03      1.00000E+00      0.00000E+00      8.39420E-01      8.39420E-01
3.14884E+03      1.00000E+00      0.00000E+00      8.39420E-01      8.39420E-01
3.14987E+03      1.00000E+00      0.00000E+00      8.39422E-01      8.39422E-01

```

```

TIME (days) = 1.93266E-02
TIME STEP SIZE (days) = 1.12885E-03
INITIAL RESERVOIR PRESSURE (psia) = 3.15000E+03
INJECTION PRESSURE (psia) = 3.15000E+03
WELLBORE PRESSURE (psia) = 2.46893E+03
AVERAGE RESERVOIR PRESSURE (psia) = 3.14371E+03

```

RESERVOIR PROPERTIES DISTRIBUTION

```

*****
PRESSURE          GAS SATURATION    MOLES OF LIQUID    GAS MOLE FRAC.    OVERALL MOLE FRAC.
*****

```

```

*****
psia
*****
C1
*****
2.56597E+03      4.61435E-01      5.96727E-01      8.61002E-01      6.46131E-01
2.72900E+03      4.82094E-01      5.66613E-01      8.56069E-01      6.70527E-01
2.82615E+03      5.79358E-01      4.63449E-01      8.52602E-01      7.10096E-01
2.86772E+03      7.77861E-01      2.51817E-01      8.50977E-01      7.75738E-01
2.89811E+03      8.66821E-01      1.52419E-01      8.49744E-01      8.05164E-01
2.92396E+03      9.16506E-01      9.58798E-02      8.48623E-01      8.21122E-01
2.94772E+03      9.43955E-01      6.43365E-02      8.47568E-01      8.29445E-01
2.97029E+03      9.60441E-01      4.53200E-02      8.46530E-01      8.33986E-01
2.99213E+03      9.71038E-01      3.30850E-02      8.45492E-01      8.36493E-01
3.01344E+03      9.78444E-01      2.45447E-02      8.44445E-01      8.37886E-01
3.03427E+03      9.84119E-01      1.80210E-02      8.43389E-01      8.38657E-01
3.05458E+03      9.88854E-01      1.26044E-02      8.42327E-01      8.39076E-01
3.07420E+03      9.93088E-01      7.79003E-03      8.41269E-01      8.39295E-01
3.09278E+03      9.97030E-01      3.33619E-03      8.40234E-01      8.39403E-01
3.10978E+03      1.00000E+00      0.00000E+00      8.39425E-01      8.39425E-01
3.12478E+03      1.00000E+00      0.00000E+00      8.39423E-01      8.39423E-01
3.13675E+03      1.00000E+00      0.00000E+00      8.39421E-01      8.39421E-01
3.14474E+03      1.00000E+00      0.00000E+00      8.39420E-01      8.39420E-01
3.14863E+03      1.00000E+00      0.00000E+00      8.39420E-01      8.39420E-01
3.14984E+03      1.00000E+00      0.00000E+00      8.39423E-01      8.39423E-01

```

```

TIME (days) = 2.04220E-02
TIME STEP SIZE (days) = 1.09543E-03
INITIAL RESERVOIR PRESSURE (psia) = 3.15000E+03
INJECTION PRESSURE (psia) = 3.15000E+03
WELLBORE PRESSURE (psia) = 2.44518E+03
AVERAGE RESERVOIR PRESSURE (psia) = 3.14336E+03

```

RESERVOIR PROPERTIES DISTRIBUTION

```

*****
PRESSURE          GAS SATURATION      MOLES OF LIQUID      GAS MOLE FRAC.      OVERALL MOLE FRAC.
psia
*****
2.54322E+03      4.60140E-01      5.99424E-01      8.61614E-01      6.43082E-01
2.70826E+03      4.79917E-01      5.69981E-01      8.56754E-01      6.67713E-01

```


3.07017E+03
 3.08901E+03
 3.10641E+03
 3.12188E+03
 3.13459E+03
 3.14346E+03
 3.14814E+03
 3.14976E+03
 9.92233E-01
 9.96231E-01
 9.99895E-01
 1.00000E+00
 1.00000E+00
 1.00000E+00
 1.00000E+00
 1.00000E+00
 1.00000E+00
 1.00000E+00
 8.76007E-03
 4.23736E-03
 1.17901E-04
 0.00000E+00
 0.00000E+00
 0.00000E+00
 0.00000E+00
 0.00000E+00
 0.00000E+00
 8.41489E-01
 8.40446E-01
 8.39453E-01
 8.39423E-01
 8.39421E-01
 8.39420E-01
 8.39420E-01
 8.39425E-01
 8.39260E-01
 8.39387E-01
 8.39424E-01
 8.39423E-01
 8.39421E-01
 8.39420E-01
 8.39420E-01
 8.39425E-01

TIME (days) = 2.22560E-02
 TIME STEP SIZE (days) = 4.08038E-04
 INITIAL RESERVOIR PRESSURE (psia) = 3.15000E+03
 INJECTION PRESSURE (psia) = 3.15000E+03
 WELLBORE PRESSURE (psia) = 2.39494E+03
 AVERAGE RESERVOIR PRESSURE (psia) = 3.14279E+03

RESERVOIR PROPERTIES DISTRIBUTION

 PRESSURE
 psia

 GAS SATURATION

 MOLES OF LIQUID

 GAS MOLE FRAC.
 C1

 OVERALL MOLE FRAC.
 C1

2.49514E+03
 2.66451E+03
 2.81208E+03
 2.85923E+03
 2.89143E+03
 2.91804E+03
 2.94216E+03
 2.96496E+03
 2.98694E+03
 3.00836E+03
 3.02931E+03
 3.04975E+03
 3.06956E+03
 3.08844E+03
 3.10592E+03
 3.12144E+03
 3.13424E+03
 4.57507E-01
 4.75517E-01
 5.01396E-01
 7.45236E-01
 8.50190E-01
 9.07536E-01
 9.38743E-01
 9.57227E-01
 9.68903E-01
 9.76894E-01
 9.82882E-01
 9.87781E-01
 9.92103E-01
 9.96111E-01
 9.99793E-01
 1.00000E+00
 1.00000E+00
 6.05064E-01
 5.76919E-01
 5.42722E-01
 2.87580E-01
 1.71186E-01
 1.06148E-01
 7.03399E-02
 4.90312E-02
 3.55503E-02
 2.63305E-02
 1.94409E-02
 1.38298E-02
 8.90738E-03
 4.37247E-03
 2.32156E-04
 0.00000E+00
 0.00000E+00
 8.62842E-01
 8.58135E-01
 8.53127E-01
 8.51314E-01
 8.50021E-01
 8.48878E-01
 8.47816E-01
 8.46776E-01
 8.45739E-01
 8.44695E-01
 8.43642E-01
 8.42582E-01
 8.41522E-01
 8.40479E-01
 8.39482E-01
 8.39423E-01
 8.39421E-01
 6.36549E-01
 6.61713E-01
 6.84663E-01
 7.64876E-01
 7.99710E-01
 8.18297E-01
 8.27917E-01
 8.33148E-01
 8.36030E-01
 8.37629E-01
 8.38516E-01
 8.38999E-01
 8.39255E-01
 8.39385E-01
 8.39425E-01
 8.39423E-01
 8.39421E-01

3.14325E+03 1.00000E+00 0.00000E+00 8.39420E-01 8.39420E-01
 3.14805E+03 1.00000E+00 0.00000E+00 8.39420E-01 8.39420E-01
 3.14974E+03 1.00000E+00 0.00000E+00 8.39425E-01 8.39425E-01

TIME (days) = 2.29783E-02
 TIME STEP SIZE (days) = 7.22222E-04
 INITIAL RESERVOIR PRESSURE (psia) = 3.15000E+03
 INJECTION PRESSURE (psia) = 3.15000E+03
 WELLBORE PRESSURE (psia) = 2.37762E+03
 AVERAGE RESERVOIR PRESSURE (psia) = 3.14256E+03

RESERVOIR PROPERTIES DISTRIBUTION

 PRESSURE psia

 PRESSURE GAS SATURATION MOLES OF LIQUID GAS MOLE FRAC. OVERALL MOLE FRAC.
 psia C1 C1

2.48059E+03	4.53290E-01	6.10068E-01	8.63203E-01	6.33303E-01
2.65501E+03	4.70236E-01	5.82657E-01	8.58427E-01	6.58941E-01
2.80859E+03	4.93550E-01	5.50697E-01	8.53256E-01	6.81918E-01
2.85722E+03	7.37005E-01	2.96543E-01	8.51393E-01	7.62136E-01
2.88986E+03	8.46063E-01	1.75831E-01	8.50085E-01	7.98351E-01
2.91667E+03	9.05331E-01	1.08668E-01	8.48936E-01	8.17597E-01
2.94089E+03	9.37472E-01	7.18031E-02	8.47872E-01	8.27539E-01
2.96375E+03	9.56450E-01	4.99275E-02	8.46831E-01	8.32941E-01
2.98577E+03	9.68394E-01	3.61386E-02	8.45794E-01	8.35915E-01
3.00722E+03	9.76530E-01	2.67503E-02	8.44751E-01	8.37566E-01
3.02819E+03	9.82596E-01	1.97695E-02	8.43699E-01	8.38481E-01
3.04867E+03	9.87536E-01	1.41093E-02	8.42639E-01	8.38980E-01
3.06852E+03	9.91881E-01	9.15920E-03	8.41578E-01	8.39245E-01
3.08747E+03	9.95905E-01	4.60406E-03	8.40532E-01	8.39380E-01
3.10506E+03	9.99613E-01	4.34279E-04	8.39531E-01	8.39424E-01
3.12068E+03	1.00000E+00	0.00000E+00	8.39423E-01	8.39423E-01
3.13365E+03	1.00000E+00	0.00000E+00	8.39421E-01	8.39421E-01
3.14288E+03	1.00000E+00	0.00000E+00	8.39420E-01	8.39420E-01
3.14790E+03	1.00000E+00	0.00000E+00	8.39420E-01	8.39420E-01
3.14971E+03	1.00000E+00	0.00000E+00	8.39426E-01	8.39426E-01

TIME (days) = 2.40957E-02
 TIME STEP SIZE (days) = 1.11739E-03
 INITIAL RESERVOIR PRESSURE (psia) = 3.15000E+03
 INJECTION PRESSURE (psia) = 3.15000E+03
 WELLBORE PRESSURE (psia) = 2.36391E+03
 AVERAGE RESERVOIR PRESSURE (psia) = 3.14222E+03

RESERVOIR PROPERTIES DISTRIBUTION

```

*****
PRESSURE          GAS SATURATION    MOLES OF LIQUID    GAS MOLE FRAC.    OVERALL MOLE FRAC.
      psia          C1              C1              C1              C1
*****
2.46910E+03      4.50085E-01      6.13893E-01      8.63484E-01      6.30763E-01
2.64701E+03      4.66770E-01      5.86522E-01      8.58670E-01      6.56922E-01
2.80308E+03      4.90290E-01      5.54236E-01      8.53459E-01      6.80388E-01
2.85421E+03      7.24079E-01      3.10568E-01      8.51511E-01      7.57837E-01
2.88755E+03      8.39643E-01      1.83042E-01      8.50180E-01      7.96235E-01
2.91467E+03      9.01927E-01      1.12557E-01      8.49021E-01      8.16513E-01
2.93903E+03      9.35519E-01      7.40509E-02      8.47954E-01      8.26955E-01
2.96198E+03      9.55264E-01      5.12967E-02      8.46912E-01      8.32621E-01
2.98405E+03      9.67621E-01      3.70312E-02      8.45875E-01      8.35738E-01
3.00554E+03      9.75982E-01      2.73825E-02      8.44833E-01      8.37467E-01
3.02655E+03      9.82169E-01      2.02605E-02      8.43781E-01      8.38427E-01
3.04707E+03      9.87172E-01      1.45246E-02      8.42722E-01      8.38950E-01
3.06699E+03      9.91552E-01      9.53258E-03      8.41661E-01      8.39229E-01
3.08603E+03      9.95600E-01      4.94922E-03      8.40612E-01      8.39371E-01
3.10376E+03      9.99339E-01      7.41281E-04      8.39606E-01      8.39423E-01
3.11954E+03      1.00000E+00      0.00000E+00      8.39422E-01      8.39422E-01
3.13275E+03      1.00000E+00      0.00000E+00      8.39421E-01      8.39421E-01
3.14231E+03      1.00000E+00      0.00000E+00      8.39420E-01      8.39420E-01
3.14765E+03      1.00000E+00      0.00000E+00      8.39420E-01      8.39420E-01
3.14967E+03      1.00000E+00      0.00000E+00      8.39427E-01      8.39427E-01
  
```

TIME (days) = 2.62839E-02
 TIME STEP SIZE (days) = 2.18829E-03
 INITIAL RESERVOIR PRESSURE (psia) = 3.15000E+03
 INJECTION PRESSURE (psia) = 3.15000E+03
 WELLBORE PRESSURE (psia) = 2.34840E+03

AVERAGE RESERVOIR PRESSURE (psia) = 3.14155E+03

RESERVOIR PROPERTIES DISTRIBUTION

```

*****
PRESSURE          GAS SATURATION    MOLES OF LIQUID    GAS MOLE FRAC.    OVERALL MOLE FRAC.
psia
*****
2.45433E+03      4.49096E-01      6.15813E-01      8.63840E-01      6.28615E-01
2.63401E+03      4.65203E-01      5.88840E-01      8.59058E-01      6.54984E-01
2.79148E+03      4.88525E-01      5.56642E-01      8.53882E-01      6.78728E-01
2.84850E+03      6.97932E-01      3.38751E-01      8.51735E-01      7.49155E-01
2.88332E+03      8.26940E-01      1.97269E-01      8.50354E-01      7.92039E-01
2.91102E+03      8.95263E-01      1.20159E-01      8.49177E-01      8.14380E-01
2.93566E+03      9.31725E-01      7.84125E-02      8.48103E-01      8.25810E-01
2.95878E+03      9.52981E-01      5.39303E-02      8.47058E-01      8.31997E-01
2.98095E+03      9.66149E-01      3.87296E-02      8.46022E-01      8.35394E-01
3.00251E+03      9.74952E-01      2.85702E-02      8.44981E-01      8.37277E-01
3.02359E+03      9.81376E-01      2.11715E-02      8.43931E-01      8.38322E-01
3.04419E+03      9.86505E-01      1.52877E-02      8.42873E-01      8.38893E-01
3.06420E+03      9.90951E-01      1.02158E-02      8.41811E-01      8.39199E-01
3.08339E+03      9.95038E-01      5.58282E-03      8.40760E-01      8.39357E-01
3.10134E+03      9.98830E-01      1.31267E-03      8.39745E-01      8.39421E-01
3.11741E+03      1.00000E+00      0.00000E+00      8.39423E-01      8.39423E-01
3.13105E+03      1.00000E+00      0.00000E+00      8.39421E-01      8.39421E-01
3.14119E+03      1.00000E+00      0.00000E+00      8.39420E-01      8.39420E-01
3.14713E+03      1.00000E+00      0.00000E+00      8.39420E-01      8.39420E-01
3.14957E+03      1.00000E+00      0.00000E+00      8.39431E-01      8.39431E-01

```

```

TIME (days) = 2.85525E-02
TIME STEP SIZE (days) = 2.26854E-03
INITIAL RESERVOIR PRESSURE (psia) = 3.15000E+03
INJECTION PRESSURE (psia) = 3.15000E+03
WELLBORE PRESSURE (psia) = 2.33307E+03
AVERAGE RESERVOIR PRESSURE (psia) = 3.14086E+03

```

RESERVOIR PROPERTIES DISTRIBUTION

```

*****
PRESSURE          GAS SATURATION    MOLES OF LIQUID    GAS MOLE FRAC.    OVERALL MOLE FRAC.
      psia
*****
2.43940E+03      4.48783E-01      6.17102E-01      8.64192E-01      6.26680E-01
2.62010E+03      4.64429E-01      5.90446E-01      8.59467E-01      6.53200E-01
2.77863E+03      4.87248E-01      5.58641E-01      8.54344E-01      6.77084E-01
2.84264E+03      6.69856E-01      3.68744E-01      8.51962E-01      7.39848E-01
2.87915E+03      8.13629E-01      2.12119E-01      8.50524E-01      7.87633E-01
2.90746E+03      8.88353E-01      1.28027E-01      8.49328E-01      8.12155E-01
2.93240E+03      9.27822E-01      8.28973E-02      8.48246E-01      8.24620E-01
2.95569E+03      9.50652E-01      5.66170E-02      8.47199E-01      8.31349E-01
2.97797E+03      9.64663E-01      4.04457E-02      8.46163E-01      8.35037E-01
2.99960E+03      9.73923E-01      2.97564E-02      8.45123E-01      8.37079E-01
3.02074E+03      9.80594E-01      2.20702E-02      8.44074E-01      8.38213E-01
3.04141E+03      9.85854E-01      1.60330E-02      8.43017E-01      8.38834E-01
3.06151E+03      9.90368E-01      1.08790E-02      8.41956E-01      8.39167E-01
3.08083E+03      9.94495E-01      6.19733E-03      8.40902E-01      8.39341E-01
3.09897E+03      9.98332E-01      1.87121E-03      8.39881E-01      8.39418E-01
3.11532E+03      1.00000E+00      0.00000E+00      8.39423E-01      8.39423E-01
3.12937E+03      1.00000E+00      0.00000E+00      8.39421E-01      8.39421E-01
3.14004E+03      1.00000E+00      0.00000E+00      8.39421E-01      8.39421E-01
3.14658E+03      1.00000E+00      0.00000E+00      8.39420E-01      8.39420E-01
3.14946E+03      1.00000E+00      0.00000E+00      8.39435E-01      8.39435E-01

```

```

TIME (days) = 3.07463E-02
TIME STEP SIZE (days) = 2.19380E-03
INITIAL RESERVOIR PRESSURE (psia) = 3.15000E+03
INJECTION PRESSURE (psia) = 3.15000E+03
WELLBORE PRESSURE (psia) = 2.31619E+03
AVERAGE RESERVOIR PRESSURE (psia) = 3.14021E+03

```

RESERVOIR PROPERTIES DISTRIBUTION

```

*****
PRESSURE          GAS SATURATION    MOLES OF LIQUID    GAS MOLE FRAC.    OVERALL MOLE FRAC.
      psia
*****

```


2.99239E+03	9.71201E-01	3.28979E-02	8.45471E-01	8.36526E-01
3.01368E+03	9.78568E-01	2.44032E-02	8.44427E-01	8.37907E-01
3.03451E+03	9.84196E-01	1.79330E-02	8.43374E-01	8.38666E-01
3.05481E+03	9.88902E-01	1.25491E-02	8.42314E-01	8.39077E-01
3.07442E+03	9.93135E-01	7.73652E-03	8.41256E-01	8.39295E-01
3.09299E+03	9.97075E-01	3.28545E-03	8.40221E-01	8.39403E-01
3.10998E+03	1.00000E+00	0.00000E+00	8.39424E-01	8.39424E-01
3.12497E+03	1.00000E+00	0.00000E+00	8.39422E-01	8.39422E-01
3.13693E+03	1.00000E+00	0.00000E+00	8.39421E-01	8.39421E-01
3.14495E+03	1.00000E+00	0.00000E+00	8.39420E-01	8.39420E-01
3.14910E+03	1.00000E+00	0.00000E+00	8.39454E-01	8.39454E-01